AAiT
Addis Ababa Institute of Technology
አዲስ አበባ ቴክኖሎጂ ኢንስቲትዩት
Addis Ababa University
አዲስ አበባ ዩኒቨርሲቲ

SCHOOL OF GRADUATE STUDIES

CIVIL ENGINEERING DEPARTMENT

COMPARISON OF CONVENTIONAL INCREMENTAL LOAD AND CONSTANT RATE OF STRAIN CONSOLIDATION TEST RESULTS FOR RED CLAY OF ADDIS ABABA.

By:

MUSTEFA TEHA

Advisor:

PROF. ALEMAYEHU TEFERRA

A Thesis Submitted to the School of Graduate Studies of
Addis Ababa University in Partial Fulfillment of the
Requirements for the Degree of
Masters of Science in
Civil Engineering (Geotechnical Engineering)

November, 2016

Addis Ababa, Ethiopia

AAiT
Addis Ababa Institute of Technology
አዲስ አበባ ቴክኖሎጂ ኢንስቲትዩት
Addis Ababa University
አዲስ አበባ ዩኒቨርሲቲ

SCHOOL OF GRADUATE STUDIES

CIVIL ENGINEERING DEPARTMENT

COMPARISON OF CONVENTIONAL INCREMENTAL LOAD AND CONSTANT RATE OF STRAIN CONSOLIDATION TEST RESULTS FOR RED CLAY OF ADDIS ABABA.

By

MUSTEFA TEHA

November, 2016

Approved by board Examiners:

Advisor	**Signature**	**Date**
External Examiner	**Signature**	**Date**
Internal Examiner	**Signature**	**Date**
Chairman	**Signature**	**Date**

DECLARATION

I, the undersigned, declare that this thesis is my original work performed under the supervision of my research advisor Prof. Alemayehu Teferra and has not been presented as a thesis for a degree in any other university. All sources of materials used for this thesis have also been duly acknowledged.

Name: Mustefa Teha

Signature: _____

Place : Addis Ababa institute of technology (AAiT)

Addis Ababa University

School of graduate studies

Addis Ababa.

Date: November, 2016.

ACKNOWLEDGEMENTS

I would like to express my sincere appreciation to my supervisor Prof. Alemayehu Teferra for his advice, guidance, and useful comments throughout my thesis work. Wolkite University, my sponsor, also deserves thanks for its financial support until the completion of the study. I also value the contributions of the staff members, especially Ato Admasu T., of the Geotechnical Engineering Laboratory of Addis Ababa Institute of Technology (AAiT).

I would like to say thank you to my father, Teha Mohammed, and my friends for their support and encouragement. Their encouragements provided the energy to concentrate on my studies.

Lastly, I would like to say thank you also to those individuals that I did not mention above that had help me directly or indirectly in my research works.

ABSTRACT

The conventional incremental loading consolidation tests are carried out for determining consolidation parameters. Due to the longer duration taken for the conventional incremental loading (CIL) consolidation tests, nowadays constant rate of strain consolidation (CRSC) tests are also used to study the consolidation behavior of clayey soils. The results of conventional incremental loading (CIL) consolidation tests and constant rate of strain consolidation (CRSC) tests for undisturbed red clay soil samples from 3 boreholes in Addis Ababa, Ethiopia, have been presented, compared and discussed. The main parameters investigated are compression index (C_c), pre-consolidation pressure (σ'_p) and coefficient of consolidation (C_v). For undisturbed red clay of Addis Ababa, e – log σ'_v curve of CRSC test is more non-linear than that of CIL test. Considering the slope (C_c) of e – log σ'_v curve just after pre-consolidation pressure (σ'_ρ), CRSC test resulted in a larger C_c and σ'_p value than CIL test for Kolfe and Rufa'el soil samples. But for Addisu Gebeya CRSC test, values are smaller than CIL test. To get comparable result the strain rate should be increased. The values of the coefficient of consolidation (C_v) from CIL and CRSC tests are comparable after the pre-consolidation stress. The excess pore pressures produced during the CRSC test show condition of CRSC test in which C_v values are acceptable and compatible with conventional consolidation test. The steady state condition is achieved when the C_v values from drained and undrained face of CRSC test converge with the C_v value from conventional (CIL) consolidation test. The time required to complete a CIL consolidation test in this study was 12 days. Whereas CRSC tests required an average of 1.8 days, consider only loading stage.

TABLE OF CONTENTS

LIST OF TABLES

LIST OF FIGURES

LIST OF APPENDICES

LIST OF SYMBOLS

ADU	Data Acquisition Unit
A_0	cross section of the specimen
ASTM	American society for testing of materials
a_v	Coefficient of Compressibility
C_c	Compression Index
CF	Clay Fraction
CH	Clay of High Plasticity Soil
CI	Clay of Intermediate Plasticity
CIL	Conventional Incremental Loading
CRSC	Constant Rate of Strain Consolidation Test
C_v	Coefficient of Consolidation
C_v drain	Drained Coefficient of Consolidation
C_v undrain	Undrained Coefficient of Consolidation
d_o	initial displacement reading at the start of load increment
d_{90}	displacement at 90 percent consolidation
d_f	final displacement reading
D	Constrained Modulus
e	Void Ratio
e_f	Final Void Ratio
e_i	Initial Void Ratio
e_o	Void Ratio at Start of Test
e_1	Void Ratio at Starting Effective Stress
e_2	Void Ratio at Ending Effective Stress
$\bar{e}$	Average Void Ratio
G_s	Specific Gravity
h_o	Height at Starting Test
H	Length of the Maximum Drainage Path
H_i	Initial Height
k	Coefficient of Permeability
LL	Liquid Limit
LVDT	Linear Displacement Transducer
M	Tangent Modulus
MI	Silt of Intermediate Plasticity
m_v	Coefficient of Volume Compressibility
n	Porosity
NC	Normally consolidated
OC	Over consolidated
OCR	Over consolidation ratio
p	Vertical Load
P_0	initial weight of wet specimen

P_1	final weight of wet specimen
P_2	weight of dried specimen
pb	Back Pressure
r	strain rate
t	Time
T_v	Time factor
t_{90}	Time Corresponding to 90% of Primary Consolidation
u	Pore Pressure
u_a	Excess Pore Pressure
u_b	Initial Back Pressure
USCS	Unified soil classification system
w_f	Final Moisture Content
wi	Initial Moisture Content
ε	Strain
ε_{ave}	Average Strain
σ	Total Stress
σ’	Effective Stress
σ'_1	Effective Stress for Starting Range
σ'_2	Effective Stress for Ending Range
σ_v	Vertical Applied Pressure
σ'_v	Vertical Effective Stress
σ'_{ave}	Average Effective Stress
$\sigma_v'_{(bottom)}$	Bottom Effective Stress
$\sigma_v'_{(top)}$	Top Effective Stress
σ'_p	Preconsolidation Pressure
β	Normalized Strain Rate
Δe	Changes in Void Ratio
ΔH	Displacement
ρ_d	Dry Density
ρ_w	Water Density
Δe,	change in voids ratio
Δσ	Increment Pressure
ζ	Consolidation Ratio

CHAPTER 1

INTRODUCTION

1.1 General

Consolidation characteristics of clays play important role in estimating the settlement of foundations and simulation of other structures for their stress -deformation response. The samples collected through geotechnical investigations are generally used in the laboratory to find the compressibility of clay. The traditional one-dimensional consolidation test (conventional incremental loading test, CIL) has been commonly used to determine the consolidation properties of clayey soil based on the theory proposed by Terzaghi in the early 1920's. As its name suggests, in the incremental loading consolidation test the load is increased in increments and the resulting vertical deformations are measured as a function of time for each increment. Conventional incremental loading (CIL) consolidation test is more convenient to be conducted and the equipment is relatively simple**.** Typically, one increment of load lasts for 24 hours. The equilibrium strain for each load can be determined from the measured deformations.

Since Terzaghi formulated his consolidation theory in the early 1920's, many extensions had been made continuously to solve many of the unrealistic assumptions made in the original theory. Today, consolidation theory had reached an advanced development that solutions are available for most practical problems. Some researcher refined Terzaghi's theory by solving a more generalized form of the differential equation of consolidation [1].

Numerous new techniques to measure the compressibility of soils were introduced after the conventional incremental loading test is standardized.

These new techniques include constant rate of strain consolidation test, constant rate of load consolidation test, constant pore pressure gradient, constant pressure ratio, restricted flow consolidation and back pressure control.

Constant rate of strain consolidation (CRSC) test is one of the new developments suggested by many researchers. Consolidation test under constant rate of strain was first presented by Hamilton and Crawford [2] as a quick way of determining pre-consolidation pressure, σ'_p. Despite the fact that more than 50 years have passed, there is lack of awareness about this test because of which it has not come to practice as much as it should have. The theories proposed by Smith and Wahls (1969) and Wissa et al. (1971) (as cited in [3]) have been conventionally used to interpret the CRSC test data. Although there is no Ethiopian testing standard available for this test, ASTM D4186-89 is available with good description of the test and its interpretation scheme. It is well known that the consolidation behavior of clayey soils is strain-rate dependent [4, 5] and the degree of this dependency is different from soil to soil [6]. An understanding of the strain rate effect on consolidation behavior is useful for designing geotechnical projects such as embankments, foundations in areas of clayey deposits.

Also, in comparison with the CIL test, the CRSC test has several merits. Constant rate of strain consolidation test can reduce the time needed for consolidation test using CIL test from almost two weeks times to few days and it provides continuous data points for a plot of void ratio (*e*) against effective vertical stress (σ'_v), which can increase the accuracy of determining pre-consolidation stress (σ'_p) and compressive index (C_c).

1.2 Statement of Problem

Since the 1950's, the standard compressibility test that has been used to measure the soil compression characteristic is the one-dimensional Compression Test (Incremental Loading Test) based on Terzaghi's theory. Conventional oedometer (CIL) test based on Terzaghi's theory is a step loading test which takes about two weeks for one complete test with loading and unloading stages.

Many researchers have introduced other methods to measure the compressibility characteristics of the soil. One of the new developments is the CRSC test. Through the CRSC test, the testing time for a completed test can be reduced from around two weeks to few days. The compression test can be conducted up to a very high pressure. There were no previously conducted CRSC test on red clays of Ethiopia. CRSC test may be a good method that provides reliable results for consolidation if proper strain rates are used. This research is aimed at comparing results from CIL and CRSC tests on such soils.

1.3 Objectives of the Study

The main objective of this thesis paper is to compare the results of conventional incremental load (CIL) and constant rate of strain (CRSC) consolidation tests for Addis Ababa red clay soil.

The following specific objectives are set forth;

- To illustrate the drawback of CIL test comparing to CRSC test.
- To check the suitability of strain rate suggested for CRSC test
- To compare the result of the compression characteristic of the soil, i.e. coefficient of consolidation (C_v), compression index (C_c) and pre-consolidation pressure, σ'_p obtained from CIL and CRSC tests.

1.4 Methodology

In order to achieve the objective of the research, index property tests i.e. specific gravity, grain size analysis, and Atterberg limit tests and one dimensional consolidation tests i.e. conventional incremental loading (CIL) tests, and Constant rate of strain consolidation (CRSC) tests, are conducted on six red clay soil samples. Test pits were excavated and soil samples of disturbed and undisturbed states have been collected from selected three locations of Addis Ababa city where red clay is found. Two samples from each test pit at two different depths (1.5 m and 3.0 m) were collected. The disturbed and undisturbed samples were used to conduct index property tests and one dimensional consolidation tests respectively. Based on the theories and laboratory tests performed, the results of conventional incremental loading test (CIL) and Constant rate of strain consolidation (CRSC) tests have been analyzed, discussed and compared thoroughly. Finally important conclusions are drawn that shade light on the relative advantages of the two procedures.

1.5 Scope of the Study

This research focuses on different locations within Addis Ababa where red clay soils are prevalent. Red clays are known to be found in Northern and Western parts of Addis Ababa [7]. Samples are collected from Kolfe, Addisu Gebeya and Rufa'el area. A test pit is opened at each site to a depth of 3m and disturbed and undisturbed samples are collected.

For the intended purpose, CIL and CRSC tests are conducted on undisturbed soil samples.

1.6 Organization of the Thesis

This thesis contains five chapters. Following the introductory chapter which describes the background, objective and scope of the work, Chapter 2 reviews the literature related to the CIL and CRSC testing, and comparison of previous tests of CIL and CRSC. Chapter 3 describes relevant details of the experimental investigations carried out in this study and presents test results and analysis. Chapter 4 discusses and compares the results of both tests. Finally, the conclusions drawn from this study and recommendations for future works are given in Chapter 5.

CHAPTER 2

LITERATURE REVIEW

2.1 Consolidation of the Soils

When a load is applied on a standard soil mass, the entire load is first carried by the pore water, then due to the loading the water will drain out from the soil, transferring the loading to the soil skeleton. The differences between total applied stress and the pore pressure at any instant known as “effective stress” [8]. That is the same stress carried by the soil skeleton.

$$\sigma' = \sigma - u \tag{2.1}$$

In essence, the consolidation process is a gradual transfer of stress from the pore water to the soil skeleton.

2.1.1 Principle of consolidation

Soil is a compressible structure. When soil is subjected to a load it tends to decrease its volume. Three stages will occur during the compression.

i. Compression of the solid grain
ii. Compression of water within the voids between grains.
iii. Escape of water from void.

2.1.2 Consolidation theory

Terzaghi made assumptions on the process of consolidation and designed the first consolidation apparatus for consolidation test. Many of the geotechnical engineers use the Terzaghi theory to solve various types of problem related to soils.

The classical one-dimensional consolidation Terzaghi theory is based on the following assumptions [8].

a) Homogeneous clay layer.
b) Fully saturated clay layer.
c) Compressibility of soil grains and water is negligible.
d) Deformation of soil occurs only in the direction of the load application.
e) Darcy's law is valid.
f) Flow is in one direction only
g) The coefficient of permeability is constant within the layer.

In case of simple one-dimensional consolidation of clay layer that is subjected to a uniform load the following equation of Terzaghi is proposed.

$$\frac{\partial u}{\partial t} = \frac{k}{\gamma_w m_v}\frac{\partial^2 u}{\partial z^2} \tag{2.2}$$

where ,

u = excess pore water pressure at time t, at a given point.

z = vertical height of that point.

k = coefficient of permeability of the clay.

m_v = coefficient of volume compressibility of the clay.

Υ_w = unit weight of water.

Defining the coefficient of consolidation, C_v as:

$$C_v = \frac{k}{\gamma_w m_v} \tag{2.3}$$

Equation 2.2 becomes,

$$\frac{\partial u}{\partial t} = c_v \frac{\partial^2 u}{\partial z^2} \tag{2.4}$$

Equation (2.4) is the basic differential equation of Terzaghi's consolidation theory and can be solved by combining two boundary conditions and initial condition.

- Boundary conditions (for all time t)

  - On the surface of the layer, z = 0, we have: $u(0,t) = 0$

  - At the bottom of the layer, z = 2H, then: $u(2H,t) = 0$

- Initial condition (for t = 0)

$$u(z,0) = \Delta\sigma_v \quad \text{except for z} = 0 \text{ and z} = 2\text{H}$$

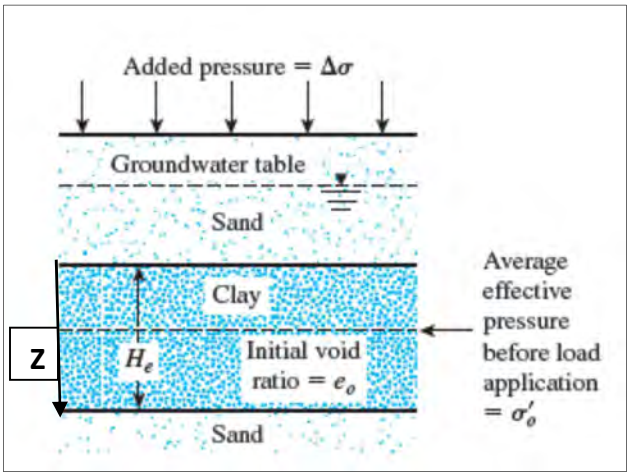

Fig. 2.1: Clay layer drained on the two faces [9].

The analytical solution of equation in conjunction with the conditions is obtained through Fourier series transformation function. The general solution of Terzaghi equation [10] is

$$u = \sum_{n=1}^{n=\infty} \left(\frac{1}{H} \int_0^{2H} u_i \, sin \frac{n\pi z}{2H} \, dz \right) sin \frac{n\pi z}{2H} \, exp \left(\frac{-n^2 \pi^2 C_v t}{4h^2} \right) \tag{2.5}$$

Expression of $\left(\frac{C_v\, t}{h^2}\right)$ is a dimensionless number and replaced by a time factor, T_v as

$$T_v = \frac{c_v t}{h^2} \tag{2.6}$$

By substituting Equation 2.6 into the general solution equation, the simplified equation becomes,

$$u = \sum_{n=1}^{n=\infty}\left(\frac{1}{H}\int_0^{2H} u_i \sin\frac{n\pi z}{2H}\, dz\right) \sin\frac{n\pi z}{2H}\, exp\left(\frac{-n^2\pi^2 T_v}{4}\right) \tag{2.7}$$

where, u = pore water pressure

u_i = initial pore water pressure

H = height of specimen

T_v = time factor

z = vertical height (top to bottom of specimen)

So far, no assumptions have been made regarding the variation of u_i with the depth of the clay layer. Several possible types of variation for u_i are shown in Fig. 2.2.

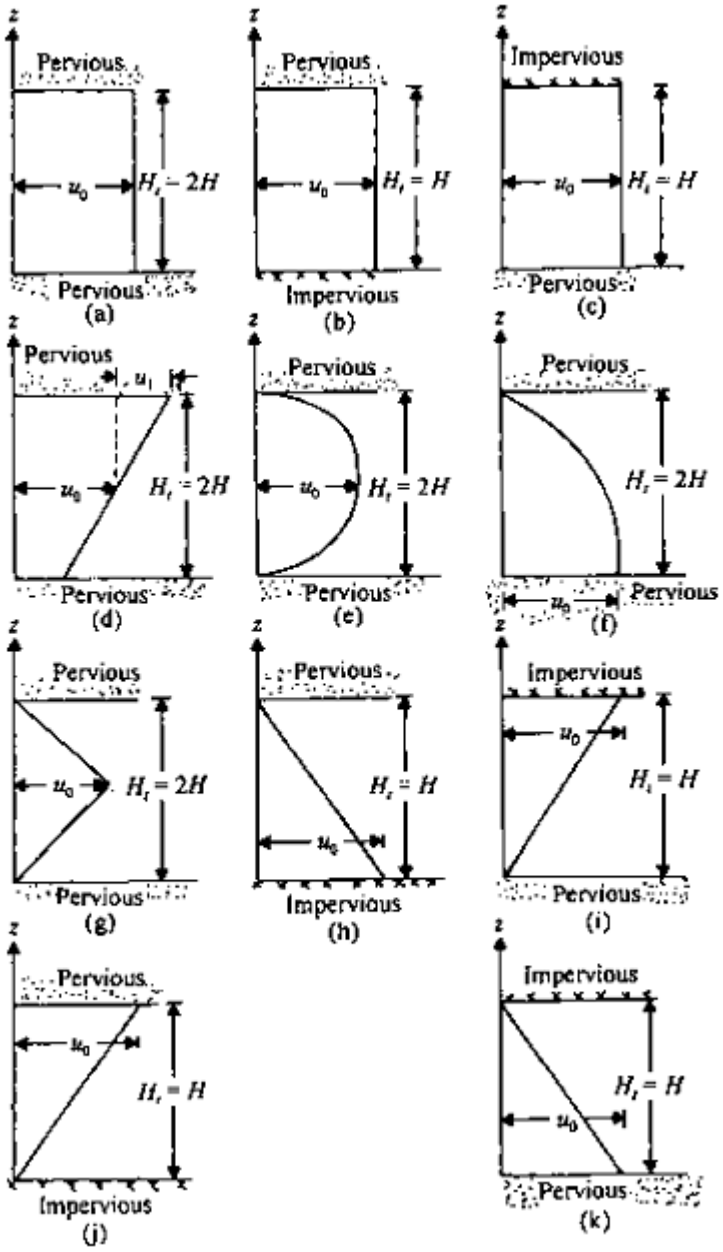

Fig. 2.2: Variation of u_i with depth [9].

At any stage during the consolidation process, transfer of stress from the pore water to soil skeleton are known as degree of consolidation, U. This process is expressed in percentage. Degree of consolidation, U at time t can be calculated by the Equation 2.8.

At a given time the degree of consolidation at any depth z is defined as

$$U_z = \frac{\text{excess pore water pressu re dissipated}}{\text{initial excess pore water pressure}}$$

$$= \frac{u_i - u}{u_i} = 1 - \frac{u}{u_i} = \frac{\Delta\sigma'}{u_i} = \frac{\Delta\sigma'}{u_0} \qquad (2.8)$$

From Equations 2.7 and 2.8 [9].

$$U_z = 1 - \sum_{m=0}^{m=\infty} \frac{2}{M} \sin\frac{Mz}{H} exp(-M^2 T_v) \qquad (2.9)$$

Where M=(2m+1)π/2

Figure 2.3 shows the variation of U_z with depth for various values of the non-dimensional time factor T_v;

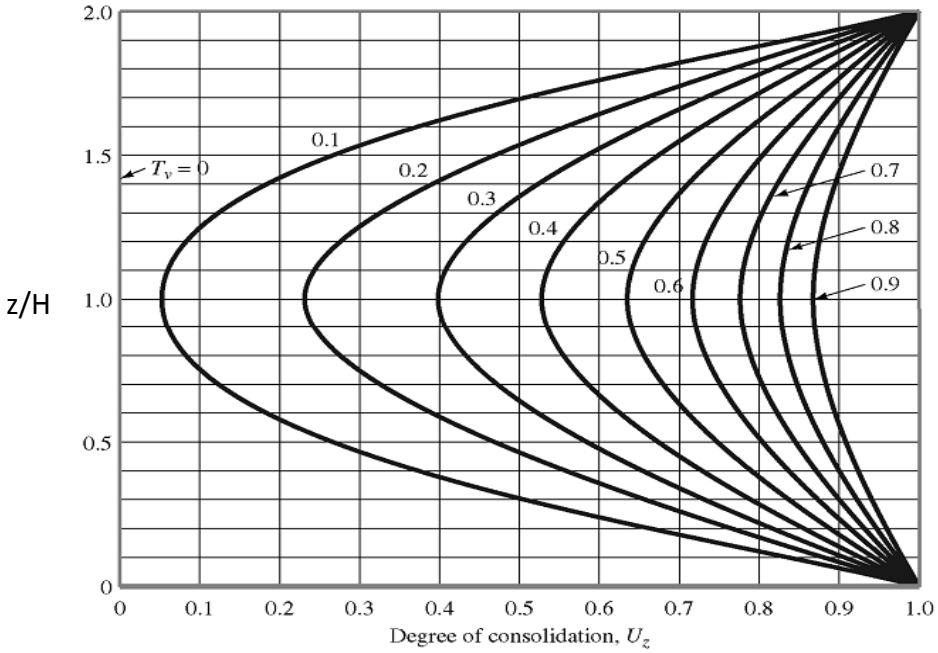

Fig.2.3: Variation of U_z with z/H and T_v [9].

The average degree of consolidation is also the ratio of consolidation settlement at any time to maximum consolidation settlement. Average degree of consolidation (U) for the entire depth of the clay layer at any time, t is [10].

$$U_{av} = 1 - \sum_{m=0}^{m=\infty} \frac{2}{M^2} \exp(-M^2 T_v) \qquad (2.10)$$

Hence the representation of the function U_{av} vs (T_v) and the inverse function T_v vs (U_{av}) are given in Fig.2.4.

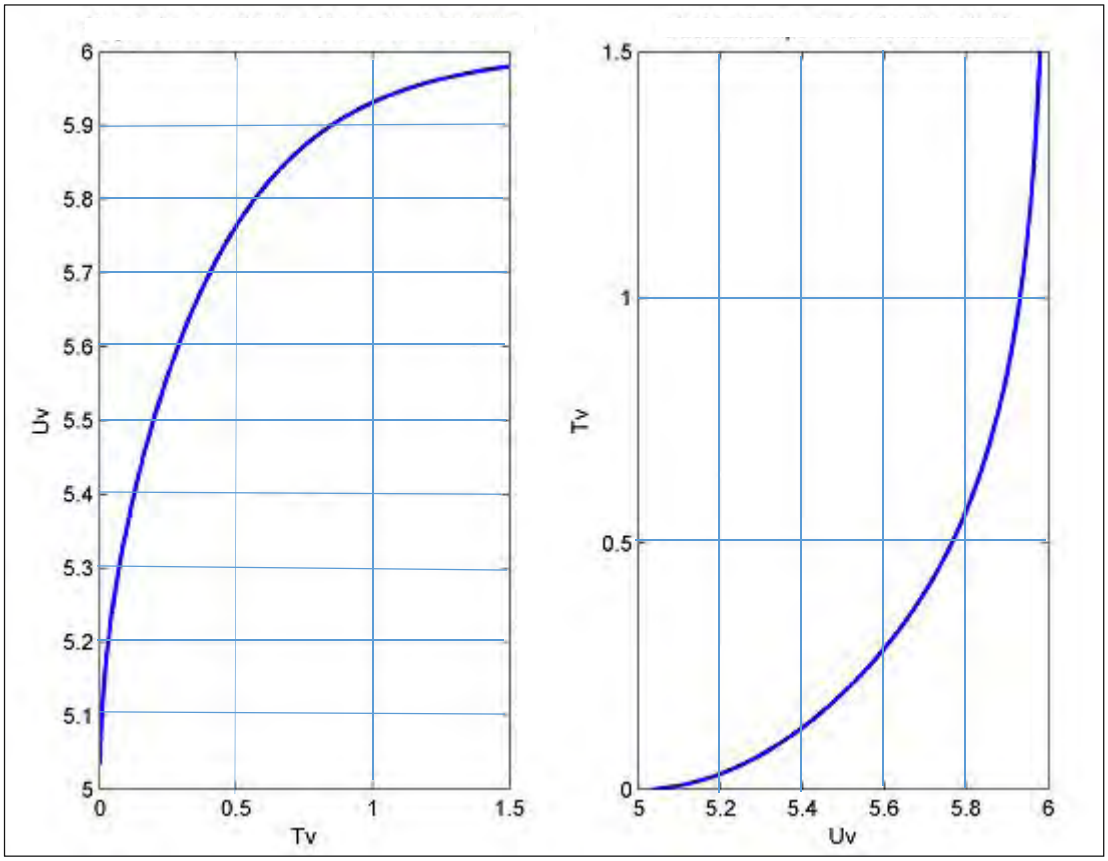

Fig. 2.4: Respective changes of U_{av} and T_v [11].

2.2 One-Dimensional Consolidation Laboratory Test

The usual way to conduct a one-dimensional consolidation test is to confine a soil sample in a fixed stiff metal ring with the sample loaded along the vertical axis of the ring. In terms of loading procedure, consolidation tests fall into two broad categories; incremental loading and continuous loading, i.e. constant rate of strain, constant rate of loading, controlled hydraulic gradient, test methods [12]. The common methods in which consolidation testing can be conducted are; conventional incremental loading (CIL) and constant rate of strain consolidation (CRSC) test [13].

2.2.1 Conventional incremental loading (CIL) consolidation test

The conventional incremental loading test is usually carried out on saturated specimens about 20 mm thick and 50 mm in diameter. The soil specimen is kept inside a metal ring, with a porous stone at the top and another at the bottom (Fig. 2.5). The load on the specimen is applied through a lever arm, and the compression of the specimen is measured by a micrometer dial gauge. The load is usually doubled every 24 hour. The specimen is kept under water throughout the test. The procedure is continued until the desired limit of stress on the clay specimen is reached [9].

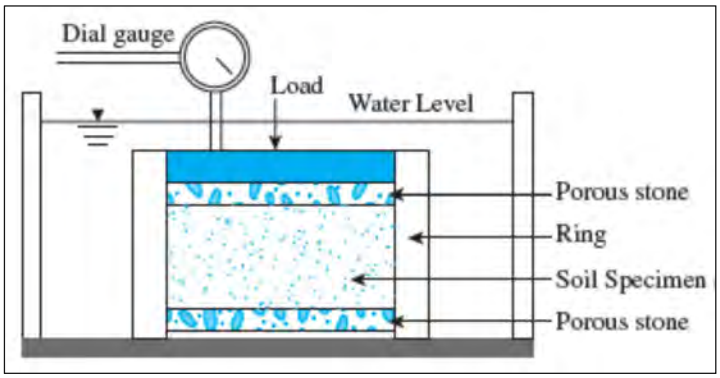

Fig.2.5: CIL test consolidometer [9].

After the time-deformation plots for various loadings are obtained in the laboratory, it is necessary to study compression and consolidation characteristics of soil, i.e.

Coefficient of Rate of Consolidation, Coefficients of Compressibility, Coefficient of Volume Compressibility and pre-consolidation pressure.

2.2.1.1 Coefficient of rate of consolidation, C_v

The process of comparing a laboratory consolidation curve with the theoretical curve is known as "curve fitting". It is related only to the primary consolidation phase and enables the coefficient of consolidation, C_v to be determined for each loading increment. Two curve fitting procedures are normally used by the geotechnical engineers, one is the log-time/settlement curve (log-time method), and the other one is the square-root-time/settlement curve (square-root-time method).

a) Square-root-time method

This procedure was introduced by Taylor (1942) (as cited in [9]), and also known as Taylor's Method. Fig. 2.6 shows the principle of the square-root-time method.

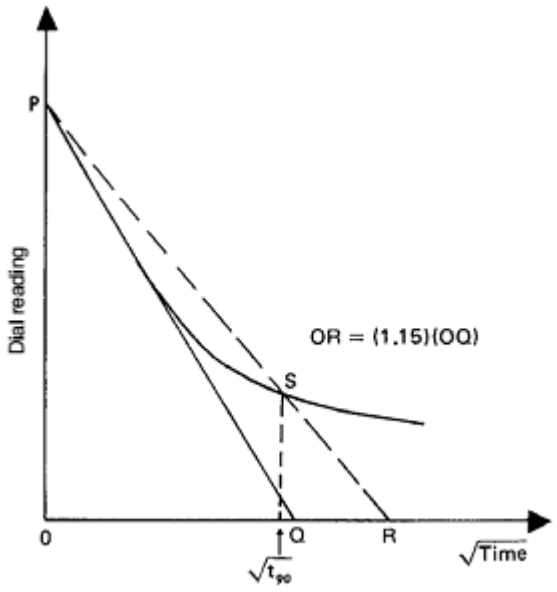

Fig. 2.6: Analysis of Square-Root-Time Curve [10].

When the actual time, t for a given percentage of primary consolidation is known for a particular load increment of the test, coefficient of consolidation, C_v can be calculated by Equation 2.3. Where the T_v is equal to 0.848 for the 90% of primary consolidation and the h is the length of the maximum drainage path.

b) Log-time method

Casagrande introduced this method to calculate the compressibility coefficients from a graph and is known as Casagrande method. Fig.2.7 shows the principle of the log-time method.

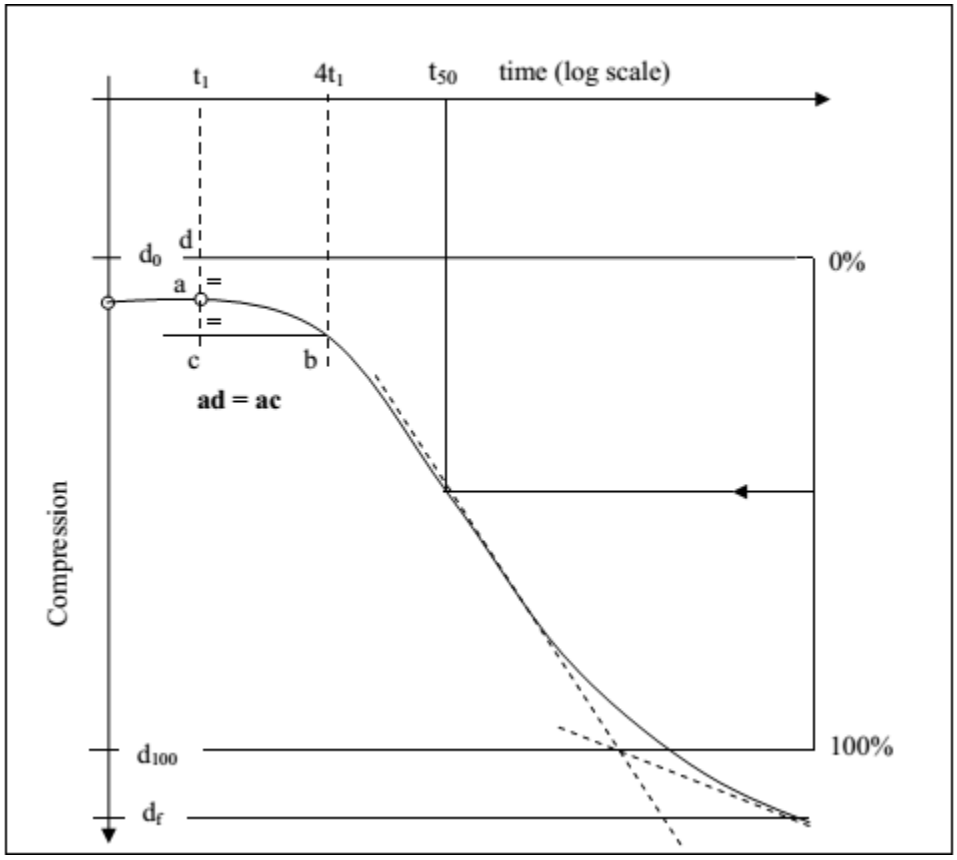

Fig. 2.7: Analysis of Log -Time/Settlement Curve [14].

Where,

d_o = initial displacement reading at 0% consolidation

d_{100} = displacement at 100% consolidation

d_f = final displacement reading

t_1 = time near the head of the initial portion of the curve

t_{50} = time at which 50% consolidation has occurred.

ad, ac = vertical distance

Coefficient of consolidation, C_v can be calculated when the time for 50% consolidation is known by Equation 2.3. Where the T_v is equal to 0.197 for the 50% of primary consolidation and h is the length of the maximum drainage path.

2.2.1.2 Coefficient of compressibility (a_v)

Coefficient of compressibility is equal to the change in voids ratio Δe , divided by corresponding stress increment $\Delta\sigma$**.** Fig. 2.8 shows the typical graph of the void ratio versus stress in linear scale. The change in void ratio denoted by Δe, and the change in stress denoted by $\Delta\sigma$.

$$a_v = \frac{(e_1 - e_2)}{(\sigma_2 - \sigma_1)} = \frac{\Delta e}{\Delta \sigma} \tag{2.11}$$

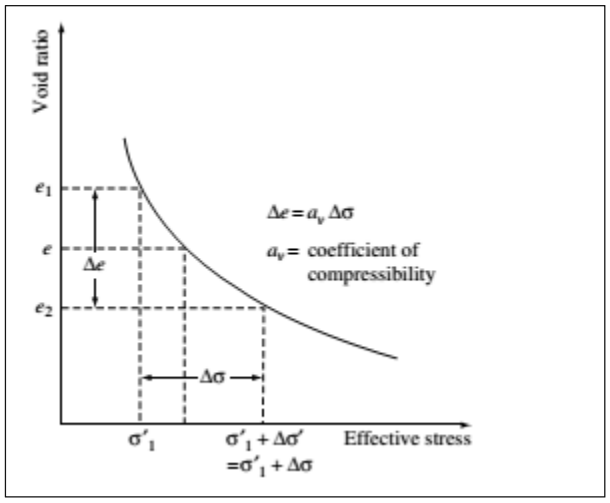

Fig.2.8: Void ratio versus effective stress Curve (e-σ') [9].

2.2.1.3 Coefficient of volume compressibility (m_v)

The compressibility of the soil is usually expressed in terms of the coefficient of volume compressibility (m_v) which indicates the compressibility per unit volume of the soil. This is also known as the coefficient of volume change which can be expressed as:

$$m_v = \frac{a_v}{(1+e_1)} = \left(\frac{1}{1+e_1}\right)\left(\frac{\Delta e}{\Delta \sigma}\right) \tag{2.12}$$

where a_v is the coefficient of compressibility and $e_1$is the void ratio at the start of the load increment $\Delta\sigma$.

2.2.1.4 Compression index (C_c)

The compression index, C_c is the slope of the straight-line portion (the latter part) of the loading curve. This slope is represented by the Equation 2.15.

$$c_c = \frac{e_1 - e_2}{\log \sigma'_2 - \log \sigma'_1} = \frac{(e_1 - e_2)}{\log \left[\frac{\sigma'_2}{\sigma'_1}\right]} \tag{2.13}$$

Where e_1 and e_2 are the void ratios at the end of consolidation under effective stresses σ'_1 and σ'_2, respectively.

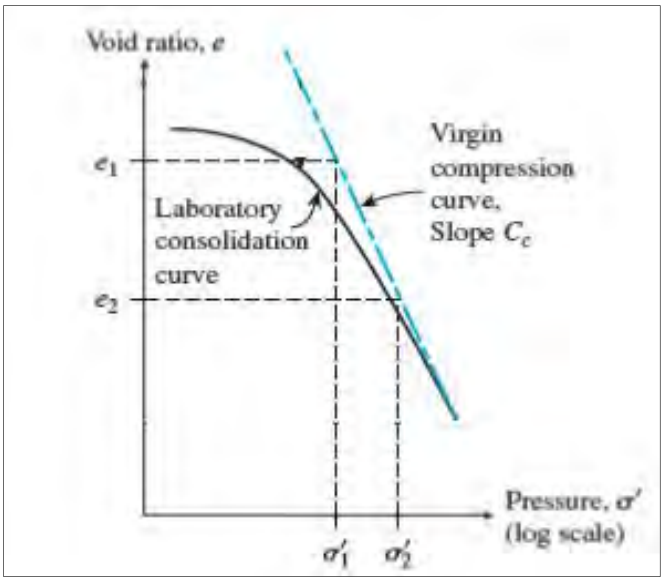

Fig. 2.9: Curve for compression index determination (e- log σ') [9].

The compression index has been found to be related to the liquid limit of clay to a reasonable degree of approximation by the equation [15].

$$C_c = 0.009(LL - 10\ \%) \tag{2.14}$$

But for the remolded clay the corresponding compression index, c_c is given approximately by the equation [15].

$$C_c = 0.007(LL - 10\%) \tag{2.15}$$

A similar study carried out by Nagaraj and Murthy, expressed compressive index as function of liquid limit and specific gravity [15]:

$$C_c = 023\ 43\left(\frac{LL}{100}\right)G_s \qquad (2.16)$$

2.2.1.5 Pre-consolidation pressure (σ'_p)

The pre-consolidation pressure, σ'_p is the maximum past effective overburden pressure to which the soil specimen has been subjected. The importance of determining σ'_p has attracted many researchers. Different methods such as by Casagrande (1936), Burmister (1951), Schmertmann (1955), Janbu (1967), and Butterfield (1979) have been developed [16]. Wang and Frost [16] suggest these methods are usually based on the experimental void ratio (e) – effective consolidation stress (σ') relations and are empirical by nature. Among the established methods, the most popular is Casagrande graphical method (e−log σ').

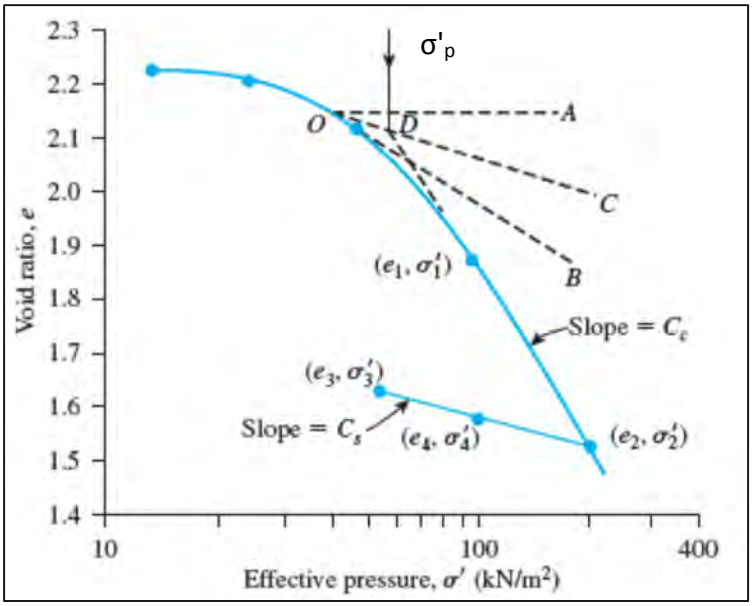

Fig.2.10: e - log σ' curve for preconsolidation pressure [9].

In the typical e versus log σ' plot shown in the above figure, the upper part is curved because when the soil specimen was obtained from the field, it was subjected to a certain maximum effective pressure.

During the process of soil exploration, the pressure is released. In the laboratory, when the soil specimen is loaded, it will show relatively small decrease of void ratio with load up to the maximum effective stress to which the soil was subjected in the past.

If the effective stress on the soil specimen is increased further, the decrease of void ratio with stress level will be larger [15].

Based on the stress history, we can define the two conditions of a clay:

a) Normally consolidated. A soil is called normally consolidated if the present effective overburden pressure is the maximum to which the soil has ever been subjected,

i.e., $\sigma'_{present} = \sigma'_{past\ maximum}$.

b) Over-consolidated. A soil is called over-consolidated if the present effective overburden pressure is less than the maximum to which the soil was ever subjected in the past, i.e., $\sigma'_{present} < \sigma'_{past\ maximum}$.

2.2.2 Constant rate of strain consolidation (CRSC) test

Constant rate of strain consolidation test is a test which the vertical deformation of the sample is applied at a constant rate [$\delta(\Delta H/ \delta t)$ = constant] as shown in the Fig. 2.11 [14]. A soil specimen is taken in a fixed-ring consolidometer and saturated. For conducting the test, drainage is permitted at the top of the specimen but not at the bottom. A continuously increasing load is applied to the top of the specimen so as to produce a constant rate of compressive strain, and the excess pore water pressure ,u_a (generated by the continuously increasing stress σ at the top) at the bottom of the specimen is measured [17]. Loading for the CRSC test is applied continuously at suitable strain rate.

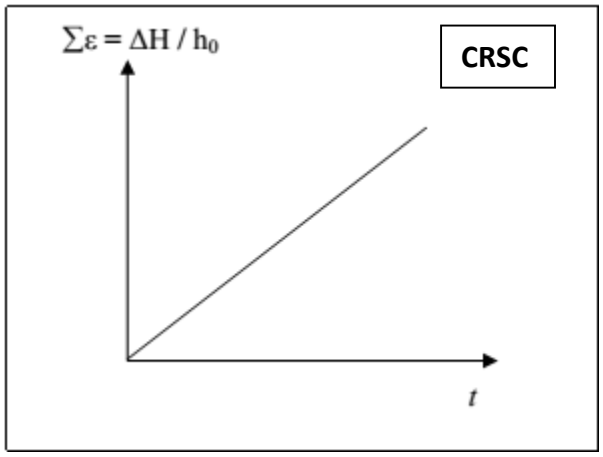

Fig.2.11 Representation of loading patterns for CRSC test [14].

The CRSC test was first described in 1959 by Hamilton and Crawford [2] as a rapid means of determining the pre-consolidation pressure and for testing material under strain rates that more closely approximate the field strain rates. They found that the relationship between void ratio and vertical effective stress depended significantly on the rate of strain of the test and concluded that some significant excess pore water pressure developed at the bottom of the specimen if the test is performed at a slow rate.

After the first proposal on the CRSC test by the Hamilton and Crawford, several modification of the constant rate of strain concept and procedures have been suggested.

Smith and Wahls (1969), Wissa et al (1971), Umehara and Zen (1980), and Lee (1981) (as cited in [17, 18, and 19]) had conducted and analyzed the CRSC test. All of them had used the Hamilton and Crawford concepts as a basic to suggest the new ways of analysis to improve the result of the CRSC test.

2.2.2.1 Theories for interpreting CRSC test results

There are several theoretical studies about strain distribution within the sample of CRSC test and interpreting CRSC test results. The existing theories can be divided into small strain theory and large strain theory according to whether considering the change of the thickness of the sample during a time interval [18, 20].

a) Small strain theory

i) Smith and Wahls method

Smith and Wahls (1969) developed the governing equation for CRSC test based on the continuity of flow through a soil element as follows [18]:

$$\frac{\partial}{\partial z}\left(\frac{k}{\gamma_w}\frac{\partial u}{\partial z}\right) = \frac{1}{1+e}\frac{\partial e}{\partial t} \qquad (2.17)$$

Where z = the vertical coordinate of a point,

k = hydraulic conductivity,

e = void ratio,

γ_w= unit weight of water,

u = pore water pressure and

t = time.

The void ratio is assumed as a linear function of time and space variable as:

$$e = e_0 - r_e t\left[1 - \frac{b}{r_e}\left(\frac{z-0.5H}{H}\right)\right] \quad (2.18)$$

Where e_0 = initial void ratio,

r_e = the rate of change of the average void ratio,

H = thickness of the sample;

b = a constant that depends on the variation in void ratio with depth and time

By assuming that the term (1+e) in Equation (2.17) can be replaced by (1+e_{av}), where e_{av} is not a function of z, and introducing the boundary conditions u (0, t) = 0 and $\partial u / \partial z$ (H, t) = 0, the solution to Equation (2.17) is obtained in the form as:

$$u = \frac{\gamma_w r_e}{k(1+e_{av})}\left[\left(Hz - \frac{z^2}{2}\right) - \frac{b}{r_e}\left(\frac{z^2}{4} - \frac{z^3}{6H}\right)\right] \quad (2.19)$$

An average effective vertical stress (σ'_v), and coefficient of consolidation (C_v) can be calculated as:

$$\sigma'_v = \sigma_v - \left[\frac{1/3-1/24(b/r_e)}{1/2-1/12(b/r_e)}\right]u \quad (2.20)$$

$$C_v = \frac{r_e H^2}{a_v u_{z=H}}\left(\frac{1}{2} - \frac{1}{12}\frac{b}{r_e}\right) \quad (2.21)$$

This theory has two major problems. First is the consequences of the assumption that the void ratio is a linear function of the time and space variables cannot be evaluated, and therefore the degree of accuracy of the obtained material properties is not known.

The second problem is that the parameter b is not known, and there is no procedure for its determination. Since the resulting material characteristics depend on the chosen value of *b*, one cannot ascertain which value to use unless some other reference test are performed on similar specimens.

ii) Wissa et al.'s method

The Wissa et al. analysis starts from the governing equation for consolidation written in terms of strains (ε) as follows [3, 18]:

$$\frac{\partial \varepsilon}{\partial t} = c_v \frac{\partial^2 \varepsilon}{\partial z^2} \tag{2.22}$$

By considering boundary and initial conditions; Wissa et al. (1971) obtained the solution for Equation 2.22 as follows:

$$\varepsilon(z,t) = rt + \frac{rH^2}{6c_v}\left(3\frac{z^2}{H^2} - 6\frac{z}{H} + 2\right) - \frac{2rH^2}{\pi^2 c_v}\sum_{n=1}^{\infty}\frac{cosn\pi z}{n^2 H} exp(-n^2\pi^2 T_v) \tag{2.23}$$

Where ε = vertical strain

r = strain rate;

C_v = coefficient of consolidation ($C_v = k/\gamma_w m_v$);

m_v = the coefficient of volume compressibility;

T_v = time factor ($T_v = C_v t/H^2$).

The above equation containing the exponential function vanishes for large values of time and in the limit, when time tends to infinity, the strains have a parabolic distribution within the specimen. This is called as "steady state" by Wissa et al. For small values of time, the specimen is in a transient state and the term containing the exponential function cannot be neglected. The analysis procedure is accordingly divided into two parts.

For the steady state condition, the term containing the exponential function in the Equation 2.23 is neglected, and a parabolic strain distribution within the specimen is obtained as:

$$\varepsilon(z,t) = rt + \frac{rH^2}{C_v}\left[\frac{1}{6}\left(3\frac{z^2}{H^2} - 6\frac{z}{H} + 2\right)\right] \tag{2.24}$$

The strain distribution within the sample is shown in Fig.2.12.

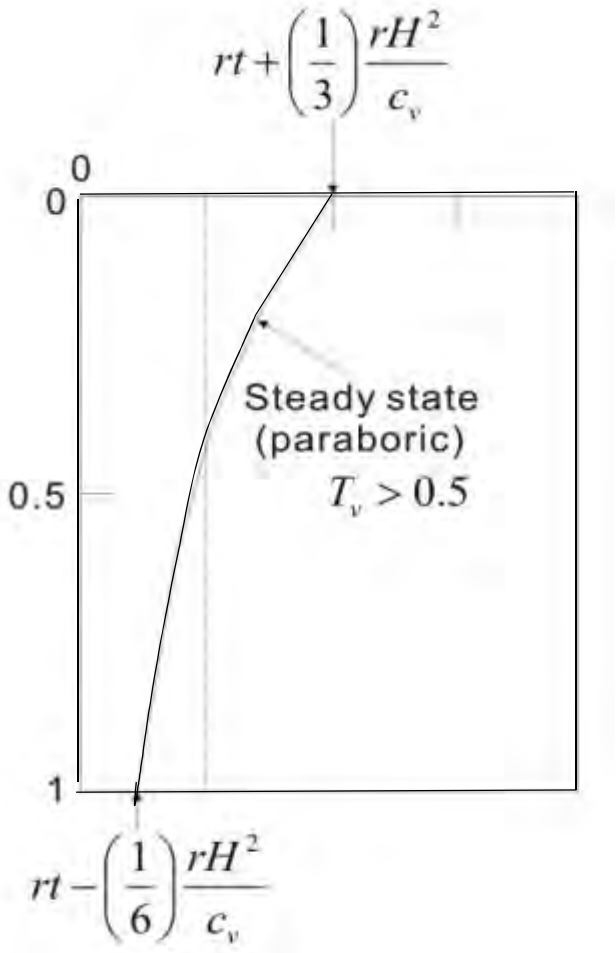

Fig. 2.12: Strain distribution within the sample (after Wissa et al.) as cited in [18].

For the linear assumption, the coefficient of consolidation is obtained as,

$$c_v = \frac{H_0^2}{2u}\frac{\Delta\sigma_v}{\Delta t} \tag{2.25}$$

Where u = pore water pressure at the bottom of the sample,

$\Delta\sigma_v$ = total vertical stress increment in a time interval of Δt and

Δt = time interval.

H_0 = initial thickness of specimen

The strains at the top and bottom of the specimen can be calculated by Equation 2.24, and the stress-strain relationship of the specimen can be determined since the applied load and pore-water pressure are measured. The average effective stress is

$$\sigma'_{\text{ave}} = \sigma - \left(\frac{2}{3}\text{u}\right) \tag{2.26}$$

Where $^2/_3$ u = was used for mean pore pressure in sample assuming parabolic distribution.

which can be associated with the average strain,

$$\varepsilon_{ave} = \left(\frac{1}{3}\right)(2\varepsilon_2 + \varepsilon_1) = rt \tag{2.27}$$

The expression for the average strain is the same since the strain distribution does not depend on the applied void ratio-effective stress model. The expression for the coefficient of consolidation and the average effective stress are changed in the case of the nonlinear assumptions.

$$c_v = -\frac{H_0^2}{2\log\left(1-\frac{u}{\sigma_v}\right)}\frac{d\log\sigma_v}{dt} \tag{2.28}$$

and

$$\sigma'_v = (\sigma_v^3 - 2\sigma_v^2 u + \sigma_v u^2)^{1/3} \tag{2.29}$$

Although the analysis described above is theoretically consistent, but some of the assumption are not always justified. First, the analysis is based on the assumptions that the coefficient of the consolidation is constant throughout the test.

The second assumption is that the coefficient of volume change (linear assumption) or compression index (nonlinear assumption) is constant.

The consequence of those two assumptions is that the analysis for the transient state yields two distinct curves for the void ratio-effective stress relationship.

One curve is obtained from strains calculated at the drained end of the specimen and the other from the undrained end. During the steady state, assumption for the constant coefficient of consolidation is somewhat less restrictive since the incremental change in the material behavior is observed. However, the steady state condition is a consequence of the assumption of a constant coefficient of consolidation.

b) Large strain theory

i) Umehara and Zen method

The analysis method proposed by Umehara and Zen [21] is based on the large strain consolidation theory developed by Mikasa. The governing equation is

$$\frac{\partial \zeta}{\partial t} = c_v \zeta^2 \left(\frac{\partial^2 \zeta}{\partial {z_0}^2}\right) \tag{2.30}$$

where $\zeta = \frac{1}{1-\varepsilon}$, ζ = consolidation ratio

ε = axial strain

t = time

z_o = original coordinate

The governing equation is solved numerically with the appropriate boundary conditions and for various values of a non-dimensional parameter C_v/RH_o (where R is the rate of deformation, and the H_o is the initial specimen height). They have been constructed a series of charts with curves relating the consolidation ratio to the strains and the non-dimensional parameter C_v/RH_o (Appendix G).

A ratio F of strains at the two ends of the specimen is determined in the same way as suggested by Wissa from experiment,

$$F = \frac{[\log\,(\sigma - u) - \log \sigma'_o]}{(\log \sigma - \log \sigma'_o)} \tag{2.31}$$

where σ'_0 = initial effective vertical stress

σ = total vertical stress

u = pore water pressure at the base

Using the constructed charts, a value for the parameter C_v/ rH_o corresponding to the ratio F can be obtained. From this parameter, the consolidation ratio at both ends of the specimen can be found from the other charts and both coefficient of consolidation and the effective stress-void ratio relationship are obtained. Two major restrictive assumptions are made in the Umehara and Zen analysis. They are the coefficient of consolidation and the compression index which are assumed to be constant throughout the test.

The consequence of these two assumptions is that the analysis yields two distinct curves for the effective stress void ratio relation. One curve is obtained from data concerning one end of the specimen and the second from the other end. The authors have noticed this discrepancy and claim that this is a consequence of the inaccuracy of the transducers for load and pore-pressure measurement. It can be shown that the suggested analysis would yield a unique void ratio-effective stress relation if the two assumptions were fulfilled.

ii) K. Lee's method

The method proposed by K. Lee (1981) starts with the governing equation written with the porosity n as the dependent variable [18]:

$$\frac{\partial n}{\partial t} = \left(\frac{\partial}{\partial \xi}\right)\left[c_v \left(\frac{\partial n}{\partial \xi}\right)\right] \tag{2.32}$$

where **ξ** is a convective coordinate system, and therefore its domain is variable with time. This formulation includes some unnecessary difficulties in solving the problem because of the variable domain. Solution for the above equation with the appropriate boundary condition is obtained numerically by assuming the coefficient of consolidation to be constant throughout the test. A dimensionless parameter β (normalized deformation rate) is defined as,

$$\beta = \frac{rH_o^2}{c_v} \tag{2.33}$$

and solutions for different values of β are obtained. It is observed that for small values of β (less than 0.1), the finite strain solution is closely approximated by the infinitesimal strain solution.

Based on this finding, a test analysis procedure, which closely follows the Wissa et al is suggested. The procedure is also divided into two parts, the steady state and the transient state.

In the transient state, the similarity between infinitesimal and finite strain theories is invoked, and therefore exactly the same analysis as suggested by Wissa et al. is recommended.

The steady state analysis represents a slight modification of the above. First, it is recognized that a true steady state does not exist during the test when the finite strain formulation is used. Therefore, some additional assumptions are needed in order to apply an analysis similar to the one proposed by Wissa et al. for the steady state condition [21]. The first assumption is that the strain distribution within the specimen can be approximated by a parabolic function. This assumption is a result of the analysis when an infinitesimal strain theory is used. After neglecting higher powers of the parameter β, a simple expression for the coefficient of consolidation is obtained,

$$c_v = \left(\frac{H^2}{2u}\right)\left(\frac{\Delta\sigma}{\Delta t}\right) \tag{2.34}$$

This expression is equivalent to Equation 2.25. The only difference is that here H represents the current height of the specimen.

The void ratio-effective stress relation can be found when the value of the coefficient of consolidation and the strains within the specimen are found.

In the discussion of the proposed analysis, Lee recognized a strong possibility that distinct curves can be found when the calculation is performed for strains and stresses at different ends of the specimen. There is no rational procedure to decide which of the curves are the best approximate to the true material behavior.

2.2.2.2 Estimation of strain rate

The process of the selecting the appropriate strain rate when conducting the constant rate of strain consolidation test is the most important procedure in order to obtain compressibility characteristic which are compatible with the oedometer test.

High CRSC strain rate will result in the rapid increase in excess pore pressure [2]. Steady state condition in CRSC test will not be achieved when the increase in pore pressure is too rapid. On the other hand when the rate is too low, there will be no significant increase in pore water pressure which will result in unreasonable high values in C_v (ASTM D-4186).

a) Liquid Limit

A standard procedure to determine the strain rate for the CRSC test based on liquid limit is given in ASTM Designation D 4186-82, "Standard Test Method for One-Dimensional Consolidation Properties of Soils using the Controlled Strain Loading"[22]. Table 2.1 shows a first estimate of the rate of strain to apply based on the liquid limit of the soil.

Table 2.1: Suggested rates of strain for CRSC test (ASTM D4186-82) [22].

Liquid limit range , %	Rate of strain, % per minute
Up to 40	0.04
40-60	0.01
60-80	0.004
80-100	0.001
100-120	0.0004
120-140	0.0001

b) Maximum allowable ratio of excess pore pressure and applied pressure (u_a/σ_v)

This is the earliest recommendation for the selection of test rate and originally proposed by Smith and Wahls [22] which suggest that the maximum excess pore water pressure should be within a certain fraction of applied pressure during the test (u_a/σ_v) . Table 2.2 shows a maximum allowable ratio recommended by many researchers:

Table 2.2: Maximum allowable ratio of excess pore pressure and applied pressure, (u_a/σ_v) [14].

References	Recommended Values of u_a/σ_v
Smith and Wahls [22]	0.5, Tested on kaolinite, calcium montmorillonite and messana clay
Wissa et al. [22]	0.05,test on artificially sedimented Boston blue clay
Sallfors [18]	0.1-0.5, tested on Bakebol clay
Gorman et al.[25]	0.3 – 0.5 , tested on Kentucky soils
Lee K et al. [18]	0.15, tested on Singapore marine clay,
ASTM [35]	0.3, to restrict the likehood of transient conditions in CRSC tests.

Table 2.2 clearly shows that the allowable ratio recommended by Smith and Wahls was the highest among the researchers. Wissa et al. [22] recommended u_a/σ_v value lowest of all the published values. Gorman et al. [25] suggested that an approximate minimum value of 7kPa excess pore pressure must develop at the bottom of the sample to get more actual coefficient of consolidation value.

c) Dimensionless normalized strain rate, β

Lee [23] recommended a new method of interpreting test results for Singapore marine clay. He developed the moving boundary theory for the finite strain consolidation under step loading.

The dimensionless parameter β is introduced which is defined as,

$$\beta = \frac{rh_o^2}{c_v} \tag{2.36}$$

Where: r = strain rate

C_v = coefficient of consolidation

h_o = initial thickness of the specimen

The estimation of the strain rate from the normalized strain rate β requires an estimation of coefficient of consolidation, C_v before starting the CRSC test. Lee suggested the maximum input value of β to be 0.1 but did not suggest the minimum value.

2.2.3 Previous studies of comparison between CIL and CRSC test

2.2.3.1 Gorman et al. [25]

14 CRSC and 22 CIL tests were conducted by Gorman et al. [25] .The tests were conducted on samples from three sites, and the results of CRSC tests were compared with those obtained from conventional oedometer tests. From these test results, Gorman et al. concluded that an agreement among CRSC and CIL stress-strain curves at one of the site (H-3, S-7) was very good.

The CRSC test gave slightly lower values of CR and Pc than did the CIL test. The CRSC compression ratio is 0.308 which is smaller than that of CIL, 0.381. They accomplished estimation of σ'_p from CRSC data by noting the value of σ_v at which pore pressure tends to increase. The CIL test give σ'_p, 250 kPa, which was larger than CRSC test, 226kPa.

With regard to the estimation of C_v, they notified that at pressures below σ'_p very little or no pore pressure is generated. Therefore the estimated C_v values are erratic and too high, but tend to show some convergence above σ'_p

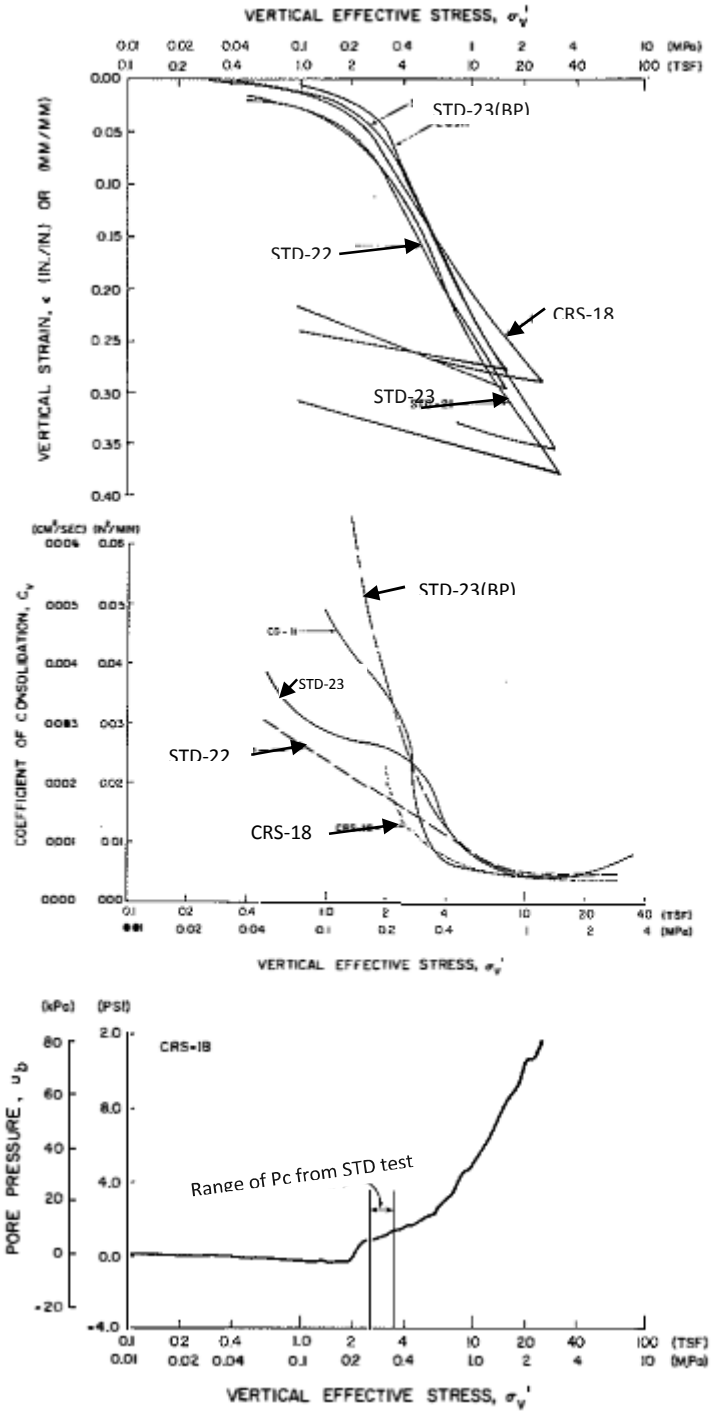

Fig.2.13: Comparison of CIL, and CRSC test results according to [25].

2.2.3.2 Seah and Juirnarongrit [27]

[27] used Bangkok clay as the testing material for constant rate of strain consolidation (CRSC) tests at different strain rates and conventional oedometer tests (CIL). The CRSC consolidation tests were performed with four different strain rates ranging from $0.3*10^{-6}$/s to $5*10^{-6}$/s. The conventional oedometer tests were conducted as reference tests for comparison with the results of CRSC tests. From results of tests, they indicated compression curves of tests are shift to the right with increasing strain rate. So pre-consolidation pressure, σ'_p increases with increasing strain rate. The CRSC with small strain rate ($0.3*10^{-6}$/s) curves are in close agreement with oedometer tests (CIL).

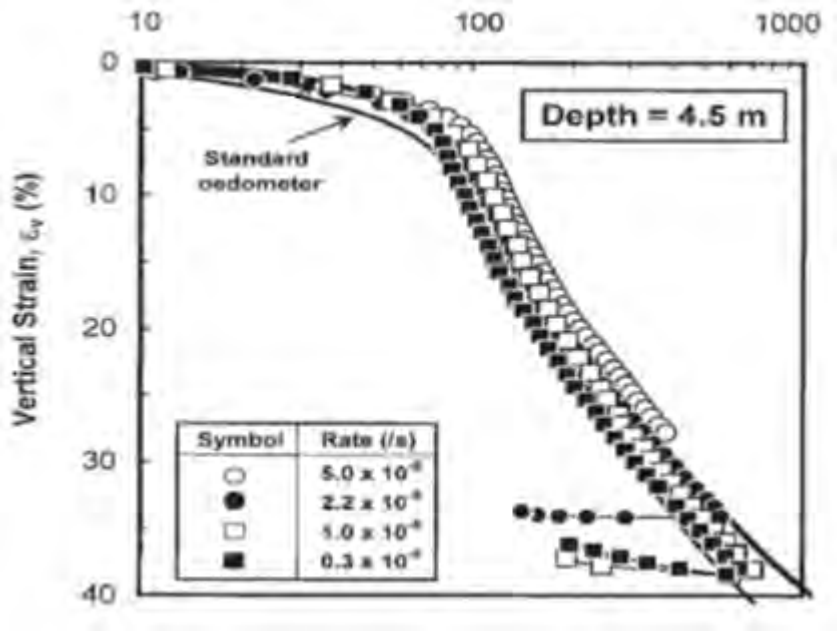

Fig. 2.14: Compression curves for different rates of strain [27].

Seah and Juirnarongrit presented the relationship of coefficient of consolidation (C_v) versus effective vertical stress conducted at different strain rates, showed that the C_v values in the over-consolidated range are much higher than those in the normally consolidated range. An abrupt change occurred close to the pre-consolidation pressure.

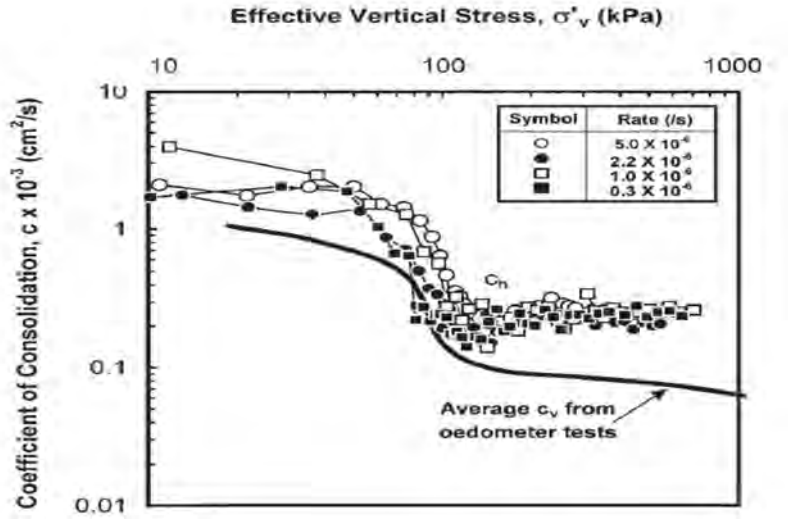

Fig. 2.15: Relationship between coefficient of consolidation and effective vertical stress [27]

2.4.3 Chai et al. [29]

[29] presented the results of conventional incremental loading (CIL) consolidation tests and constant rate of strain consolidation (CRSC) tests for the undisturbed soil samples from 5 boreholes of Ariake clay in Saga, Japan.

They concluded that the result of CRSC test is more non-linear than that of CIL test, and considering the C_c value just after yielding stress (σ'_p), CRSC test resulted in a larger C_c value than that of CIL test (Fig.2.17). Also comparing the σ'_p values from CIL tests and CRSC tests, it is suggested that the σ'_p values of CRSC tests with a strain-rate of 0.02%/min are comparable with that of CIL tests, and practically they can be judged as similar.

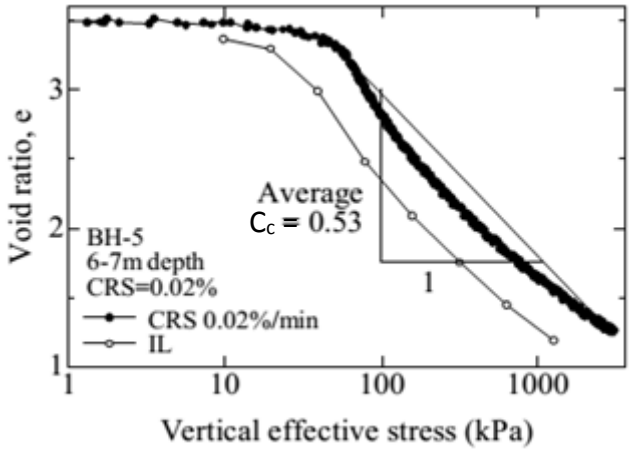

Fig. 2.16: e – log σ'_v curve [29].

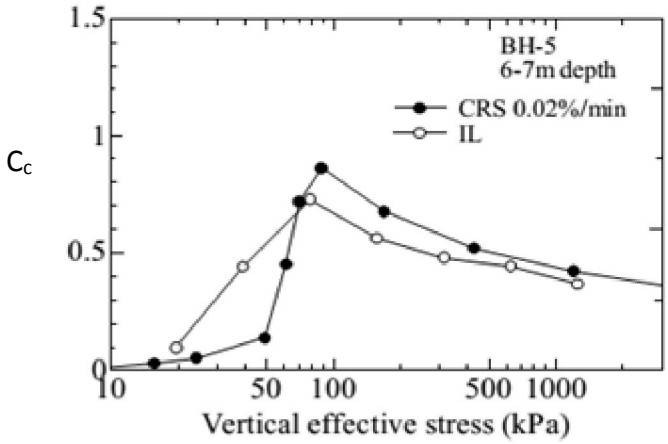

Fig. 2.17: C_c - σ'_v relationship [29].

Chai et al. [29] determined C_v values from CIL tests by $\sqrt{t}$ method (t is time). They saw that at low consolidation stress range CRSC tests yielded higher C_v values and after that the C_v values are similar (Fig.2.18).

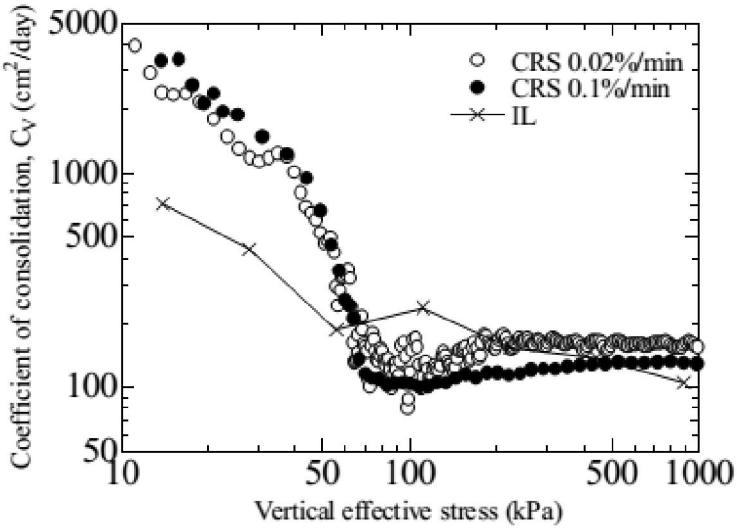

Fig. 2.18: Variation of C_v with σ'_v [29].

2.2.3.4 **Rui Jia** [18]

Rui Jia conducted 114 Constant rate of strain consolidation tests and 15 incremental loading consolidation tests for undisturbed Ariake clay samples from three boreholes in the Saga Plain, Kyushu, Japan, to systematically investigate the strain-rate effect on the consolidation behavior of Ariake clay.

Comparing the σ'_p values from CIL and CRSC tests, he suggested that the σ'_p values from CRSC tests with a strain rate of 0.02% / min are comparable to those from CIL tests.

In the e – log σ_v' plot, the compression curve from the CRSC test is more non -linear than that from the CIL test, and the largest difference in the C_c value from the CRSC and CIL tests occurred around the value of σ'_p .

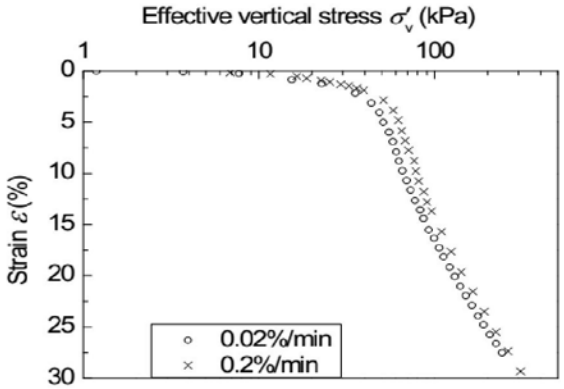

Fig. 2.19: Stress-strain rate relation [18].

Coefficient of consolidation, C_v for the Ariake clay obtained using of CRSC tests with a strain rate of 0.02% / min are comparable with those of CIL tests.

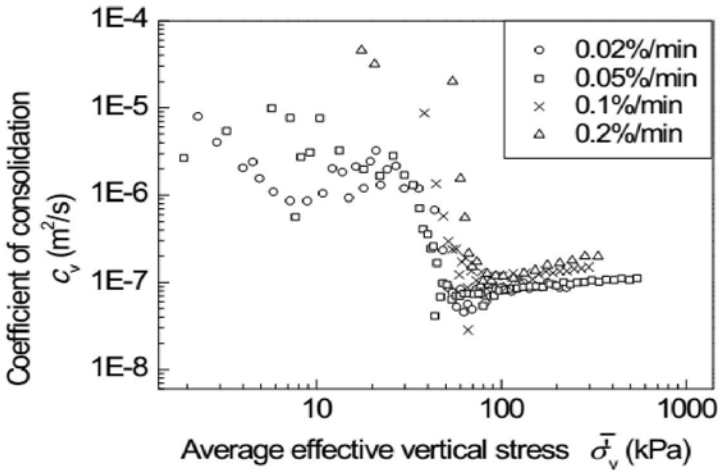

Fig. 2.20: C_v-stress-strain rate relation [18].

2.2.3.5 **Kassim et al.** [32]

Kassim et al. [32] collected four different types of soil samples from southern part of West Malaysia. Their study were conducted on typical tropical soil. In total, 12 CRSC tests had been conducted for four samples of soil. They applied three different intensities of pre-consolidation for the preparation of sample. Also two tests of conventional oedometer test (CIL) were conducted on each sample to get confidence on their work.

The average coefficient of consolidation pressure, C_v from conventional oedometer test were used to estimate the strain rate before the CRS test.

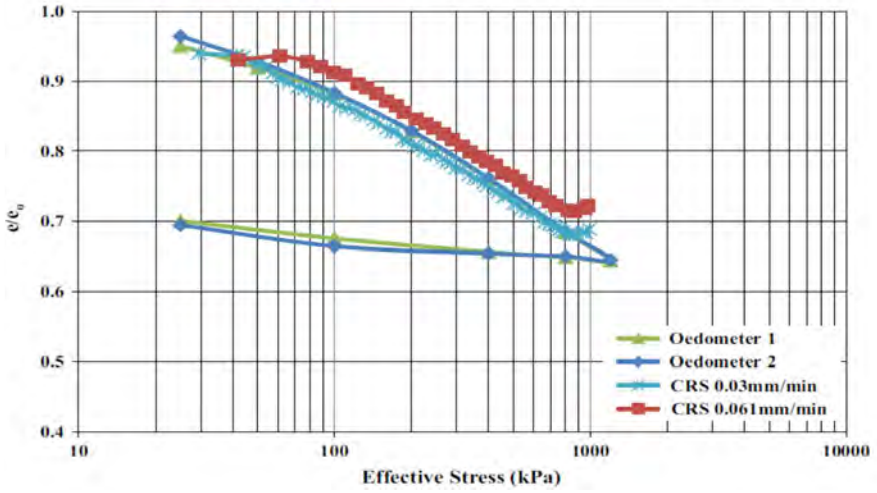

Fig 2.21: e/e_o versus effective stress relationship [32].

Undrained and drained coefficient of consolidation values were derived from the top and bottom of the soil sample in the CRSC test. The steady state condition is achieved when the C_v values from drained and undrained face of CRSC converged with the Cv from Oedometer test. Kassim et al. concluded that the tested samples had produced compatible results with those conducted with Oedometer (Fig.2.22). Both CRSC curves (drained and undrained) indicated that the steady state condition has been achieved. In comparison, slower strain rate, 0.0125 mm/min produce somewhat better CRSC test results.

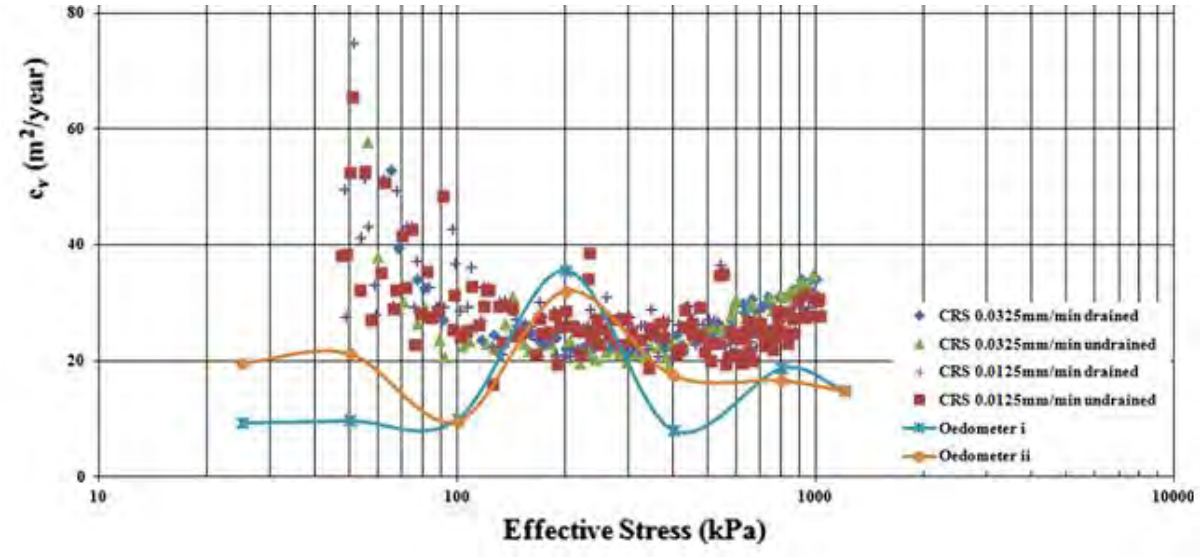

Fig. 2.22: Comparison of the relationship of C_v and effective stress [32].

2.3 Consolidation properties of Addis Ababa red clay

It was shown that the predominant mineral of Addis Ababa red clay is kaolinite and halloysite [7]. Studies on the general characteristics of Addis Ababa red clays have been carried out to date by many researchers. The geotechnical properties of Addis Ababa red clay have been reported by [7] and other researchers. The laboratory measured soil compressibility and compression characteristics are investigated by different researchers.

The following Tables (Table 2.3 --2.5) show consolidation properties of Addis Ababa red clay according to researchers.

Table2.3 Consolidation properties of undisturbed red clay of Addis Ababa [7].

No.	Location	Depth(m)	C_V(avg.)(10^{-4} cm^2/sec)	C_C	σ'_p
1	Kolfe	3.0	19.630	0.136	200
2	Semen -mazegaja	1.5	17.665	0.146	180
3	Rufa'el	1.5	18.975	0.153	215

Table 2.4 Consolidation properties of red clay of Addis Ababa [33].

No.	Location	Depth (m)	C_V(avg.) (m^2/sec)		C_C		σ'_p	
			UND.	REM.	UND.	REM.	UND.	REM.
1	Kolfe Pit -1	2.5	46.0183	25.2183	0.147	0.175	320	220
2	Kolfe Pit- 2	2.5	46.300	23.370	0.196	0.240	380	180
3	Addisu Gebeya Pit- 1	2.5	46.3567	16.993	0.152	0.204	380	140
4	Addisu Gebeya Pit -2	2.5	40.7983	16.725	0.178	0.236	280	100

where UND. = Undisturbed Soil Sample

REM. = Remolded Soil Sample

Table 2.5 Consolidation properties of Remolded red clay of Addis Ababa [34].

No.	Location	Depth(m)	C_C	σ'_p (kpa)
1	Kolfe Pit -1	1.5	0.199	
2	Kolfe Pit- 2	3.0	0.186	75
3	Addisu Gebeya Pit- 1	1.5	0.199	
4	Addisu Gebeya Pit -2	3.0	0.191	60
5	Atena tera Pit-1	1.5	0.203	
6	Atena tera Pit-2	3.0	0.227	260
7	Athari Pit-1	1.5	0.209	
8	Athari Pit-2	3.0	0.225	70
9	Awelya pit -1	1.5	0.176	
10	Awelya pit -2	3.0	0.180	100
11	Shegole Pit-1	1.5	0.209	
12	Shegole Pit-2	3.0	0.180	160

All researchers used conventional incremental load (CIL) consolidation test to describe the consolidation properties of Addis Ababa red clay, which is common test in our country.

CHAPTER 3

LABORATORY TEST RESULTS

3.1 Introduction

This chapter gives the relevant details of the experimental investigations carried out in this study. All laboratory test procedures are based on the manual of soil laboratory testing in accordance with the American Standard Testing Methods (ASTM) [35].The soil samples, test equipment, test methods and the result interpretation are described for each kind of test.

3.2 Index property tests

The purpose of index property tests are to separate groups of soils with different behavior. Index property tests are conducted at the early stage of the research to get the properties of the soil samples, which are described in Table 3.1. These tests include sieve and hydrometer analysis, Atterberg limit, and specific gravity test.

Table 3.1. Sample description

Soil Sample Area	**Soil Type**	**Sample taken at Depth (m)**	**Sample Designation**
Kolfe	Red Clay	1.5	**K-1**
		3.0	**K-2**
Addisu- Gebeya	Red clay	1.5	**AG-1**
		3.0	**AG-2**
Rufa'el	Red Clay	1.5	**R-1**
		3.0	**R-2**

3.2.1 Particle size distribution

The particle size distribution of all soil samples was determined by wet sieving and hydrometer test. The tests are conducted in accordance with ASTM D422-98 [35]. The combined particle size distributions are plotted for a complete particle size curve (Fig.3.1). The details are given in the Laboratory report of Appendix D.

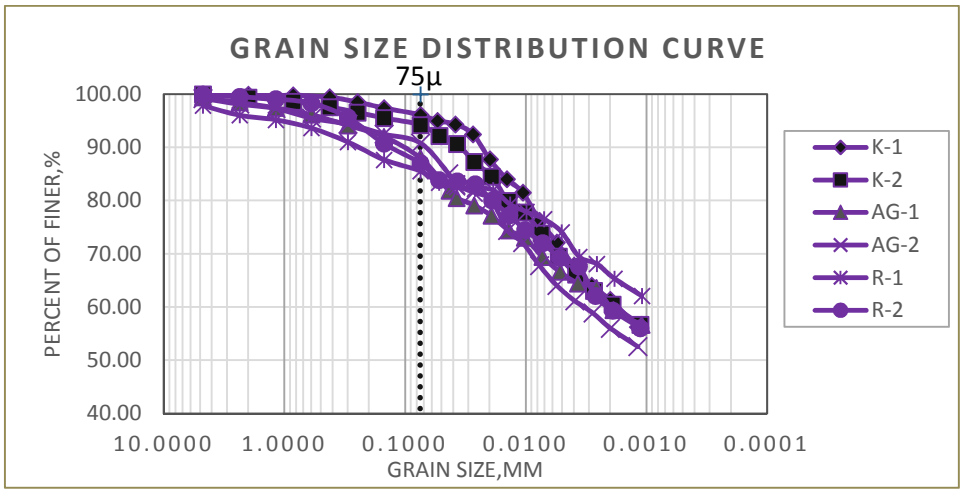

Fig. 3.1: Particle size curve for all soil sample

It can be observed from Fig.3.1 that the percentage passing 75µm for all soil samples ranges from 85% to 96%. **K-1** has the highest percentage of fines followed by **K-2**, whereas **R-1** has the smallest percentage of fines.

Table 3.2 percentage of the clay, silt and sand fractions for the soil samples tested.

Soil type	Soil sample type percentage (%)					
	K-1	**K-2**	**AG-1**	**AG-2**	**R-1**	**R-2**
Clay (<0.002mm)	61.37	60.79	60.07	56.04	65.78	59.68
Silt (0.002-0.075mm)	34.77	33.45	27.96	34.82	19.80	27.39
Sand (0.075-2mm)	3.78	5.16	10.44	7.30	10.48	12.46

The physical properties of fine-grained soils are dictated to a great extent by the types and amounts of clay fraction present in them.

Over 50 % of the material tested consists of clay fraction in all samples. So tested soil samples are identified as clay soil. **R-1** soil has the highest clay fraction compared to other soils. The curves do not extend beyond 0.001 mm, since according to ASTM procedure for hydrometer analysis terminate at 24 hrs.

3.2.2 Atterberg limits

The Atterberg limits test (plastic limit and liquid limit test) were performed in accordance with ASTM D4318-98 [35]. Dry soils passing through 425 μm sieve were used for this purpose.

Results of the liquid limit and plastic limit tests for three types of soil sample are shown in Table 3.3 while the complete data analyses for both tests are provided in Appendix C. The plasticity index (PI) of the soil samples ranges from 31 to 49 with the K-2 soil showing the highest PI and R-1 the lowest. AG-2 soil has the highest Plastic Limit (PL), and K-2 soil has the highest liquid limit. Liquid limit (LL) of soil sample increases as depth of tested soil increases.

Table 3.3: Atterberg limit for the soil sample

Atterberg Limits	Soil Sample Type					
	K-1	**K-2**	**AG-1**	**AG-2**	**R-1**	**R-2**
Liquid Limit (%)	60	73	63	67	60	71
Plastic Limit (%)	25	24	32	32	29	30
Plastic Index (%)	35	49	35	35	31	41

3.2.3 Specific Gravity

Small pycnometer were used to obtain the specific gravity (Gs) of the samples. The test was conducted in accordance with ASTM D854-98 [35].

Table 3.4 shows the result of the specific gravity for the three types of soil Samples. AG-1 soil has the highest specific gravity compared the other type of soil specimens with 2.75. Detail calculations of the specific gravity test are shown in the Lab report of Appendix B.

Table 3.4: Specific gravity for the soil sample

	Soil Sample Type					
	K-1	**K-2**	**AG-1**	**AG-2**	**R-1**	**R-2**
Specific Gravity, G_S	2.60	2.74	2.75	2.72	2.69	2.71

3.2.4 Soil classification

Classification of the soil samples is based on the ASTM D-2487 (Unified soil classification system) [35]. From the plasticity chart in Fig.3.2, all soils are classified as clay of high plasticity (CH). Table 3.5 shows the classification of the three types of soils used in this research.

Table 3.5: Soil sample classification

Soil Sample type	**Soil Classification**
Kolfe (K-1 and K-2)	Inorganic Clays of high plasticity (**CH**)
Addisu-Gebeya (AG-1 and AG-2)	Inorganic Clays of high plasticity(**CH**)
Rufa'el (R-1 and R-2)	Inorganic Clays of high plasticity(**CH**)

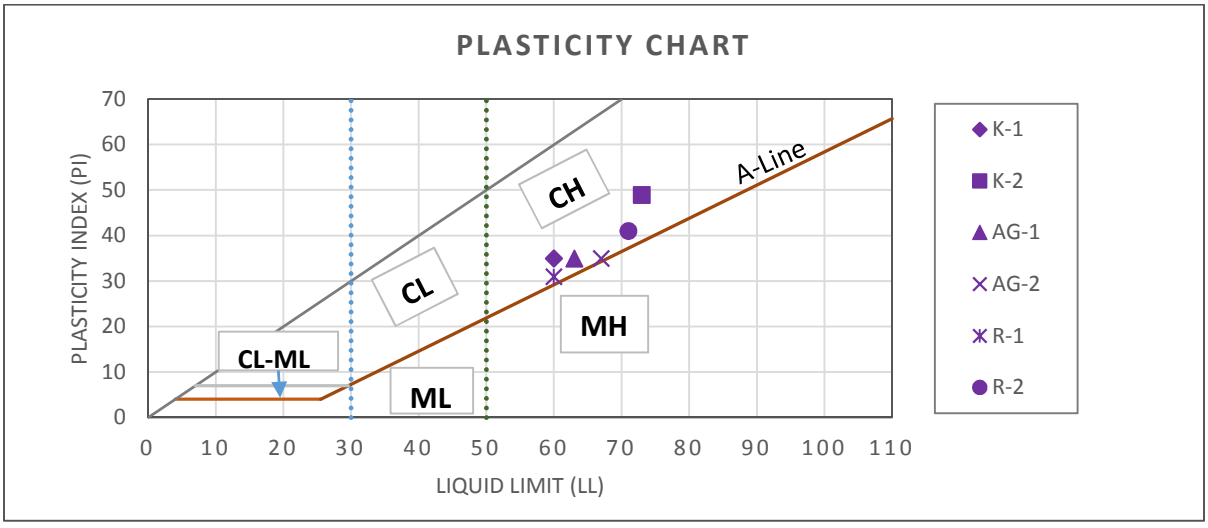

Fig. 3.2: Plasticity chart for soil classification

3.3 One-Dimensional Consolidation Tests

3.3.1 Sample preparation

Undisturbed soil samples were collected from Kolfe, Addisu Gebeya and Rufa'el, which are located in the western and northern part of Addis Ababa. Undisturbed samples were taken using hydraulic Jack to minimize the disturbance of the sample as much as possible. After sample tubes were transported to the laboratory, soil samples were taken from them.

After the soil is ready, the consolidation ring was pushed inside the sampler to extract the soil sample. The sample contained in the consolidation ring are treamed to size on both sides as shown in Fig. 3.3. The consolidation ring used for the CIL test is 50mm in diameter and 20mm in thickness and that for CRSC test is 63.5mm in diameter and 25.4mm thickness. The sample contained in the consolidation ring was then used for CIL Test and Constant rate of strain Consolidation Test (CRSC Test).

a) Sample mount for CIL b) Sample mount for CRSC

Fig. 3.3: Sample mount for CIL and CRSC tests

3.3.2 Conventional Incremental Loading (CIL) Test

The conventional consolidation tests are used to explore the consolidation behavior of Addis Ababa red clay, since it is the most popular method. Six CIL tests are carried out for three red clay soil samples representing different areas.

The soil sample contained in the consolidation ring was placed in a consolidometer. Two porous stones are placed on both top and bottom faces of the sample in the ring to make water freely access to both faces of the soil specimen as shown in Fig.3.4.

The compressive load is applied to the specimen by means of a system of levers. The compression is measured manually. The soil sample is kept submerged in water during the test. Loads are applied in steps in such a way that the successive load intensity, p, is twice the preceding one. The load intensities commonly used are 25, 50, 100, 200, 400,800 and 1600 kPa. Unloading stage sequences are 800kPa, 400kPa, 200kPa, 100kPa and 50kPa. Each load is allowed to stand until compression has practically ceased (i.e. for 24 hours).

Dial readings are taken at elapsed times of 1/10, 1/4, 1/2, 1, 2, 4, 8, 15, 30, 60, 120,240 and 1440 minutes from the time the new increment of load is put on the sample.

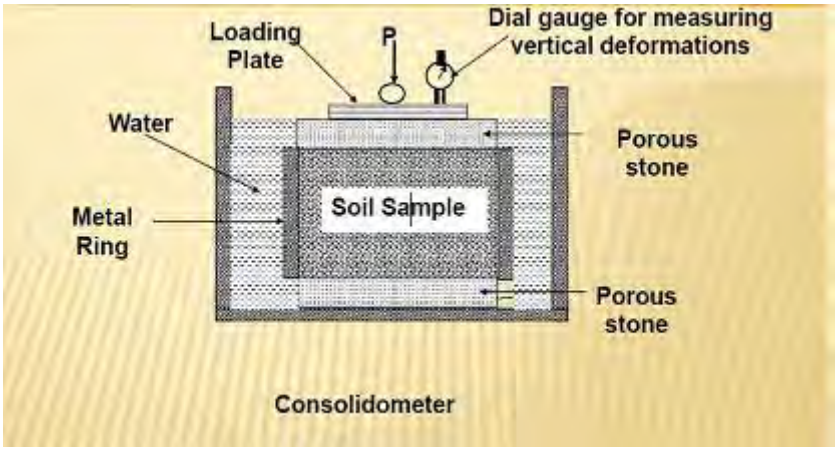

Fig. 3.4: One Dimensional Consolidometer [9].

3.3.2.1 Data analysis of CIL test

The test schedule for the CIL test are given in Table 3.6.

Table. 3.6 CIL test schedule

Soil Sample Area	Depth(m)	Soil Designation	Soil Type	CIL Tests
Kolfe	1.5	**K-1**	Red Clay	√
	3.0	**K-2**	Red Clay	√
Addisu Gebeya	2.0	**AG-1**	Red Clay	√
	3.0	**AG-2**	Red Clay	√
Rufa'el	1.5	**R-1**	Red Clay	√
	3.0	**R-2**	Red Clay	√
Total No. of Tests				**6**

A graph relating the void ratio at the end of each loading stage with the effective pressure on logarithmic scale was plotted for a complete set of consolidation test data.

The e–log σ'_v curve is used to obtain compression indices, C_c and thus the coefficient of axial compressibility, a_v. e–log σ'_v is also used to obtain the coefficient of volume compressibility, m_v. The pre-consolidation pressure can also be determined by the Cassagrande method from this curve [9]. The compression - time curve is used to obtain the coefficient of consolidation, C_v for the CIL test as outlined in Section 2.2.1.1. Of the two methods, the root time method proposed by Taylor and the log time method proposed by Casagrande that can be used to calculate C_v [9], the root time method is employed for this study.

The output of the CIL test is presented in terms of compression indexes, C_c, pre-consolidation pressure, σ'_p, and coefficient of consolidation, C_v.

3.3.2.2 CIL test results

a) Void ratio versus effective stress

Figs. 3.5 (a)-(c) show the void ratio versus effective stress plot for soil sample obtained from Kolfe, Addisu-Gebeya and Rufa'el. The details for the oedometer (CIL) tests and their determination are shown in the Lab report of Appendix E. Table 3.7 shows the compression index and pre-consolidation pressure values. The compression index values for the K-2 soil is the highest, while the corresponding pre-consolidation pressure is the lowest one. K-1 soil sample has highest pre-consolidation pressure.

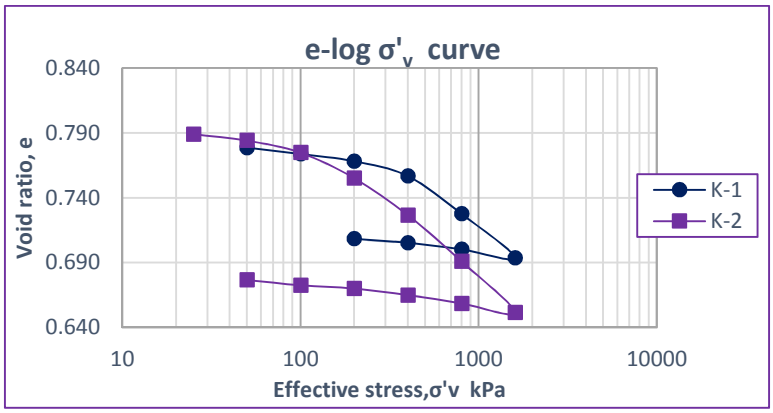

Fig.3.5 (a) Void ratio vs Effective pressure curve for Kolfe.

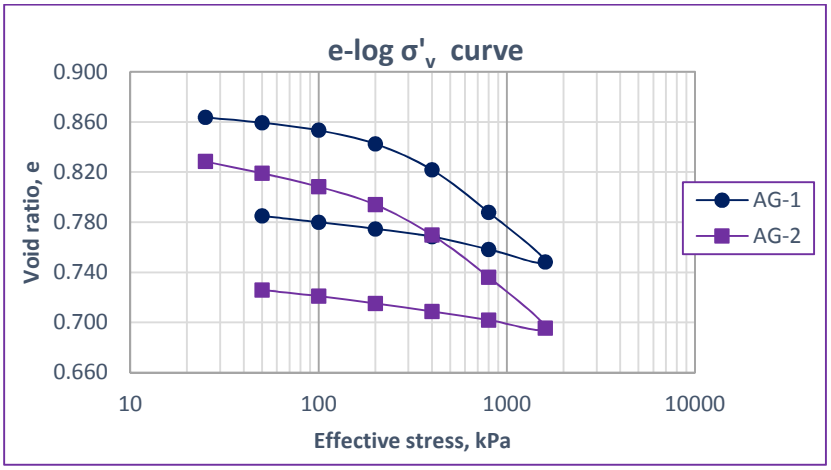

Fig.3.5 (b) Void ratio vs Effective pressure curve for Addisu- Gebeya.

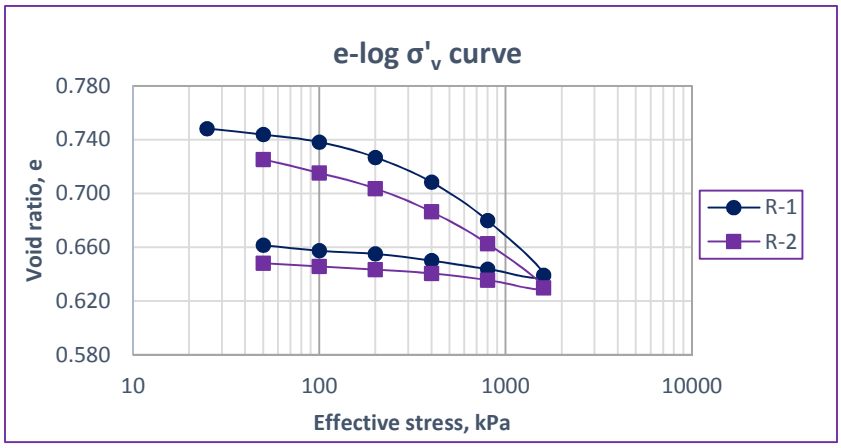

Fig.3.5 (c) Void ratio vs Effective pressure curve for Rufa'el.

Table 3.7 Consolidation properties from CIL tests.

Soil Sample	Compression index ,C_c			C_s	C_s/C_c	Pre-consolidation pressure σ'_p ,(kPa)
	From e - log σ'_v plot graph	From Empirical formula				
		Terzaghi and peck	Nagaraj and Murthy			
K-1	0.105	0.450	0.366	0.020	0.186	360
K-2	0.125	0.567	0.469	0.022	0.179	198
AG-1	0.122	0.477	0.406	0.034	0.276	300
AG-2	0.123	0.513	0.427	0.022	0.180	290
R-1	0.124	0.450	0.378	0.018	0.143	300
R-2	0.103	0.549	0.451	0.017	0.168	320

From the Table 3.7 it can be noticed that the range of C_C values calculated from e-log σ'_v curve is smaller as compared to C_C values calculated by using empirical formula.

b) Coefficient of Consolidation versus Effective Stress

Beside the compression index, the coefficient of consolidation (C_v) of soil for each effective pressure stage is also calculated from CIL test.The coefficient of consolidation versus effective stress plot obtained for the three soil sample are presented as shown in Figs.3.6 (a)-(c).

The calculation of the coefficient of consolidation values for CIL consolidation tests are provided in the Lab. report of Appendix E. Rufa'el soil samples have the lowest C_v value among the other type of soil samples.

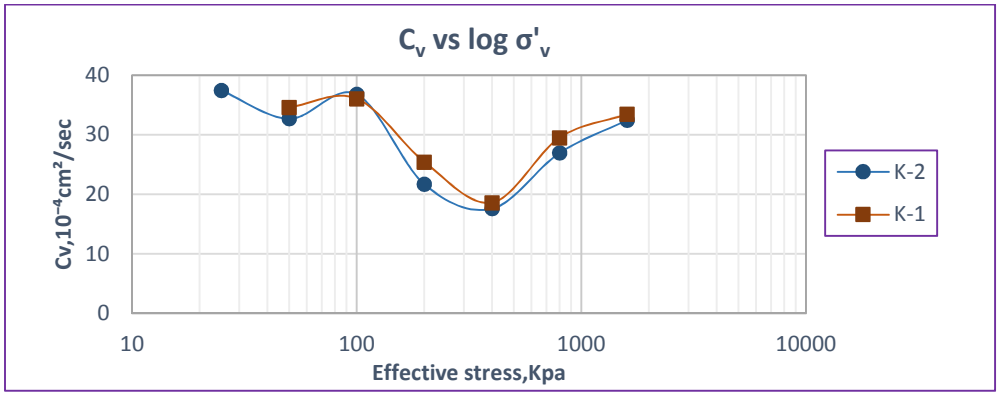

Fig.3.6 (a) Coefficient of Consolidation (C_v) for Kolfe soil samples

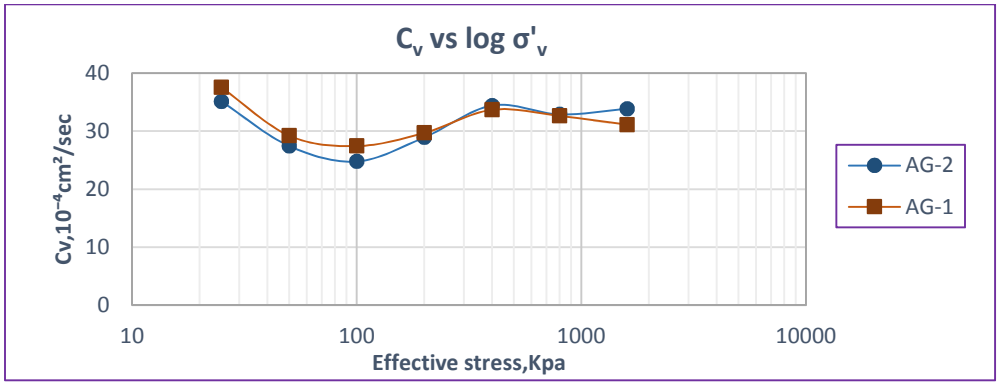

Fig.3.6 (b) Coefficient of Consolidation (C_v) for Addisu Gebeya soil samples

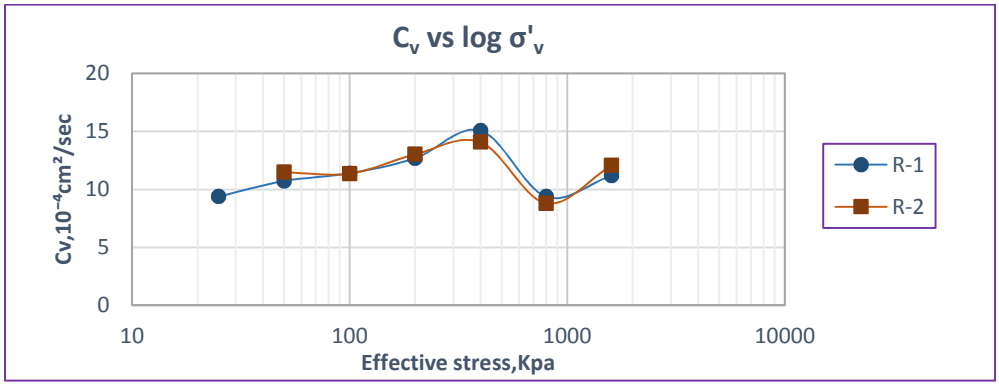

Fig.3.6 (c) Coefficient of Consolidation (C_v) for Rufa'el soil samples.

3.3.3 Constant Rate of Strain Consolidation (CRSC) Test

Six Constant Rate of Strain Consolidation (CRSC) Test were carried out for three red clay soil from different areas of Addis Ababa.

CRSC Cell

The CRS consolidation cell is used to attempt to achieve a constant rate of strain by using a mechanical compression machine capable of carrying out the test with a very low velocity on the soil sample. In all cases, drainages were allowed at the top of the specimens (drained surface), while the pore water pressure was measured at the base (undrained surface) [17].

The equipment itself is very similar to a triaxial chamber, properly modified to keep a soil specimen laterally constrained in a steel ring without the possibility of radial strain. Inside the cell, two independent chambers are created, separated by a special rubber membrane so that two different water pressures can be applied [36]:

a) The outer chamber for cell pressure;

b) The inner chamber where the sample is placed and backpressure can be applied for saturation and accurate measurement of pore pressure.

Fig.3.7: CRS consolidation cell [36].

3.3.3.1 CRSC Test Setup

The CRS consolidation testing apparatus includes the axial loading frame, axial loading device (load cell), pore water transducer, deformation indicator (LVDT) and CRS consolidation cell.

Fig.3.8: Linear Variable Displacement Trasducer (LVDT)

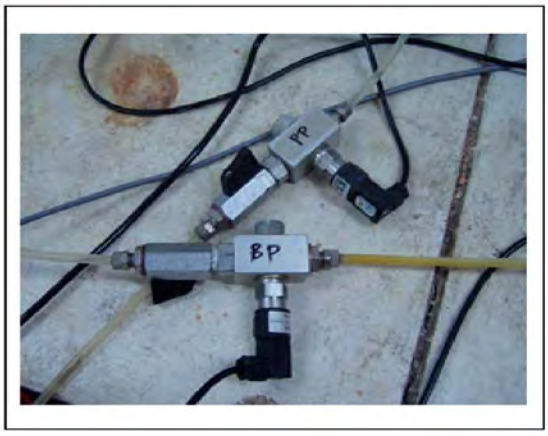

Fig.3.9: Pressure Transducer

Fig.3.10: Load Cell

The loading frame with multi speed drive unit is the main loading machine used in the CRSC test. It can provide constant motor drive speed ranging from 0.0001 to 9.0 mm/min.

Three types of measuring devices were used in the CRS test for data measurement. These measuring devices are the linear variable displacement transducer (LVDT), pressure transducer and the load cell. A 10 mm LVDT with an accuracy of 0.001 mm is used to measure vertical displacement of the soil sample in the CRS test. Fig.3.8 shows the 10 mm LVDT.

This LVDT is attached to the loading piston during the CRSC test. 2000 kPa pressure transducers with an accuracy of 0.1 kPa as shown in Fig. 3.9 were used to measure back pressure and pore pressure from the top and the bottom of the specimen. All connecting to pore pressure and back pressure must be saturated to ensure accurate readings of pressures [36].

A 50kN capacity load cell was used for load measurement on the 63.5 mm diameter soil specimen. The load cell was attached between the loading frame and the load piston that transfer the load to the load platen and subsequently to the soil sample. The load cell can give to the nearest 0.001 kN. Fig. 3.10 shows the load cell.

A Data acquisition unit (ADU) is used to read and store the measured data systematically. The ADU used for the CRSC test is **GEODATALOG series 6000** with 16 channel PC unit [37]. Load cell, pressure transducer and LVDT are attached to the ADU when the CRSC test are running. All the back pressure, pore pressure, load and the displacement are read and stored by the personal computer.

DATACOMM is the software that used to control the testing data saving progress for all the data collected from the ADU [37]. Fig. 3.11 and 3.12 below show the Data Acquisition Unit (ADU) and the main page for the DATACOMM software.

Fig.3.11: GEODATALOG series 6000 Data Acquisition Unit (ADU) [37].

Fig.3.12: Main Page of the DATACOMM software for Collecting Data System

3.3.3.2 Saturation of the CRSC Soil Specimen

It is essential to saturate the CRSC soil sample before starting the test to ensure the accuracy of measurement of the pressures. The trimmed sample is placed on the base of the cell and the perforated platen placed on the top of the porous stone to transmit the load from the piston to the sample. After the cell chamber and the cell top are tightly fitted, screws and nuts are used to secure the cell chamber and cell top to the base [36].

The cell was placed on the loading frame machine and apply a cell pressure of about 220 kPa and a back pressure of 200 kPa (at least 20 kPa less than cell pressure) [36]. Then the piston is brought into place just touching the perforated platen. A seating pressure of about 5 kPa is applied manually by adjusting the top platen of the compressing machine. At least 12 hours are required to saturate the CRSC soil specimen [25]. Fully saturated condition of the CRS specimen was reached when the pore pressure at the bottom of the cell achieved 90% of the cell pressure applied [36].

After the saturation is achieved, appropriate strain rate is selected. In this paper, strain rates as suggested by ASTM D4186-82 are used as a function of the liquid limit of the soil. The strain rates used are tabulated in Table 3.8 on the basis of the relationship between acceptable strain rate and liquid limit.

Table 3.8 Strain rate used for CRSC tests of soil sample

Soil Sample	Liquid Limit (%)	Strain rate (%/min)	Strain rate (mm/min*)
K-1	60	0.01	0.00254
K-2	73	0.004	0.00102
AG-1	63	0.004	0.00102
AG-2	67	0.004	0.00102
R-1	60	0.004	0.00102
R-2	71	0.004	0.00102

*when initial height of specimen is 25.4mm.

Then selected strain rate is entered into the control box and the tests started .The specimen is loaded up to the desired stress.

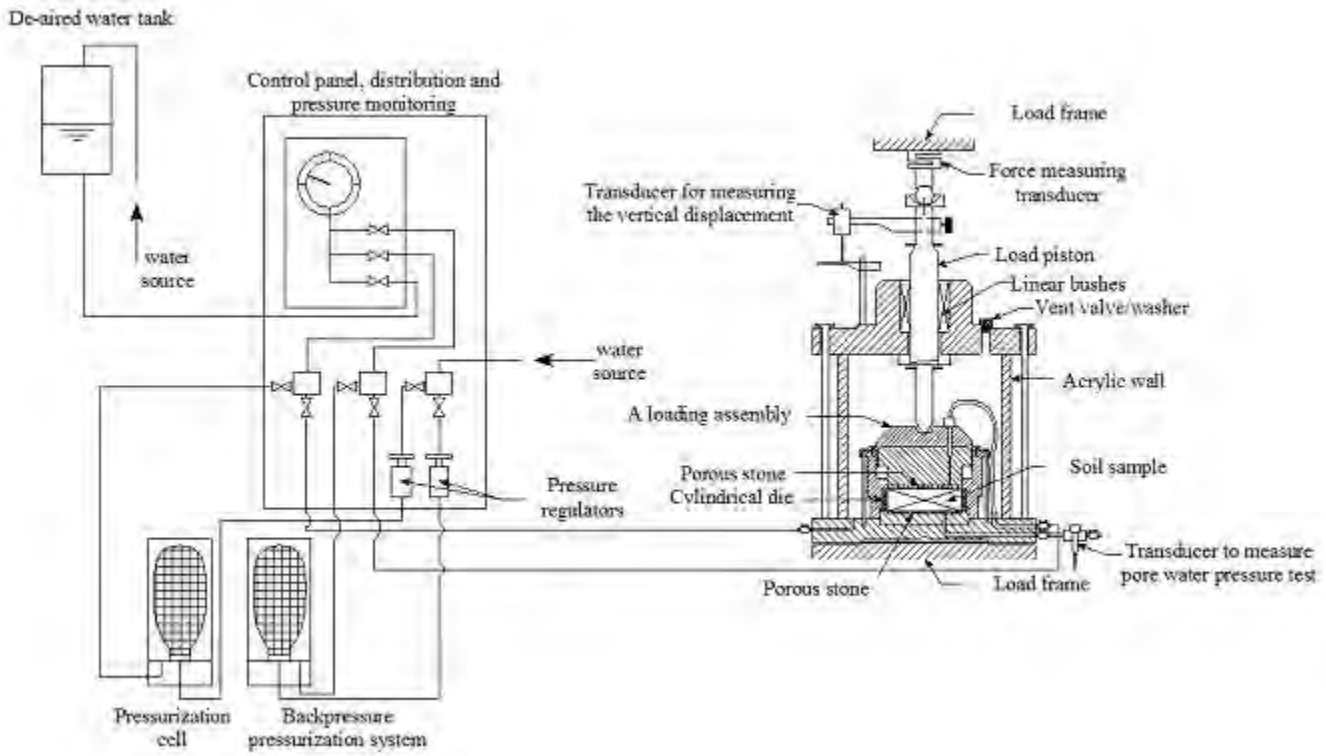

Fig. 3.13: Schematic diagram of a CRSC test [12].

The main steps of the test are summarized below:

a) Connection and filling up the system with de-aired water.

b) Saturation of the drainage lines and pore pressure de-airing block.

c) Assemble the specimen.

d) Saturation stage.

e) Consolidation stage

3.3.3.3 Interpretation of the CRSC data

An instruction manual referencing ASTM Standard D4186, is used to calculate average effective stress, coefficient of consolidation and other parameter as follow;

1) The net applied axial load, P, is the load required to cause axial deformation additional to that needed to balance the initial back pressure u_b.

The net applied axial stress on the sample during the test is

$$\sigma = P/A. \tag{3.1}$$

where σ = axial stress (kPa)

P=total vertical load applied to the specimen (kPa)

A=cross section of the specimen (cm²)

Total vertical pressure on the sample,

$$\sigma_v = \sigma + u_b \tag{3.2}$$

where σ_v= total vertical stress (kPa)

u_b= initial back pressure (kPa)

Pore pressure at drained face (u_d) during test is equal to the back pressure, $u_d = u_b$

2) Effective pressures at the top and bottom of specimen are derived from,

Top effective pressure, $\sigma_v'(top) = \sigma_v - u_b$ (3.3)

Bottom effective pressure, $\sigma_v'(bottom) = \sigma_v - u$ (3.4)

Average effective pressure according to Wissa et al. for steady state condition

$$\sigma_v' = (\sigma_v^3 - 2\sigma_v^2 u_a + \sigma_v {u_a}^2)^{1/3} \tag{3.5}$$

where u_a= excess pore pressure = $u - u_b$

u= pore water pressure at the bottom of specimen (kPa)

3) Initial void ratio can be calculated as follows from the specific gravity of particles and initial dried unit weight of specimen [36].

a) Initial and final moisture content (%)

$$w_i = \frac{P_0 - P_2}{P_2} 100 \qquad w_f = \frac{P_1 - P_2}{P_2} 100 \tag{3.6}$$

Where P_0=initial weight of wet specimen (g)

P_1= final weight of wet specimen (g)

P_2=weight of dried specimen (g)

b) Initial and final wet unit weight (g/cm^3)

$$\gamma_i = \frac{P_0}{A_0 H_0} \qquad \gamma_f = \frac{P_1}{A_0 H_f} \tag{3.7}$$

where H_0=initial height of the specimen (cm)

H_f= final height of the specimen (cm)

A_0=cross section of the specimen (cm^2)

c) Initial and final dried unit weight (g/cm^3)

$$\gamma_{di} = \frac{\gamma_i}{1+w_i} \qquad \gamma_{df} = \frac{\gamma_f}{1+w_f} \tag{3.8}$$

So, initial void ratio is expressed as

$$e_0 = \left(\frac{G_s}{\gamma_{di}}\right) - 1 \tag{3.9}$$

$$H_s = \frac{H_0}{1+e_0} \tag{3.10}$$

where H_s =height of solids

H_0 =initial height of specimen

e_0 =initial void ratio

4) Void ratio is calculated from e_0 and H_s

$$e = e_0 - \frac{H}{H_s} \tag{3.11}$$

where e= void ratio

H=current height of specimen

5) Compression index, C_c and pre-consolidation pressure, σ'_p are calculated from e-log σ'_v curve.

$$C_c = \frac{e_1 - e_2}{log\sigma'_2 - log\sigma'_1} \tag{3.12}$$

Where e_1 =void ratio at t_1

e_2 = void ratio at t_2

σ'_1 =effective stress at t_1

σ'_2 =effective stress at t_2

Casagrande graphical method is used to estimate pre-consolidation pressure, σ'_p.

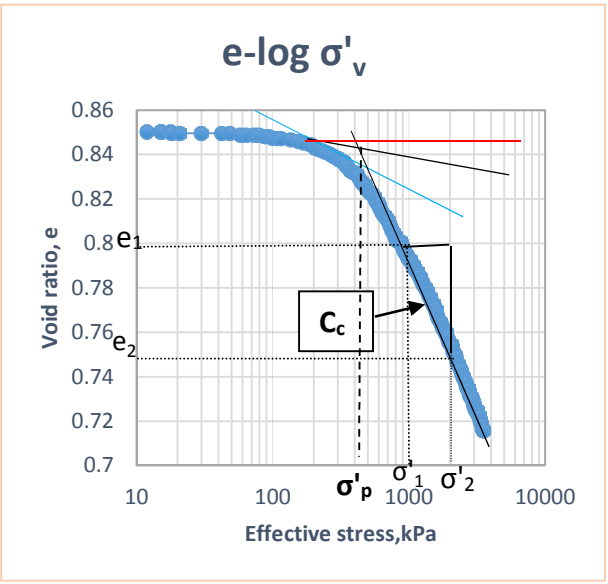

Fig. 3.14: e-log σ'_v curve from CRSC tests

6) Axial strain expressed in %

$\varepsilon = (\Delta H / Ho)\ 100$

where ΔH=settlement of the specimen

7) The coefficient of consolidation c_v can be calculated from the following expression:

At the drained face of the specimen

$$c_{vd} = \left(\frac{h^2}{2u_a}\right)\left(\frac{\sigma'_{vd}}{\Delta t}\right) \tag{3.13}$$

where h= is the current thickness of the specimen (cm)

u_a= is the excess pore pressure

$\sigma_{v\,d}'$ / Δt= the rate of change of effective stress at the drained face.

At the undrained face of the specimen

$$c_{vu} = \left(\frac{h^2}{2u_a}\right)\left(\frac{\sigma'_{vu}}{\Delta t}\right) \tag{3.14}$$

σ_{vu}' / Δt= the rate of change of effective stress at the undrained face.

8) Lee et al. (1993) suggested the rate of change of effective stress at the undrained face and at the drained face can be calculates from the "three-point formula" or "five-point formula" as follows [14]:

$$\left(\frac{\sigma'_v}{\Delta t}\right)_o = \left(\frac{1}{2\Delta t}\right)[-(\sigma'_v)_{-1} + (\sigma'_v)_{+1}] \tag{3.15}$$

$$\left(\frac{\sigma'_v}{\Delta t}\right)_o = \left(\frac{1}{2\Delta t}\right)[(\sigma'_v)_{-2} - 8(\sigma'_v)_{-1} + 8(\sigma'_v)_{+1} - (\sigma'_v)_{+2}] \tag{3.16}$$

and the expression for the first and the last few readings may be obtained by using one-sided formula as follows:

$$\left(\frac{1}{2\Delta t}\right)_o = \left(\frac{1}{2\Delta t}\right)[-3(\sigma'_v)_0 + 4(\sigma'_v)_{+1} - (\sigma'_v)_{+2}] \tag{3.17}$$

$$\left(\frac{1}{2\Delta t}\right)_o = \left(\frac{1}{2\Delta t}\right)[-25(\sigma'_v)_0 + 48(\sigma'_v)_{+1} - 36(\sigma'_v)_{+2} + 16(\sigma'_v)_{+3} - 3(\sigma'_v)_{+4}] \tag{3.18}$$

the subscripts -1, +1 and +2 refer to the readings taken immediately before and after the present reading denoted by subscript 0

9) The constrained modulus, M can be calculate as follows

$$M = \frac{\sigma'_{v2} - \sigma'_{v1}}{\varepsilon_2 - \varepsilon_1} \tag{3.19}$$

Where $(\sigma'_v)_1$ =average effective stress at t_1
$(\sigma'_v)_2$ = average effective stress at t_2

ε_1 =axial strain at t_1

ε_2 = axial strain at t_2

t = time

3.3.3.4 Data analysis of the CRSC test

In this study, constant rate of strain consolidation tests were conducted on three soil samples from different areas of Addis Ababa. The test schedule for CRSC tests is given in Table 3.9.

Table. 3.9 CRSC test programme

Soil Sample Area	Depth (m)	Soil Designation	Soil Type	Strain rate (mm/min)	CRSC Tests
Kolfe	1.5	**K-1**	Red Clay	0.00254	√
	3.0	**K-2**	Red Clay	0.00102	√
Addisu Gebeya	2.0	**AG-1**	Red Clay	0.00102	√
	3.0	**AG-2**	Red Clay	0.00102	√
Rufa'el	1.5	**R-1**	Red Clay	0.00102	√
	3.0	**R-2**	Red Clay	0.00102	√
Total no. of Tests					**6**

The CRSC test data presented herein are analyzed in accordance with the nonlinear small-strain theories and the large-strain theory [20]. Graphical plots of void ratio, coefficient of consolidation, and pore-water pressure as a function of average effective stress are obtained from each loading stage of a CRSC tests.

Coefficient of consolidation from CRSC test can be calculated by using Equations 3.13 and 3.14. As pointed out in CIL test data analysis, the output of the study is presented in terms of compression indexes, c_c, pre-consolidation pressure, σ'_p, and coefficient of consolidation, c_v. These values are required for comparison with the corresponding CIL test results.

3.3.3.5 CRSC test results

Results of the constant rate of strain consolidation tests are presented in this section in terms of void ratio curve and coefficient of consolidation (C_V) curve. Results obtained for all CRSC tests are given in the Lab. report of Appendix F.

a) Void Ratio Curve

The void ratio versus effective stress curve is an important result in consolidation test. Soil settlement with corresponding applied loading was calculated.

For this research, three different type of soil sample had been tested. For each type of sample, compression curves were produced from the testing data.

Figs.3.15 (a) –(c) shows the curves of void ratio against effective stress for all three types of soil sample from CRS tests.

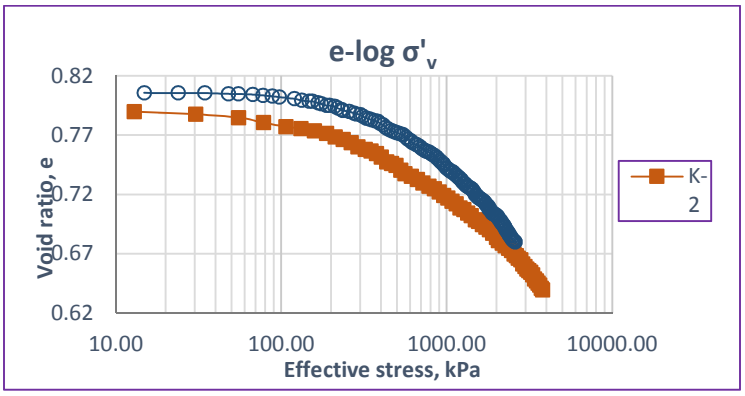

Fig. 3.15 (a) CRSC test void ratio vs effective stress curve for Kolfe

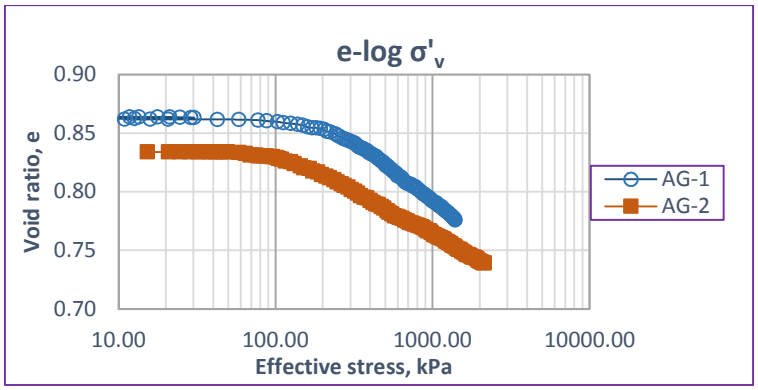

Fig. 3.15 (b) CRSC test void ratio vs effective stress curve for Addisu Gebeya

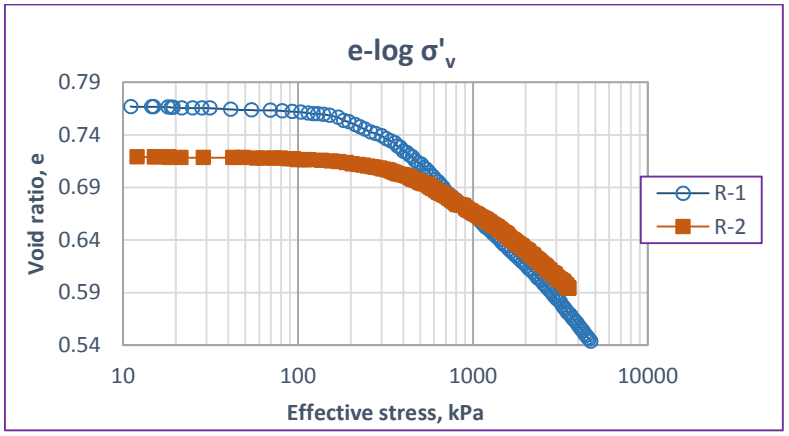

Fig. 3.15 (c) CRSC test void ratio vs effective stress curve for Rufa'el

Table 3.10 shows the compression index and pre-consolidation pressure values obtained from the void ratio curves in Figs.3.15 (a) – (c). Fig.3.16 shown that compression index values for R-1 soil sample is the highest. Compression index and pre-consolidation pressure of AG-2 is the lowest of others soil. The K-2 soil sample has the highest pre-consolidation pressure.

Table 3.10 Consolidation properties from CRSC tests

Soil Sample	Strain Rate (mm/min)	compression index C_c	Pre-consolidation pressure σ'_p ,(kPa)
K-1	0.00254	0.131	400
K-2	0.00102	0.140	420
AG-1	0.00102	0.114	230
AG-2	0.00102	0.082	170
R-1	0.00102	0.177	310
R-2	0.00102	0.127	400

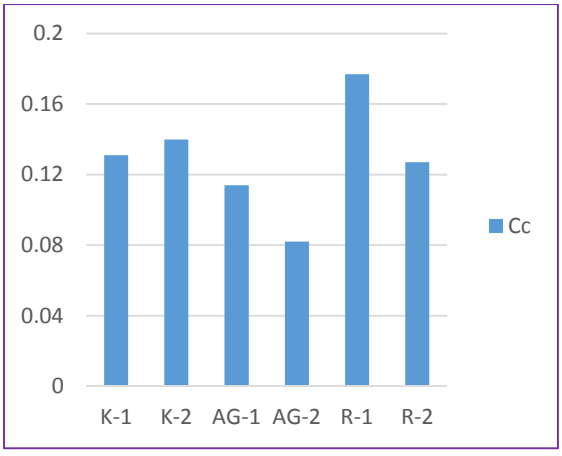

a) Compression index comparison

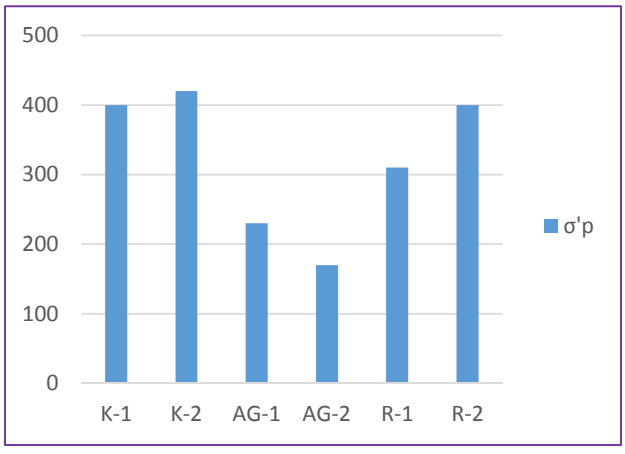

b) Preconsoidation pressure comparisson

Fig.3.16. CRSC C_c and σ'_p comparison of soil samples

b) Coefficient of Consolidation, C_V

Wissa's theory gives that the values of coefficient of consolidations, C_v as calculated from drained surface and undrained surface as shown in Equations 3.13 and 3.14. [38] proposed that a successful CRSC test would be one for C_v values obtained from the undrained and drain surface agreed, it means that the values of C_v obtained in these tests are reliable. Convergence of undrained and drained C_v values shows that constant rate of strain soil sample reach the stable condition from top to bottom of the soil sample.

Figs.3.17 – 3.19a show the coefficient of consolidation (C_v) versus vertical average effective stress ($\sigma'_{v)}$ for the CRSC tests corresponding to the undrained surface and drained surface. It is found that the values of coefficient of consolidations calculated from the drain surface and undrained surface agree very well, it means that the values of C_v obtained in these two surface are reliable. The excess pore pressure increase was much steeper for K-2, AG-2 and R-2 than K-1, AG-1 and R-1 respectively (Figs.3.17 – 3.19b).

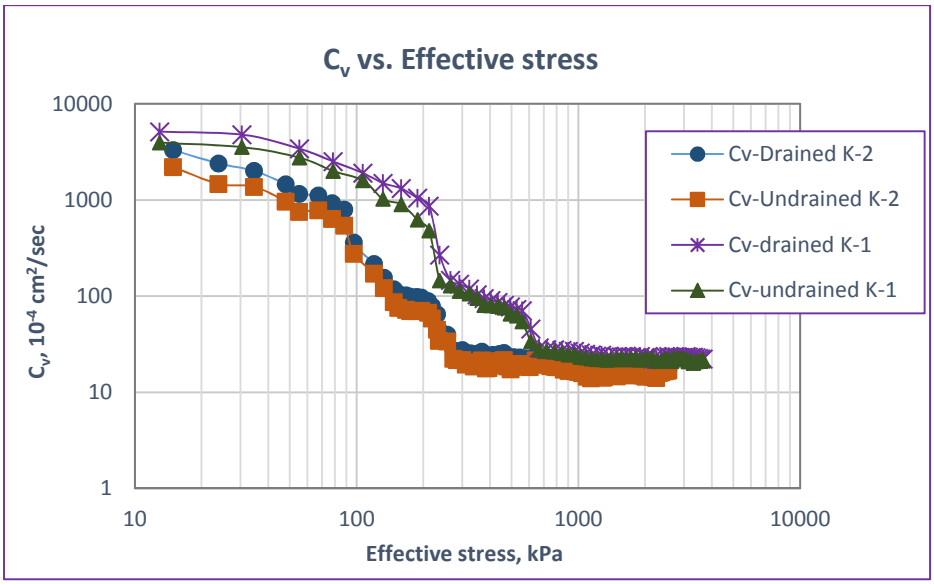

Fig. 3.17 (a) C_v -curve of CRSC test for kolfe soil sample.

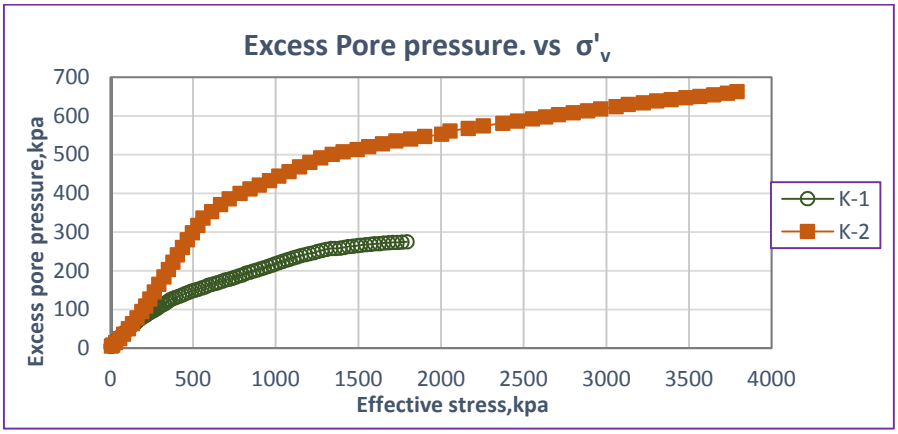

Fig.3.17 (b) Excess pore pressure development for Kolfe

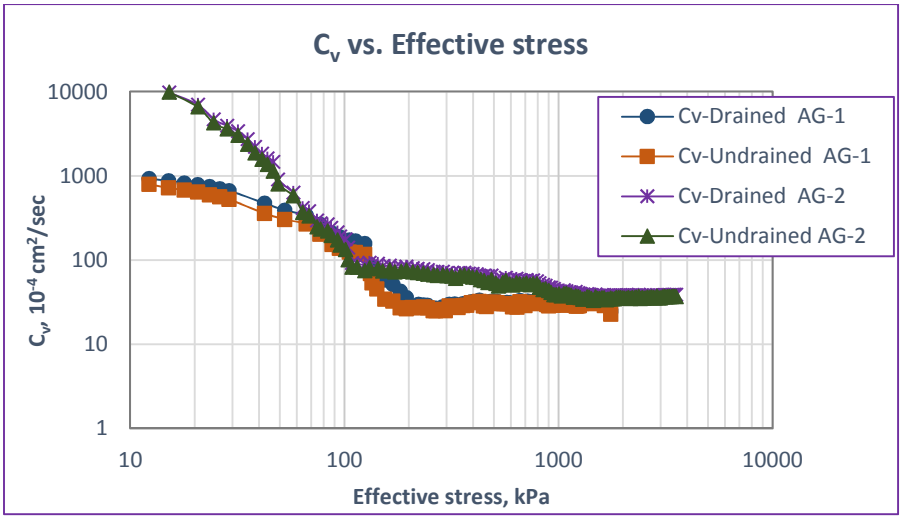

Fig. 3.18 (a) C_v -curve of CRSC test for Addisu Gebeya soil sample.

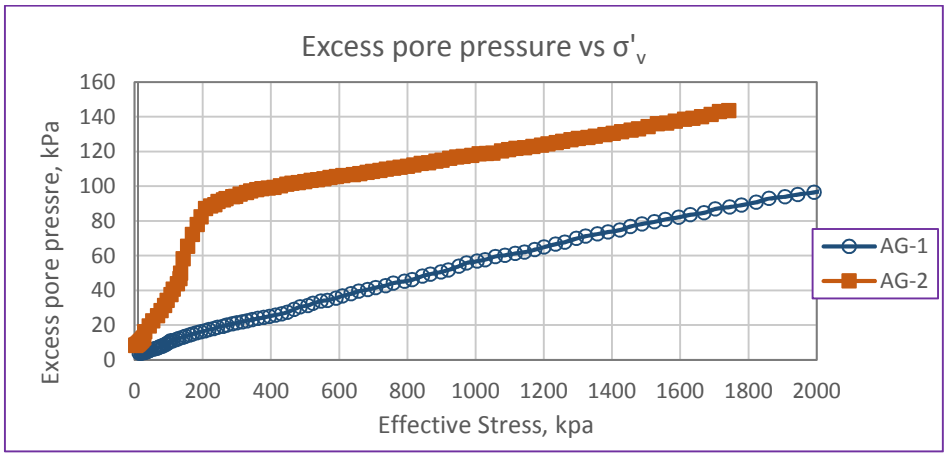

Fig.3.18 (b) Excess pore pressure development for Addisu Gebeya

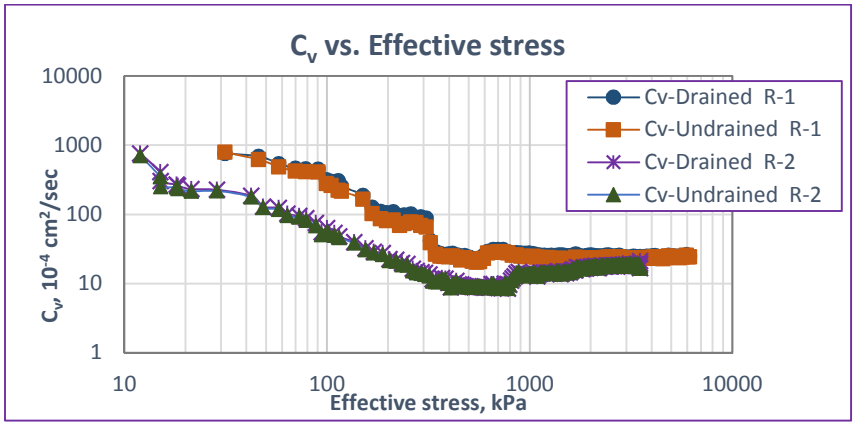

Fig. 3.19 (a) C_v -curve of CRSC test for Rufa'el soil sample.

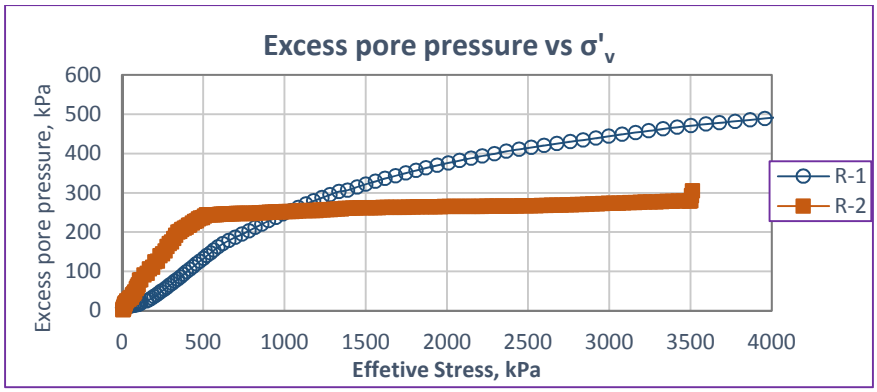

Fig.3.19 (b) Excess pore pressure development for Rufa'el

From the figures, it can be seen that the value of C_v decreases rapidly with the increasing of vertical average stress in the Over Consolidated (OC) stage and converge in the range of the Normally Consolidated (NC) stage.

The plots also show the relationship between the coefficient of consolidation and effective stress (σ'_v) of CRSC tests from soil sample at 1.5 m and 3 m depths. The values of C_v obtained from K-1 and R-1 are slightly larger than that obtained from K-2 and R-2 respectively after C_v values converges, though the AG samples show some kind of a reverse trend. As Gorman [26] pointed out, the value of C_v increases with increased strain rate. The above condition is happened since soils with higher LL, the pore pressure increase, normally have lower C_v (Figs.3.17 - 3.19). It show that both depths give similar results of C_v values after 1000 kPa effective stress.

CHAPTER 4

DISCUSSION OF TEST RESULTS

The results of the CIL test and CRSC tests at various depths are plotted together and compared. The comparison is made with respect to the compression index, the pre-consolidation pressure and the coefficient of consolidation.

4.1 Compression Curves (e-log σ'_v)

The compression curves of the two sets of consolidation tests were compared for samples taken from the same depth, as shown in Figs. 4.1 - 4.3. This figures show the relationship between void ratio and log effective stress for CIL and CRSC tests. The results indicate relatively good agreement for 1.5m samples (Figs.4.1- 4.3a). But for 3m samples (Figs.4.1-4.3b) the CRSC tests compression curve shift up. The reason for this could be the higher LL of depth than 1.5m, because with higher LL the pore pressure increase was much steeper than for the lower. The steeper shape of the excess pore pressure curves from 3m depth in comparison to 1.5m implies that the excess pore pressure is dependent on the LL of the sample (Figs. 3.17 - 3.19b). Also during CRSC test pore pressure control is difficult and compression curve is mainly affected by strain rate selection. This clarifies why the CRSC test, dependent of the drainage condition, produced relatively higher compression curves than the CIL tests. In general, the data points from conventional oedometer tests lie very close to or on the compression curves of the CRSC tests.

Since initial loading for CRSC test is almost zero while for CIL test is 25kPa, the compression curve for CRSC tests have higher initial void ratio than the CIL consolidation tests. So the compression curves were higher than the CIL compression curve.

CRSC compression curves were very similar to the Conventional oedometer consolidation compression curve although the compression curve was shifted upward. With the similar curve, compression index for the CRSC tests are nearly the same with the CIL test results.

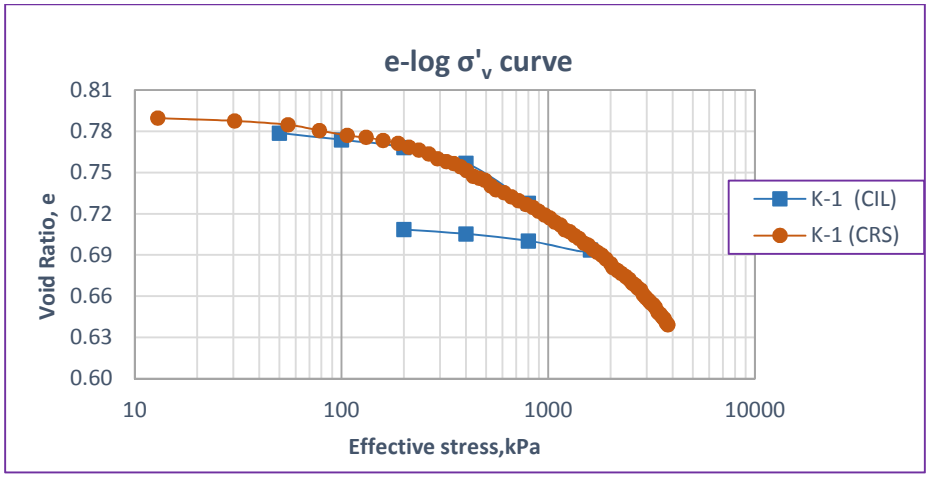

Fig. 4.1: (a) Compression curves comparison for K-1 sample.

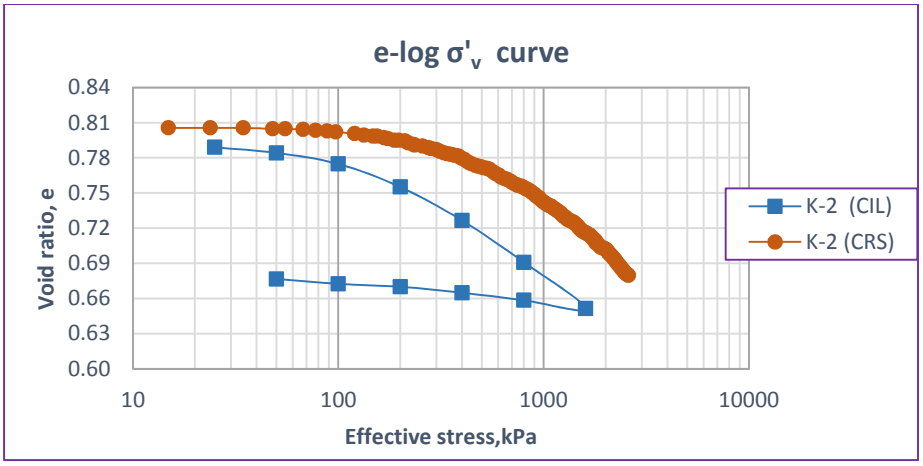

Fig. 4.1: (b) Compression curves comparison for K-2 sample.

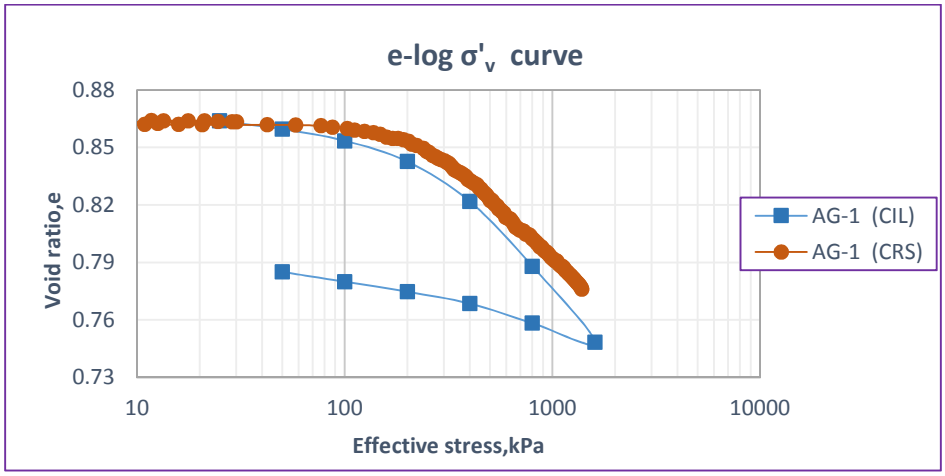

Fig. 4.2: (a) Compression curves comparison for AG-1 sample.

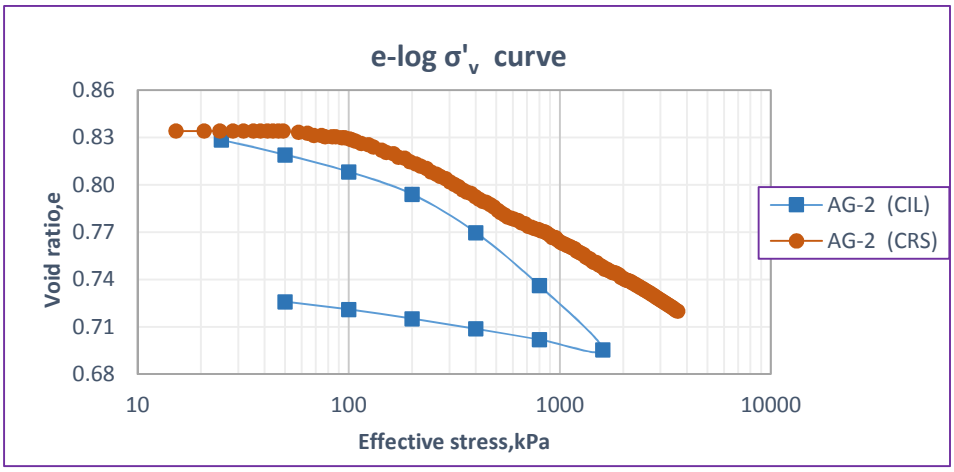

Fig. 4.2: (b) Compression curves comparison for AG-2 sample.

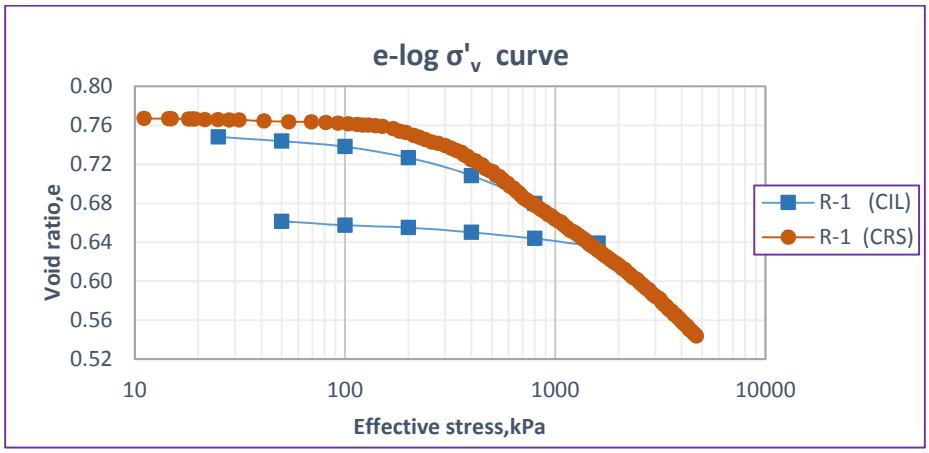

Fig. 4.3: (a) Compression comparison curves for R-1 sample.

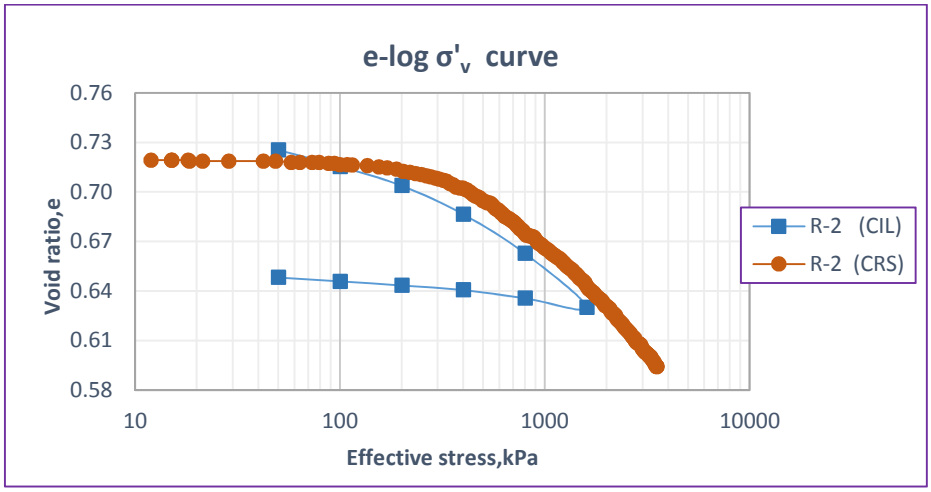

Fig. 4.3: (b) Compression comparison curves for R-2 sample.

Table 4.1 summarizes the consolidation properties obtained from the six conventional incremental (CIL) and CRSC consolidation tests. It is found that the pre-consolidation pressure obtained from CRSC test is higher than that obtained from CIL consolidation tests. This observation is reasonable since the pre-consolidation pressure is strain rate dependent [33] and the strain rate used in this study may be a little too large for Kolfe and Rufa'el red clay. However strain rate used for Addisu Gebeya is small since CRSC test pre-consolidation pressure is smaller than CIL test. The Addisu Gebeya pre-consolidation pressure, from previous studies, by Merihun [19] was 280 kPa which is almost the same as the result shown in Table 4.1. According to Tanaka [33] pre-consolidation pressure value increases linearly with increase in strain rate in logarithm scale.

It is also observed that the compression index, C_c obtained from the CRSC tests is slightly larger than that obtained from conventional oedometer tests, whereas the Addisu Gebeya samples (AG-1 and AG-2) smaller values as in the pre-consolidation pressure.

Table 4.1 Consolidation properties from CIL and CRSC tests.

Soil Sample	**CIL Tests**		**CRSC Tests**		
	C_C	**σ'_p (kPa)**	Strain rate **(mm/min)**	**C_C**	**σ'_p (kPa)**
K-1	0.105	360	0.00254	0.131	400
K-2	0.125	198	0.00102	0.140	420
AG-1	0.122	300	0.00102	0.114	230
AG-2	0.123	290	0.00102	0.082	170
R-1	0.124	300	0.00102	0.177	310
R-2	0.103	320	0.00102	0.127	400

4.2 Coefficient of Consolidation

According to Lee (1981), CRSC test could only be accepted when there is a good agreement with the coefficient of consolidation from CIL test [14]. For the comparison of coefficient of consolidation, CIL test result was compared with the CRSC undrained (C_v-undrain) and drained (C_v-drain) coefficient of consolidation for rate of strain given to the soil (Figs.4.4 - 4.9 (a)). Drained and undrained coefficient of consolidation values were derived from the top and bottom of the soil sample in the CRSC test. Convergence of **C_v** values from drained and undrained face indicates that the steady state condition is achieved and can produce the acceptable C_v values compared with oedometer test.

The steady state condition for excess pore water pressure is also important in determining the coefficient of consolidation (Figs. 4.4- 4.9 (b)). This is to show that the soil condition is in steady state condition during the process.

Figs. 4.4 – 4.9 show C_v curves from the conventional incremental (CIL) and CRSC consolidation tests.

4.2.1 For K - 1 soil sample

Range of the C_v value for CIL test of **K–1** sample were from 18.63 - 36.10*10^{-4} cm^2/sec as shown in Appendix E2. Coefficient of consolidation values curve for conventional and CRSC test are shown in the Fig. 4.4a. The C_v from the CRSC test value were acceptable because the CRSC tests converge around 300 kPa to achieve steady state and compatible with oedometer test results after 600 kPa effective stress. As shown in Fig. 4.4b excess pore pressure increase slowly after 600 kPa effective stress that led to steady state condition.

The values of C_v obtained from CRSC tests are extremely larger than those obtained from conventional tests before pre-consolidation pressure.

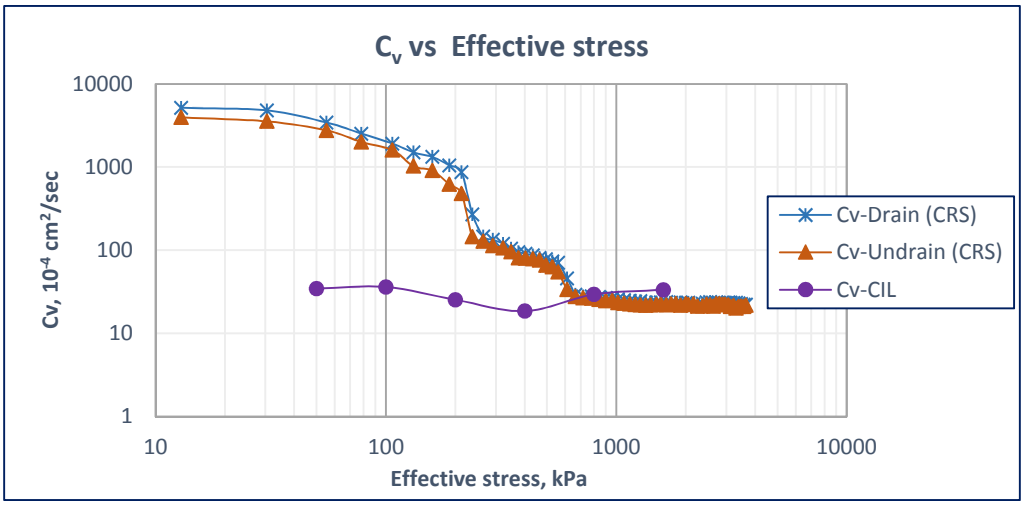

Fig. 4.4: a) C_v curves comparison for **K-1** sample.

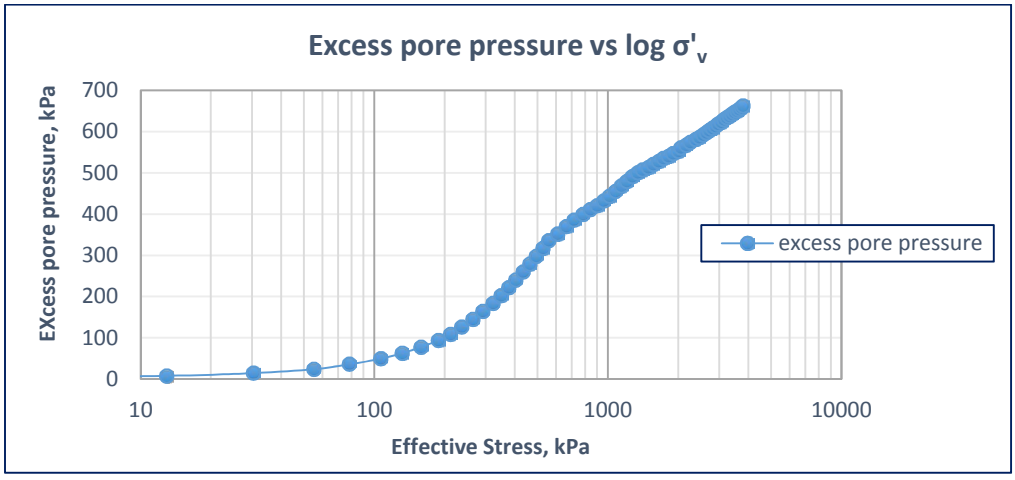

Fig. 4.4: b) Excess pore pressure curve for **K-1** CRSC test.

4.2.2 For K - 2 soil sample

Fig. 4.5a show the C_v curves for CIL and CRSC tests for K-2 sample. The C_v value of CRSC test decreases rapidly with increasing vertical average stress in the over consolidated stage and converge in the range of 300 – 2600 kPa in the normally consolidated stage. Both undrained and drained C_v values from CRSC test converge with C_v values from conventional oedometer (CIL) test after 300 kPa effective stress and become compatible. The compatibility can be seen from the overlapping of both curves.

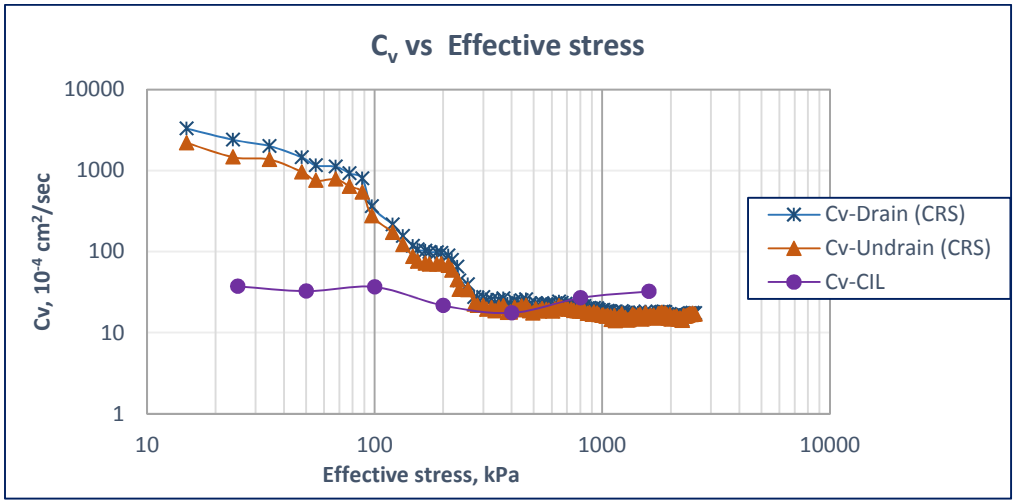

Fig. 4.5 a) C_v curve comparison for **K-2** sample.

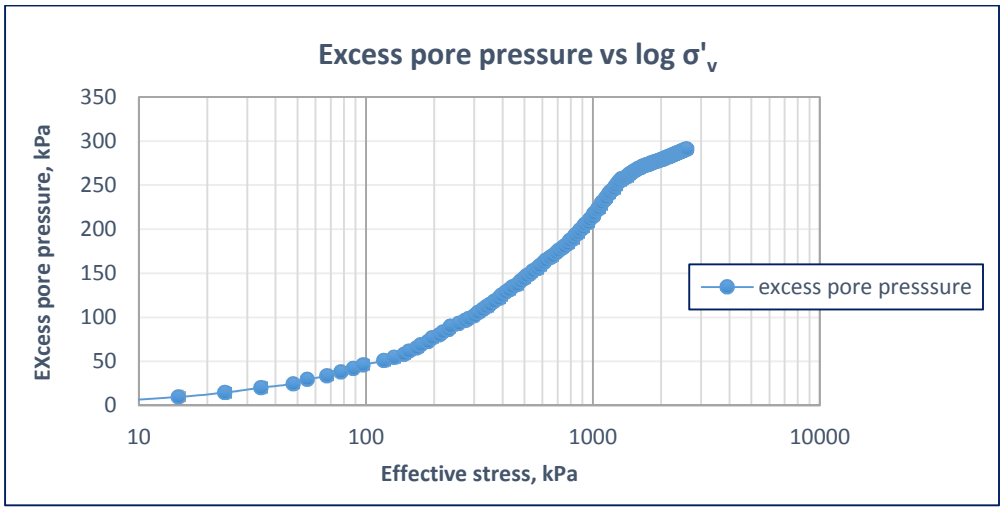

Fig. 4.5 b) Excess pore pressure curve for **K-2** CRSC test

4.2.3 For AG - 1 soil sample

Fig. 4.6a show the C_v curves of **AG-1** sample for the CIL and CRSC tests. It is found that CRSC test results produced very good agreement with the conventional test results and the values of C_v fall into the range of 25 - 30*10^{-4} cm^2/sec in the normally consolidated stage .

The rapid increases of the excess pore pressure up to 200 kPa effective stress cause unstable and higher Cv-undrain and Cv-drain value (Fig.4.6b).

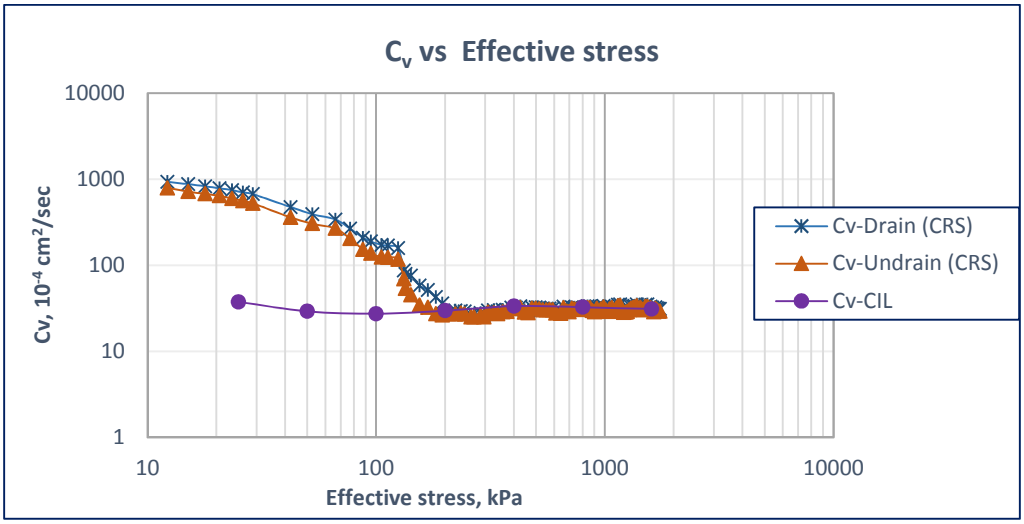

Fig. 4.6 a) C_v curve comparison for **AG-1** sample.

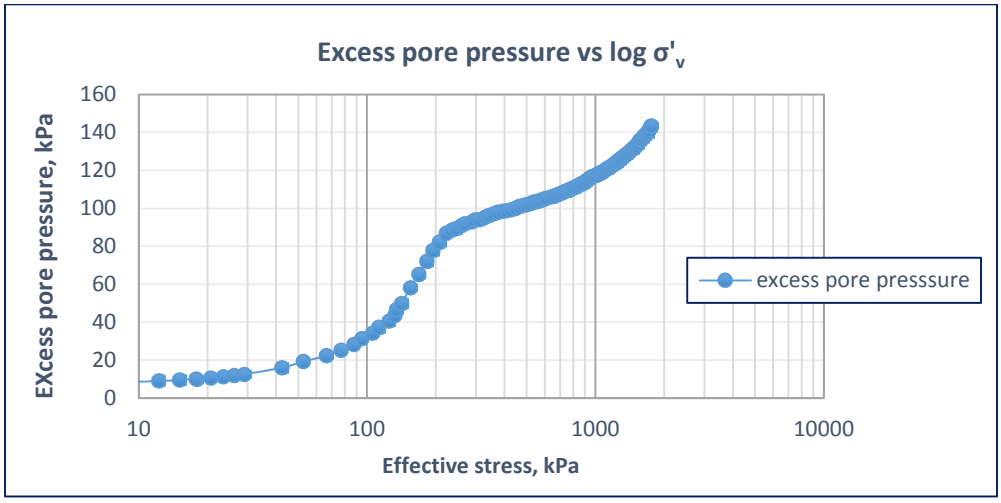

Fig. 4.6 b) Excess pore pressure curve for **AG-1** CRSC test

4.2.4 For AG - 2 soil sample

Fig.4.7a show the C_v curves of **AG-2** sample for CIL and CRS tests. The coefficient of consolidation for the CRSC decreases slowly and stabilizes at the end of the test. The value of coefficient of consolidation for the CRSC reached a steady state after an effective stress of 100 kPa and became stable between 35 - 42*10^{-4} cm^2/sec.

CRSC tests results are considered satisfactory as they converge with the Oedometer (CIL) test results.

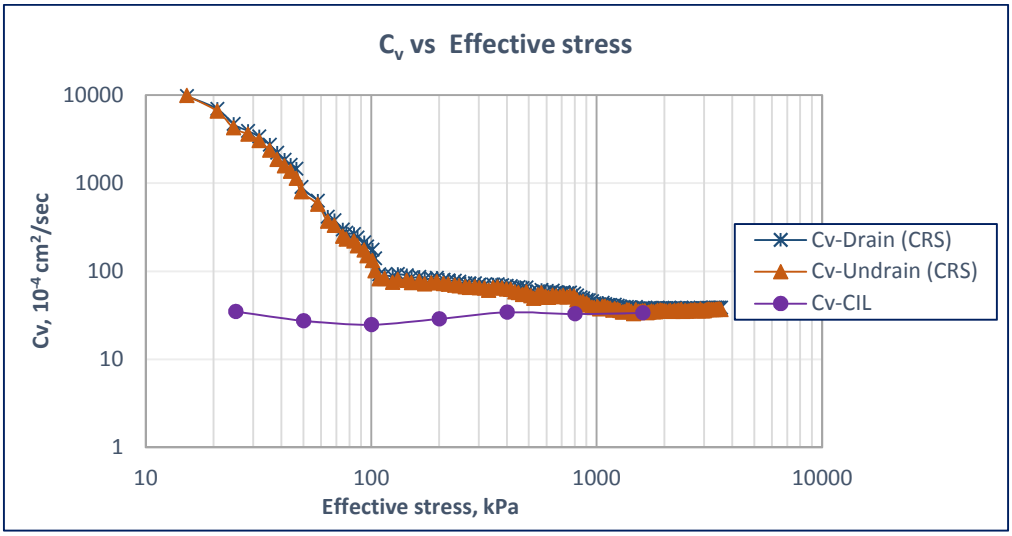

Fig. 4.7 a) C_v curve comparison for **AG-2** sample.

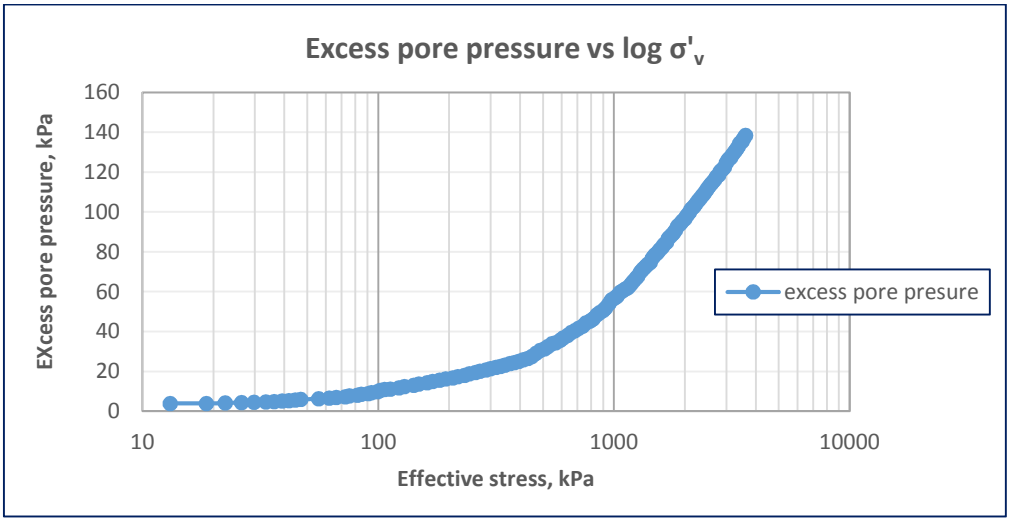

Fig. 4.7 b) Excess pore pressure curve for **AG-2** CRSC test

4.2.5 For R - 1 soil sample

Coefficient of consolidation from conventional test for **R-1** sample range from 9.40 to 15.10*10^{-4} cm^2/sec as shown in Appendix E5. Fig.4.8a shows the comparison of C_v value for CIL and CRSC tests.

Coefficient of consolidation value for CRSC test is close to the CIL test as shown in the Figure. The results are acceptable because of the convergence of the two curves.

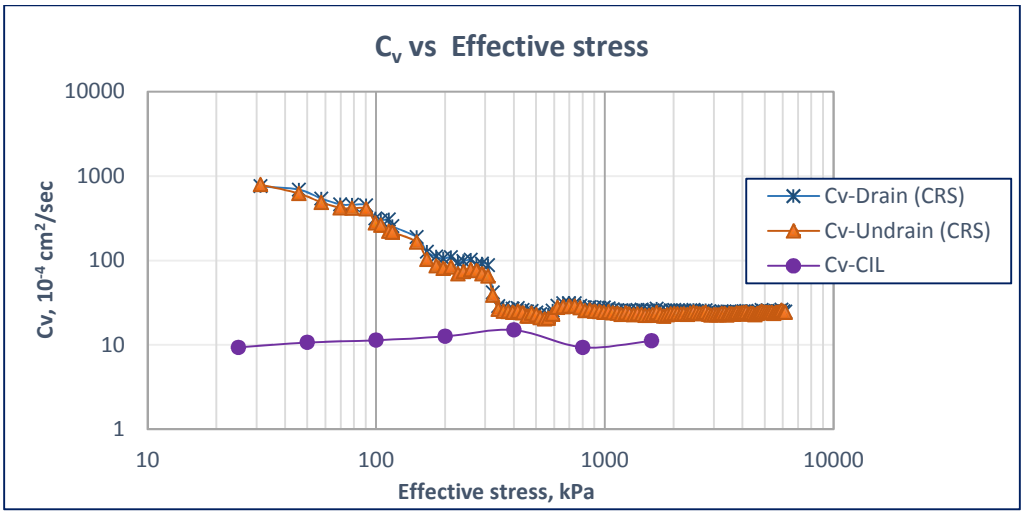

Fig. 4.8 a) C_v curve comparison for **R-1** sample.

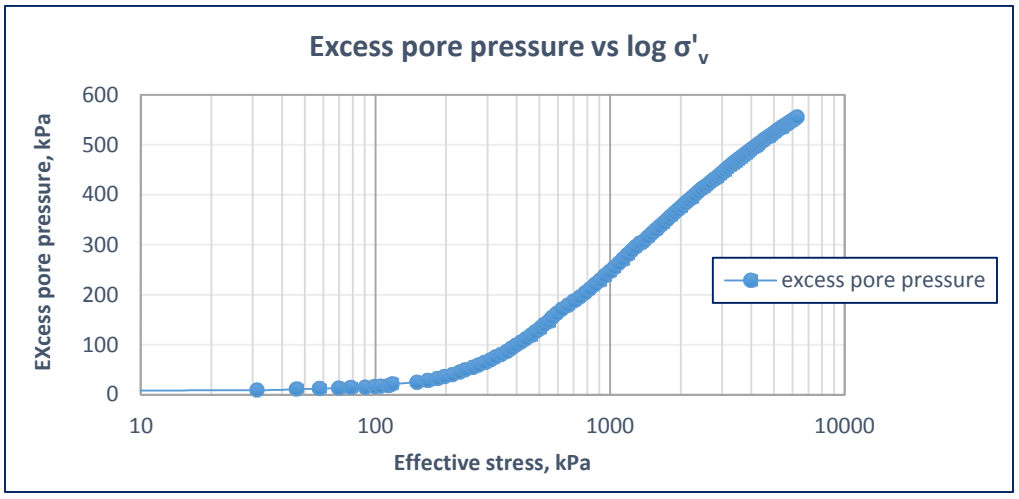

Fig. 4.8 b) Excess pore pressure curve for **R-1** CRSC test

4.2.6 For R - 2 soil sample

Coefficient of consolidation for R-2 from CIL test are from 8.81 - 14.09 *10^{-4}cm^2/sec as shown in Appendix E6. Fig.4.9a shows C_v against effective stress curve for CIL and CRSC test results. The CRSC curve shows that the steady state condition exists. CRSC test for R-2 sample had a good agreement with CIL test results.

Fig. 4.9b shows that the excess pore pressure versus effective stress graph for CRSC test. The observed steady state condition shows that the C_v value for the CRSC test is acceptable.

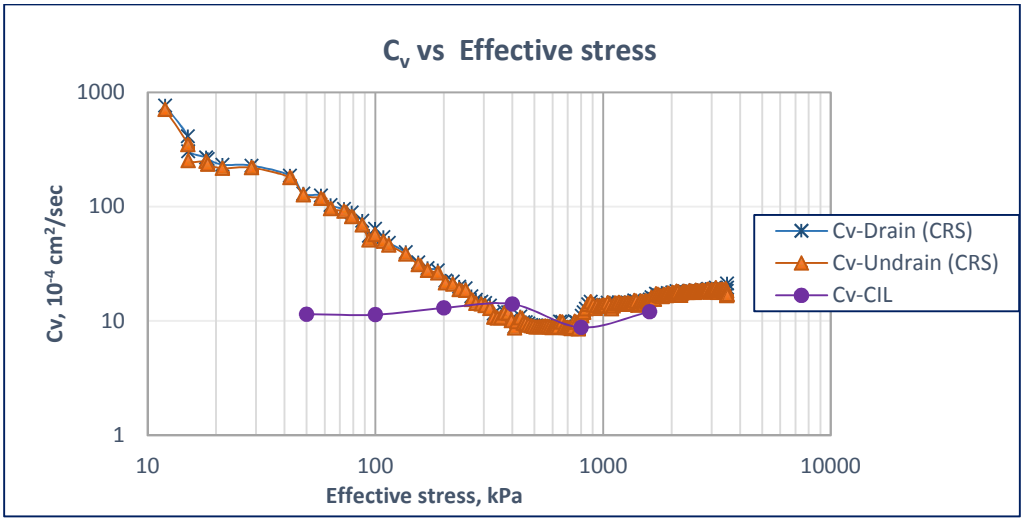

Fig. 4.9 a) C_v curve comparison for **R-2** sample.

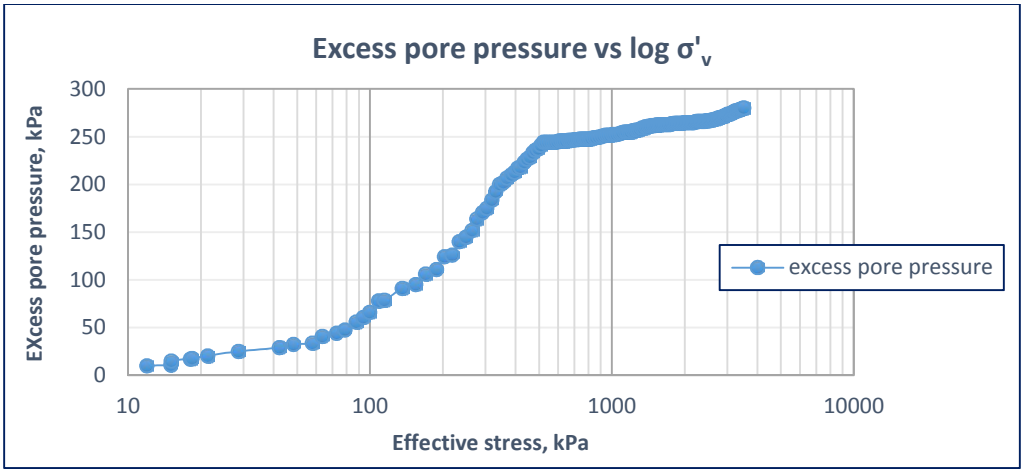

Fig. 4.9 b) Excess pore pressure curve for **R-2** CRSC test

At the early stage of the CRSC tests, the ASTM code and Wissa's theory provide unrealistic interpretation for C_v and show a notable disparity between *e* versus σ' relationship obtained from CRSC consolidation test and that obtained from CIL consolidation test [36] as shown in the above Figure.

CHAPTER 5

CONCLUSION AND RECOMMENDATION

5.1 Conclusion

A series of conventional incremental loading (CIL) and CRSC consolidation tests on kolfe, Addisu Gebeya and Rufa'el undisturbed samples were conducted. All the soil samples were red clay soils which are founded in Addis Ababa. Conventional incremental tests were used to validate the CRSC test results. This chapter summarizes the results and draws conclusions which could be applied by geotechnical engineers.

The void ratio curves from the CRSC tests are found to be compatible with conventional consolidation test. The values of pre- consolidation stress, σ'_p and compression index, C_c obtained from CRSC tests are a little larger than that obtained from conventional consolidation tests in Kolfe and Rufa'el soil sample. The CRSC evaluation method of Casagrande generates higher values of σ'_p than CIL. Nevertheless, it is questionable if it should be used for evaluation of CRS tests since it is designed for CIL tests. But Addisu Gebeya soil sample CRSC test values were found to be smaller than CIL test. This value show that the strain rate used, 0.00102 mm/min, for CRSC tests cannot give comparable result of CIL test. So it is suggested to use increased strain rate for CRSC test to get compatible result with CIL test. Furthermore, it is easier to determine pre-consolidation stress or compression index in CRSC tests than in conventional consolidation tests, since the specimens in CRSC tests are fully saturated and continuous data points are recorded in the test.

The values of coefficient of consolidation, C_v in the over consolidated stage are much larger than that in the normally consolidated stage for CRSC tests.

CRSC test interpretation theories provide unrealistic results at the early stage of the test. So values of C_v should be considered valid only above the pre consolidation stress.

The coefficient of consolidation results from CRSC tests are compatible with the conventional incremental consolidation (CIL) test when vertical loading stress is larger than the pre-consolidation stress. With the increase in pressure there is reorientation of the grains due to which there is reduction in void ratio and subsequently C_v reduces.

The excess pore pressure produced during the CRSC test also play an important role in producing reasonable values for C_v. Rapid increase in excess pore pressure will give rise to transient condition which is unacceptable for CRSC test to be compatible with conventional consolidation test as the mode of pore pressure development during conventional test is in steady state condition.

The problem with the CRS test is that when testing a specific soil for the first time, a preselected strain rate must be set. This can lead to unreliable results, meaning the test must be repeated with another strain rate.

The time required to complete a CIL test in this study was 12 days. Time to completion in the CRSC test depends on the selected strain rate and the compressibility and permeability of the soil. CRSC tests reported herein required an average of 1.8 days, considered only the loading stage, to complete the test., Of the two test methods considered, the CRSC test required the least time, though difficult to perform.

5.2 Recommendation for Future Analysis

Constant rate of strain consolidation test (CRSC) is a unique consolidation test compared with the conventional incremental consolidation (CIL) test.

More CRSC tests should be performed with different values of strain rate and the optimum strain rate for Addis Ababa red clay. It is advisable to let the soil sample reach the steady state condition completely during the CRSC test.

Further researches can be conducted with increased number of tests and additional areas that are not included in this research, where red clay soil found.

REFERENCES

[1] Davis, E. H., & Raymond, G. P. (1965). A non-linear theory of consolidation. *Geotechnique, 15*(2), 161-173.

[2] Hamilton, J. J., & Crawford, C. B. (1959). Improved determination of preconsolidation pressure of a sensitive clay. *American Society for Testing and Materials*, 254-270.

[3] Prasad, S. (2012). *Consolidation behavior of organic clay under constant rate of strain.* Master Thesis, Jadavpur University, Kolkata.

[4] Leroueil, S., Kabbaj, M., Tavenas, F., & Bouchard, R. (1985). Stress-strain - strain rate relation for the compressibility of sensitive natural clays. *Geotechnique, 35*(2), 159-180.

[5] Tanaka, H. (2005). Consolidation behavior of natural soils around pc value - long term consolidation test. *Soils and Foundations, 45*(3), 83-95.

[6] Tanaka, H., Udaka, K., & Nosaka, T. (2006). Strain rate dependency of cohesive soils in consolidation settlement. *Soils and Foundations, 46*(3), 315-322.

[7] Samuel, T. (1989). *Investigation in to some of engineering properties of Addis Ababa red clay soils.* Master Thesis, Addis Ababa University, Addis Ababa.

[8] Terzaghi, K. (1943). *Theoretical Soils Mechanics.* New York: John Wiley & Sons, Inc.

[9] Das, B. M. (2008). *Advanced Soil Mechanics* (3rd ed.). New York, 270 Madison Ave.: Taylor & Francis.

[10] Alemayehu, T., & Mesfin, L. (1999). *Soil Mechanics.* Addis Ababa: Addis Ababa University Printing Press.

[11] Ndiaye, C., Fall, M., Ndiaye, M., Sangare, D., & Tall, A. (2014). A review and update of analytical and numerical solutions of the Terzaghi one- dimensional consolidation equation . *Open Journal of Civil Engineering, 4*, 274-284. Retrieved from http://dx.doi.org/10.4236/ojce.2014.43023.

[12] Khansari, H. (1996). *An investigation of one-dimensional compression and consolidation of intact and reconstituted bothkennar soft soil.* PhD Dissertation, university of the West of England, Bristol.

[13] Powell, J. S. (2010). *Geotechnical characterization of the bearpaw shale.* PhD Dissertation, Queen's University, Kingston,Canada.

[14] Siang, L. C. (2011). *Criteria of acceptance for constant rate of strain consolidation test for cohesive soil.* PhD Dissertation, Universiti Teknoogi Malaysia.

[15] Budhu, M. (2000). *Soil Mechanics and Foundations.* (w. Anderson, Ed.) Arizona: John Wiley & Sons, Inc.

[16] Wang, L., & Frost, J. D. (2004). Dissipated strain energy method for determining preconsolidation pressure. *Canadian Geotechnical Journal, 41*, 760-768. doi:10.1139/T04-013.

[17] Lok, T. H., & Shi, X. (2008). *Consolidation and strength properties of Macau Marine clay.* PhD Dissertation, University Macau.

[18] Jia, R. (2010). *Consolidation behavior of Ariake clay under constant rate of strain.* PhD Dissertation, Saga University, Saga.

[19] Crawford, C. B. (1986). State of the art: Evaluation and Interpretation of soil consolidation tests. *Consolidation of soils*, 71-103.

[20] Sample, K. M., & Shackelford, C. D. (2012). Apparatus for constant rate -of -strain consolidation of slurry mixed soils. *Geotechnical Testing Journal, 35*(3), 409-418.

[21] Umehara, Y., & Zen, K. (1980). Constant rate of strain consolidation for very soft clayey soils. *Soils and Foundations, 20*(2), 79-93.

[22] Ozer, A. T., Lawton, E. C., & Bartlett, S. F. (2012). New method to determine proper strain rate for constant rate-of-strain consolidation tests. *Canadian Geotechnical Journal, 49*, 18-26. doi:10.1139/T11-086.

[23] Premchitt, J., Ho, K. S., & Evans, N. C. (1996). Conventional and CRS rowe cell consolidation test on some Hong Kong clas. *Geo Report*(55), 8-40.

[24] Aboshi, H., Yoshikuni, H., & Maruyama, S. (1970). Constant loading rate consolidation test. *Soils and Foundations, 10*(1), 43-56.

[25] Gorman, C. T., Hopkins, T. C., Deen, R. C., & Drnevich, V. P. (1978). Constant rate of strain and controlled gradient consolidation testing. *Geotechnical Test Journal, 1*(1), 3-15.

[26] Gorman, C. T. (1981). Strain -rate selection in the constant rate of-strain consolidation test. *Geotechnical test journal, 1*(1), 1-15.

[27] Seah, T. H., & Juirnarongrit, T. (2003). Constant rate of strain consolidation with radial drainage. *Geotechnical Testing journal, 26*(4), 1-11.

[28] Suzuki, K., & Yasuhara, K. (2005). Normalization of stress-strain curves from CRSC consolidation test and its application to consolidation analysis. *Lowland technology international, 7*(1), 65-75.

[29] Chai, J. C., Iribe, K., & Hino, T. (2006). Comparison of incremental load and Constant rate of strain consolidation test results. *Recent development of geotechnical and Geo-Environmental engineering*, 47-52.

[30] Sandeep, M. N., & Reshma, T. C. (2014). Consolidation behavior of cochin Marine clay under constant rate of strain. *International journal of scientific and Engineering research, 5*(7), 1317-1322.

[31] Kassim, K. A., A.Rashid, A. S., Hong Kueh, A. B., Yah, C. S., Siang, C. L., & Moayedi, H. (2014). Development of rapid consolidation Equipment for cohesive soil. *Geotechnical and Geological Engineering, 1*(1), 2-7. doi:10.1007/s10706-014-9819-7.

[32] Kassim, K. A., A.Rashid, S. A., Hong Kueh, A. B., Yah, C. S., & Siang, L. C. (2016). Criteria of acceptance for constant rate of strain consolidation test for Tropical cohesive soil. *Geotechnical and Geological Engineering, 1*(1), 2-17.doi:10.1007/s10706-016-0016-8.

[33] Merihun, L. (2010). *A study on the effect of remolding on the mechanical behavior of Addis Ababa red clay soil.* Master Thesis, Addis Ababa University, Addis Ababa.

[34] Yodit, M. (2012). *Correlation between critical state soil parameters and index properties of remolded red clay soils of Addis Ababa.* Master Thesis, Addis Ababa University, Addis Ababa.

[35] American Society for Testing and Materials (1998).Standard Test Method for Soil and Rock, Annual Book of ASTM Standards, Vol.04.08 and 04.09.Philadelphia, USA.

[36] Instruction Manual for Continuous Consolidation Test, Mod. 26-WF24670, Rev. 0, 22.11.2006. CONTROLS, Italy.

[37] Instruction Manual of Geodatalog and Datacomm, Mod. 30-WF6016/30-WF6032.Rev. 2 EN, 23.12.2008. CONTROLS, Italy.

[38] Vikash, G., & Prashant, A. (2014). Consolidation characteristics of clay using constant rate of deformation test. *Golden Jubilee Conference of the IGS Bangalore Chapter,Geo-Innovations*, (pp. 1-10). bangalore.

Appendix

A–F

(Laboratory Report)

A. Moisture content Determination

A1. Moisture content test for kolfe sample #1

Location: ***Kolfe area (bethel)***	Job ref.	***Thesis research***
Soil Description: ***Red clay***	Sample no.	**#1**
	Depth	**1.5m**
Test method : Oven dried , ASTM standard: D 2216 -98	Date	16/03/2016.

Specimen ref.	#1	#2
Container no.	A40	T70
Mass of wet soil + container (m_2)g	124.00	115.00
Mass of dry soil + container (m_3)g	99.29	91.70
Mass of container (m_1)g	10.80	15.60
Mass of moisture(Water) (m_2-m_3)g	24.71	23.30
Mass of dry soil (m_3-m_1)g	88.49	76.10
Moisture content = (m_2-m_3)/ (m_3-m_1)*100, %	**27.9**	**30.60**
Average (%)	**29.27**	

A2. Moisture content test for kolfe sample #2

Location: ***Kolfe area (bethel)***	Job ref.	***Thesis research***
Soil Description: ***Red clay***	Sample no.	**#2**
	Depth	**3m**
Test method : Oven dried , ASTM standard: D 2216 -98	Date	16/03/2016.

Specimen ref.	#1	#2
Container no.	A302	H50
Mass of wet soil + container (m_2)g	117.60	104.70
Mass of dry soil + container (m_3)g	93.10	83.50
Mass of container (m_1)g	15.50	15.90
Mass of moisture(Water) (m_2-m_3)g	24.50	21.20
Mass of dry soil (m_3-m_1)g	77.60	67.60
Moisture content = (m_2-m_3)/ (m_3-m_1)*100, %	**31.60**	**31.40**
Average (%)	**31.47**	

A3. Moisture content test for Addisu-Gebeya sample #1

Location: ***Addisu-Gebeya area (Hamle19/67 primary school)***	Job ref.	***Thesis research***
Soil Description: ***Red clay***	Sample no.	**#1**
	Depth	**1.5m**
Test method : Oven dried , ASTM standard: D 2216 -98	Date	05/04/2016.

Specimen ref.	#1	#2
Container no.	G52	625
Mass of wet soil + container (m_2)g	44.76	37.67
Mass of dry soil + container (m_3)g	38.52	32.86
Mass of container (m_1)g	15.68	15.74
Mass of moisture(Water) (m_2-m_3)g	6.24	4.81
Mass of dry soil (m_3-m_1)g	22.84	17.12
Moisture content = (m_2-m_3)/ (m_3-m_1)*100, %	**27.30**	**28.10**
Average (%)	**27.71**	

A4. Moisture content test for Addisu-Gebeya sample #2

Location: ***Addisu-Gebeya area (Hamle19/67 primary school)***	Job ref.	***Thesis research***
Soil Description: ***Red clay***	Sample no.	**#2**
	Depth	**3m**
Test method : Oven dried , ASTM standard: D 2216 -98	Date	05/04/2016.

Specimen ref.	#1	#2
Container no.	H50	A320
Mass of wet soil + container (m_2)g	43.31	41.43
Mass of dry soil + container (m_3)g	37.03	35.82
Mass of container (m_1)g	15.87	15.79
Mass of moisture(Water) (m_2-m_3)g	6.28	5.61
Mass of dry soil (m_3-m_1)g	21.16	20.03
Moisture content = (m_2-m_3)/ (m_3-m_1)*100, %	**29.70**	**28.00**
Average (%)	**28.84**	

A5. Moisture content test for Rufa'el sample #1

Location: ***Rufa'el area (primary school)***		Job ref.	***Thesis research***
Soil Description: ***Red clay***		Sample no.	**#1**
		Depth	**1.5m**
Test method : Oven dried , ASTM standard: D 2216 -98		Date	19/05/2016.
Specimen ref.	#1	#2	#3
Container no.	K6	62	D51
Mass of wet soil + container (m_2)g	42.4	62.00	52.40
Mass of dry soil + container (m_3)g	37.1	52.90	45.30
Mass of container (m_1)g	11.00	15.50	16.10
Mass of moisture(Water) (m_2-m_3)g	5.30	9.10	7.10
Mass of dry soil (m_3-m_1)g	26.10	37.40	29.20
Moisture content = (m_2-m_3)/ (m_3-m_1)*100, %	**20.30**	**24.30**	**24.32**
Average (%)	**22.98**		

A6. Moisture content test for Rufa'el sample #2

Location: ***Rufa'el area (primary school)***		Job ref.	***Thesis research***
Soil Description: ***Red clay***		Sample no.	**#2**
		Depth	**3m**
Test method : Oven dried , ASTM standard: D 2216 -98		Date	19/05/2016.
Specimen ref.	#1	#2	#3
Container no.	G-F	G-19	PL
Mass of wet soil + container (m_2)g	43.70	56.60	44.50
Mass of dry soil + container (m_3)g	37.60	48.70	38.50
Mass of container (m_1)g	10.90	15.70	13.80
Mass of moisture(Water) (m_2-m_3)g	6.10	7.90	6.00
Mass of dry soil (m_3-m_1)g	26.70	33.00	24.70
Moisture content = (m_2-m_3)/ (m_3-m_1)*100, %	**22.85**	**23.94**	**24.3**
Average (%)	**23.69**		

B. Specific Gravity Determination

B1. Specific Gravity test for kolfe sample #1

Location: ***Kolfe area (bethel)***		Job ref.	***Thesis research***
Soil Description: ***Red clay***		Sample no.	**#1**
		Depth	**1.5m**
Test method : Small pycnometer ASTM standard: D 854-98		Date	08/04/2016.
Specimen ref.	#1		#2
Pycnometer number.	A6		B7
Mass of Pycnometer + soil + water (m_3)g	162.70		158.80
Mass of Pycnometer + soil (m_2)g	72.40		69.60
Mass of Pycnometer full of water (m_4)g	146.80		144.00
Mass of empty Pycnometer (m_1)g	47.40		44.60
Mass of soil (m_2-m_1)g	25		25.00
Mass of water in full Pycnometer (m_4-m_1)g	99.40		99.40
Mass of water used (m_3-m_2)g	90.30		89.20
Volume of soil particles (m_4-m_1)- (m_3-m_2)ml	9.10		10.20
Tx, suspension Temperature ,^{0}C	25.70		25.70
Correction factor value, K	0.9987		0.9987
Specific Gravity = (m_2-m_1)/ ((m_4-m_1)- (m_3-m_2))	**2.74**		**2.45**
Average	**2.60**		

B2. Specific Gravity test for kolfe sample #2

Location: ***Kolfe area (bethel)***		Job ref.	***Thesis research***
Soil Description: ***Red clay***		Sample no.	**#2**
		Depth	**3m**
Test method : Small pycnometer ASTM standard: D 854-98		Date	08/04/2016.
Specimen ref.	#1		#2
Pycnometer number.	9A		MR
Mass of bottle + soil + water (m_3)g	158.80		164.40
Mass of bottle + soil (m_2)g	68.30		73.90
Mass of bottle full of water (m_4)g	142.90		148.50
Mass of bottle (m_1)g	43.30		48.90
Mass of soil (m_2-m_1)g	25		25.00
Mass of water in full bottle (m_4-m_1)g	99.60		99.60
Mass of water used (m_3-m_2)g	90.50		90.50
Volume of soil particles (m_4-m_1)- (m_3-m_2)ml	9.10		9.10
Tx, suspension Temperature ,^{0}C	25.80		25.80
Correction factor value, K	0.9987		0.9987
Specific Gravity =(m_2-m_1)/ ((m_4-m_1)- (m_3-m_2))	**2.74**		**2.74**
Average	**2.74**		

B3. Specific Gravity test for Addisu-Gebeya sample #1

Location: ***Addisu-Gebeya area (Hamle19/67 primary school)***		Job ref.	***Thesis research***
Soil Description: ***Red clay***		Sample no.	**#1**
		Depth	**1.5m**
Test method : Small pycnometer ASTM standard: D 854-98		Date	21/04/2016.
Specimen ref.	#1		#2
Pycnometer number.	C21		B11
Mass of Pycnometer + soil + water (m_3)g	160.40		161.50
Mass of Pycnometer + soil (m_2)g	70.60		72.10
Mass of Pycnometer full of water (m_4)g	144.60		144.80
Mass of empty Pycnometer (m_1)g	45.80		45.80
Mass of soil (m_2-m_1)g	24.80		26.30
Mass of water in full Pycnometer (m_4-m_1)g	98.80		99.00
Mass of water used (m_3-m_2)g	89.80		89.40
Volume of soil particles (m_4-m_1)- (m_3-m_2)ml	9.00		9.60
Tx, suspension Temperature ,^{0}C	22.50		22.50
Correction factor value, K	0.9996		0.9996
Specific Gravity=(m_2-m_1)/ ((m_4-m_1)- (m_3-m_2))	**2.76**		**2.74**
Average	**2.75**		

B4. Specific Gravity test for Addisu-Gebeya sample #2

Location: ***Addisu-Gebeya (Hamle19/67 P. school)***		Job ref.	***Thesis research***
Soil Description: ***Red clay***		Sample no.	**#2**
		Depth	**3m**
Test method : Small pycnometer ASTM standard: D 854-98		Date	21/04/2016.
Specimen ref.	#1		#2
Pycnometer number.	F19		C23
Mass of Pycnometer + soil + water (m_3)g	162.40		158.60
Mass of Pycnometer + soil (m_2)g	73.80		70.50
Mass of Pycnometer full of water (m_4)g	145.12		142.90
Mass of empty Pycnometer (m_1)g	46.30		45.80
Mass of soil (m_2-m_1)g	27.50		24.70
Mass of water in full Pycnometer (m_4-m_1)g	98.82		97.10
Mass of water used (m_3-m_2)g	88.60		88.10
Volume of soil particles (m_4-m_1)- (m_3-m_2)ml	10.22		9
Tx, suspension Temperature ,^{0}C	22.50		22.50
Correction factor value, K	0.9996		0.9996
Specific Gravity =(m_2-m_1)/ ((m_4-m_1)- (m_3-m_2))	**2.69**		**2.74**
Average	**2.72**		

B5. Specific Gravity test for Rufa'el sample #1

Location: ***Rufa'el area (primary school)***		Job ref.	***Thesis research***
Soil Description: ***Red clay***		Sample no.	**#1**
		Depth	**1.5m**
Test method : Small pycnometer ASTM standard: D 854-98		Date	21/06/2016.
Specimen ref.		#1	#2
Pycnometer number.		A6	B7
Mass of Pycnometer + soil + water (m_3)g		160.59	160.47
Mass of Pycnometer + soil (m_2)g		70.80	70.8
Mass of Pycnometer full of water (m_4)g		144.83	144.81
Mass of empty Pycnometer (m_1)g		45.80	45.80
Mass of soil (m_2-m_1)g		25.00	25.00
Mass of water in full Pycnometer (m_4-m_1)g		99.03	99.01
Mass of water used (m_3-m_2)g		89.79	89.67
Volume of soil particles (m_4-m_1)- (m_3-m_2)ml		9.24	9.34
Tx, suspension Temperature ,^{0}C		21.10	21.10
Correction factor value, K		0.9998	0.9998
Specific Gravity =(m_2-m_1)/ ((m_4-m_1)- (m_3-m_2))		**2.71**	**2.68**
Average		**2.69**	

B6. Specific Gravity test for Rufa'el sample #2

Location: ***Rufa'el area (primary school)***		Job ref.	***Thesis research***
Soil Description: ***Red clay***		Sample no.	**#2**
		Depth	**3m**
Test method : Small pycnometer ASTM standard: D 854-98		Date	21/06/2016.
Specimen ref.		#1	#2
Pycnometer number.		A6	B7
Mass of Pycnometer + soil + water (m_3)g		161.25	161.16
Mass of Pycnometer + soil (m_2)g		70.80	70.8
Mass of Pycnometer full of water (m_4)g		145.48	145.36
Mass of empty Pycnometer (m_1)g		45.80	45.80
Mass of soil (m_2-m_1)g		25.00	25.00
Mass of water in full Pycnometer (m_4-m_1)g		99.68	99.56
Mass of water used (m_3-m_2)g		90.45	90.36
Volume of soil particles (m_4-m_1)- (m_3-m_2)ml		9.23	9.20
Tx, suspension Temperature ,^{0}C		21.10	21.10
Correction factor value, K		0.9998	0.9998
Specific Gravity =(m_2-m_1)/ ((m_4-m_1)- (m_3-m_2))		**2.71**	**2.72**
Average		**2.71**	

C. Atterberg limits Determination

C1. Liquid limit test for kolfe sample #1

Location: ***Kolfe area (bethel)***	Job ref.	***Thesis research***
Soil Description: ***Red clay***	Sample no.	**#1**
	Depth	**1.5m**
Test method : air dried, ASTM standard: D 4318-98	Date	09/04/2016.

Plastic limit test		
Test no.	#1	#2
Container no.	142	136
Mass of wet soil + container (m_2)g	47.20	48.10
Mass of dry soil + container (m_3)g	44.50	45.20
Mass of container (m_1)g	33.60	33.70
Mass of moisture(Water) (m_2-m_3)g	2.70	2.90
Mass of dry soil (m_3-m_1)g	10.90	11.50
Moisture content = (m_2-m_3)/ (m_3-m_1)*100, %	**24.80**	**25.20**
Average (%)	**25**	

Liquid Limit test				
Test no.	#1	#2	#3	#4
Container no.	106	52.40	55.50	54.80
Mass of wet soil + container (m_2)g	52.50	52.40	55.50	54.80
Mass of dry soil + container (m_3)g	45.30	45.30	47.10	46.80
Mass of container (m_1)g	33.10	33.40	33.20	33.60
Mass of moisture(Water) (m_2-m_3)g	7.20	7.10	8.40	8.00
Mass of dry soil (m_3-m_1)g	12.20	11.90	13.90	13.20
Moisture content = (m_2-m_3)/ (m_3-m_1)*100, %	59.00	59.70	60.40	60.60
No. of blows	35	27	21	17

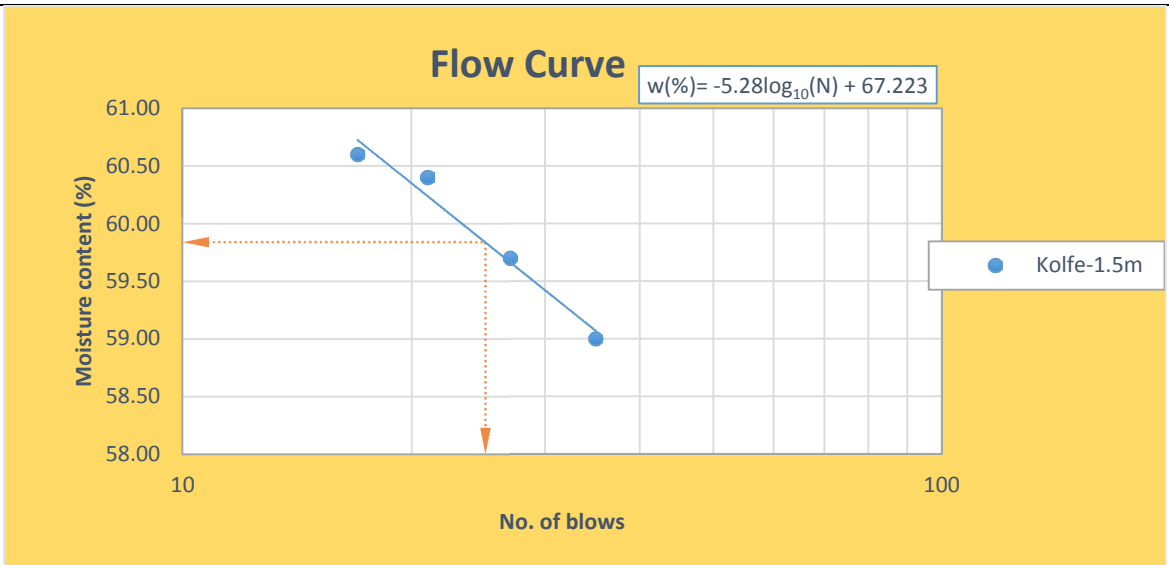

$w(\%)= -5.28\log_{10}(25)+67.233 = 59.84$		
LL=60	**PL=25**	**PI**=LL-PL=**35**

C2. Liquid limit test for kolfe sample #2

Location: ***Kolfe area (bethel)***	Job ref.	***Thesis research***
Soil Description: ***Red clay***	Sample no.	**#2**
	Depth	**3m**
Test method : air dried, ASTM standard: D 4318-98	Date	16/04/2016.

Plastic limit test		
Test no.	#1	#2
Container no.	128	101
Mass of wet soil + container (m_2)g	40.40	39.80
Mass of dry soil + container (m_3)g	38.90	38.50
Mass of container (m_1)g	32.90	32.90
Mass of moisture(Water) (m_2-m_3)g	1.50	1.30
Mass of dry soil (m_3-m_1)g	6.00	5.60
Moisture content = (m_2-m_3)/ (m_3-m_1)*100, %	**25.00**	**23.20**
Average (%)	**24**	

Liquid Limit test				
Test no.	#1	#2	#3	#4
Container no.	112	168	147	94
Mass of wet soil + container (m_2)g	54.40	52.70	51.10	54.60
Mass of dry soil + container (m_3)g	45.40	44.70	43.50	45.70
Mass of container (m_1)g	32.80	33.70	33.20	34.00
Mass of moisture(Water) (m_2-m_3)g	9.00	8.00	7.60	8.90
Mass of dry soil (m_3-m_1)g	12.60	11.00	10.30	11.70
Moisture content = (m_2-m_3)/ (m_3-m_1)*100, %	71.40	72.70	73.80	76.10
No. of blows	34	28	22	18

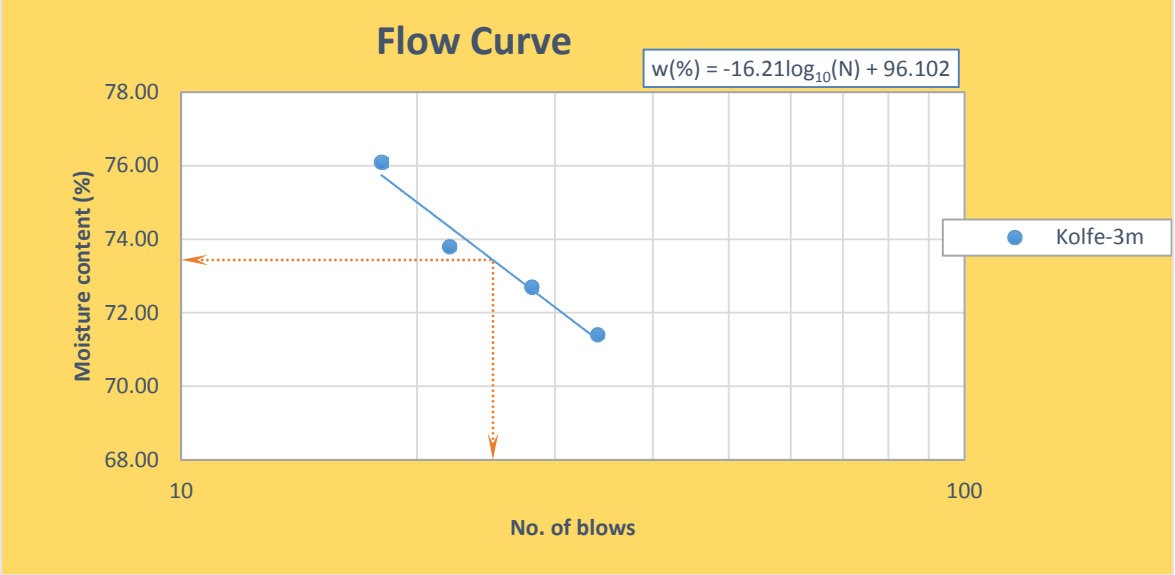

w(%) = -16.21$\log_{10}$(25) + 96.102 = 73.44		
LL = 73	**PL = 24**	**PI** = LL-PL= **49**

C3. Liquid limit test for Addisu-Gebeya sample #1

Location: ***Addisu-Gebeya area (Hamle19/67 primary school)***	Job ref.	***Thesis research***
Soil Description: ***Red clay***	Sample no.	**#1**
	Depth	**1.5m**
Test method : air dried, ASTM standard: D 4318-98	Date	21/04/2016.

Plastic limit test

Test no.	#1	#2
Container no.	C13	D114
Mass of wet soil + container (m_2)g	21.05	18.92
Mass of dry soil + container (m_3)g	19.89	17.80
Mass of container (m_1)g	15.88	13.69
Mass of moisture(Water) (m_2-m_3)g	1.16	1.12
Mass of dry soil (m_3-m_1)g	4.01	4.11
Moisture content = (m_2-m_3)/ (m_3-m_1)*100, %	**28.90**	**27.30**
Average (%)	**28**	

Liquid Limit test

Test no.	#1	#2	#3	#4
Container no.	C18	E3	D5	C54
Mass of wet soil + container (m_2)g	49.56	50.39	45.24	54.80
Mass of dry soil + container (m_3)g	36.28	36.86	33.89	39.80
Mass of container (m_1)g	15.69	15.65	15.75	15.59
Mass of moisture(Water) (m_2-m_3)g	13.28	13.53	11.35	15.00
Mass of dry soil (m_3-m_1)g	20.59	21.21	18.14	24.21
Moisture content = (m_2-m_3)/ (m_3-m_1)*100, %	64.50	63.8	62.60	62.00
No. of blows	16	21	24	28

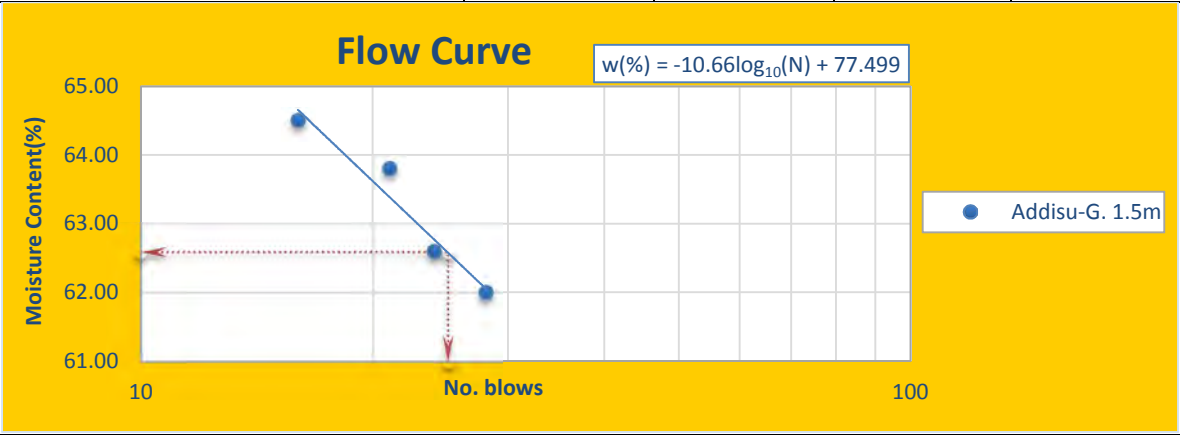

w(%) = -10.66log$_{10}$(25) + 77.499 = 62.59		
LL=63	**PL=28**	**PI**=LL-PL=**35**

C4. Liquid limit test for Addisu-Gebeya sample #2

Location: ***Addisu-Gebeya area (Hamle19/67 primary school).***	Job ref.	***Thesis research***
Soil Description: ***Red clay***	Sample no.	**#2**
	Depth	**3m**
Test method : air dried, ASTM standard: D 4318-98	Date	22/04/2016.

Plastic limit test

Test no.	#1	#2
Container no.	H77	B1
Mass of wet soil + container (m_2)g	21.17	19.02
Mass of dry soil + container (m_3)g	19.89	18.14
Mass of container (m_1)g	15.65	15.50
Mass of moisture(Water) (m_2-m_3)g	1.28	0.88
Mass of dry soil (m_3-m_1)g	4.28	2.64
Moisture content = (m_2-m_3)/ (m_3-m_1)*100, %	**30.20**	**33.30**
Average (%)	**32**	

Liquid Limit test

Test no.	#1	#2	#3	#4
Container no.	D3C3	H5	102	A20
Mass of wet soil + container (m_2)g	47.17	43.29	46.11	43.46
Mass of dry soil + container (m_3)g	33.95	31.82	33.79	30.47
Mass of container (m_1)g	15.70	15.50	15.70	10.70
Mass of moisture(Water) (m_2-m_3)g	13.22	11.47	12.32	12.99
Mass of dry soil (m_3-m_1)g	18.25	16.32	18.09	19.77
Moisture content = (m_2-m_3)/ (m_3-m_1)*100, %	72.4	70.3	68.1	65.7
No. of blows	17	20	25	27

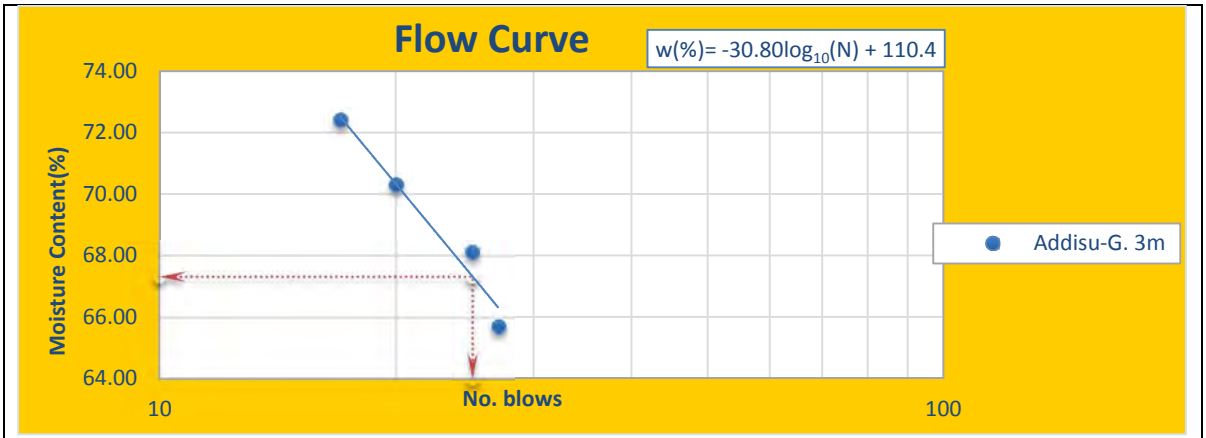

w(%)= -30.80log$_{10}$(25) + 110.4 = 67.33		
LL = 67	**PL = 32**	**PI** = LL – PL = **35**

C5. Liquid limit test for Rufa'el sample #1

Location: ***Rufa'el area (primary school).***	Job ref.		***Thesis research***	
Soil Description: ***Red clay***	Sample no.		**#1**	
	Depth		**1.5m**	
Test method : air dried, ASTM standard: D 4318-98	Date		25/06/2016.	
Plastic limit test				
Test no.	#1	#2	#3	
Container no.	C9	P2	19	
Mass of wet soil + container (m_2)g	21.70	22.50	26.80	
Mass of dry soil + container (m_3)g	20.00	20.90	24.30	
Mass of container (m_1)g	14.10	15.40	15.60	
Mass of moisture(Water) (m_2-m_3)g	5.90	1.60	2.50	
Mass of dry soil (m_3-m_1)g	1.70	5.50	8.70	
Moisture content = (m_2-m_3)/ (m_3-m_1)*100, %	**28.80**	**29.10**	**28.70**	
Average (%)	**29**			
Liquid Limit test				
Test no.	#1	#2	#3	#4
Container no.	WB	D58	19	4
Mass of wet soil + container (m_2)g	30.80	30.60	30.10	28.40
Mass of dry soil + container (m_3)g	25.30	25.10	24.70	23.40
Mass of container (m_1)g	16.00	15.90	15.70	15.20
Mass of moisture(Water) (m_2-m_3)g	5.50	5.50	5.41	5.00
Mass of dry soil (m_3-m_1)g	9.30	9.20	9.00	8.20
Moisture content = (m_2-m_3)/ (m_3-m_1)*100, %	59.10	59.8	60.10	61
No. of blows	35	29	24	18

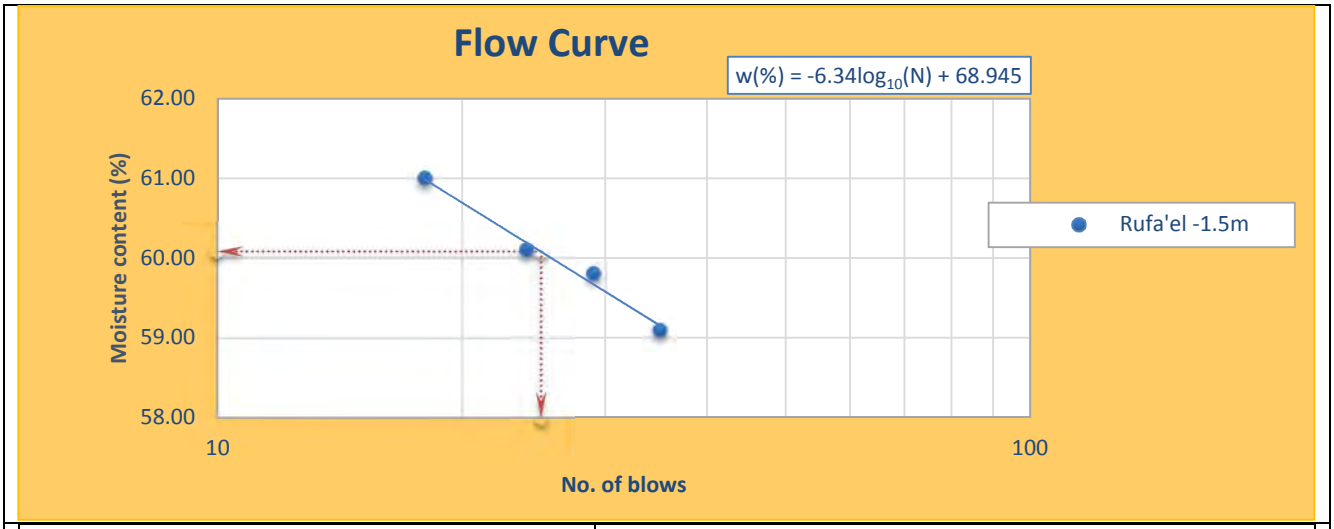

w(%) = -6.34log$_{10}$(25) + 68.945 =60.08		
LL = 60	**PL = 29**	**PI** = LL – PL = **31**

C6. Liquid limit test for Rufa'el sample #2

Location: ***Rufa'el area (primary school).***	Job ref.	***Thesis research***
Soil Description: ***Red clay***	Sample no.	**#2**
	Depth	**3m**
Test method : air dried, ASTM standard: D 4318-98	Date	26/06/2016.

Plastic limit test			
Test no.	#1	#2	#3
Container no.	201	14	AH
Mass of wet soil + container (m_2)g	30.30	30.70	32.00
Mass of dry soil + container (m_3)g	26.90	27.20	28.30
Mass of container (m_1)g	15.70	15.70	15.40
Mass of moisture(Water) (m_2-m_3)g	3.40	3.50	3.70
Mass of dry soil (m_3-m_1)g	11.20	11.50	12.90
Moisture content = (m_2-m_3)/ (m_3-m_1)*100, %	**30.40**	**30.40**	**28.70**
Average (%)	**30**		

Liquid Limit test				
Test no.	#1	#2	#3	#4
Container no.	W35	G15	T4	19
Mass of wet soil + container (m_2)g	31.70	30.30	35.60	31.20
Mass of dry soil + container (m_3)g	25.20	23.68	27.30	24.70
Mass of container (m_1)g	15.70	14.20	15.70	15.80
Mass of moisture(Water) (m_2-m_3)g	6.50	6.62	8.30	6.50
Mass of dry soil (m_3-m_1)g	9.50	9.48	11.60	8.90
Moisture content = (m_2-m_3)/ (m_3-m_1)*100, %	68.40	69.80	71.60	73.00
No. of blows	35	28	24	17

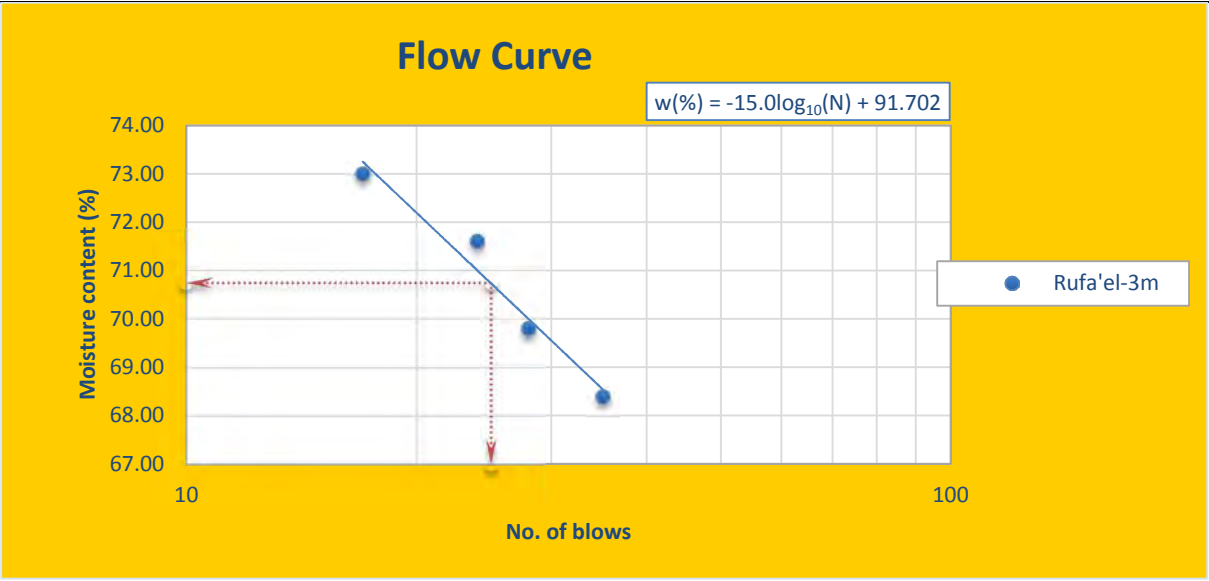

w(%) = -15.0log$_{10}$(25) + 91.702 = 70.73		
LL = 71	**PL = 30**	**PI** = LL - PL = **41**

D. Particle Size Analysis

D1. Grain size analysis for Kolfe sample #1

Location: ***Kolfe area (bethel)***	Job ref.	***Thesis research***
Soil Description: ***Red clay***	Sample no.	**#1**
	Depth	**1.5m**
Test method : **ASTM standard: D 422-63**		

Sieve Analysis

	Date	***16/04/2016***
	Total mass of sample	***500g***

Sieve Number	Diameter (mm)	Mass of empty sieve (g)	Mass of Sieve+ Soil Retained (g)	Soil Retained (g)	Percent Retained %	Percent Passing %
4	4.75	1263.5	1263.5	0	0	100
8	2.36	983.9	984.3	0.4	0.08	99.92
16	1.18	895	895.5	0.5	0.1	99.82
30	0.6	831.5	833.5	2	0.4	99.42
50	0.3	754.5	759	4.5	0.9	98.52
100	0.15	779.6	785.3	5.7	1.14	97.38
200	0.075	731.2	737.4	6.2	1.24	96.14
pan	-	708.7				-

Hydrometer Analysis

Specific gravity	***2.60***	Date	***18/04/2016***
Mass of sample	***50g***	Hydrometer type	***151H***

Elapsed time (min)	Test Temperature, deg.c	Actual Hydrometer Reading	Composite correction	Corrected Hydrometer Reading	Effective Depth (cm)	Coefficient K	Grain Size (mm)	Percent Finer (%)	Percent Finer Combined (%)
0.5	19	1.0333	-0.0029	1.0304	7.49	0.01403	0.0543	98.80	94.99
1	19	1.0331	-0.0029	1.0302	7.54	0.01403	0.0385	98.15	94.36
2	19	1.0325	-0.0029	1.0296	7.70	0.01403	0.0275	96.20	92.49
4	19	1.0310	-0.0029	1.0281	8.10	0.01403	0.0200	91.33	87.80
8	19	1.0298	-0.0029	1.0269	8.42	0.01403	0.0144	87.43	84.05
15	19	1.0290	-0.0029	1.0261	8.63	0.01403	0.0106	84.83	81.55
30	19	1.0273	-0.0029	1.0244	9.08	0.01403	0.0077	79.30	76.24
60	19	1.0260	-0.0029	1.0231	9.42	0.01403	0.0056	75.08	72.18
120	19	1.0246	-0.0029	1.0217	9.79	0.01403	0.0040	70.53	67.80
240	20	1.0232	-0.0027	1.0205	10.16	0.01386	0.0029	66.63	64.05
480	21.7	1.0220	-0.00236	1.0196	10.48	0.01358	0.0020	63.83	61.37
1440	21.1	1.0205	-0.00248	1.0180	10.88	0.01367	0.0012	58.56	56.30

Kolfe 1.5m Grain size distribution curve

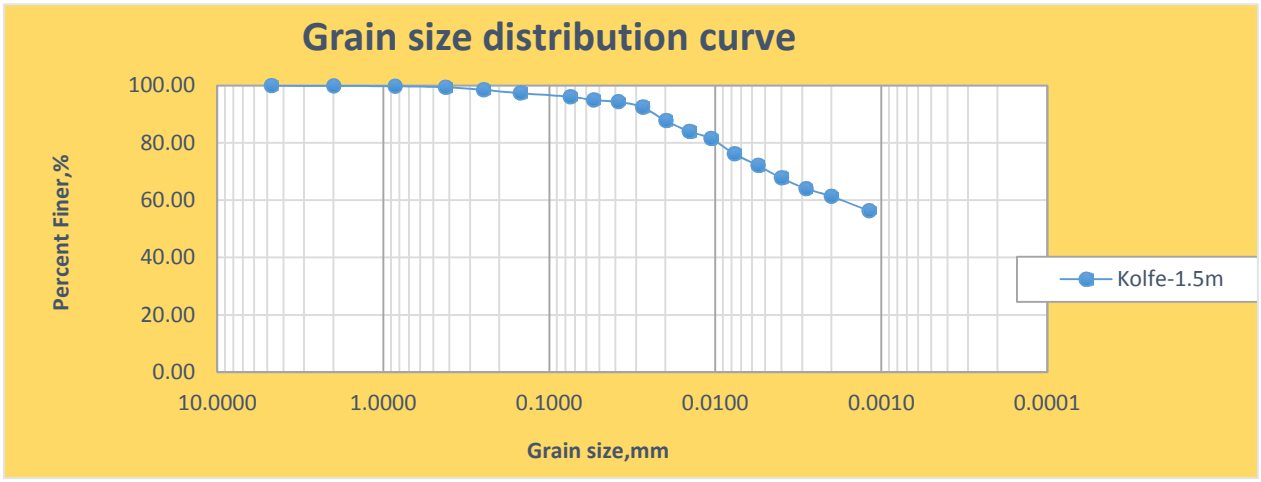

D2. Grain size analysis for Kolfe sample #2

Location: ***Kolfe area (bethel)***	Job ref.	***Thesis research***
Soil Description: ***Red clay***	Sample no.	**#2**
	Depth	**3m**
Test method : **ASTM standard: D 422-63**		

Sieve Analysis

	Date	***16/04/2016***
	Total mass of sample	***500g***

Sieve Number	Diameter (mm)	Mass of empty sieve (g)	Mass of Sieve+ Soil Retained (g)	Soil Retained (g)	Percent Retained %	Percent Passing %
4	4.75	1263.5	1263.5	0	0	100
8	2.36	983.9	986.9	3	0.6	99.4
16	1.18	895	898.9	3.9	0.78	98.62
30	0.6	831.5	836.7	5.2	1.04	97.58
50	0.3	754.5	759.6	5.1	1.02	96.56
100	0.15	779.6	784.8	5.2	1.04	95.52
200	0.075	731.2	737.6	6.4	1.28	94.24
pan	-	708.7				-

Hydrometer Analysis

	Specific gravity	***2.74***	Date	***18/04/2016***
	Mass of sample	***50g***	Hydrometer type	***151H***

Elapsed Time (min)	Test Temperature, deg.c	Actual Hydrometer Reading	Composite Correction	Corrected Hydrometer Reading	Effective Depth (cm)	Coefficient K	Grain Size (mm)	Percent Finer (%)	Perc. Finer Combined (%)
0.5	19	1.0330	-0.0029	1.0301	7.57	0.01346	0.0524	97.83	92.19
1	19	1.0325	-0.0029	1.0296	7.70	0.01346	0.0374	96.20	90.66
2	19	1.0314	-0.0029	1.0285	7.99	0.01346	0.0269	92.63	87.29
4	19	1.0305	-0.0029	1.0276	8.23	0.01346	0.0193	89.70	84.53
8	19	1.0290	-0.0029	1.0261	8.63	0.01346	0.0140	84.83	79.94
15	19	1.0283	-0.0029	1.0254	8.81	0.01346	0.0103	82.55	77.80
30	19	1.0270	-0.0029	1.0241	9.16	0.01346	0.0074	78.33	73.81
60	19	1.0256	-0.0029	1.0227	9.53	0.01346	0.0054	73.78	69.53
120	19	1.0245	-0.0029	1.0216	9.82	0.01346	0.0039	70.20	66.16
240	20	1.0231	-0.0025	1.0206	10.19	0.01329	0.0027	66.95	63.09
480	21.7	1.0221	-0.00236	1.0197	10.45	0.01302	0.0019	64.16	60.46
1440	21.1	1.0210	-0.00248	1.0185	10.75	0.01311	0.0011	60.19	56.72

Kolfe 3m Grain size distribution curve

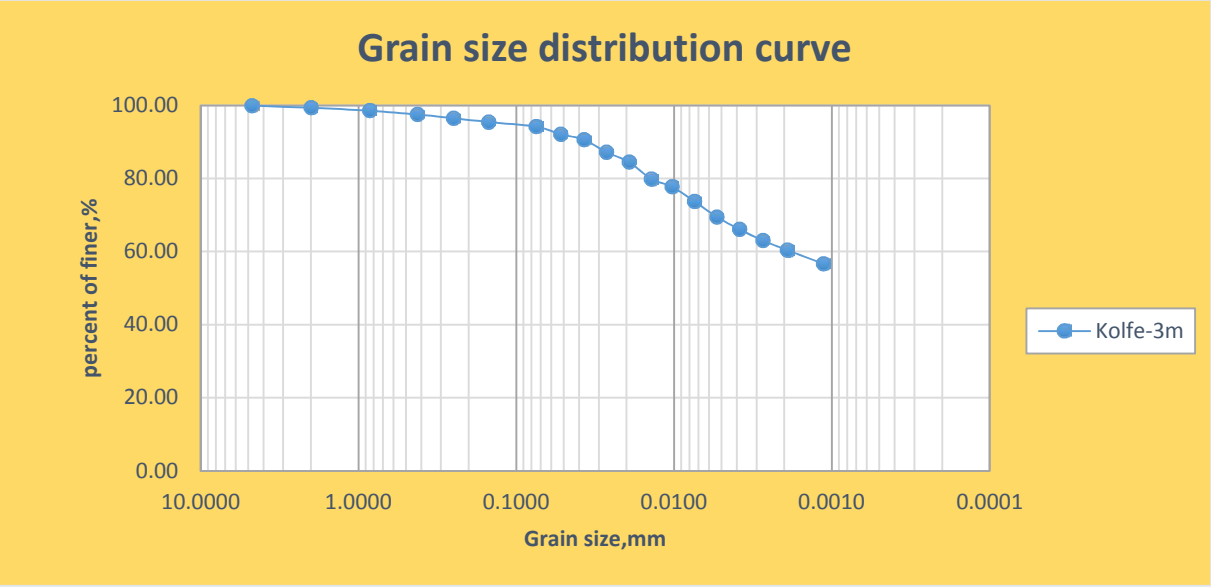

D3. Grain size analysis for Addisu-Gebeya sample #1

Location: ***Addisu-Gebeya area***	Job ref.	***Thesis research***
Soil Description: ***Red clay***	Sample no.	**#1**
	Depth	**1.5m**
Test method : **ASTM standard: D 422-63**		

Sieve Analysis

	Date	***09/05/2016***
	Total mass of sample	***1000g***

Sieve Number	Diameter (mm)	Mass of empty sieve (g)	Mass of Sieve+ Soil Retained (g)	Soil Retained (g)	Percent Retained %	Percent Passing %
4	4.75	1263.5	1269.1	5.6	0.56	99.44
8	2.36	983.9	993.6	9.7	0.97	98.47
16	1.18	895	905.2	10.2	1.02	97.45
30	0.6	831.5	844	12.5	1.25	96.2
50	0.3	754.5	774.7	20.2	2.02	94.18
100	0.15	779.6	801.2	21.6	2.16	92.02
200	0.075	731.2	771.1	39.9	3.99	88.03
pan	-	708.7	708.7	0	0	-

Hydrometer Analysis

	Specific gravity	***2.75***	Date	***10/05/2016***
	Mass of sample	***50g***	Hydrometer type	***151H***

Elapsed Time (min)	Test Temperature, deg.c	Actual Hydrometer Reading	Composite Correction	Corrected Hydrometer Reading	Effective Depth (cm)	Coefficient K	Grain Size (mm)	Percent Finer (%)	Perc. Finer Combined (%)
0.5	19	1.0325	-0.0029	1.0296	7.70	0.01342	0.0430	93.03	81.89
1	19	1.0320	-0.0029	1.0291	7.84	0.01342	0.0376	91.46	80.51
2	19	1.0315	-0.0029	1.0286	7.97	0.01342	0.0268	89.89	79.13
4	18	1.0310	-0.0031	1.0279	8.10	0.01359	0.0193	87.69	77.19
8	18	1.0300	-0.0031	1.0269	8.36	0.01359	0.0139	84.54	74.42
15	18	1.0295	-0.0031	1.0264	8.50	0.01359	0.0102	82.97	73.04
30	19	1.0280	-0.0029	1.0251	8.89	0.01342	0.0073	78.89	69.44
60	19	1.0270	-0.0029	1.0241	9.16	0.01342	0.0052	75.74	66.68
120	20	1.0260	-0.0027	1.0233	9.42	0.01325	0.0037	73.23	64.46
240	21	1.0255	-0.0025	1.0230	9.55	0.01309	0.0026	72.29	63.63
480	21	1.0240	-0.0025	1.0215	9.95	0.01309	0.0019	67.57	59.48
1440	21	1.0230	-0.0025	1.0205	10.22	0.01309	0.0011	64.43	56.72

Addisu-Gebeya 1.5m Grain size distribution curve

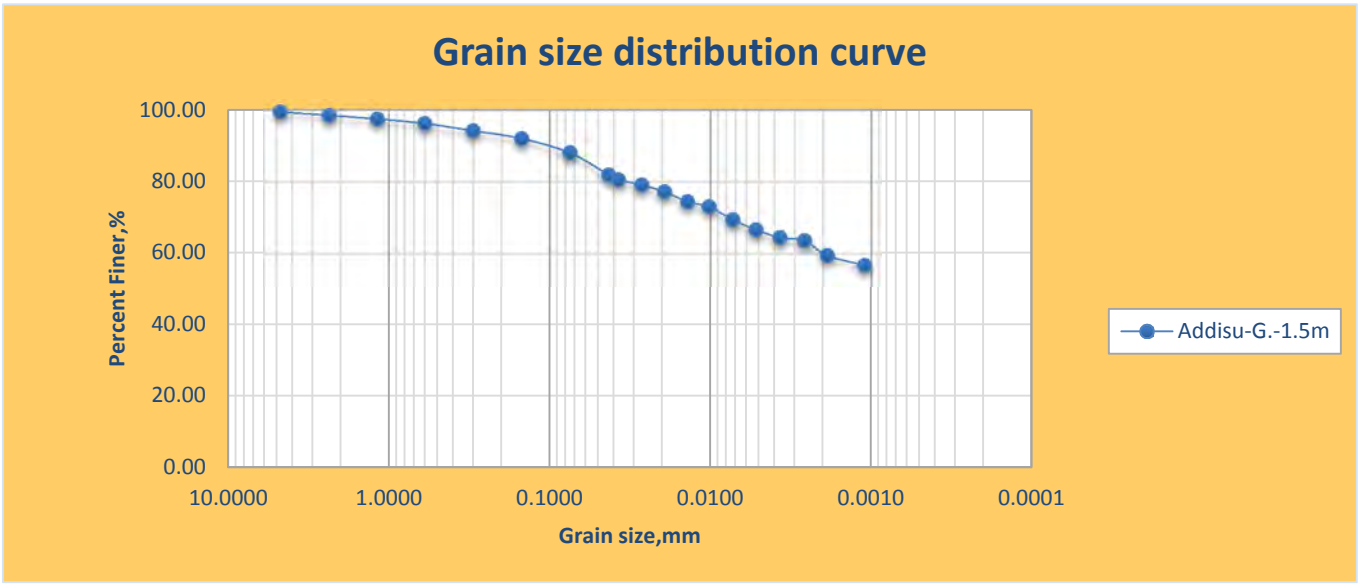

D4. Grain size analysis for Addisu-Gebeya sample #2

Location: ***Addisu-Gebeya area***	Job ref.	***Thesis research***
Soil Description: ***Red clay***	Sample no.	**#2**
	Depth	**3m**
Test method : **ASTM standard: D 422-63**		

Sieve Analysis

	Date	***09/05/2016***
	Total mass of sample	***1000g***

Sieve Number	Diameter (mm)	Mass of empty sieve (g)	Mass of Sieve+ Soil Retained (g)	Soil Retained (g)	Percent Retained %	Percent Passing %
4	4.75	1263.5	1271.5	8	0.8	99.2
8	2.36	983.9	994.3	10.4	1.04	98.16
16	1.18	895	903.4	8.4	0.84	97.32
30	0.6	831.5	849.5	18	1.8	95.52
50	0.3	754.5	765.5	11	1.1	94.42
100	0.15	779.6	798.4	18.8	1.88	92.54
200	0.075	731.2	748	16.8	1.68	90.86
pan	-	708.7	708.7	0	0	-

Hydrometer Analysis

	Specific gravity	***2.72***	Date	***10/05/2016***
	Mass of sample	***50g***	Hydrometer type	***151H***

Elapsed Time (min)	Test Temperature, deg.c	Actual Hydrometer Reading	Composite Correction	Corrected Hydrometer Reading	Effective Depth (cm)	Coefficient K	Grain Size (mm)	Percent Finer (%)	Perc. Finer Combined (%)
0.5	18	1.0322	-0.0031	1.0296	7.65	0.0137	0.0438	93.62	85.06
1	18	1.0320	-0.0031	1.0289	7.84	0.0137	0.0383	91.40	83.05
2	18	1.0315	-0.0031	1.0284	7.97	0.0137	0.0273	89.82	81.61
4	18	1.0310	-0.0031	1.0279	8.10	0.0137	0.0195	88.24	80.18
8	18	1.0290	-0.0031	1.0259	8.63	0.0137	0.0142	81.92	74.43
15	19	1.0280	-0.0029	1.0251	8.89	0.01388	0.0107	79.39	72.13
30	19	1.0265	-0.0029	1.0236	9.29	0.01388	0.0077	74.64	67.82
60	19	1.0252	-0.0029	1.0223	9.63	0.01388	0.0056	70.53	64.08
120	20	1.0240	-0.0027	1.0213	9.95	0.013704	0.0039	67.37	61.21
240	21	1.0230	-0.0025	1.0205	10.22	0.013534	0.0028	64.84	58.91
480	21	1.0220	-0.0025	1.0195	10.48	0.013534	0.0020	61.67	56.04
1440	20	1.0210	-0.0027	1.0183	10.75	0.013704	0.0012	57.88	52.59

Addisu-Gebeya 3m Grain size distribution curve

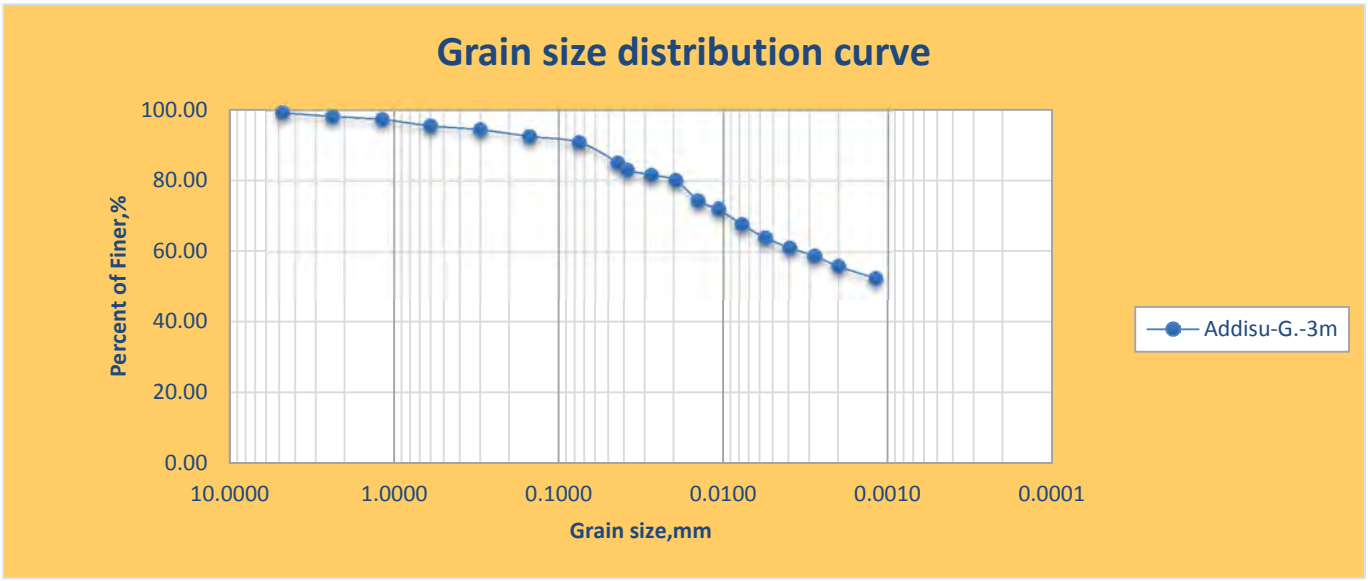

D5. Grain size analysis for Rufa'el sample #1

Location: ***Rufa'el area***	Job ref.	***Thesis research***
Soil Description: ***Red clay***	Sample no.	**#1**
	Depth	**1.5m**
Test method : **ASTM standard: D 422-63**		

Sieve Analysis

	Date	***30/05/2016***
	Total mass of sample	***1000g***

Sieve Number	Diameter Of sieve (mm)	Mass of empty sieve (g)	Mass of Sieve+ Soil Retained (g)	Soil Retained (g)	Percent Retained %	Percent Passing %
4	4.75	1263.5	1284.8	21.3	2.13	97.87
8	2.36	983.9	1002	18.1	1.81	96.06
16	1.18	895	903.5	8.5	0.85	95.21
30	0.6	831.5	847	15.5	1.55	93.66
50	0.3	754.5	780.7	26.2	2.62	91.04
100	0.15	779.6	813.1	33.5	3.35	87.69
200	0.075	731.2	752.3	21.1	2.11	85.58
pan	-	708.7	708.7	-		-

Hydrometer Analysis

	Specific gravity	***2.69***	Date	***07/06/2016***
	Mass of sample	***50g***	Hydrometer type	***151H***

Elapsed Time (min)	Test Temperature, deg.c	Actual Hydrometer Reading	Composite Correction	Corrected Hydrometer Reading	Effective Depth (cm)	Coefficient K	Grain Size (mm)	Percent Finer (%)	Perc. Finer Combined (%)
0.5	19	1.0335	-0.0029	1.0306	7.44	0.013652	0.0527	97.41	83.37
1	19	1.0332	-0.0029	1.0303	7.52	0.013652	0.0374	96.46	82.55
2	19	1.0331	-0.0029	1.0302	7.54	0.013652	0.0265	96.14	82.28
4	19	1.0330	-0.0029	1.0301	7.57	0.013652	0.0188	95.82	82.00
8	19	1.0320	-0.0029	1.0291	7.84	0.013652	0.0135	92.64	79.28
15	19	1.0315	-0.0029	1.0286	7.97	0.013652	0.0099	91.05	77.92
30	19	1.0310	-0.0029	1.0281	8.10	0.013652	0.0071	89.45	76.56
60	19.5	1.0300	-0.0028	1.0272	8.36	0.013567	0.0051	86.59	74.10
120	21	1.0280	-0.0025	1.0255	8.89	0.01332	0.0036	81.18	69.47
240	21	1.0275	-0.0025	1.0250	9.03	0.01332	0.0026	79.59	68.11
480	21	1.0265	-0.0025	1.0240	9.29	0.01332	0.0019	76.40	65.39

1440	20	1.0255	-0.0027	1.0228	9.55	0.013482	0.0011	72.58	62.12

Rufa'el 1.5m Grain size distribution curve

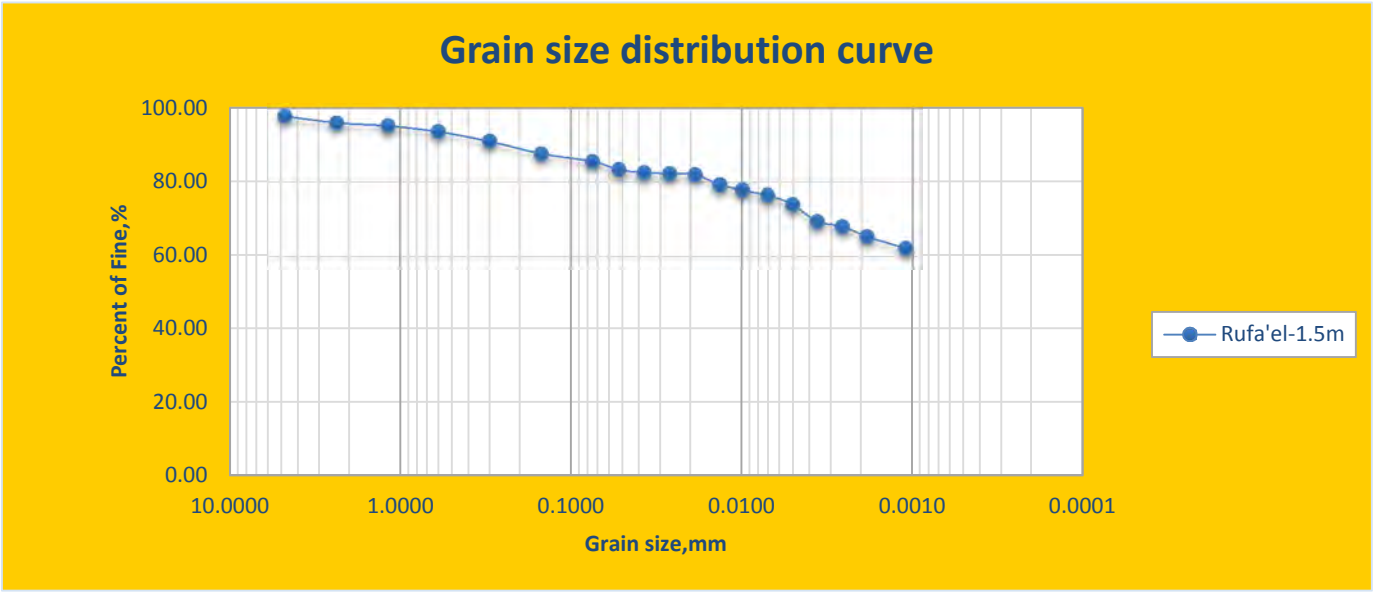

D6. Grain size analysis for Rufa'el sample #2

Location: ***Rufa'el area***	Job ref.	***Thesis research***
Soil Description: ***Red clay***	Sample no.	**#2**
	Depth	**3m**
Test method : **ASTM standard: D 422-63**		

Sieve Analysis

	Date	***30/05/2016***
	Total mass of sample	***1000g***

Sieve Number	Diameter (mm)	Mass of empty sieve (g)	Mass of Sieve+ Soil Retained (g)	Soil Retained (g)	Percent Retained %	Percent Passing %
4	4.75	1263.5	1264.4	0.9	0.09	99.91
8	2.36	983.9	987.7	3.8	0.38	99.53
16	1.18	895	899.4	4.4	0.44	99.09
30	0.6	831.5	839.2	7.7	0.77	98.32
50	0.3	754.5	781.3	26.8	2.68	95.64
100	0.15	779.6	828.8	49.2	4.92	90.72
200	0.075	731.2	767.7	36.5	3.65	87.07
pan	-	708.7	708.7	0	0	-

Hydrometer Analysis

	Specific gravity	***2.71***	Date	***07/06/2016***
	Mass of sample	***50g***	Hydrometer type	***151H***

Elapsed Time (min)	Test Temperature, deg.c	Actual Hydrometer Reading	Composite Correction	Corrected Hydrometer Reading	Effective Depth (cm)	Coefficient K	Grain Size (mm)	Perc. Finer (%)	Perc. Finer Combined (%)
0.5	19	1.0333	-0.0029	1.0304	7.49	0.013572	0.0525	96.36	83.90
1	19	1.0332	-0.0029	1.0303	7.52	0.013572	0.0372	96.04	83.62
2	19	1.0330	-0.0029	1.0301	7.57	0.013572	0.0264	95.40	83.07
4	18.5	1.0320	-0.003	1.0290	7.84	0.013657	0.0191	91.92	80.03
8	18.5	1.0310	-0.003	1.0280	8.10	0.013657	0.0137	88.75	77.27
15	18.5	1.0300	-0.003	1.0270	8.36	0.013657	0.0102	85.58	74.51
30	19	1.0290	-0.0029	1.0261	8.63	0.013572	0.0073	82.73	72.03
60	19	1.0280	-0.0029	1.0251	8.89	0.013572	0.0052	79.56	69.27
120	21	1.0270	-0.0025	1.0245	9.16	0.013242	0.0037	77.65	67.61
240	21	1.0250	-0.0025	1.0225	9.69	0.013242	0.0027	71.32	62.09
480	21	1.0240	-0.0025	1.0215	9.95	0.013242	0.0019	68.15	59.33
1440	20	1.0230	-0.0027	1.0203	10.22	0.013402	0.0011	64.34	56.02

Rufa'el 3m Grain size distribution curve

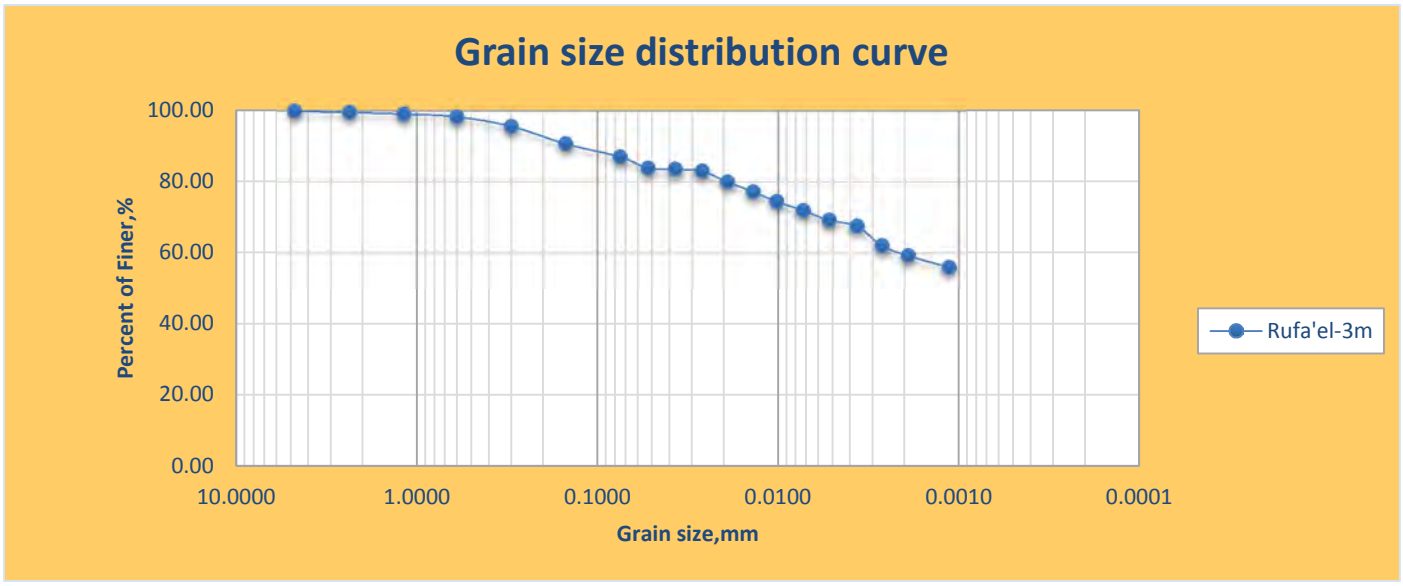

E. Conventional Incremental Load (CIL) Consolidation test.

E1. One dimensional consolidation test for kolfe sample @3m, k-2

Load increment: 25kpa

Elapsed Time (min)	Deformation Dial Reading (mm)
0	2.264
0.1	2.319
0.25	2.322
0.5	2.324
1	2.327
2	2.331
4	2.335
8	2.34
15	2.344
30	2.348
60	2.353
120	2.36
240	2.366
480	2.374
1440	2.385

Initial Height, H_O	20mm
Final height, H_f	19.879mm
Deformation	0.121mm

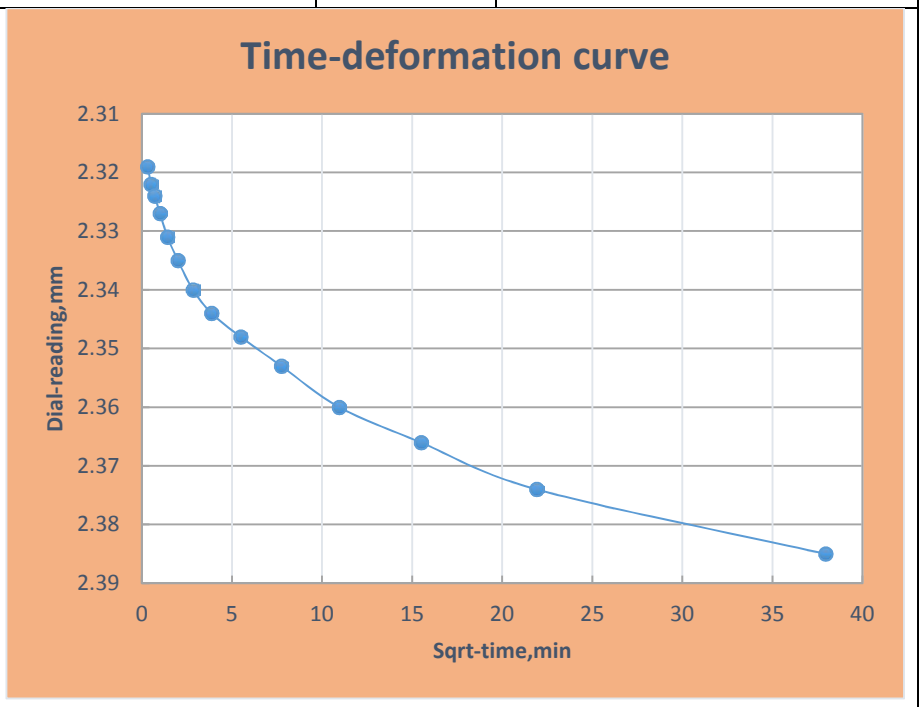

	d_o	=2.32mm	$\sqrt{t_{90}}$=3.87=15min	T=0.848	$C_V=(0.848* H_{avg}^2)/ t_{90}$
	d_{90}	=2.344mm	H_{avg}=19.9395mm		C_V=0.003746cm²/sec

Load increment: 50kpa

Elapsed Time (min)	Deformation Dial Reading (mm)
0	2.385
0.1	2.41
0.25	2.411
0.5	2.4125
1	2.4149
2	2.4173
4	2.4198
8	2.4221
15	2.4248
30	2.4282
60	2.4306
120	2.4324
240	2.4346
480	2.4362
1440	2.4392

Initial Height, H_O	19.879mm				
Final height, H_f	19.8248mm				
Deformation	0.0542mm				
	d_o	=2.409mm	$\sqrt{t_{90}}$=4.13=17min	T=0.848	$C_V=(0.848* H_{avg}^2)/ t_{90}$
	d_{90}	=2.425mm	H_{avg}=19.8519mm		C_V=0.003273cm²/sec

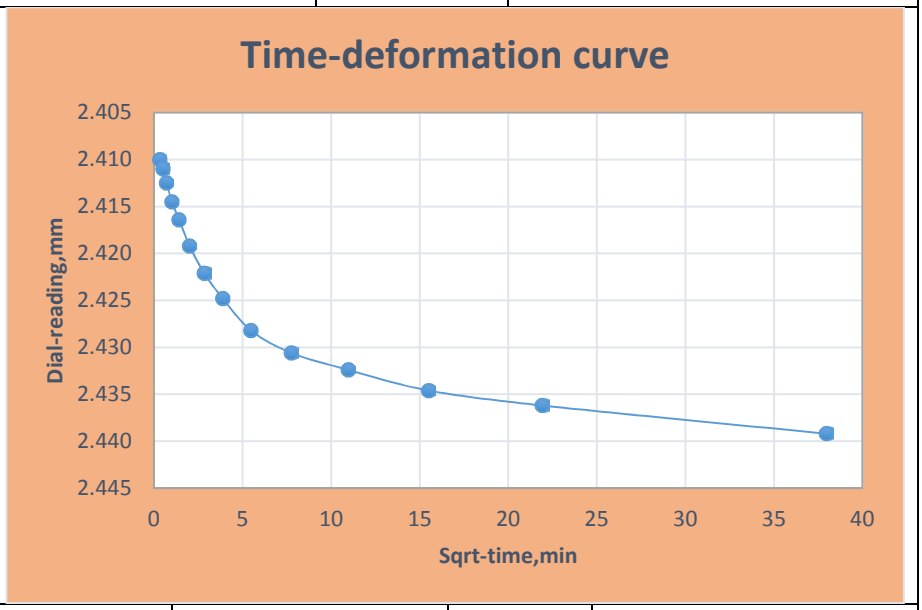

Load increment: 100kpa

Elapsed Time (min)	Deformation Dial Reading (mm)
0	2.4392
0.1	2.4782
0.25	2.4813
0.5	2.4854
1	2.4886
2	2.4917
4	2.4956
8	2.500
15	2.5043
30	2.5092
60	2.5153
120	2.5217
240	2.5301
480	2.5361
1440	2.5433

Initial Height, H_O	19.8248mm				
Final height, H_f	19.7207mm				
Deformation	0.1041mm				
	d_o	=2.478mm	$\sqrt{t_{90}}$=3.87=15min	T=0.848	$C_V=(0.848* H_{avg}^2)/ t_{90}$
	d_{90}	=2.509mm	H_{avg}=19.773mm		C_V=0.003684cm²/sec

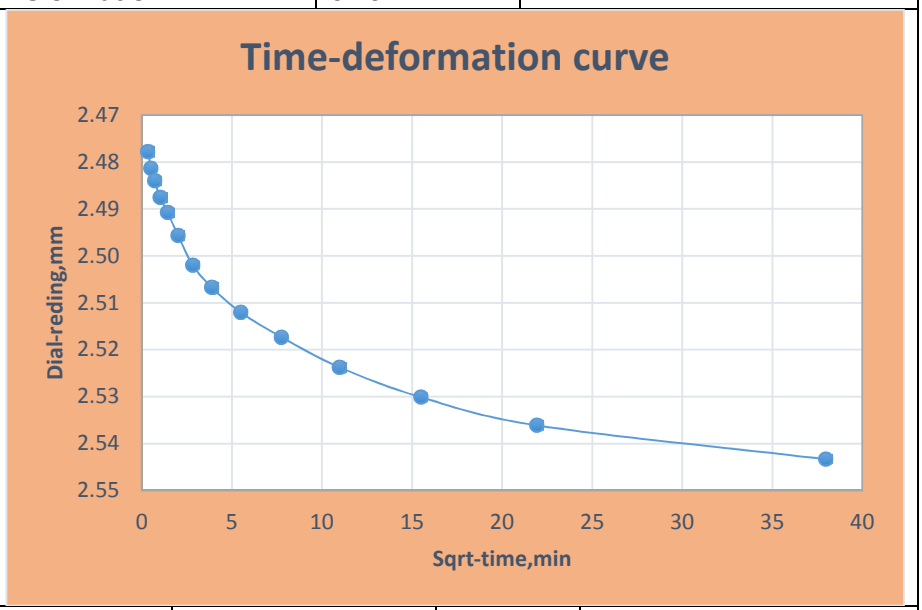

Load increment: 200kpa

Elapsed Time (min)	Deformation Dial Reading (mm)
0	2.5433
0.1	2.676
0.25	2.679
0.5	2.6824
1	2.688
2	2.6944
4	2.700
8	2.708
15	2.714
30	2.721
60	2.728
120	2.734
240	2.743
480	2.750
1440	2.761

Initial Height, H_O	19.7207mm
Final height, H_f	19.503mm
Deformation	0.2177mm

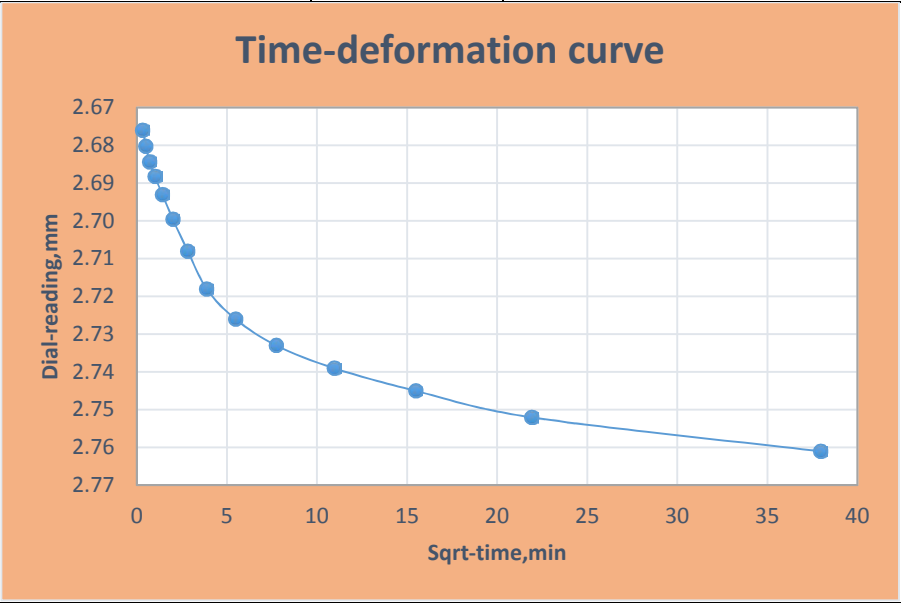

d_o	=2.677mm	$\sqrt{t_{90}}$=5=25min	T=0.848	$C_V=(0.848* H_{avg}^2)/ t_{90}$
d_{90}	=2.725mm	H_{avg}=19.612mm		C_V=0.002174cm^2/sec

Load increment: 400kpa

Elapsed Time (min)	Deformation Dial Reading (mm)
0	2.761
0.1	2.854
0.25	2.863
0.5	2.871
1	2.88
2	2.89
4	2.902
8	2.921
15	2.941
30	2.966
60	2.993
120	3.01
240	3.028
480	3.0491
1440	3.078

Initial Height, H_O	19.503mm
Final height, H_f	19.186mm
Deformation	0.317mm

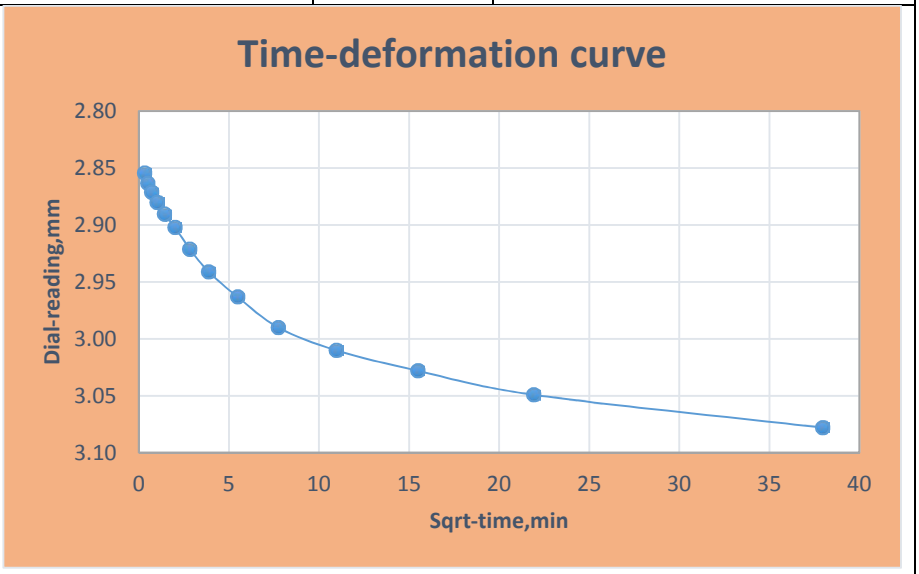

d_o	=2.855mm	$\sqrt{t_{90}}$=5.48=30min	T=0.848	$C_V=(0.848* H_{avg}^2)/ t_{90}$
d_{90}	=2.953mm	H_{avg}=19.345mm		C_V=0.001763cm^2/sec

Load increment: 800kpa					
Elapsed Time (min)	Deformation Dial Reading (mm)	Initial Height, H_O	19.186mm		
		Final height, H_f	18.79mm		
		Deformation	0.396mm		
0	3.078	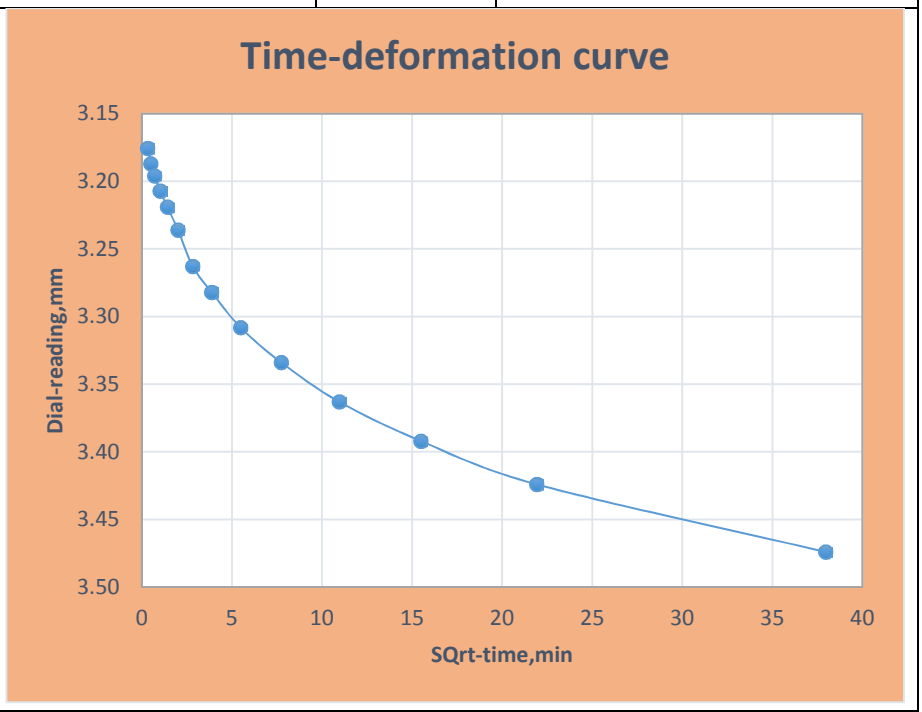			
0.1	3.1756				
0.25	3.187				
0.5	3.196				
1	3.207				
2	3.219				
4	3.236				
8	3.259				
15	3.282				
30	3.308				
60	3.334				
120	3.363				
240	3.392				
480	3.424				
1440	3.474				
	d_o	=3.172mm	$\sqrt{t_{90}}$=4.34=19min	T=0.848	C_V=(0.848* H_{avg}^2)/ t_{90}
	d_{90}	=3.290mm	H_{avg}=18.988mm		C_V=0.0027cm^2/sec

Load increment: 1600kpa

Elapsed Time (min)	Deformation Dial Reading (mm)		
		Initial Height, H_O	18.79mm
		Final height, H_f	19.352mm
		Deformation	0.438mm
0	3.474		
0.1	3.506		
0.25	3.524		
0.5	3.540		
1	3.563		
2	3.591		
4	3.6213		
8	3.651		
15	3.682		
30	3.723		
60	3.762		
120	3.806		
240	3.839		
480	3.879		
1440	3.912		

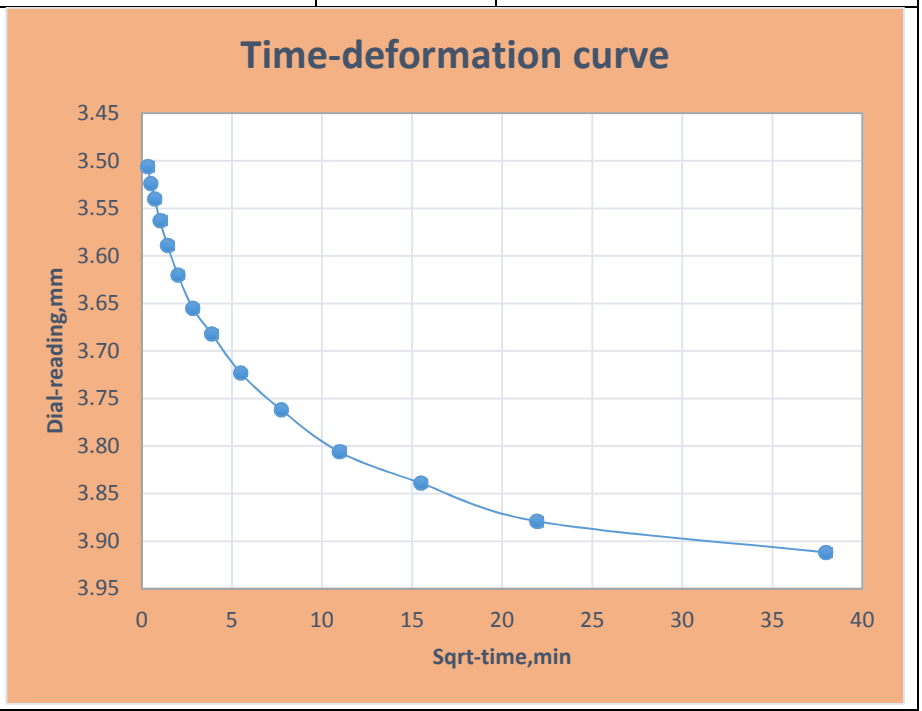

	d_o	=3.510mm	$\sqrt{t_{90}}$=3.87=15min	T=0.848	C_V=(0.848* H_{avg}^2)/ t_{90}
	d_{90}	=3.68mm	H_{avg}=18.571mm		C_V=0.00325cm^2/sec

unloading

Load Decrement, kpa	Def. Dial Reading (mm)
800	3.8333
400	3.7619
200	3.7057
100	3.6778
50	3.6324
25	

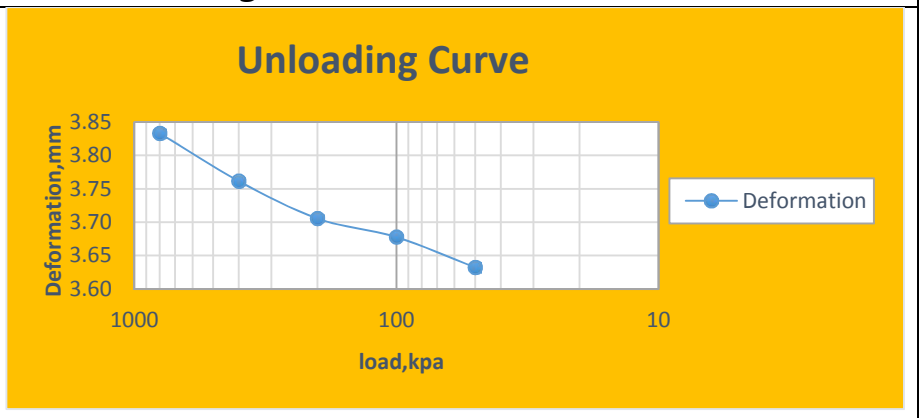

Compression at the end of each loading

Loading, kpa	Deformation, mm	Height of Specimen, mm
25	0.121	19.879
50	0.1752	19.8248
100	0.2793	19.7207
200	0.497	19.503
400	0.814	19.186
800	1.21	18.79
1600	1.648	18.35

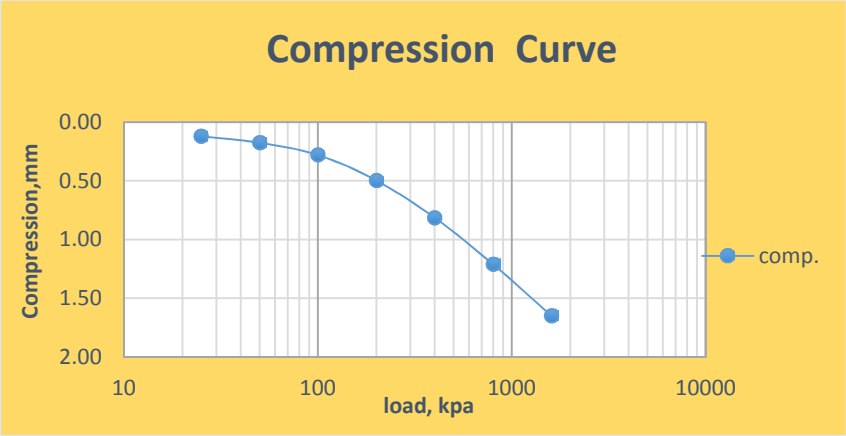

Void ratio at the end of each loading

Loading, kpa	Void ratio, e
25	0.788484031
50	0.783607737
100	0.774242015
200	0.75465587
400	0.726135852
800	0.690508322
1600	0.651064325
800	0.65814238
400	0.664567251
200	0.669626181
100	0.672134953
50	0.676221772

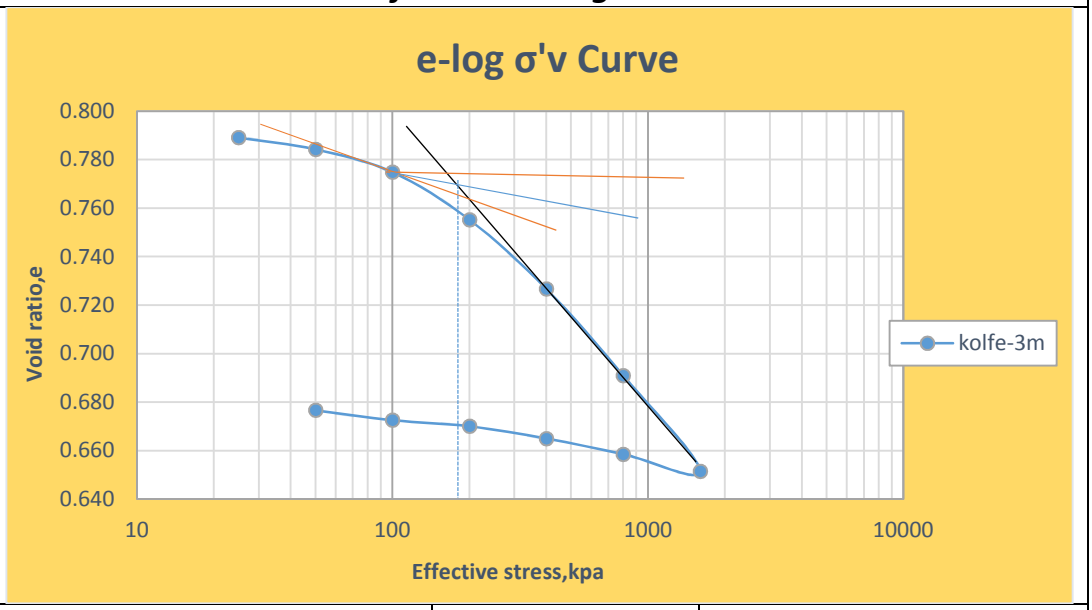

$e = (H-H_S)/H_S$	$H_S = H_O/(1+e_O)$	$C_C = (e_1-e_2)/\log(\sigma_2/\sigma_1)$	e_1=0.72613585	σ_2=1600kpa
		C_C=0.1247	e_2=0.65106432	σ_1=400kpa

Compression coefficient

Load, kpa	Void ratio, e	$a_V=(e_1-e_2)/(\sigma_2-\sigma_1)$	$m_V=a_V/(1+e_1)$	C_V(cm2/sec)	Pc, Kpa
25	0.788484031	0.000195052	0.00010906	0.00374	198
50	0.783607737	0.000187314	0.00010502	0.003273	
100	0.774242015	0.000195861	0.000110392	0.003684	
200	0.75465587	0.0001426	8.12695E-05	0.002174	
400	0.726135852	8.90688E-05	5.16001E-05	0.001763	
800	0.690508322	4.9305E-05	2.91658E-05	0.0027	
1600	0.651064325			0.00325	

Load, Kpa	Cv,$10^{-4}cm^2/sec$
25	37.46
50	32.73
100	36.84
200	21.74
400	17.63
800	27.00
1600	32.50

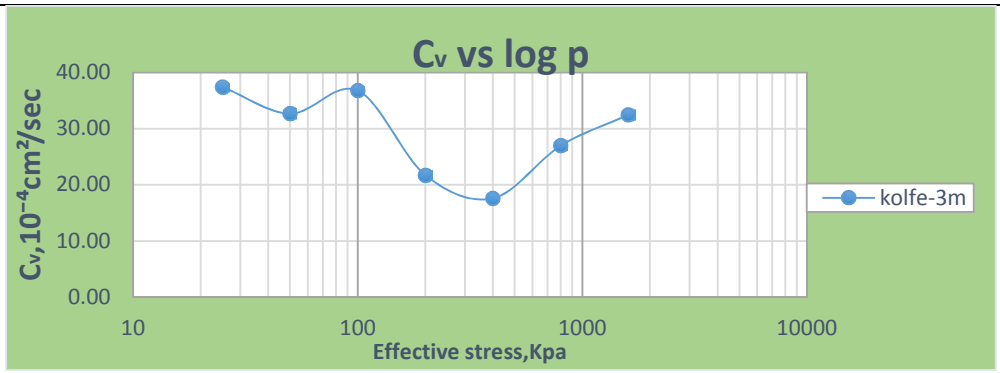

E2. One dimensional consolidation test for kolfe sample @1.5m, K-1

Load increment: 50kpa

Elapsed Time (min)	Deformation Dial Reading (mm)
0	2.25
0.1	2.382
0.25	2.396
0.5	2.407
1	2.422
2	2.44
4	2.461
8	2.491
15	2.512
30	2.541
60	2.562
120	2.584
240	2.608
480	2.622
1440	2.649

Initial Height, H_O	20mm
Final height, H_f	19.601mm
Deformation	0.399mm

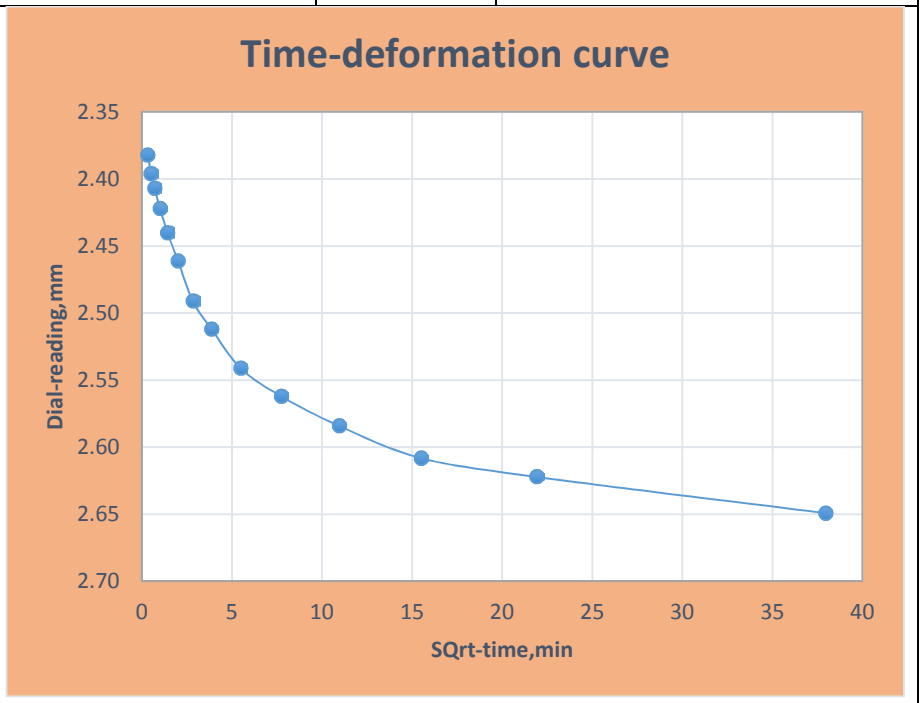

	d_o	=2.39mm	$\sqrt{t_{90}}$=4=16min	T=0.848	$C_V=(0.848* H_{avg}^2)/ t_{90}$
	d_{90}	=2.515mm	H_{avg}=19.8005mm		C_V=0.003463cm^2/sec

Load increment: 100kpa

Elapsed Time (min)	Deformation Dial Reading (mm)
0	2.649
0.1	2.666
0.25	2.668
0.5	2.671
1	2.674
2	2.677
4	2.68
8	2.683
15	2.686
30	2.689
60	2.692
120	2.695
240	2.698
480	2.701
1440	2.7026

Initial Height, H_O	19.601mm
Final height, H_f	19.5474mm
Deformation	0.0536mm

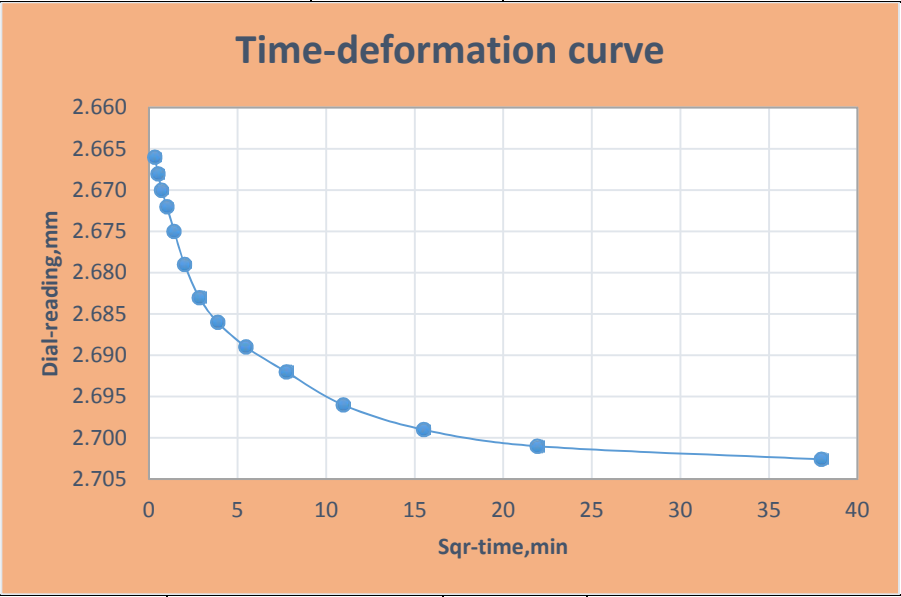

	d_o	=2.665mm	$\sqrt{t_{90}}$=3.87=15min	T=0.848	$C_V=(0.848* H_{avg}^2)/ t_{90}$
	d_{90}	=2.685mm	H_{avg}=19.5742mm		C_V=0.003610cm²/sec

Load increment: 200kpa

Elapsed Time (min)	Deformation Dial Reading (mm)
0	2.7026
0.1	2.7341
0.25	2.7358
0.5	2.7373
1	2.7388
2	2.7412
4	2.743
8	2.7453
15	2.7472
30	2.7492
60	2.7519
120	2.7543
240	2.7576
480	2.7602
1440	2.7633

Initial Height, H_O	19.5474mm
Final height, H_f	19.4867mm
Deformation	0.0607mm

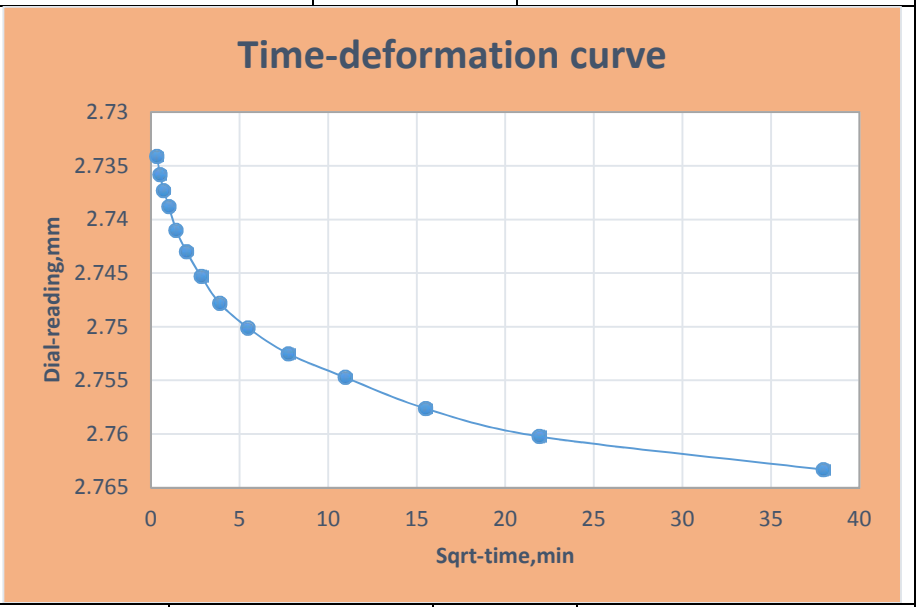

	d_o	=2.736mm	$\sqrt{t_{90}}$=4.6=21.2mi	T=0.848	$C_V=(0.848* H_{avg}^2)/ t_{90}$
	d_{90}	=2.749mm	H_{avg}=19.517mm		C_V=0.002544cm²/sec

Load increment: 400kpa

Elapsed Time (min)	Deformation Dial Reading (mm)
0	2.7633
0.1	2.796
0.25	2.802
0.5	2.809
1	2.816
2	2.826
4	2.836
8	2.847
15	2.855
30	2.863
60	2.871
120	2.88
240	2.885
480	2.8878
1440	2.8894

Initial Height, H_O	19.4867mm		
Final height, H_f	19.3606mm		
Deformation	0.1261mm		

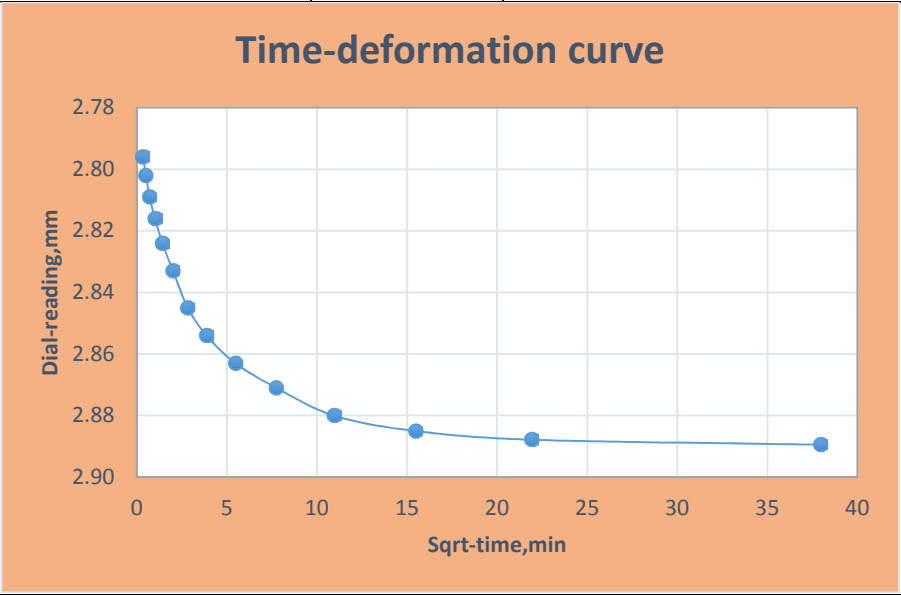

	d_o	=2.808mm	$\sqrt{t_{90}}$=5.35=28.6min	T=0.848	$C_V=(0.848* H_{avg}^2)/ t_{90}$
	d_{90}	=2.86mm	H_{avg}=19.4236mm		C_V=0.001863cm²/sec

Load increment: 800kpa

Elapsed Time (min)	Deformation Dial Reading (mm)
0	2.8894
0.1	2.958
0.25	2.968
0.5	2.976
1	2.988
2	3.000
4	3.020
8	3.040
15	3.060
30	3.090
60	3.120
120	3.140
240	3.160
480	3.180
1440	3.2104

Initial Height, H_O	19.3606mm		
Final height, H_f	19.0396mm		
Deformation	0.321mm		

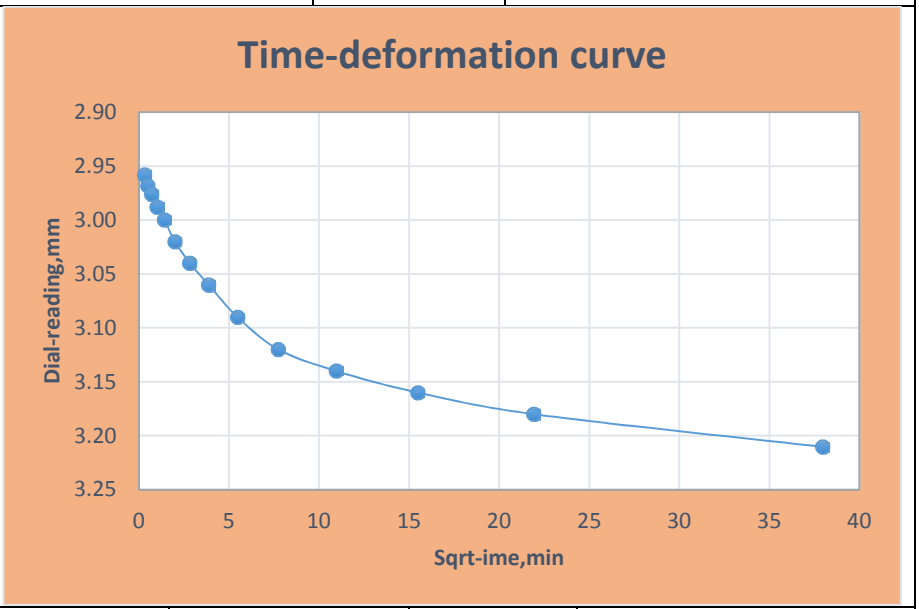

	d_o	=2.96mm	$\sqrt{t_{90}}$=4.3=17.6	T=0.848	$C_V=(0.848* H_{avg}^2)/ t_{90}$
	d_{90}	=3.070mm	H_{avg}=19.2mm		C_V=0.002954cm²/sec

Load increment: 1600kpa

Elapsed Time (min)	Deformation Dial Reading (mm)
0	3.2104
0.1	3.305
0.25	3.324
0.5	3.342
1	3.362
2	3.389
4	3.422
8	3.456
15	3.483
30	3.512
60	3.534
120	3.554
240	3.569
480	3.578
1440	3.5854

Initial Height, H_O	19.0396mm
Final height, H_f	18.6646mm
Deformation	0.375mm

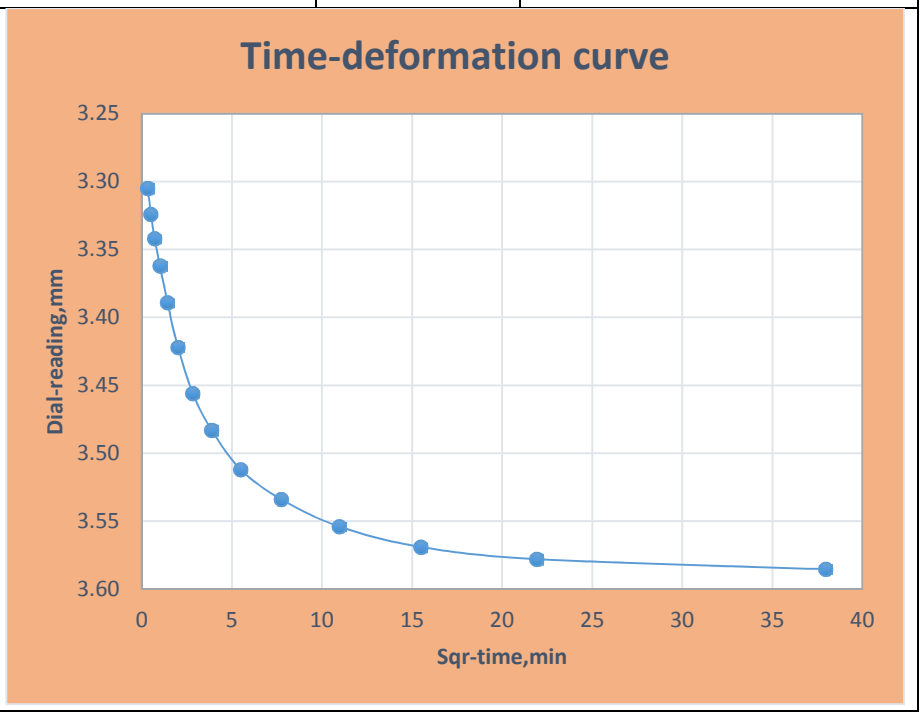

	d_o	=3.31mm	$\sqrt{t_{90}}$=3.87=15min	T=0.848	C_V=(0.848* H_{avg}^2)/ t_{90}
	d_{90}	=3.48mm	H_{avg}=18.852mm		C_V=0.003348cm^2/sec

unloading

Load Decrement, kpa	Def. Dial Reading (mm)
800	3.5112
400	3.4561
200	3.4213
100	
50	
25	

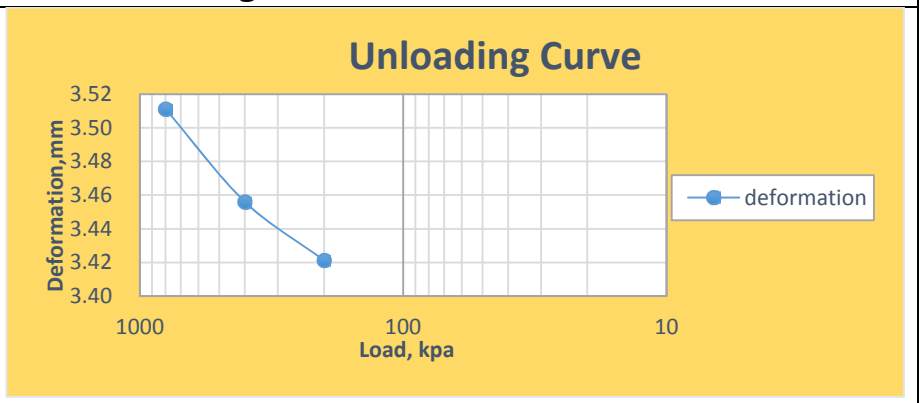

Compression at the end of each loading

Loading, kpa	Deformation, mm	Height of Specimen, mm
50	0.3986	19.601
100	0.4522	19.5478
200	0.5129	19.4871
400	0.639	19.361
800	0.96	19.04
1600	1.3352	18.6648

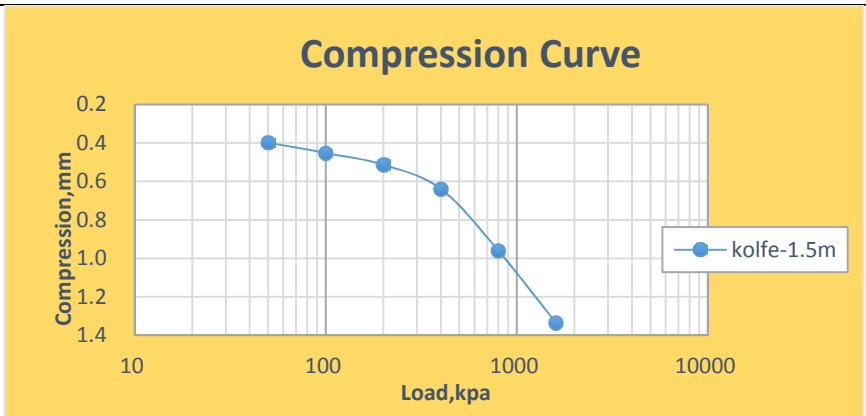

Void ratio at the end of each loading

Loading, kpa	Void ratio, e
50	0.778712256
100	0.773847247
200	0.768341032
400	0.756895204
800	0.727760213
1600	0.693719723
800	0.700455563
400	0.705460036
200	0.708621253

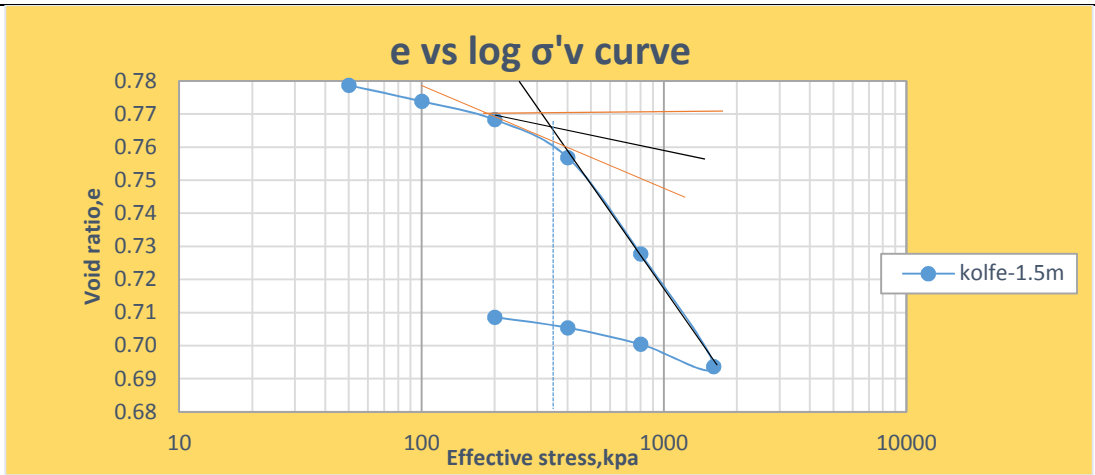

$e=(H-H_S)/H_S$	$H_S=H_O/(1+e_O)$	$C_C=(e_1-e_2)/\log(\sigma_2/\sigma_1)$	e_1=0.756895204	σ_2=1600kpa
		C_C=0.105	e_2=0.693719723	σ_1=400kpa

Compression coefficient

Load, kpa	Void ratio, e	$a_V=(e_1-e_2)/(\sigma_2-\sigma_1)$	$m_V=a_V/(1+e_1)$	C_V(cm2/sec)	Pc,kpa
50	0.778712256	9.73002E-05	5.47026E-05	0.003463	360
100	0.773847247	5.50622E-05	3.10411E-05	0.003610	
200	0.768341032	5.72291E-05	3.23632E-05	0.002544	
400	0.756895204	7.28375E-05	4.14581E-05	0.001863	
800	0.727760213	4.2550E-05	2.46276E-05	0.002954	
1600	0.693719723			0.003348	

Load, kpa	Cv,10^{-4}cm²/sec
50	34.63
100	36.10
200	25.44
400	18.63
800	29.54
1600	33.48

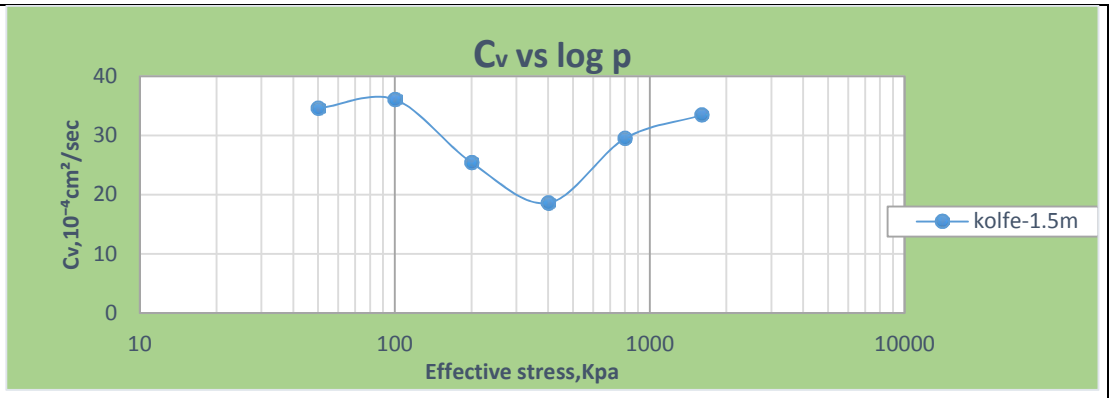

E3. One dimensional consolidation test for Addisu-Gebeya sample @1.5m, AG-1

Load increment: 25kpa

Elapsed Time (min)	Deformation Dial Reading (mm)
0	2.001
0.1	2.011
0.25	2.016
0.5	2.019
1	2.024
2	2.029
4	2.033
8	2.038
15	2.043
30	2.047
60	2.051
120	2.055
240	2.059
480	2.062
1440	2.067

Initial Height, H_O	20mm				
Final height, H_f	19.943mm				
Deformation	0.057mm				
	d_o	=2.013mm	$\sqrt{t_{90}}$=3.87=15min	T=0.848	C_V=(0.848* H_{avg}^2)/ t_{90}
	d_{90}	=2.043mm	H_{avg}=19.9715mm		C_V=0.003756cm²/sec

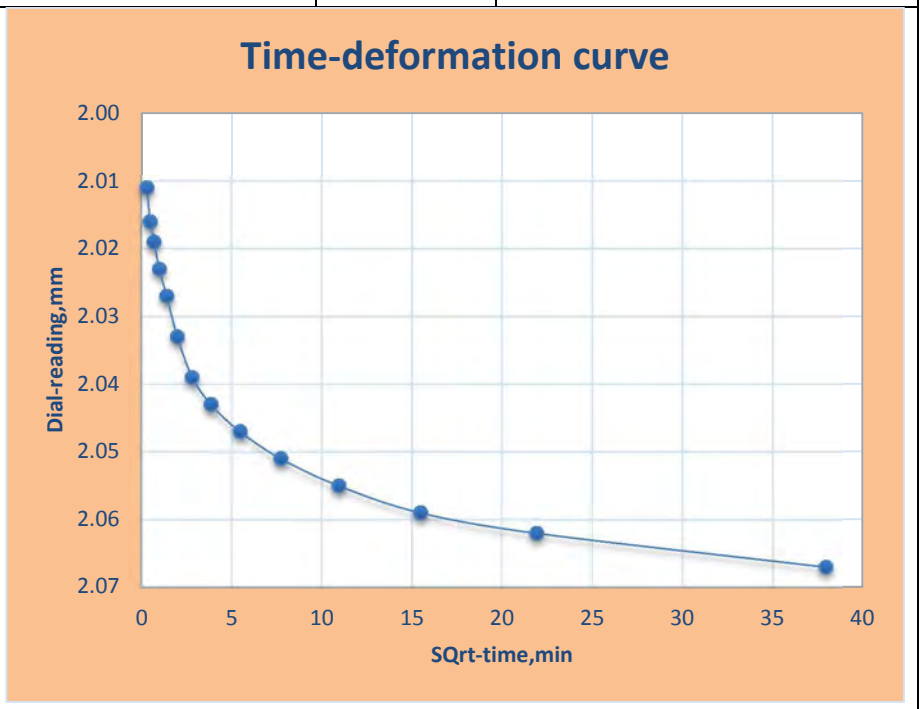

Load increment: 50kpa

Elapsed Time (min)	Deformation Dial Reading (mm)
0	2.067
0.1	2.071
0.25	2.074
0.5	2.077
1	2.080
2	2.084
4	2.087
8	2.091
15	2.094
30	2.098
60	2.102
120	2.106
240	2.110
480	2.113
1440	2.118

Initial Height, H_O	19.943mm		
Final height, H_f	19.897mm		
Deformation	0.046mm		

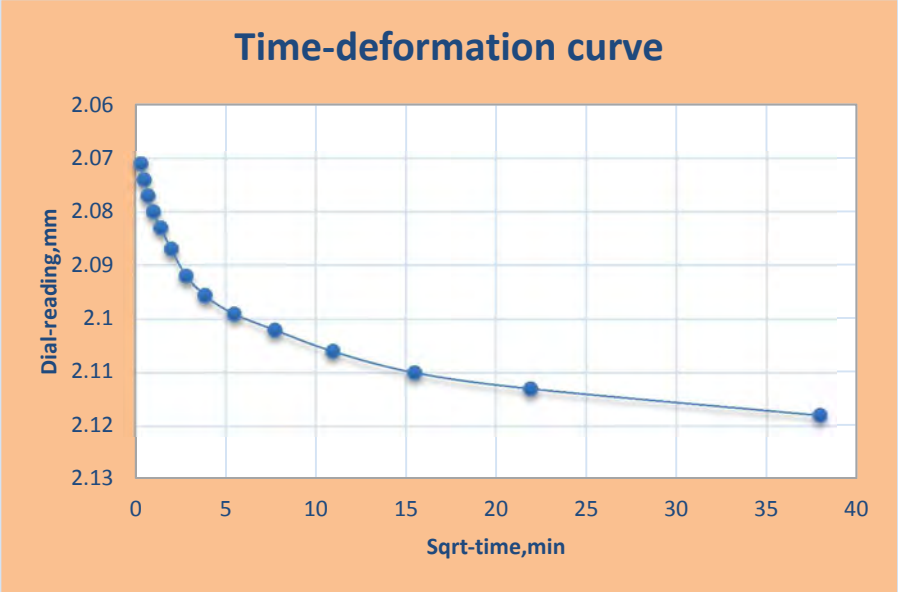

d_o	=2.071mm	$\sqrt{t_{90}}$=4.37=19.1min	T=0.848	$C_V=(0.848* H_{avg}^2)/ t_{90}$
d_{90}	=2.097mm	H_{avg}=19.92mm		C_V=0.002926cm²/sec

Load increment: 100kpa

Elapsed Time (min)	Deformation Dial Reading (mm)
0	2.118
0.1	2.170
0.25	2.174
0.5	2.176
1	2.178
2	2.181
4	2.184
8	2.187
15	2.19
30	2.193
60	2.197
120	2.201
240	2.204
480	2.206
1440	2.210

Initial Height, H_O	19.897mm		
Final height, H_f	19.832mm		
Deformation	0.065mm		

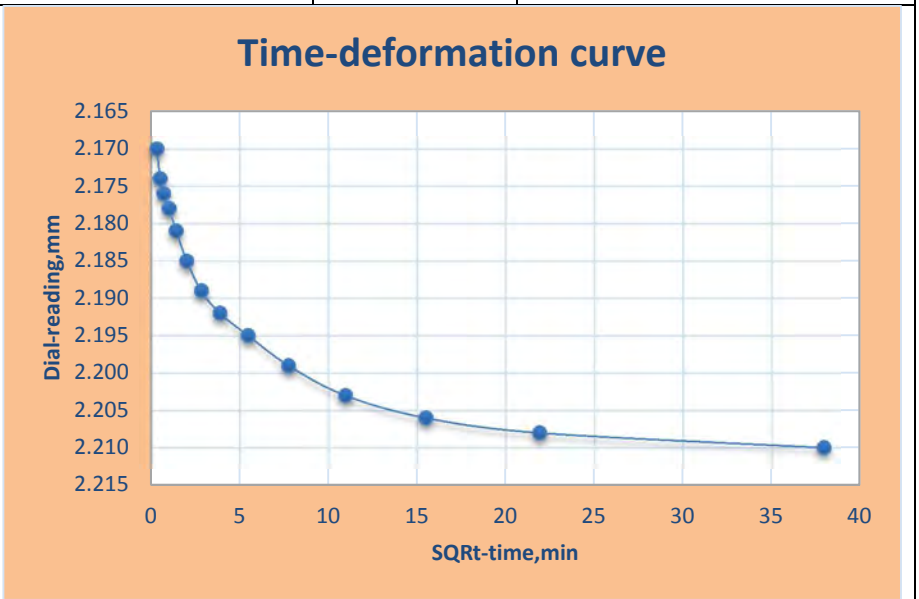

d_o	=2.172mm	$\sqrt{t_{90}}$=4.5=20.25mi	T=0.848	$C_V=(0.848* H_{avg}^2)/ t_{90}$
d_{90}	=2.194mm	H_{avg}=19.8645mm		C_V=0.002746cm²/sec

Load increment: 200kpa

Elapsed Time (min)	Deformation Dial Reading (mm)
0	2.210
0.1	2.302
0.25	2.306
0.5	2.310
1	2.314
2	2.318
4	2.322
8	2.326
15	2.330
30	2.334
60	2.337
120	2.340
240	2.343
480	2.346
1440	2.350

Initial Height, H_O	19.832mm
Final height, H_f	19.716mm
Deformation	0.116mm

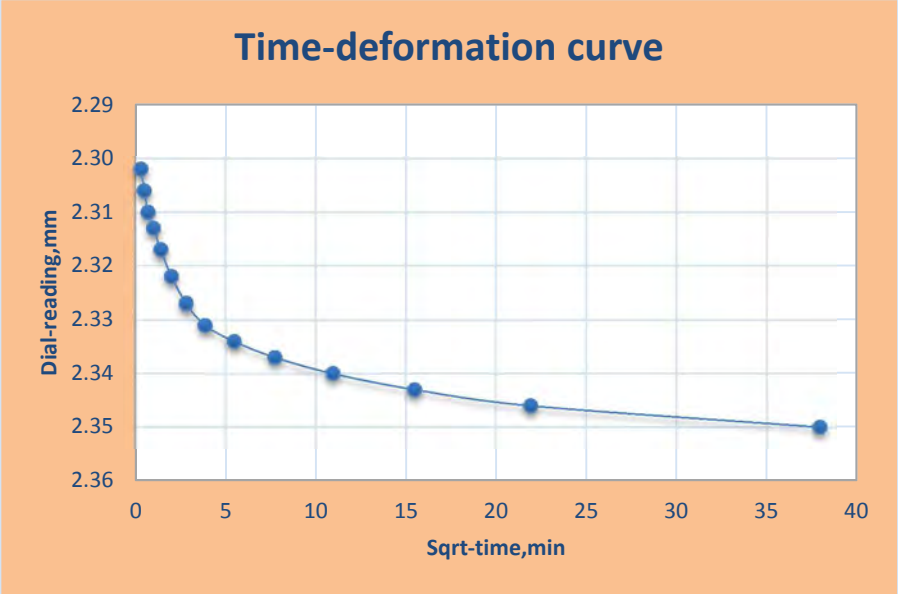

d_o	=2.308mm	$\sqrt{t_{90}}$=4.3=18.49min	T=0.848	$C_V=(0.848* H_{avg}^2)/ t_{90}$
d_{90}	=2.330mm	H_{avg}=19.774mm		C_V=0.002972cm²/sec

Load increment: 400kpa

Elapsed Time (min)	Deformation Dial Reading (mm)
0	2.350
0.1	2.510
0.25	2.518
0.5	2.523
1	2.529
2	2.536
4	2.542
8	2.548
15	2.552
30	2.558
60	2.563
120	2.568
240	2.574
480	2.578
1440	2.582

Initial Height, H_O	19.716mm
Final height, H_f	19.493mm
Deformation	0.223mm

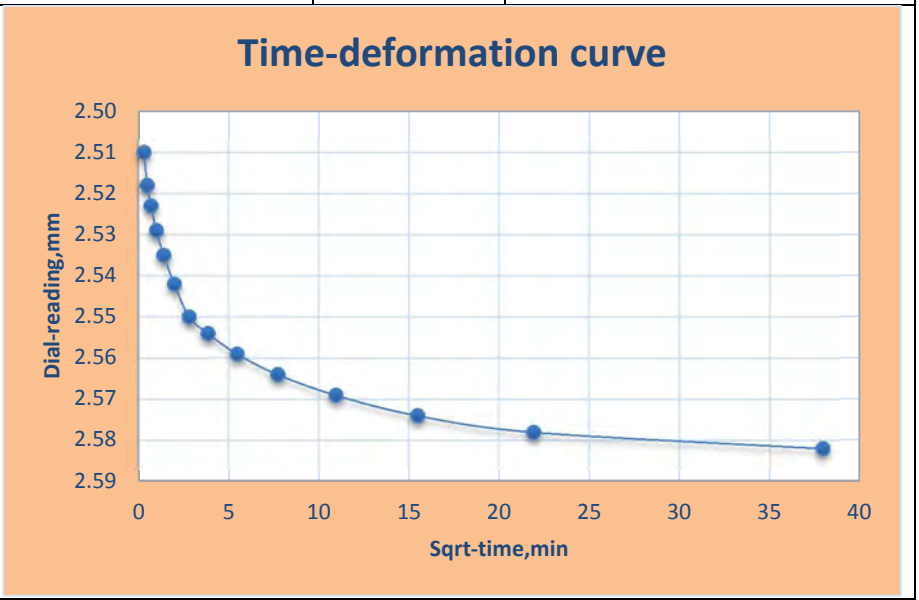

d_o	=2.51mm	$\sqrt{t_{90}}$=4=16min	T=0.848	$C_V=(0.848* H_{avg}^2)/ t_{90}$
d_{90}	=2.55mm	H_{avg}=19.6045mm		C_V=0.003370cm²/sec

Load increment: 800kpa

Elapsed Time (min)	Deformation Dial Reading (mm)		
		Initial Height, H_O	19.493mm
		Final height, H_f	19.131mm
		Deformation	0.362mm
0	2.582		
0.1	2.850		
0.25	2.864		
0.5	2.874		
1	2.885		
2	2.893		
4	2.903		
8	2.912		
15	2.920		
30	2.930		
60	2.937		
120	2.944		
240	2.952		
480	2.958		
1440	2.962		

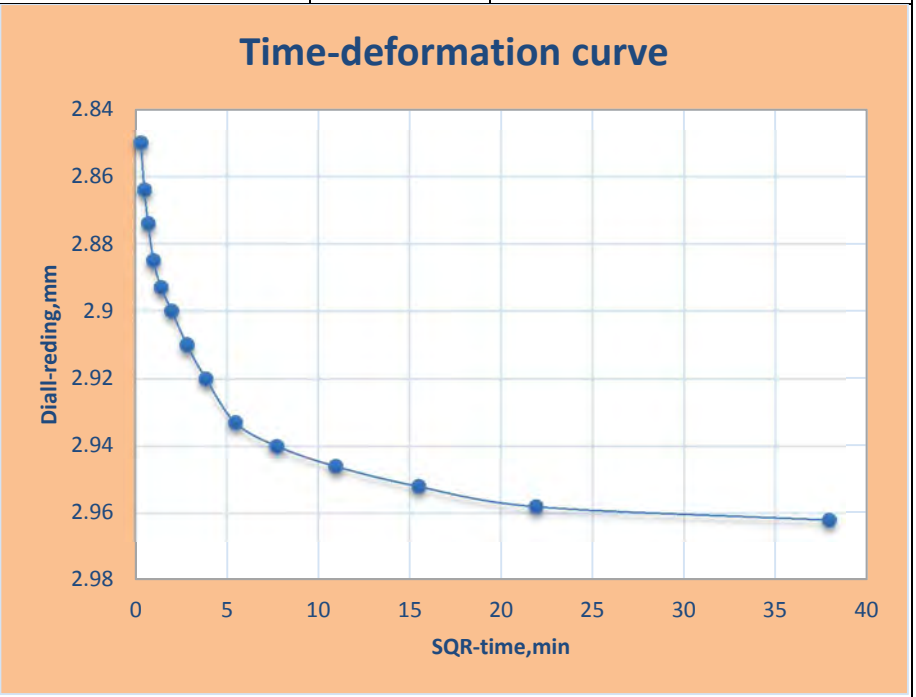

	d_o	=2.868mm	$\sqrt{t_{90}}$=4=16min	T=0.848	C_V=(0.848* H_{avg}^2)/ t_{90}
	d_{90}	=2.92mm	H_{avg}=19.312mm		C_V=0.003266cm^2/sec

Load increment: 1600kpa

Elapsed Time (min)	Deformation Dial Reading (mm)	Initial Height, H_O	19.131mm
		Final height, H_f	18.707mm
		Deformation	0.424mm
0	2.962		
0.1	3.340		
0.25	3.352		
0.5	3.367		
1	3.380		
2	3.393		
4	3.406		
8	3.418		
15	3.431		
30	3.449		
60	3.463		
120	3.473		
240	3.481		
480	3.485		
1440	3.490		

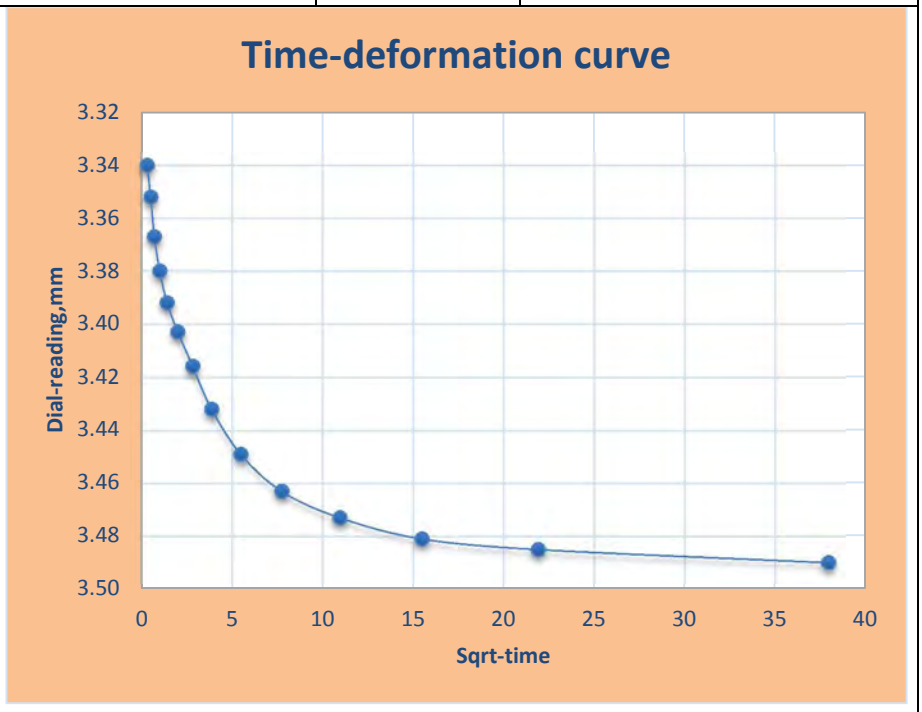

	d_o	=3.36mm	$\sqrt{t_{90}}$=3.87=15min	T=0.848	C_V=(0.848* H_{avg}^2)/ t_{90}
	d_{90}	=3.432mm	H_{avg}=18.919mm		C_V=0.003113cm^2/sec

unloading

Load Decrement, kpa	Def. Dial Reading (mm)
800	3.382
400	3.273
200	3.207
100	3.151
50	3.096
25	-

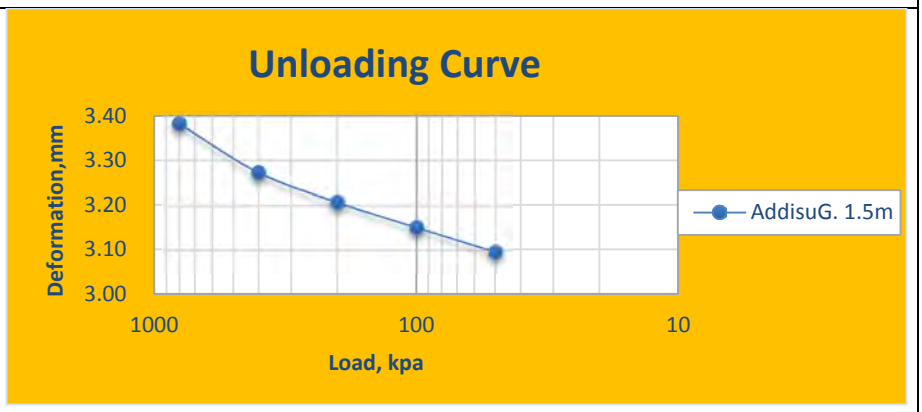

Compression at the end of each loading

Loading, kpa	Deformation, mm	Height of Specimen, mm
25	0.057	19.943
50	0.103	19.897
100	0.168	19.832
200	0.284	19.716
400	0.507	19.493
800	0.869	19.131
1600	1.293	18.707

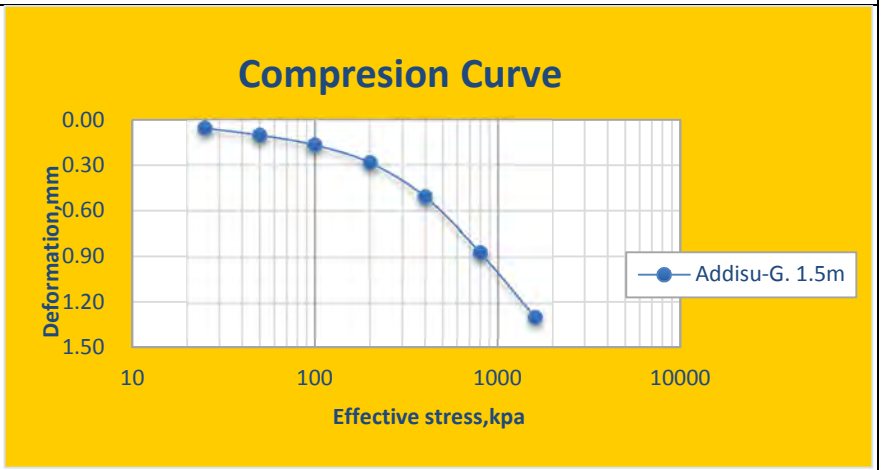

Void ratio at the end of each loading

Loading, kpa	Void ratio, e
25	0.863831776
50	0.85953271
100	0.853457944
200	0.842616822
400	0.821775701
800	0.787943925
1600	0.748317757
800	0.758411215
400	0.768598131
200	0.774766355
100	0.78
50	0.785140187
25	

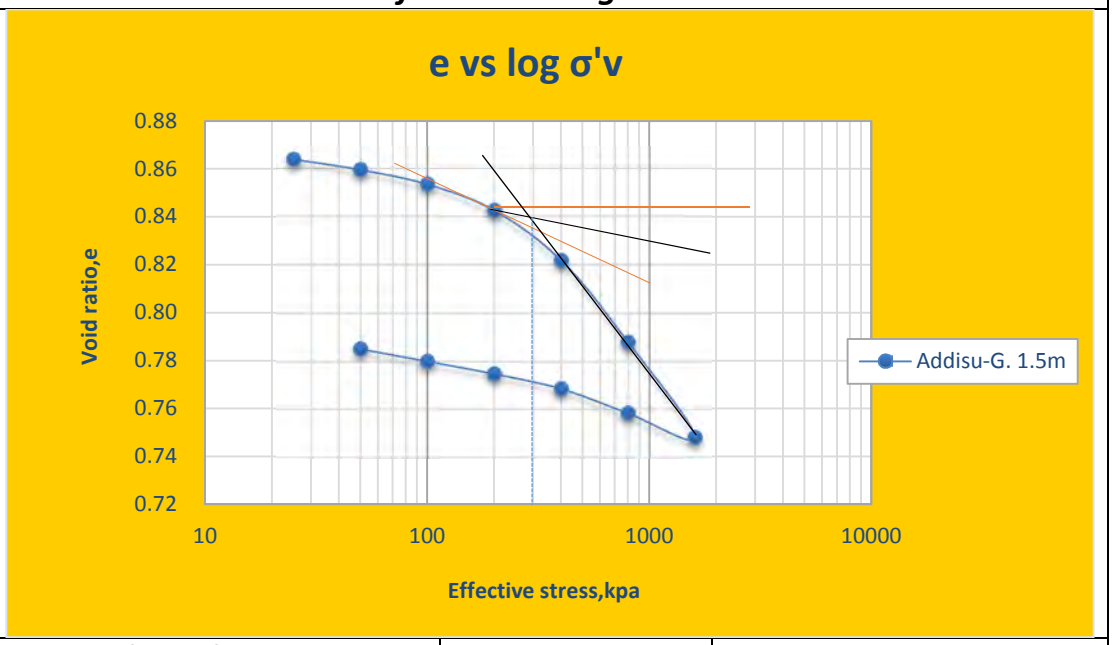

$e = (H-H_S)/H_S$	$H_S=H_O/(1+e_O)$	$C_C=(e_1-e_2)/\log(\sigma_2/\sigma_1)$	e_1=0.821775701	σ_2=1600kpa
		C_C=0.122	e_2=0.748317757	σ_1=400kpa

Compression coefficient

Load, kpa	Void ratio, e	$a_V=(e_1-e_2)/(\sigma_2-\sigma_1)$	$m_V=a_V/(1+e_1)$	C_V(cm2/sec)	Pc, kpa
25	0.863831776	0.000171963	9.22629E-05	0.003756	
50	0.85953271	0.000121495	6.53365E-05	0.002926	
100	0.853457944	0.000108411	5.84913E-05	0.002746	
200	0.842616822	0.000104206	5.65531E-05	0.002972	300
400	0.821775701	8.45794E-05	4.64269E-05	0.003370	
800	0.787943925	4.95327E-05	2.77037E-05	0.003266	
1600	0.748317757			0.003113	

Load, kpa	Cv,10^{-4}cm²/sec
25	37.56
50	29.26
100	27.46
200	29.72
400	33.70
800	32.66
1600	31.13

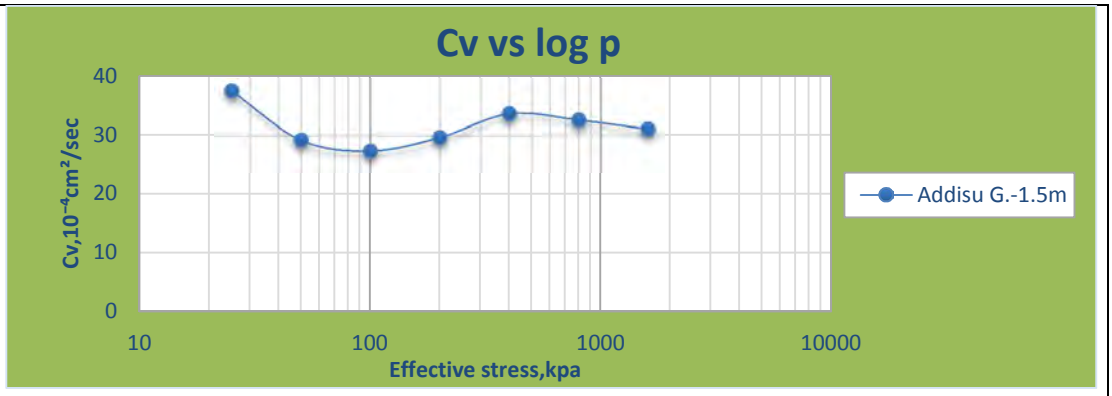

E4. One dimensional consolidation test for Addisu-Gebeya sample @3m, AG-2

Load increment: 25kpa

Elapsed Time (min)	Deformation Dial Reading (mm)
0	3.053
0.1	3.088
0.25	3.092
0.5	3.096
1	3.100
2	3.105
4	3.110
8	3.116
15	3.120
30	3.125
60	3.130
120	3.136
240	3.141
480	3.147
1440	3.154

Initial Height, H_O	20mm				
Final height, H_f	19.934mm				
Deformation	0.066mm				
	d_o	=3.088mm	$\sqrt{t_{90}}$=4=16min	T=0.848	C_V=(0.848* H_{avg}^2)/ t_{90}
	d_{90}	=3.122mm	H_{avg}=19.967mm		C_V=0.003515cm²/sec

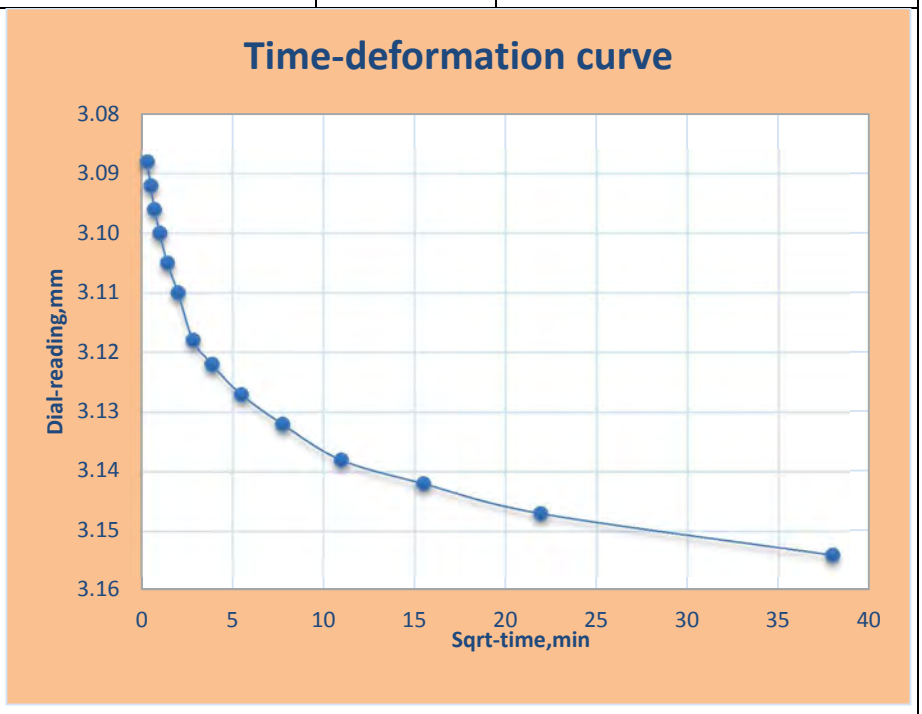

Load increment: 50kpa

Elapsed Time (min)	Deformation Dial Reading (mm)
0	3.154
0.1	3.176
0.25	3.189
0.5	3.199
1	3.206
2	3.212
4	3.216
8	3.222
15	3.228
30	3.236
60	3.244
120	3.250
240	3.256
480	3.259
1440	3.265

Initial Height, H_O	19.934mm			
Final height, H_f	19.831mm			
Deformation	0.103mm			
d_o	=3.187mm	$\sqrt{t_{90}}$=4.5=20.3mi	T=0.848	$C_V=(0.848* H_{avg}^2)/ t_{90}$
d_{90}	=3.236mm	H_{avg}=19.8825mm		C_V=0.002748cm^2/sec

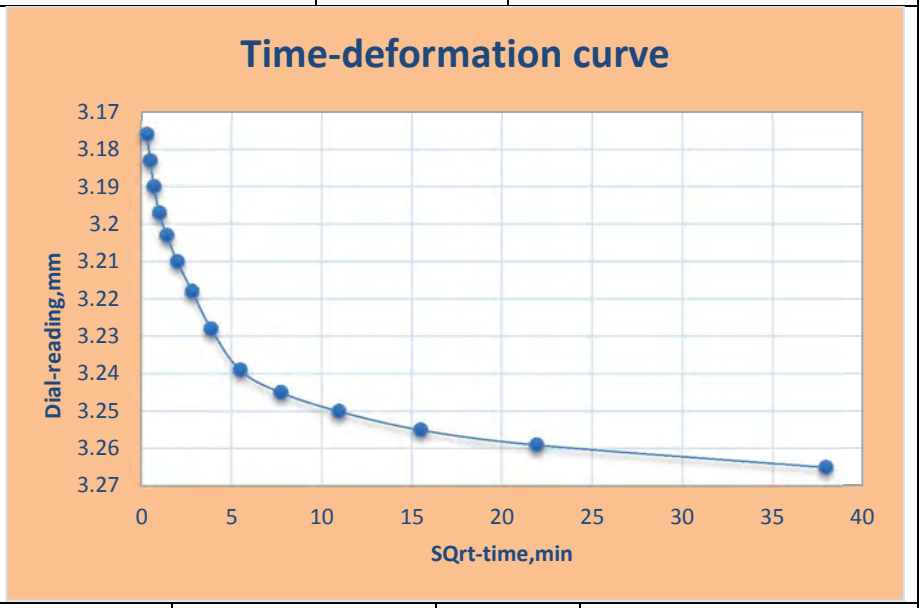

Load increment: 100kpa

Elapsed Time (min)	Deformation Dial Reading (mm)
0	3.265
0.1	3.390
0.25	3.397
0.5	3.403
1	3.408
2	3.412
4	3.416
8	3.420
15	3.423
30	3.427
60	3.430
120	3.433
240	3.437
480	3.440
1440	3.446

Initial Height, H_O	19.831mm			
Final height, H_f	19.713mm			
Deformation	0.118mm			
d_o	=3.40mm	$\sqrt{t_{90}}$=4.7=22.09	T=0.848	$C_V=(0.848* H_{avg}^2)/ t_{90}$
d_{90}	=3.425mm	H_{avg}=19.772mm		C_V=0.002482cm^2/sec

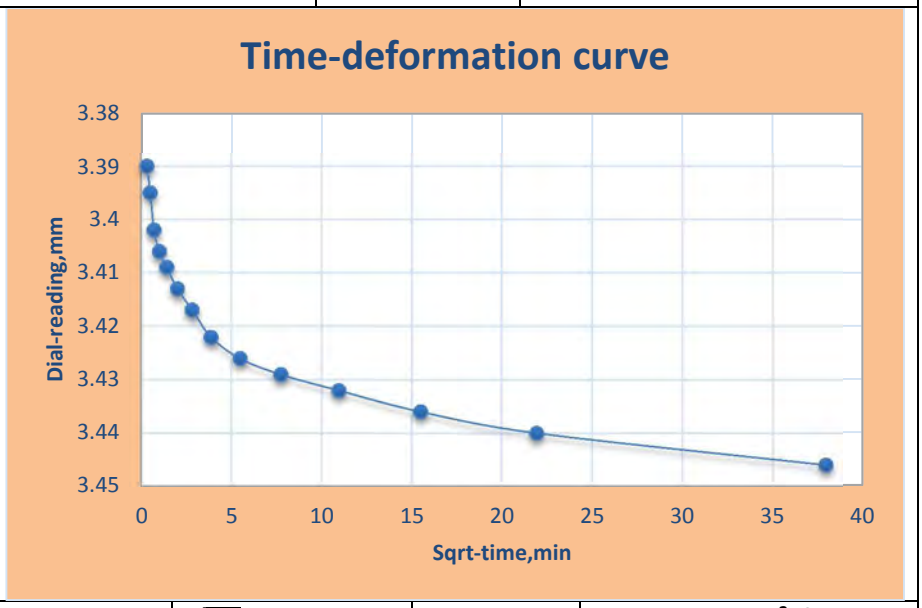

Load increment: 200kpa

Elapsed Time (min)	Deformation Dial Reading (mm)
0	3.446
0.1	3.670
0.25	3.677
0.5	3.684
1	3.690
2	3.696
4	3.699
8	3.703
15	3.707
30	3.712
60	3.716
120	3.720
240	3.7240
480	3.727
1440	3.732

Initial Height, H_O	19.713mm
Final height, H_f	19.556mm
Deformation	0.157mm

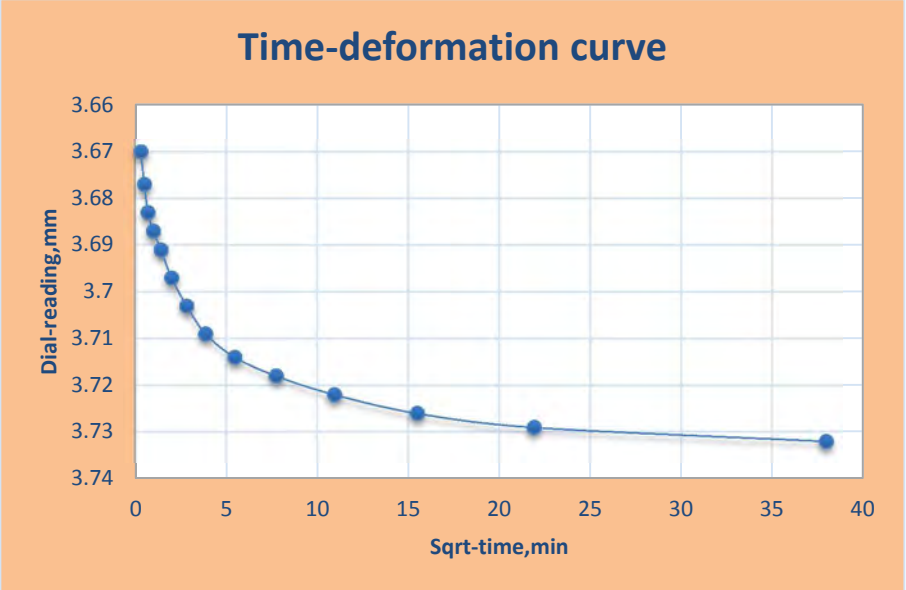

	d_o	=3.677mm	$\sqrt{t_{90}}$=4.3=18.5mi	T=0.848	C_V=(0.848* H_{avg}^2)/ t_{90}
	d_{90}	=3.712mm	H_{avg}=19.6345mm		C_V=0.002896cm^2/sec

Load increment: 400kpa

Elapsed Time (min)	Deformation Dial Reading (mm)
0	3.732
0.1	4.053
0.25	4.06
0.5	4.068
1	4.076
2	4.082
4	4.089
8	4.096
15	4.102
30	4.107
60	4.113
120	4.118
240	4.125
480	4.131
1440	4.138

Initial Height, H_O	19.556mm
Final height, H_f	19.29mm
Deformation	0.266mm

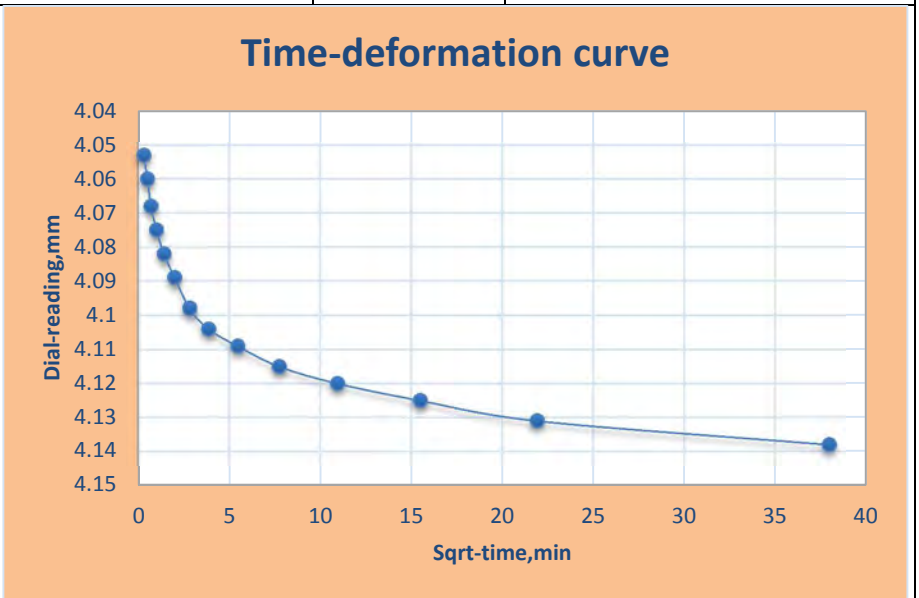

	d_o	=4.060mm	$\sqrt{t_{90}}$=3.87=15min	T=0.848	C_V=(0.848* H_{avg}^2)/ t_{90}
	d_{90}	=4.103mm	H_{avg}=19.423mm		C_V=0.003444cm^2/sec

Load increment: 800kpa					
Elapsed Time (min)	**Deformation Dial Reading (mm)**	**Initial Height, H_o**	**19.29mm**		
		Final height, H_f	**18.922mm**		
		Deformation	**0.368mm**		
0	4.138	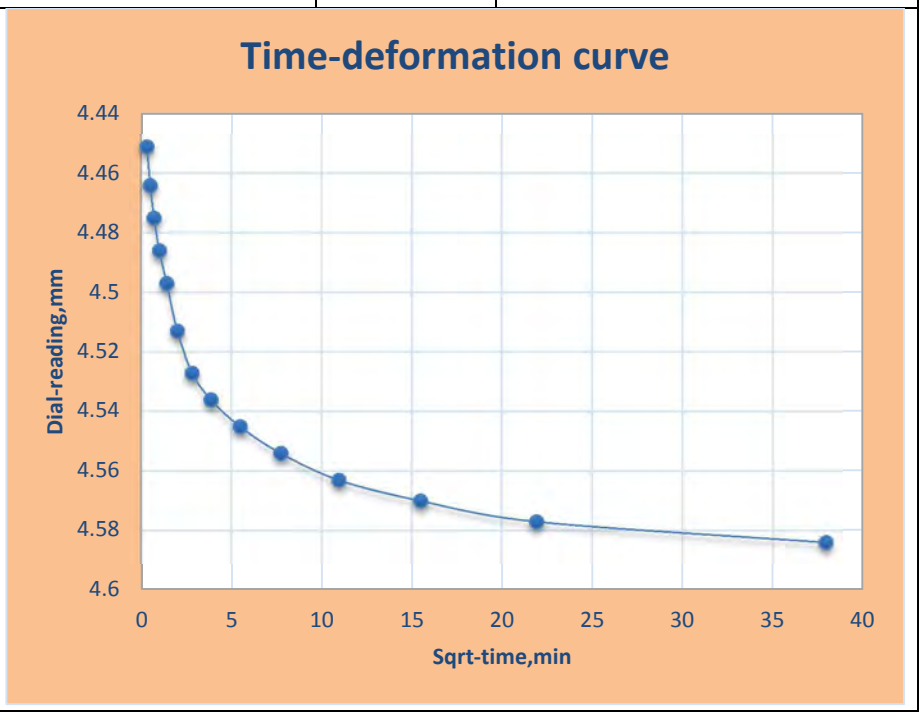			
0.1	4.451				
0.25	4.464				
0.5	4.475				
1	4.489				
2	4.503				
4	4.4515				
8	4.525				
15	4.536				
30	4.545				
60	4.554				
120	4.563				
240	4.570				
480	4.577				
1440	4.584				
	d_o	**=4.455mm**	**$\sqrt{t_{90}}$=3.87=15min**	**T=0.848**	**C_V=(0.848* H_{avg}^2)/ t_{90}**
	d_{90}	**=4.536mm**	**H_{avg}=19.106mm**		**C_V=0.003292cm^2/sec**

Load increment: 1600kpa

Elapsed Time (min)	Deformation Dial Reading (mm)		
		Initial Height, H_O	18.922mm
		Final height, H_f	18.476mm
		Deformation	0.446mm
0	4.584		
0.1	5.044		
0.25	5.058		
0.5	5.072		
1	5.088		
2	5.104		
4	5.119		
8	5.133		
15	5.143		
30	5.153		
60	5.163		
120	5.171		
240	5.179		
480	5.185		
1440	5.200		

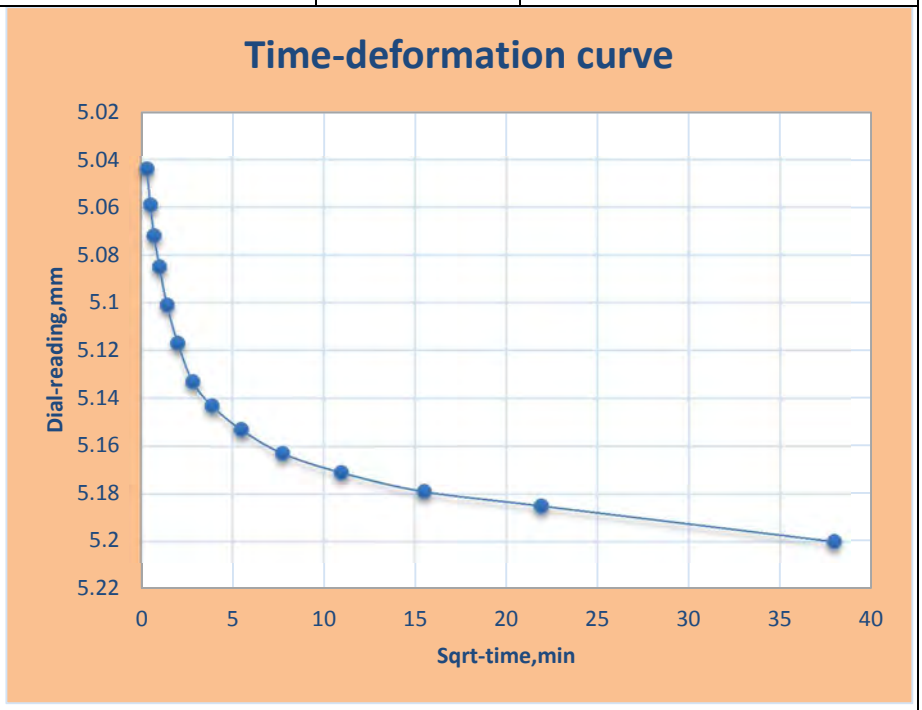

	d_o	=5.060mm	$\sqrt{t_{90}}$=3.8=14.4mi	T=0.848	C_V=(0.848* H_{avg}^2)/ t_{90}
	d_{90}	=5.143mm	H_{avg}=18.699mm		C_V=0.003388cm^2/sec

unloading

Load Decrement, kpa	Def. Dial Reading (mm)
800	5.129
400	5.054
200	4.984
100	4.92
50	4.866
25	4.684

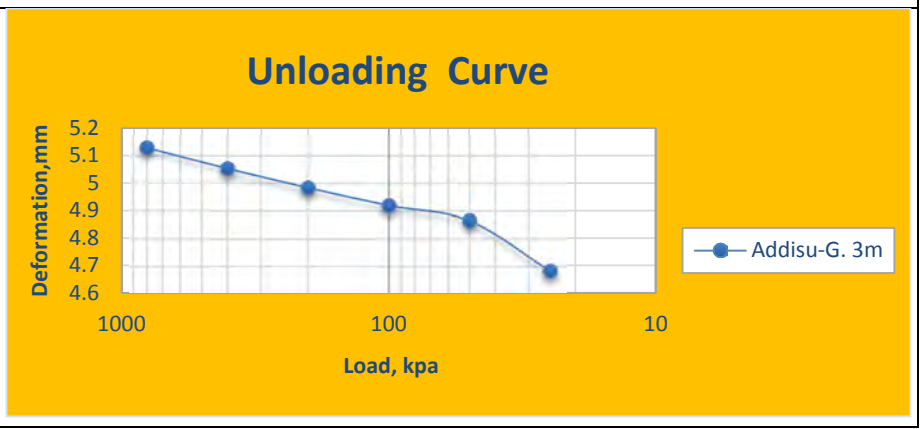

Compression at the end of each loading

Loading, kpa	Deformation, mm	Height of Specimen, mm
25	0.066	19.934
50	0.169	19.831
100	0.287	19.713
200	0.444	19.556
400	0.71	19.29
800	1.078	18.922
1600	1.524	18.476

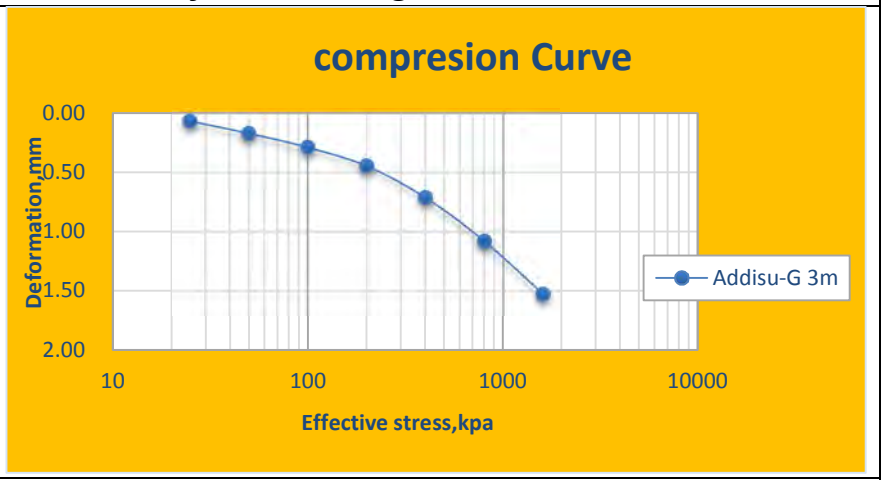

Void ratio at the end of each loading

Loading, kpa	Void ratio, e
25	0.828587076
50	0.819185834
100	0.80841548
200	0.794085433
400	0.769806499
800	0.736217598
1600	0.69550931
800	0.701989777
400	0.708835341
200	0.715224535
100	0.721066083
50	0.725994889
25	

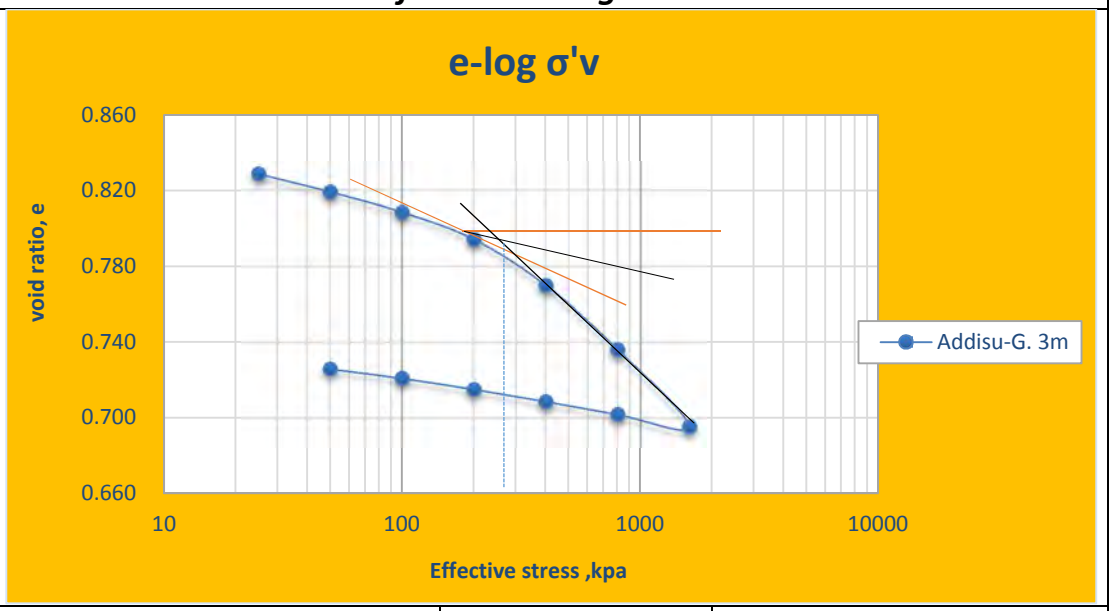

$e = (H-H_S)/H_S$	$H_S = H_O/(1+e_O)$	$C_C = (e_1-e_2)/\log(\sigma_2/\sigma_1)$	e_1=0.769806499	σ_2=1600kpa
		C_C=0.123	e_2=0.69550931	σ_1=400kpa

Compression coefficient

Load, kpa	Void ratio, e	$a_V=(e_1-e_2)/(\sigma_2-\sigma_1)$	$m_V=a_V/(1+e_1)$	C_V(cm2/sec)	Pc,kpa
25	0.828587076	0.00037605	0.00020565	0.003515	290
50	0.819185834	0.000215407	0.000118409	0.002748	
100	0.80841548	0.0001433	7.92409E-05	0.002482	
200	0.794085433	0.000121395	6.76638E-05	0.002896	
400	0.769806499	8.39723E-05	4.74471E-05	0.003444	
800	0.736217598	5.08854E-05	2.93082E-05	0.003292	
1600	0.69550931			0.003388	

Load, kpa	Cv,$10^{-4}cm^2/sec$
25	35.15
50	27.48
100	24.82
200	28.96
400	34.44
800	32.92
1600	33.88

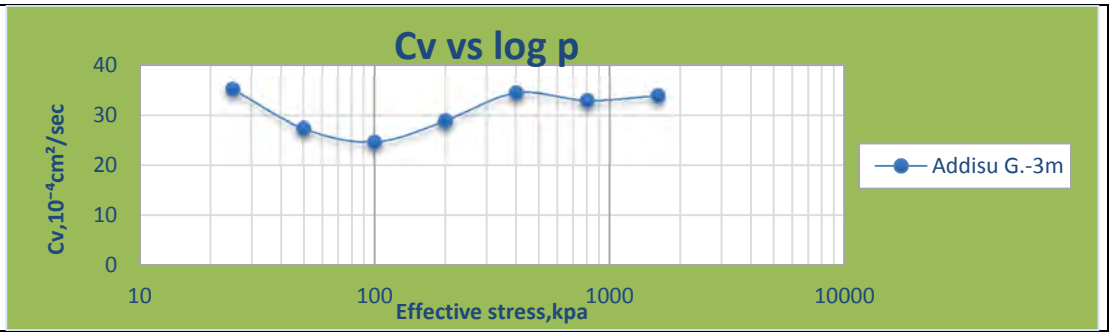

E5. One dimensional consolidation test for Rufa'el sample @1.5m, R-1

Load increment: 25kpa

Elapsed Time (min)	Deformation Dial Reading (mm)				
		Initial Height, H_O	20mm		
		Final height, H_f	19.9574mm		
		Deformation	0.0426mm		
0	5.97				
0.1	5.99				
0.25	5.992				
0.5	5.995				
1	5.9966				
2	5.9975				
4	5.9984				
8	5.9991				
15	6.0003				
30	6.0018				
60	6.0035				
120	6.0049				
240	6.0066				
480	6.009				
1440	6.0126				
	d_o	=5.996mm	$\sqrt{t_{90}}$=7.746=60mi	T=0.848	$C_V=(0.848*H_{avg}^2)/t_{90}$
	d_{90}	=6.004mm	H_{avg}=19.9787mm		C_V=0.00094cm^2/sec

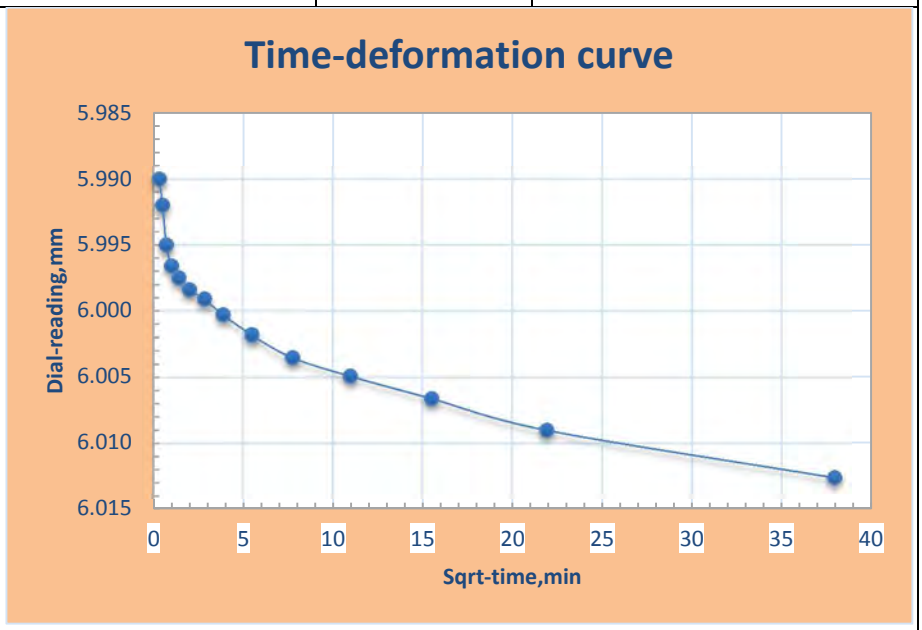

Load increment: 50kpa

Elapsed Time (min)	Deformation Dial Reading (mm)
0	6.0126
0.1	6.026
0.25	6.028
0.5	6.03
1	6.033
2	6.035
4	6.037
8	6.039
15	6.0415
30	6.045
60	6.048
120	6.051
240	6.054
480	6.057
1440	6.062

Initial Height, H_O	19.9574mm
Final height, H_f	19.908mm
Deformation	0.0494mm

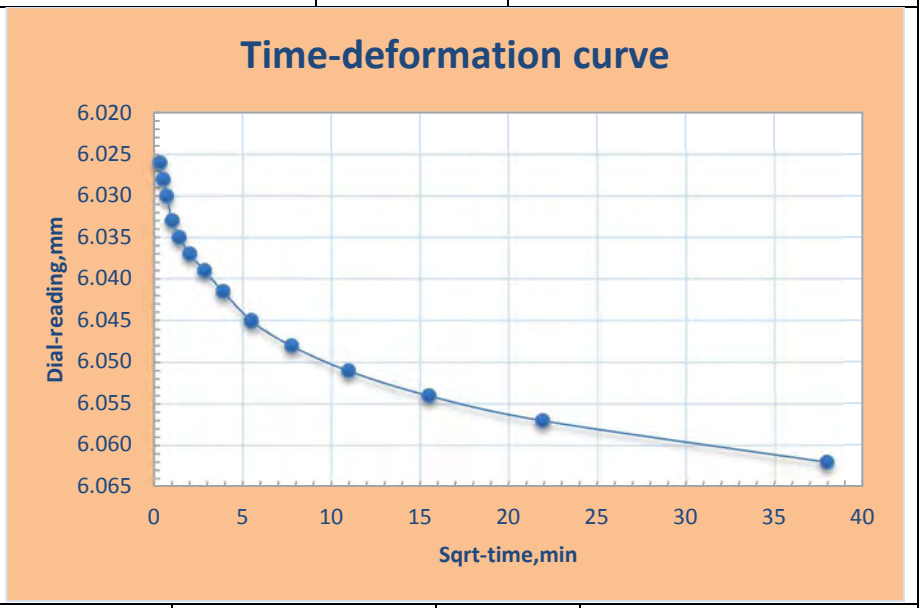

	d_o	=6.032mm	$\sqrt{t_{90}}$=7.2=51.8mi	T=0.848	$C_V=(0.848* H_{avg}^2)/ t_{90}$
	d_{90}	=6.047mm	H_{avg}=19.8519mm		C_V=0.001074cm^2/sec

Load increment: 100kpa

Elapsed Time (min)	Deformation Dial Reading (mm)
0	6.062
0.1	6.084
0.25	6.087
0.5	6.088
1	6.09
2	6.0918
4	6.094
8	6.0964
15	6.0994
30	6.102
60	6.105
120	6.108
240	6.1108
480	6.116
1440	6.126

Initial Height, H_O	19.908mm
Final height, H_f	19.844mm
Deformation	0.064mm

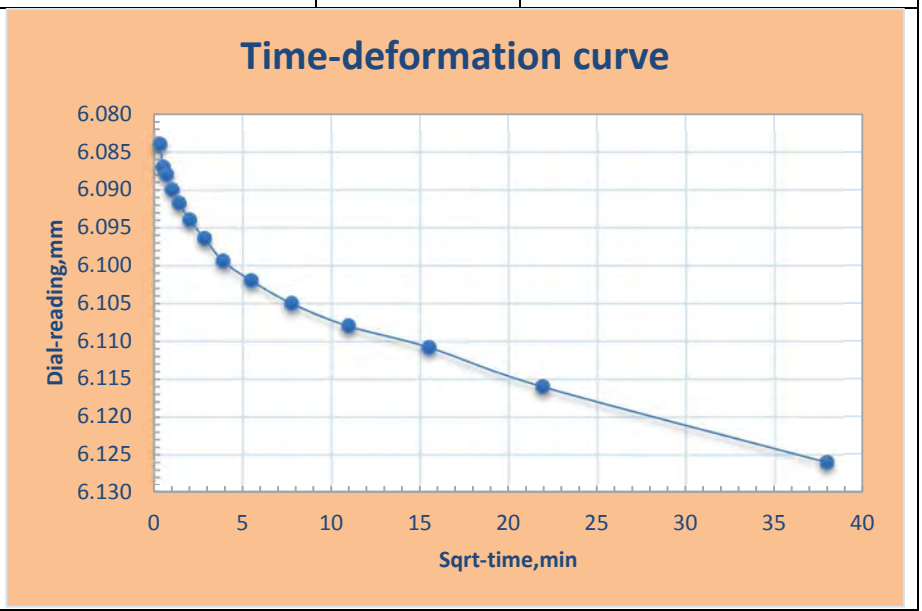

	d_o	=6.088mm	$\sqrt{t_{90}}$=5=25min	T=0.848	$C_V=(0.848* H_{avg}^2)/ t_{90}$
	d_{90}	=6.103mm	H_{avg}=19.876mm		C_V=0.002233cm^2/sec

Load increment: 200kpa

Elapsed Time (min)	Deformation Dial Reading (mm)
0	6.126
0.1	6.178
0.25	6.184
0.5	6.188
1	6.193
2	6.199
4	6.204
8	6.207
15	6.212
30	6.218
60	6.222
120	6.228
240	6.2356
480	6.244
1440	6.256

Initial Height, H_O	19.844mm
Final height, H_f	19.714mm
Deformation	0.13mm

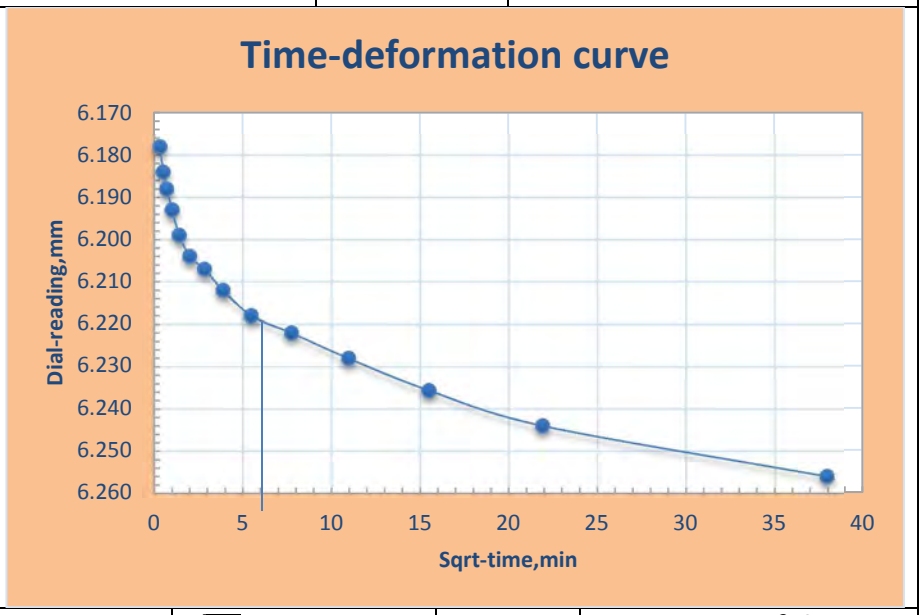

d_o	=6.195mm	$\sqrt{t_{90}}$=6.6=43.56mi	T=0.848	C_V=(0.848* H_{avg}^2)/ t_{90}
d_{90}	=6.220mm	H_{avg}=19.779mm		C_V=0.001270cm^2/sec

Load increment: 400kpa

Elapsed Time (min)	Deformation Dial Reading (mm)
0	6.256
0.1	6.332
0.25	6.348
0.5	6.356
1	6.364
2	6.372
4	6.38
8	6.39
15	6.399
30	6.41
60	6.422
120	6.434
240	6.446
480	6.458
1440	6.474

Initial Height, H_O	19.714mm
Final height, H_f	19.496mm
Deformation	0.218mm

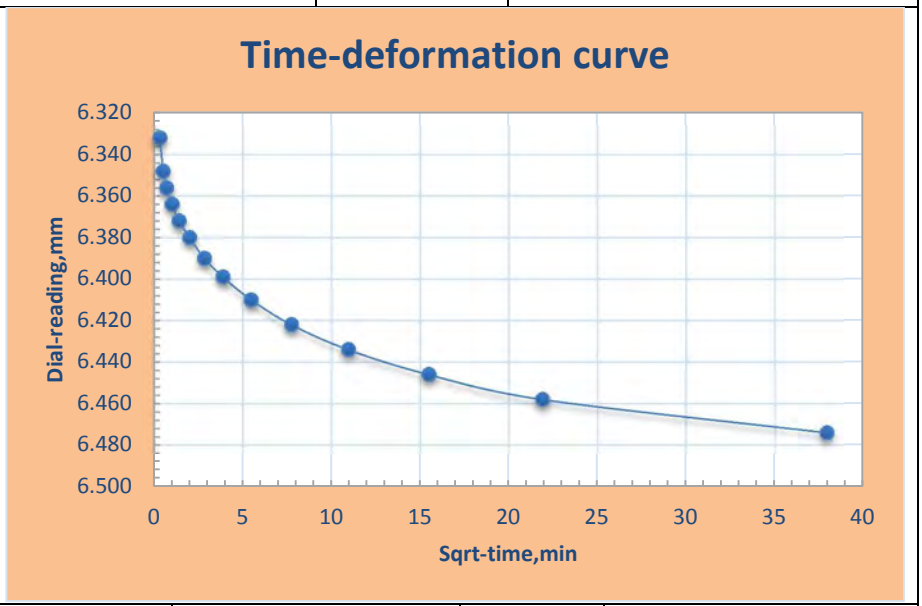

d_o	=6.360mm	$\sqrt{t_{90}}$=6=36min	T=0.848	C_V=(0.848* H_{avg}^2)/ t_{90}
d_{90}	=6.415mm	H_{avg}=19.605mm		C_V=0.001509cm^2/sec

Load increment: 800kpa					
Elapsed Time (min)	Deformation Dial Reading (mm)	Initial Height, H_o	19.496mm		
		Final height, H_f	19.178mm		
		Deformation	0.318mm		
0	6.474	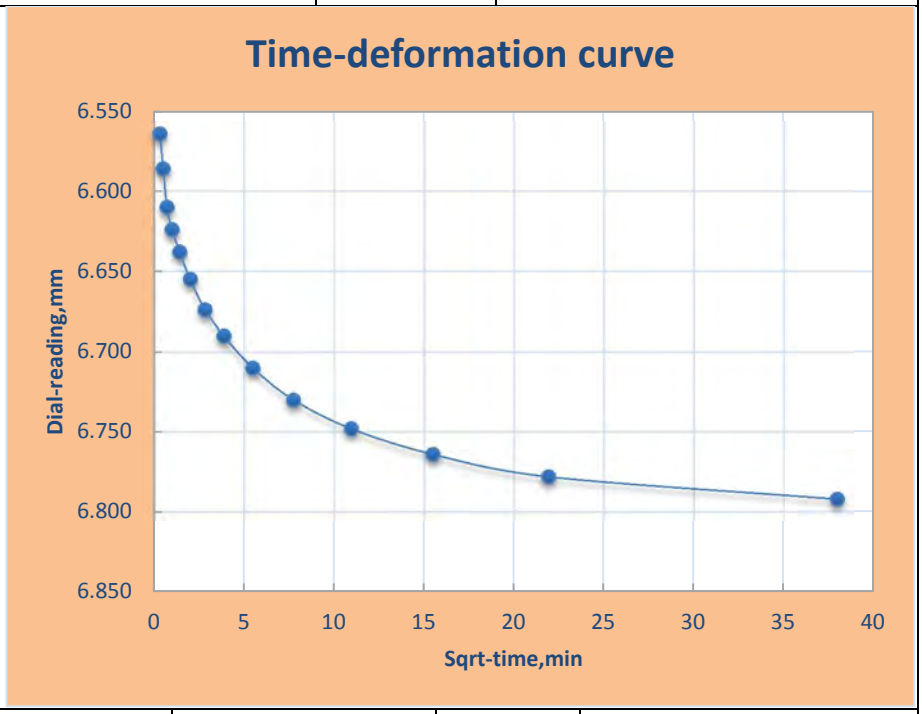			
0.1	6.564				
0.25	6.586				
0.5	6.61				
1	6.624				
2	6.638				
4	6.655				
8	6.674				
15	6.69				
30	6.71				
60	6.73				
120	6.748				
240	6.764				
480	6.778				
1440	6.792				
	d_o	=6.620mm	$\sqrt{t_{90}}$=7.5=56.3mi	T=0.848	C_V=(0.848* H_{avg}^2)/ t_{90}
	d_{90}	=6.730mm	H_{avg}=19.337mm		C_V=0.00094cm^2/sec

Load increment: 1600kpa

Elapsed Time (min)	Deformation Dial Reading (mm)
0	6.792
0.1	6.9
0.25	6.922
0.5	6.932
1	6.946
2	6.965
4	6.99
8	7.023
15	7.062
30	7.112
60	7.148
120	7.18
240	7.222
480	7.23
1440	7.258

Initial Height, H_O	19.178mm
Final height, H_f	18.712mm
Deformation	0.466mm

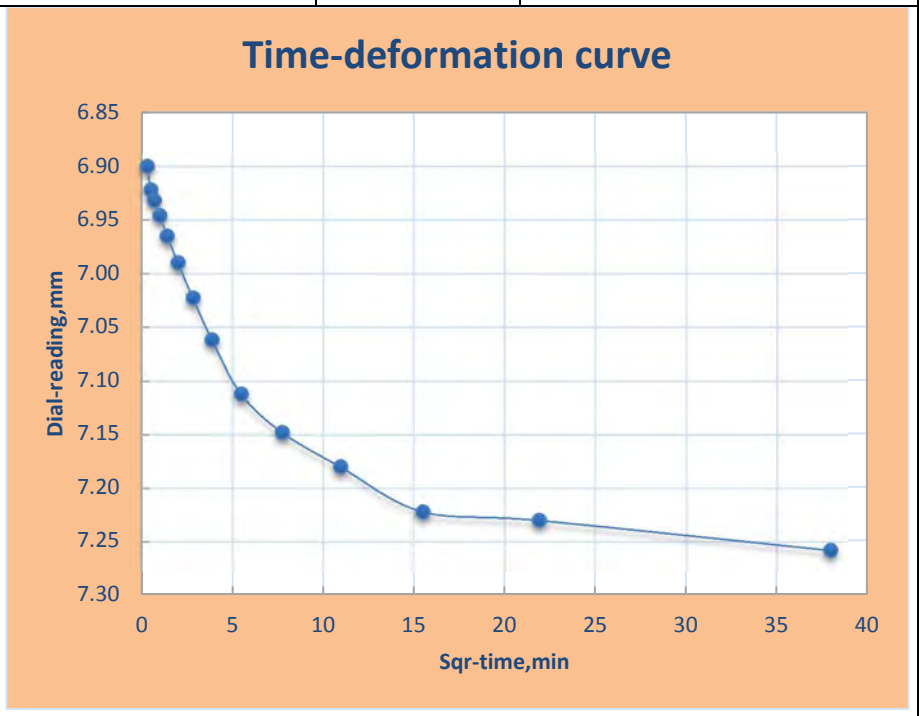

	d_o	=6.920mm	$\sqrt{t_{90}}$=6.5=42.25mi	T=0.848	$C_V=(0.848* H_{avg}^2)/ t_{90}$
	d_{90}	=7.130mm	H_{avg}=18.945mm		C_V=0.001121cm²/sec

unloading

Load Decrement, kpa	Def. Dial Reading (mm)
800	7.204
400	7.132
200	7.0758
100	7.0479
50	7.0025
25	

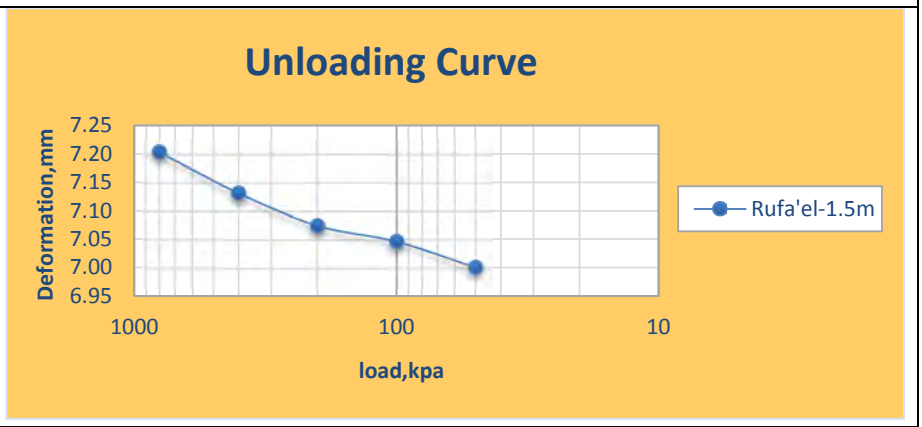

Compression at the end of each loading

Loading, kpa	Deformation, mm	Height of Specimen, mm
25	0.0426	19.9574
50	0.092	19.908
100	0.156	19.844
200	0.286	19.714
400	0.496	19.504
800	0.822	19.178
1600	1.288	18.712

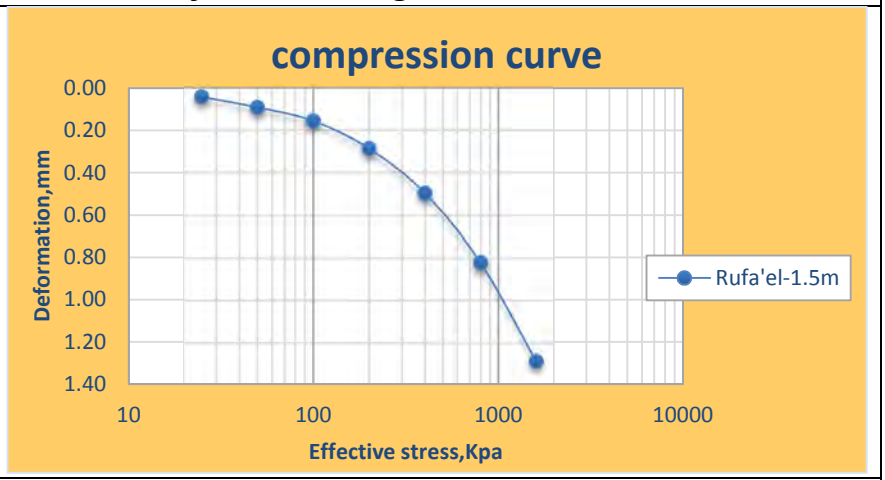

Void ratio at the end of each loading

Loading, kpa	Void ratio, e
25	0.74827
50	0.743944
100	0.73834
200	0.726956
400	0.708567
800	0.680021
1600	0.639215
800	0.643944
400	0.650249
200	0.65517
100	0.657613
50	0.661588
25	

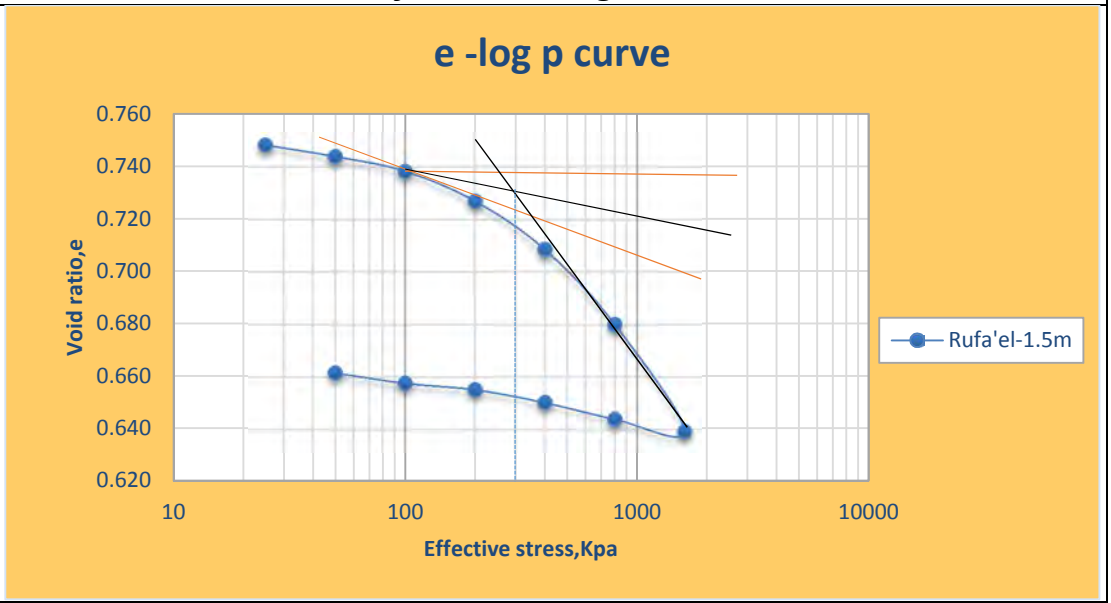

$e=(H-H_S)/H_S$	$H_S=H_O/(1+e_O)$	$C_C=(e_1-e_2)/\log(\sigma_2/\sigma_1)$	$e_1=0.709$	$\sigma_2=1600$kpa
		$C_C=0.124$	$e_2=0.639$	$\sigma_1=400$kpa

Compression coefficient

Load, kpa	Void ratio, e	$a_V=(e_1-e_2)/(\sigma_2-\sigma_1)$	$m_V=a_V/(1+e_1)$	C_V(cm2/sec)	Pc,kpa
25	0.74827	0.00017303	9.8972E-05	0.000940	
50	0.743944	0.000112084	6.427E-05	0.001074	300
100	0.73834	0.000113835	6.5485E-05	0.001140	
200	0.726956	9.1944E-05	5.324E-05	0.001270	
400	0.708567	7.1366E-05	4.177E-05	0.001509	
800	0.680021	5.1007E-05	3.0361E-05	0.000940	
1600	0.639215			0.001121	

Load, kpa	Cv,10^{-4}cm²/sec
25	9.40
50	10.74
100	11.40
200	12.70
400	15.09
800	9.40
1600	11.21

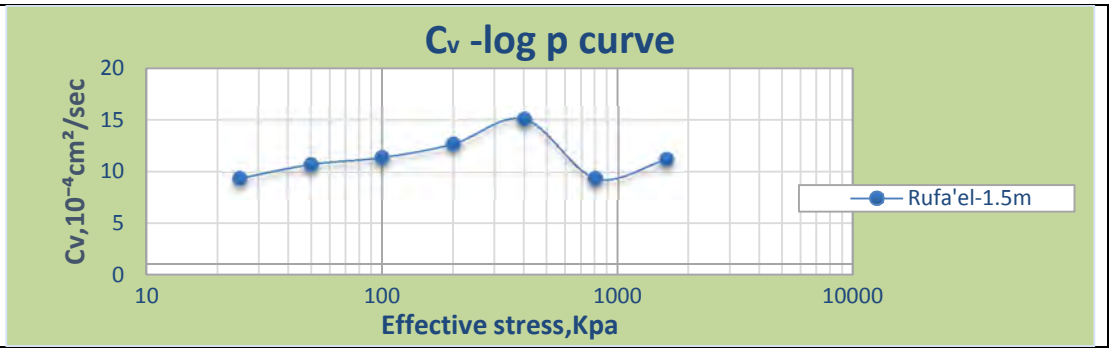

E6. One dimensional consolidation test for Rufa'el sample @3m, R-2

Load increment: 50kpa

Elapsed Time (min)	Deformation Dial Reading (mm)
0	3.281
0.1	3.32
0.25	3.324
0.5	3.3256
1	3.3276
2	3.33
4	3.332
8	3.334
15	3.336
30	3.338
60	3.3404
120	3.3426
240	3.3456
480	3.3486
1440	3.354

Initial Height, H_O	20mm				
Final height, H_f	19.927mm				
Deformation	0.073mm				
	d_o	=3.328mm	$\sqrt{t_{90}}$=7=49min	T=0.848	$C_V=(0.848* H_{avg}^2)/ t_{90}$
	d_{90}	=3.339mm	H_{avg}=19.9635mm		C_V=0.001150cm²/sec

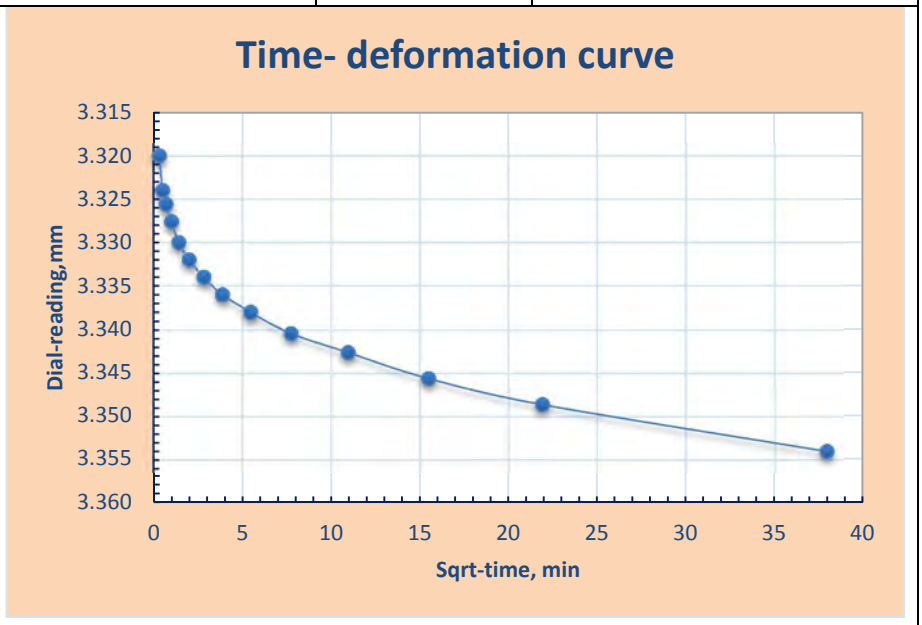

Load increment: 100kpa

Elapsed Time (min)	Deformation Dial Reading (mm)
0	3.354
0.1	3.412
0.25	3.418
0.5	3.422
1	3.426
2	3.431
4	3.436
8	3.44
15	3.4436
30	3.448
60	3.452
120	3.456
240	3.46
480	3.464
1440	3.47

Initial Height, H_O	19.927mm				
Final height, H_f	19.811mm				
Deformation	0.116mm				
	d_o	=3.43mm	$\sqrt{t_{90}}$=7=49min	T=0.848	C_V=(0.848* H_{avg}^2)/ t_{90}
	d_{90}	=3.452mm	H_{avg}=19.869mm		C_V=0.001138cm^2/sec

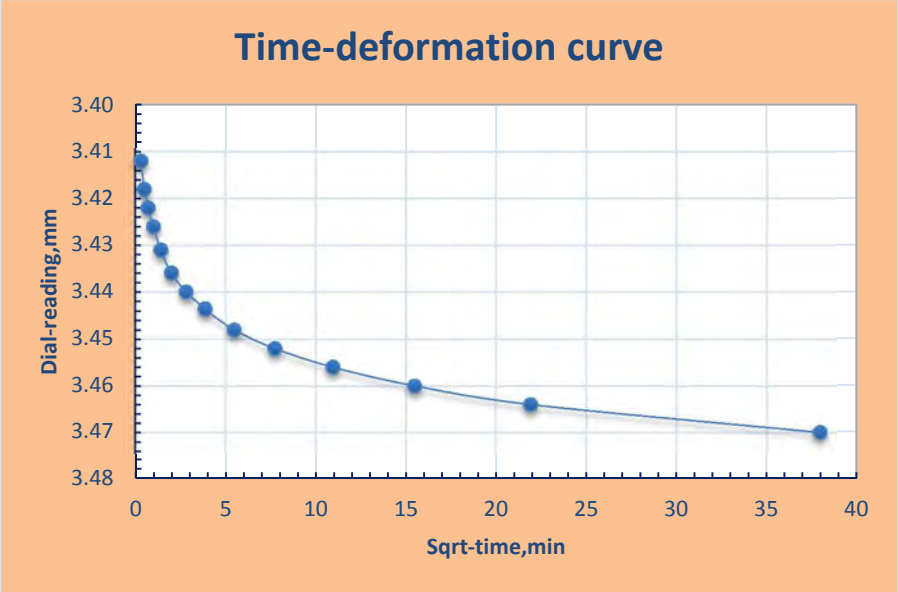

Load increment: 200kpa

Elapsed Time (min)	Deformation Dial Reading (mm)
0	3.47
0.1	3.518
0.25	3.525
0.5	3.53
1	3.536
2	3.5436
4	3.55
8	3.556
15	3.563
30	3.57
60	3.576
120	3.582
240	3.588
480	3.596
1440	3.604

Initial Height, H_O	19.811mm				
Final height, H_f	19.677mm				
Deformation	0.134mm				
	d_o	=3.54mm	$\sqrt{t_{90}}$=6.5=42.3m	T=0.848	C_V=(0.848* H_{avg}^2)/ t_{90}
	d_{90}	=3.576mm	H_{avg}=19.744mm		C_V=0.001304cm^2/sec

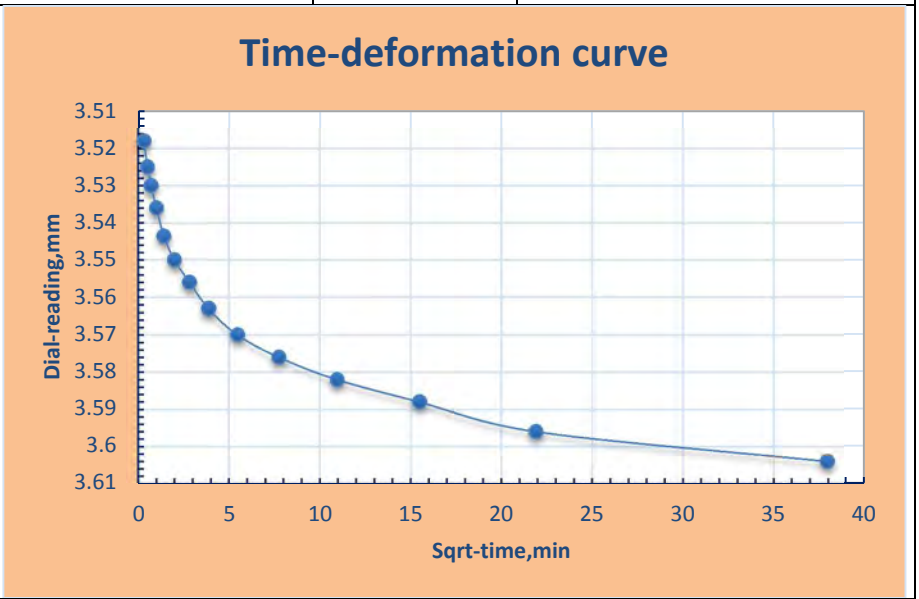

Load increment: 400kpa

Elapsed Time (min)	Deformation Dial Reading (mm)
0	3.604
0.1	3.684
0.25	3.694
0.5	3.702
1	3.711
2	3.72
4	3.732
8	3.742
15	3.752
30	3.7604
60	3.769
120	3.778
240	3.786
480	3.794
1440	3.804

Initial Height, H_O	19.677mm
Final height, H_f	19.477mm
Deformation	0.2mm

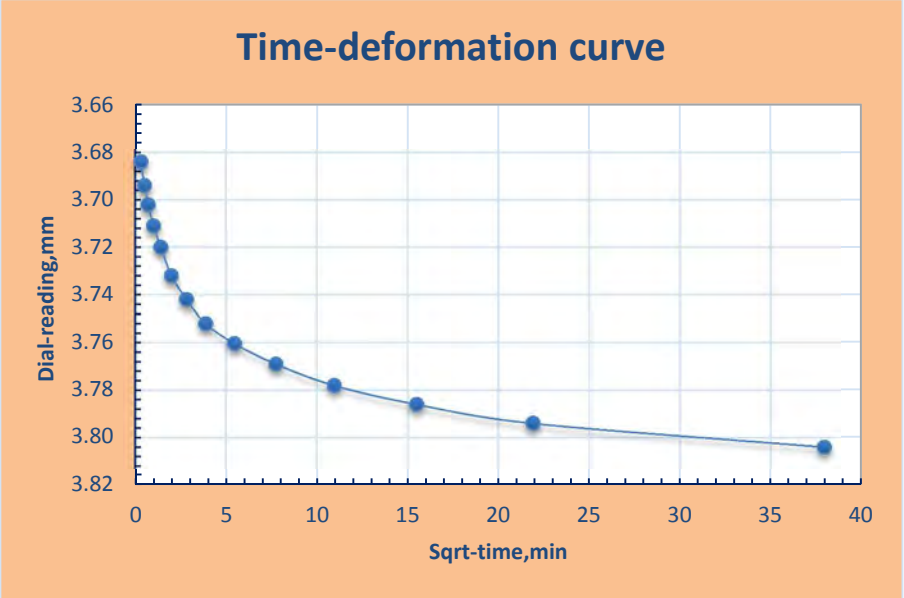

d_o	=3.716mm	$\sqrt{t_{90}}$=6.2=38.44mi	T=0.848	$C_V=(0.848* H_{avg}^2)/ t_{90}$
d_{90}	=3.764mm	H_{avg}=19.577mm		C_V=0.001409cm²/sec

Load increment: 800kpa

Elapsed Time (min)	Deformation Dial Reading (mm)
0	3.804
0.1	3.896
0.25	3.908
0.5	3.916
1	3.93
2	3.944
4	3.96
8	3.98
15	3.998
30	4.016
60	4.03
120	4.044
240	4.056
480	4.066
1440	4.078

Initial Height, H_O	19.477mm
Final height, H_f	19.203mm
Deformation	0.274mm

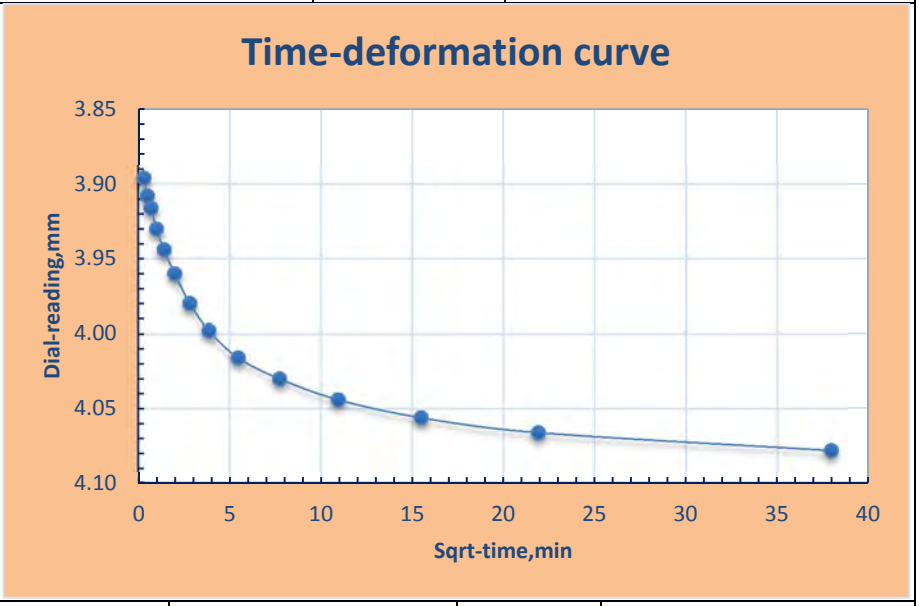

d_o	=3.95mm	$\sqrt{t_{90}}$=7.74=60min	T=0.848	$C_V=(0.848* H_{avg}^2)/ t_{90}$
d_{90}	=4.03mm	H_{avg}=19.34mm		C_V=0.000881cm²/sec

Load increment: 1600kpa

Elapsed Time (min)	Deformation Dial Reading (mm)			
		Initial Height, H_O	19.203mm	
		Final height, H_f	18.825mm	
		Deformation	0.378mm	
0	4.078			
0.1	4.182			
0.25	4.194			
0.5	4.204			
1	4.22			
2	4.241			
4	4.267			
8	4.302			
15	4.338			
30	4.3704			
60	4.398			
120	4.4172			
240	4.434			
480	4.444			
1440	4.456			

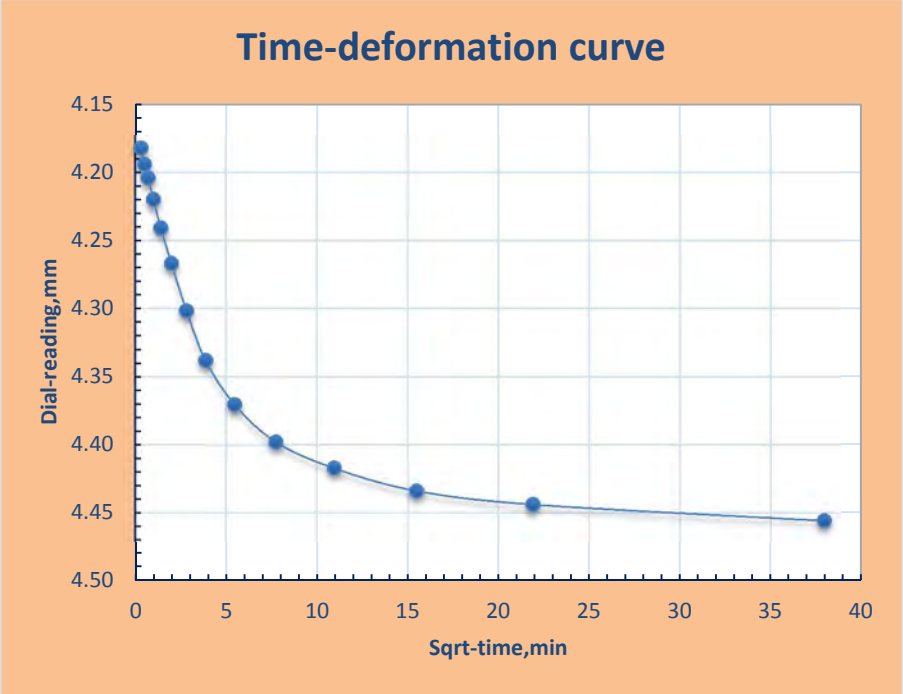

	d_o	=4.19mm	$\sqrt{t_{90}}$=6.5=42.25mi	T=0.848	$C_V=(0.848* H_{avg}^2)/ t_{90}$
	d_{90}	=4.39mm	H_{avg}=19.014mm		C_V=0.001209cm^2/sec

unloading

Load Decrement, kpa	Def. Dial Reading (mm)
800	4.38
400	4.323
200	4.2868
100	4.2589
50	4.2335
25	

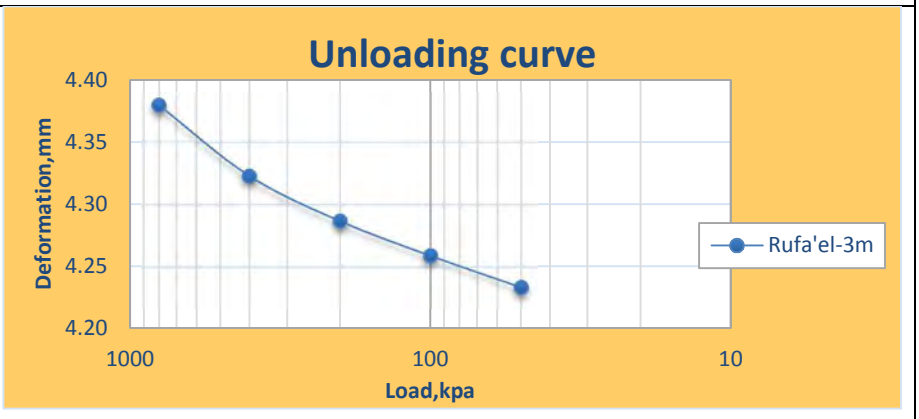

Compression at the end of each loading

Loading, kpa	Deformation, mm	Height of Specimen, mm
25		20
50	0.073	19.927
100	0.189	19.811
200	0.323	19.677
400	0.523	19.477
800	0.797	19.203
1600	1.175	18.825

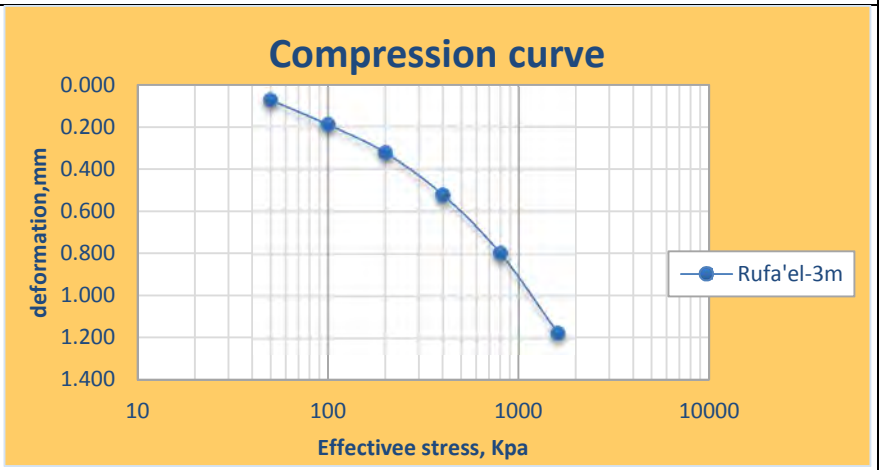

Void ratio at the end of each loading

Loading, kpa	Void ratio, e
25	
50	0.726
100	0.715
200	0.704
400	0.687
800	0.663
1600	0.630
800	0.636
400	0.641
200	0.644
100	0.646
50	0.648
25	

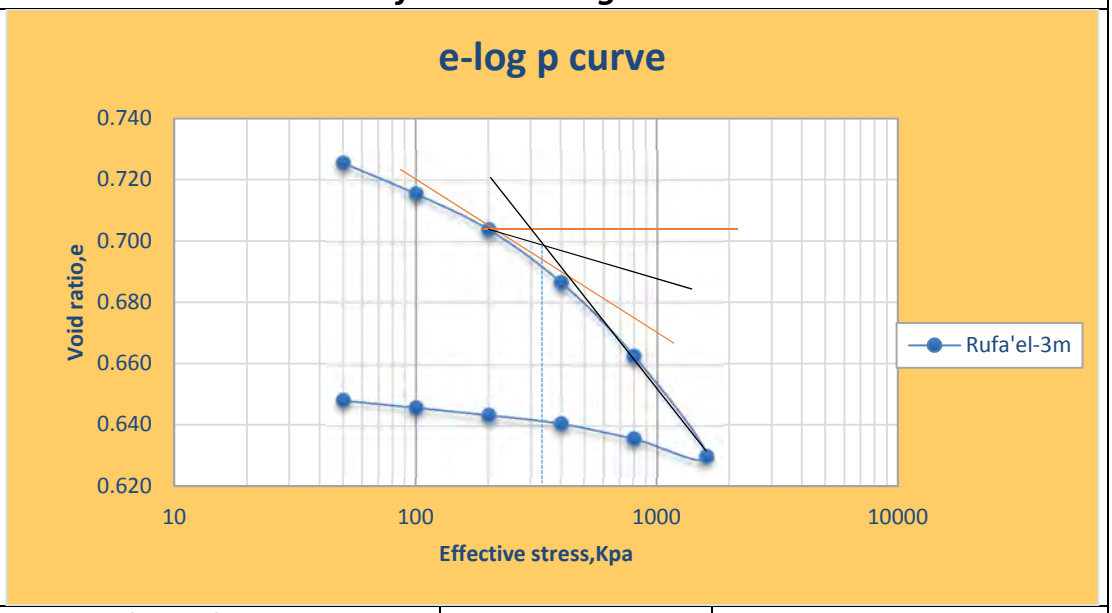

$e=(H-H_S)/H_S$, $H_S=H_O/(1+e_O)$		$C_C=(e_1-e_2)/\log(\sigma_2/\sigma_1)$	e_1=0.682	σ_2=1600kpa
		C_C=0.103	e_2=0.630	σ_1=500kpa

Compression coefficient

Load, kpa	Void ratio, e	$a_V=(e_1-e_2)/(\sigma_2-\sigma_1)$	$m_V=a_V/(1+e_1)$	C_V(cm2/sec)	Pc,kpa
25					320
50	0.726	0.000201	0.000116	0.001150	
100	0.715	0.000116	6.76E-05	0.001138	
200	0.704	8.66E-05	5.08E-05	0.001304	
400	0.687	5.93E-05	3.52E-05	0.001409	
800	0.663	4.09E-05	2.46E-05	0.000881	
1600	0.630			0.001209	

Load, kpa	Cv,$10^{-4}cm^2/sec$
25	
50	11.50
100	11.38
200	13.04
400	14.09
800	8.81
1600	12.09

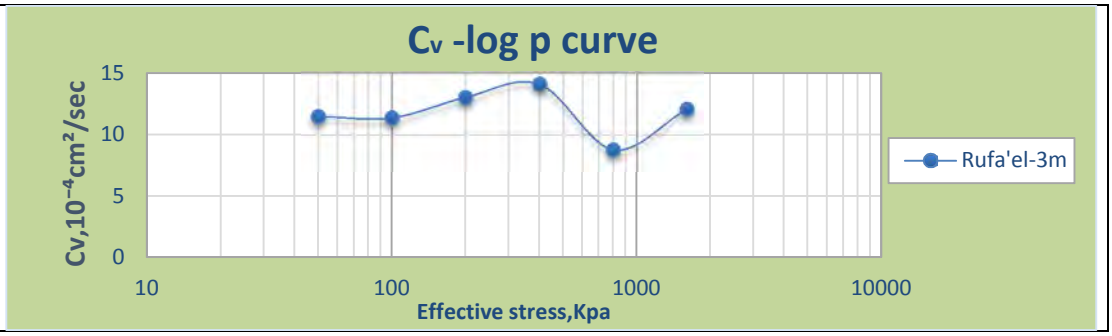

F. CONSTANT RATE OF STRAIN CONSOLIADTION (CRSC)TEST

TEST REPORT. (SAMPLE).

Location:-Kolfe-Keraneyo @ 3m, K-2

Specimen and Test conditions.

Liquid limit = 73 %	Diameter=63.5mm
Plasticity Index=49 %	height =25.4mm
Strain rate = 0.004%/min	Type = Undisturbed
Back pressure =200kpa	

u = pore pressure
Disp. =deformation
σ_v = Total stress
σ'_v (top) = Top effective stress
σ'_v (bottom) = Bottom effective stress
u_a = Excess pore pressure

h= Current thickness of specimen
dσ/dt (drain) = Rate of change of effective stress at drained face
dσ/dt (undrain) = Rate of change of effective stress at undrained face
ε = strain
e= void ratio
C_v =Coefficient of consolidation

Time (min)	u (kPa)	Disp. (mm)	Load kN	σ_v kPa	σ'_v top (kpa)	σ'_v bottom (kpa)	u_a (kPa)	h (mm)	$h^2/2u_a$	avg. σ'_v kPa	ε %	e	dσ/dt drained	dσ/dt undrained	C_v drained	C_v undrained
1	204.5	0.02	0.03	210	10.1	5.6	4.50	25.38	0.72	6.8	0.08	0.807	0.097	0.051	6968.08	3663.86
2	209.9	0.03	0.07	222	22.1	12.2	9.90	25.37	0.33	14.9	0.12	0.806	0.103	0.059	3335.88	1911.00
3	215.0	0.03	0.11	235	34.7	19.7	15.02	25.37	0.21	23.8	0.12	0.806	0.113	0.069	2418.03	1474.15
4	220.5	0.03	0.16	249	49.3	28.8	20.50	25.37	0.16	34.4	0.13	0.806	0.129	0.088	2023.74	1379.55
5	224.9	0.04	0.21	266	65.7	40.8	24.87	25.36	0.13	47.8	0.16	0.805	0.113	0.075	1463.57	966.11
6	229.7	0.04	0.24	276	76.4	46.7	29.73	25.36	0.11	55.0	0.17	0.805	0.108	0.070	1164.95	758.67
7	233.9	0.05	0.29	292	91.6	57.7	33.90	25.35	0.09	67.3	0.20	0.804	0.119	0.083	1124.55	789.38
8	238.2	0.06	0.33	305	104.8	66.6	38.20	25.34	0.08	77.5	0.24	0.804	0.111	0.076	930.70	640.51
9	242.2	0.07	0.37	318	118.1	75.9	42.17	25.33	0.08	88.0	0.28	0.803	0.105	0.072	800.70	544.90
10	246.3	0.08	0.41	330	130.1	83.8	46.27	25.32	0.07	97.0	0.31	0.802	0.053	0.040	364.34	278.19

15	251.1	0.10	0.49	356	156.0	104.9	51.13	25.30	0.06	119.7	0.39	0.801	0.035	0.028	217.41	172.81
20	254.8	0.12	0.54	372	171.8	117.0	54.82	25.28	0.06	132.9	0.47	0.799	0.027	0.021	156.46	121.92
25	258.2	0.13	0.60	388	188.2	130.0	58.24	25.27	0.05	147.0	0.51	0.799	0.022	0.016	118.29	87.36
30	261.6	0.13	0.63	398	197.7	136.1	61.59	25.27	0.05	154.1	0.52	0.799	0.021	0.015	106.40	76.29
35	265.2	0.15	0.67	413	212.8	147.6	65.21	25.25	0.05	166.8	0.59	0.797	0.021	0.015	102.90	72.55
40	269.0	0.16	0.71	423	222.9	153.9	69.04	25.24	0.05	174.1	0.63	0.797	0.022	0.015	99.52	70.35
45	272.8	0.18	0.76	439	238.7	165.9	72.80	25.22	0.04	187.3	0.71	0.795	0.023	0.016	98.81	70.17
50	276.9	0.18	0.79	450	250.1	173.2	76.91	25.22	0.04	195.7	0.71	0.795	0.023	0.017	96.84	71.13
55	280.3	0.19	0.85	467	266.8	186.6	80.26	25.21	0.04	210.2	0.75	0.794	0.023	0.017	89.61	67.96
60	283.5	0.21	0.88	477	277.2	193.8	83.47	25.19	0.04	218.3	0.83	0.793	0.021	0.016	79.04	58.92
65	286.6	0.23	0.92	492	291.8	205.1	86.61	25.17	0.04	230.7	0.91	0.792	0.018	0.012	65.43	45.02
70	290.2	0.24	0.95	499	298.7	208.5	90.17	25.16	0.04	235.1	0.94	0.791	0.013	0.010	44.33	34.43
85	293.4	0.25	1.02	522	322.1	228.7	93.38	25.15	0.03	256.3	0.98	0.790	0.012	0.010	39.79	33.87
100	296.5	0.27	1.08	541	341.0	244.6	96.46	25.13	0.03	273.2	1.06	0.789	0.008	0.007	27.52	22.49
115	298.9	0.28	1.12	552	352.4	253.5	98.92	25.12	0.03	282.9	1.10	0.788	0.008	0.007	26.78	21.76
130	302.1	0.29	1.18	571	371.3	269.2	102.14	25.11	0.03	299.7	1.14	0.787	0.009	0.007	27.58	21.84
145	305.6	0.31	1.22	585	384.6	279.0	105.62	25.09	0.03	310.5	1.22	0.786	0.008	0.007	25.16	19.54
160	308.9	0.33	1.27	602	401.6	292.7	108.91	25.07	0.03	325.3	1.30	0.785	0.009	0.007	25.56	20.35
175	312.1	0.34	1.32	616	416.5	304.4	112.12	25.06	0.03	337.9	1.34	0.784	0.008	0.007	23.31	18.64
190	314.9	0.35	1.37	632	431.6	316.7	114.92	25.05	0.03	351.1	1.38	0.783	0.009	0.008	25.41	20.64
205	318.4	0.36	1.43	650	450.0	331.5	118.41	25.04	0.03	367.1	1.42	0.782	0.010	0.008	26.62	21.61
220	321.8	0.37	1.48	668	468.0	346.2	121.76	25.03	0.03	382.8	1.46	0.782	0.009	0.007	22.71	17.84
235	325.3	0.39	1.53	682	481.8	356.6	125.25	25.01	0.02	394.2	1.54	0.780	0.009	0.007	22.73	18.00
250	328.6	0.41	1.59	701	500.8	372.2	128.60	24.99	0.02	410.9	1.61	0.779	0.010	0.008	24.72	20.57
265	331.4	0.44	1.64	718	518.5	387.1	131.40	24.96	0.02	426.7	1.73	0.777	0.010	0.008	23.13	19.17
280	334.6	0.46	1.70	736	535.8	401.2	134.61	24.94	0.02	441.8	1.81	0.775	0.011	0.009	25.17	21.30
295	337.4	0.48	1.77	758	557.6	420.2	137.42	24.92	0.02	461.8	1.89	0.774	0.011	0.010	25.89	21.74
310	341.3	0.49	1.83	777	577.2	436.0	141.25	24.91	0.02	478.7	1.93	0.773	0.010	0.008	22.69	18.65
325	344.1	0.50	1.88	795	594.9	450.8	144.05	24.90	0.02	494.5	1.97	0.772	0.010	0.008	21.22	17.44
340	347.5	0.51	1.94	813	612.6	465.0	147.54	24.89	0.02	509.8	2.01	0.772	0.011	0.009	23.27	19.75
355	350.1	0.52	2.01	835	634.7	484.6	150.07	24.88	0.02	530.2	2.05	0.771	0.010	0.009	21.58	18.54
370	352.9	0.53	2.06	850	650.5	497.6	152.87	24.87	0.02	544.1	2.09	0.770	0.011	0.010	23.10	19.95

385	355.7	0.56	2.14	876	675.7	520.0	155.67	24.84	0.02	567.5	2.20	0.768	0.011	0.010	22.57	19.40
400	358.6	0.58	2.19	892	691.5	532.9	158.63	24.82	0.02	581.2	2.28	0.767	0.012	0.010	22.52	18.98
415	362.3	0.60	2.27	918	718.0	555.7	162.32	24.80	0.02	605.3	2.36	0.765	0.011	0.010	21.69	18.39
430	364.9	0.62	2.32	933	732.6	567.7	164.86	24.78	0.02	618.0	2.44	0.764	0.012	0.011	22.46	19.62
445	367.7	0.64	2.41	961	761.0	593.2	167.74	24.76	0.02	644.6	2.52	0.762	0.013	0.012	24.19	21.56
460	370.0	0.65	2.47	980	779.9	609.9	170.02	24.75	0.02	662.0	2.56	0.762	0.013	0.011	23.41	20.53
475	373.6	0.67	2.56	1008	808.3	634.8	173.58	24.73	0.02	688.0	2.64	0.760	0.013	0.011	22.87	19.92
490	376.1	0.69	2.62	1027	827.3	651.2	176.12	24.71	0.02	705.3	2.72	0.759	0.013	0.011	21.96	19.57
505	378.5	0.71	2.70	1054	853.8	675.3	178.54	24.69	0.02	730.2	2.80	0.757	0.013	0.011	21.85	19.55
520	381.0	0.72	2.77	1073	873.1	692.1	180.95	24.68	0.02	747.8	2.83	0.757	0.013	0.011	21.28	18.79
536	383.9	0.73	2.85	1100	899.6	715.7	183.90	24.67	0.02	772.4	2.87	0.756	0.013	0.011	21.65	18.66
550	387.5	0.74	2.91	1120	920.1	732.7	187.45	24.66	0.02	790.5	2.91	0.755	0.013	0.011	21.11	18.46
565	389.7	0.76	3.00	1146	946.0	756.3	189.73	24.64	0.02	814.9	2.99	0.754	0.013	0.012	21.23	18.46
580	393.7	0.77	3.07	1168	967.8	774.1	193.68	24.63	0.02	833.9	3.03	0.753	0.014	0.012	21.31	18.53
595	396.2	0.79	3.15	1195	995.3	799.1	196.16	24.61	0.02	859.8	3.11	0.752	0.013	0.011	19.67	17.31
610	399.3	0.81	3.21	1214	1014.2	815.0	199.25	24.59	0.02	876.6	3.19	0.750	0.013	0.012	20.16	17.58
625	402.3	0.83	3.30	1243	1042.9	840.7	202.26	24.57	0.01	903.3	3.27	0.749	0.013	0.011	19.36	16.84
641	405.3	0.85	3.36	1261	1060.9	855.6	205.34	24.55	0.01	919.2	3.35	0.747	0.014	0.012	20.15	17.94
655	407.7	0.87	3.46	1293	1092.5	884.8	207.69	24.53	0.01	949.3	3.43	0.746	0.014	0.012	19.98	17.53
671	411.4	0.89	3.52	1311	1110.8	899.4	211.44	24.51	0.01	965.0	3.50	0.745	0.014	0.012	19.21	16.65
686	414.2	0.92	3.62	1341	1141.5	927.3	214.19	24.48	0.01	993.8	3.62	0.743	0.014	0.012	18.99	16.47
700	417.8	0.93	3.67	1359	1158.8	941.0	217.81	24.47	0.01	1008.6	3.66	0.742	0.014	0.012	19.21	16.51
716	421.3	0.95	3.78	1392	1192.0	970.7	221.30	24.45	0.01	1039.5	3.74	0.740	0.014	0.012	18.34	15.98
730	424.1	0.96	3.83	1408	1207.8	983.7	224.11	24.44	0.01	1053.3	3.78	0.740	0.014	0.012	18.61	16.28
746	427.6	0.97	3.93	1442	1242.2	1014.6	227.60	24.43	0.01	1085.4	3.82	0.739	0.012	0.010	15.24	12.96
761	430.5	0.98	3.96	1450	1250.4	1019.9	230.48	24.42	0.01	1091.6	3.86	0.738	0.013	0.011	16.76	14.59
775	433.6	1.00	4.08	1488	1288.3	1054.7	233.56	24.40	0.01	1127.4	3.94	0.737	0.014	0.013	18.21	16.23
790	436.0	1.01	4.12	1501	1300.9	1064.9	235.97	24.39	0.01	1138.4	3.98	0.736	0.013	0.011	16.13	14.04
805	439.5	1.03	4.23	1534	1334.4	1094.9	239.53	24.37	0.01	1169.5	4.06	0.735	0.014	0.012	17.05	15.00
821	442.1	1.04	4.28	1551	1351.4	1109.4	242.07	24.36	0.01	1184.8	4.09	0.734	0.014	0.013	17.43	15.74
836	444.6	1.06	4.39	1586	1386.2	1141.6	244.55	24.34	0.01	1217.9	4.17	0.733	0.015	0.014	18.53	17.05
850	446.4	1.08	4.45	1605	1405.1	1158.8	246.36	24.32	0.01	1235.7	4.25	0.731	0.013	0.012	15.92	14.18

865	449.7	1.10	4.54	1634	1433.5	1183.8	249.71	24.30	0.01	1261.8	4.33	0.730	0.015	0.013	17.47	15.46
880	452.5	1.11	4.62	1659	1458.8	1206.3	252.53	24.29	0.01	1285.2	4.37	0.729	0.014	0.012	16.02	14.32
895	454.9	1.13	4.70	1683	1482.8	1227.9	254.94	24.27	0.01	1307.5	4.45	0.728	0.014	0.012	15.98	14.41
911	457.5	1.14	4.78	1709	1509.3	1251.8	257.49	24.26	0.01	1332.4	4.49	0.727	0.014	0.014	16.42	15.61
925	457.5	1.15	4.86	1735	1534.6	1277.1	257.49	24.25	0.01	1357.7	4.53	0.726	0.015	0.015	17.25	16.90
940	458.6	1.16	4.95	1763	1563.0	1304.4	258.56	24.24	0.01	1385.5	4.57	0.725	0.015	0.014	16.89	16.13
956	459.9	1.17	5.03	1788	1588.3	1328.4	259.90	24.23	0.01	1409.9	4.61	0.725	0.015	0.014	16.52	15.43
971	462.1	1.19	5.12	1817	1616.7	1354.6	262.11	24.21	0.01	1436.8	4.69	0.723	0.016	0.015	17.60	16.44
986	463.7	1.21	5.21	1845	1645.1	1381.4	263.66	24.19	0.01	1464.3	4.76	0.722	0.016	0.015	17.77	16.92
1000	464.8	1.24	5.30	1874	1673.5	1408.7	264.84	24.16	0.01	1491.9	4.88	0.720	0.014	0.013	15.46	14.70
1016	466.1	1.25	5.37	1896	1695.6	1429.5	266.12	24.15	0.01	1513.2	4.92	0.719	0.015	0.014	16.09	15.37
1031	467.2	1.27	5.47	1927	1727.2	1460.0	267.23	24.13	0.01	1544.1	5.00	0.718	0.017	0.016	18.23	17.49
1045	468.6	1.28	5.56	1956	1755.6	1487.0	268.56	24.12	0.01	1571.7	5.04	0.717	0.015	0.015	16.55	15.84
1060	469.5	1.29	5.64	1981	1780.9	1511.3	269.53	24.11	0.01	1596.3	5.08	0.716	0.015	0.015	16.25	15.73
1075	470.3	1.30	5.73	2009	1809.3	1539.0	270.28	24.10	0.01	1624.3	5.12	0.715	0.016	0.015	16.90	16.33
1090	471.5	1.31	5.82	2038	1837.7	1566.2	271.46	24.09	0.01	1652.0	5.16	0.715	0.016	0.015	16.58	15.97
1106	472.4	1.32	5.91	2066	1866.1	1593.7	272.37	24.08	0.01	1679.8	5.20	0.714	0.016	0.015	16.89	16.48
1120	472.9	1.34	6.00	2095	1894.5	1621.7	272.86	24.06	0.01	1708.0	5.28	0.713	0.015	0.015	15.68	15.42
1136	473.3	1.36	6.08	2120	1919.8	1646.5	273.25	24.04	0.01	1733.0	5.35	0.711	0.015	0.014	15.43	15.14
1151	473.9	1.37	6.17	2148	1948.2	1674.3	273.87	24.03	0.01	1761.1	5.39	0.710	0.017	0.016	17.61	17.25
1166	474.5	1.39	6.27	2180	1979.8	1705.3	274.49	24.01	0.01	1792.3	5.47	0.709	0.018	0.017	19.08	18.37
1166	475.1	1.41	6.27	2181	1981.1	1706.0	275.09	23.99	0.01	1793.1	5.55	0.708	0.018	0.017	18.76	18.08
1181	475.7	1.42	6.37	2213	2012.6	1736.9	275.69	23.98	0.01	1824.4	5.59	0.707	0.018	0.018	19.15	18.80
1195	476.3	1.44	6.48	2246	2046.1	1769.8	276.29	23.96	0.01	1857.5	5.67	0.705	0.018	0.017	18.38	18.03
1211	476.9	1.46	6.58	2276	2076.1	1799.2	276.89	23.94	0.01	1887.1	5.75	0.704	0.018	0.018	18.90	18.56
1226	477.5	1.47	6.69	2312	2112.4	1834.9	277.49	23.93	0.01	1923.1	5.79	0.703	0.017	0.016	17.07	16.72
1240	478.1	1.47	6.76	2335	2134.5	1856.4	278.09	23.93	0.01	1944.8	5.79	0.703	0.015	0.015	15.47	15.12
1255	478.7	1.48	6.86	2366	2166.1	1887.4	278.69	23.92	0.01	1976.1	5.83	0.703	0.017	0.016	17.03	16.69
1271	479.3	1.49	6.95	2395	2194.5	1915.2	279.29	23.91	0.01	2004.1	5.87	0.702	0.015	0.014	15.01	14.68
1286	479.9	1.50	7.03	2420	2219.8	1939.9	279.89	23.90	0.01	2029.0	5.91	0.701	0.015	0.015	15.44	15.09
1300	480.5	1.52	7.12	2448	2248.2	1967.7	280.49	23.88	0.01	2057.1	5.98	0.700	0.016	0.015	16.09	15.75
1316	481.1	1.54	7.21	2477	2276.6	1995.5	281.09	23.86	0.01	2085.1	6.06	0.698	0.016	0.015	15.85	15.52

1330	481.7	1.55	7.30	2505	2305.0	2023.3	281.69	23.85	0.01	2113.2	6.10	0.698	0.016	0.016	16.34	15.99
1345	482.3	1.57	7.39	2533	2333.4	2051.1	282.29	23.83	0.01	2141.2	6.18	0.696	0.015	0.015	15.20	14.86
1360	482.9	1.58	7.47	2559	2358.7	2075.8	282.89	23.82	0.01	2166.1	6.22	0.696	0.015	0.015	14.99	14.66
1375	483.5	1.60	7.56	2587	2387.1	2103.6	283.49	23.80	0.01	2194.2	6.30	0.694	0.017	0.016	16.51	16.18
1390	484.1	1.61	7.66	2619	2418.7	2134.6	284.09	23.79	0.01	2225.4	6.34	0.693	0.014	0.013	13.71	13.39
1406	484.7	1.63	7.72	2638	2437.6	2152.9	284.69	23.77	0.01	2243.9	6.42	0.692	0.014	0.013	13.51	13.19
1421	485.3	1.65	7.82	2669	2469.2	2183.9	285.29	23.75	0.01	2275.2	6.50	0.691	0.017	0.016	16.57	16.24
1435	485.9	1.67	7.91	2698	2497.6	2211.7	285.89	23.73	0.01	2303.2	6.57	0.689	0.017	0.016	16.32	16.00
1451	486.5	1.68	8.01	2729	2529.2	2242.7	286.49	23.72	0.01	2334.4	6.61	0.688	0.017	0.016	16.46	16.13
1466	487.1	1.70	8.10	2759	2558.9	2271.8	287.09	23.70	0.01	2363.7	6.69	0.687	0.017	0.017	16.68	16.35
1481	487.7	1.72	8.20	2789	2589.2	2301.5	287.69	23.68	0.01	2393.7	6.78	0.685	0.017	0.017	16.97	16.64
1496	488.3	1.73	8.30	2821	2620.8	2332.5	288.29	23.67	0.01	2424.9	6.81	0.685	0.018	0.018	17.44	17.11
1511	488.9	1.75	8.40	2854	2653.6	2364.7	288.89	23.65	0.01	2457.3	6.89	0.683	0.018	0.017	17.03	16.71
1526	489.5	1.77	8.50	2885	2684.6	2395.1	289.49	23.63	0.01	2487.9	6.97	0.682	0.018	0.018	17.63	17.32
1541	490.1	1.78	8.62	2921	2720.6	2430.5	290.09	23.62	0.01	2523.6	7.01	0.681	0.018	0.018	17.21	16.88
1555	490.7	1.79	8.70	2947	2747.4	2456.7	290.69	23.61	0.01	2550.0	7.05	0.681	0.018	0.018	17.41	17.09
1571	491.3	1.80	8.82	2985	2785.0	2493.7	291.29	23.60	0.01	2587.2	7.09	0.680	0.015	0.013	14.08	12.59

F1. K-1 CRSC Test Results.

Strain Curve

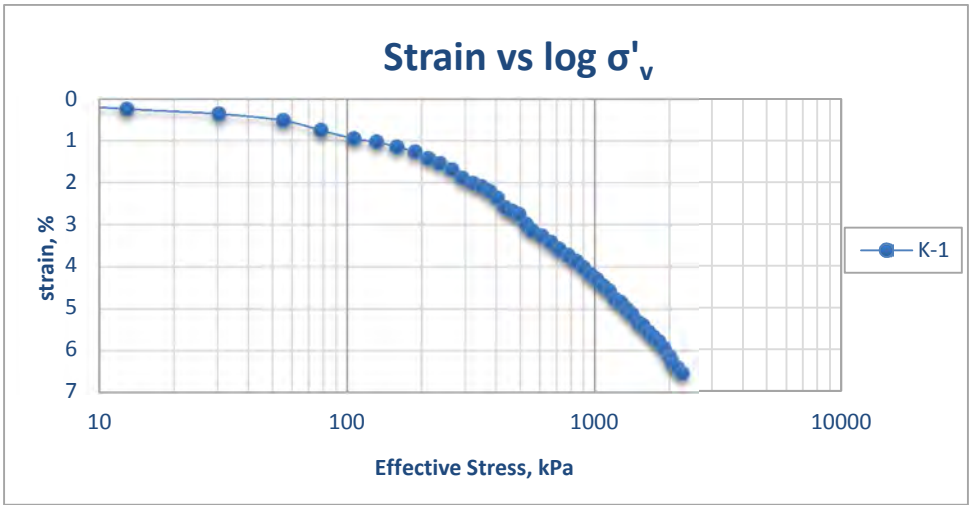

Fig.F-1: Axial strain versus log of average effective vertical stress.

Void Ratio curve

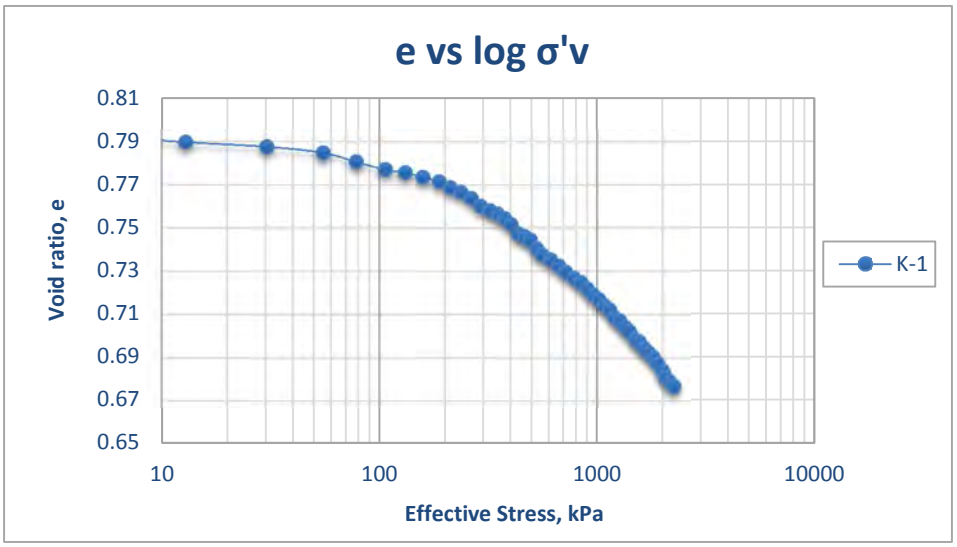

Fig. F-2: Void ratio versus log of average effective vertical stress.

Coefficient of Consolidation Curve

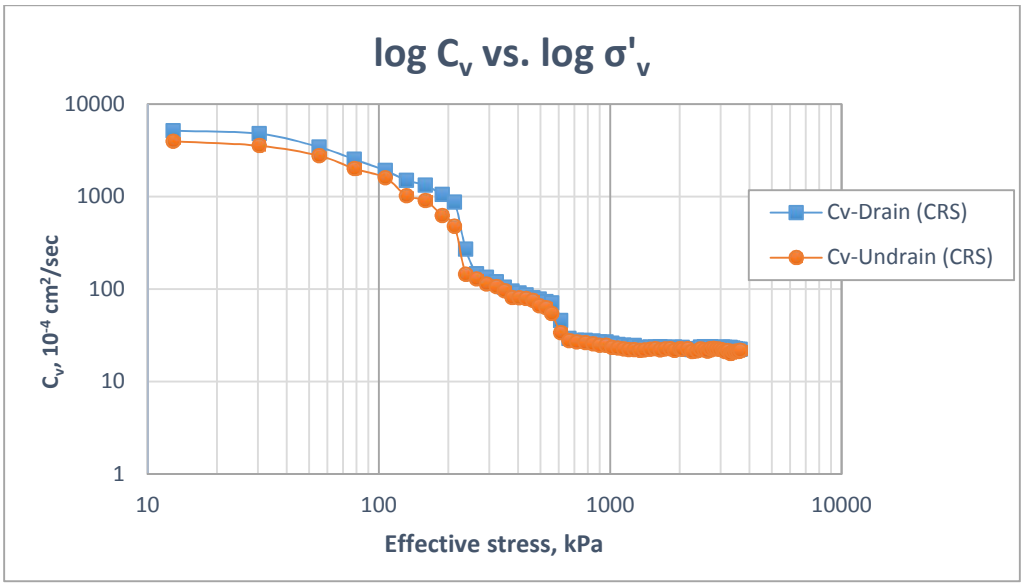

Fig. F-3 Log of coefficient of consolidation versus log of average effective vertical stress.

Excess pore pressure of K-1

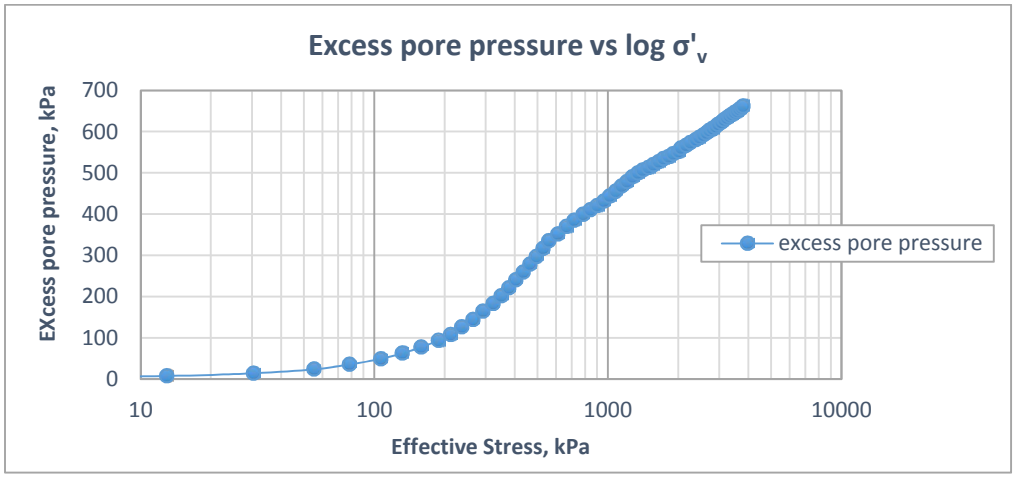

Fig. F-4: Excess pore pressure versus log of average effective vertical stress

F2. K-2 CRSC Test Results.

Strain Curve

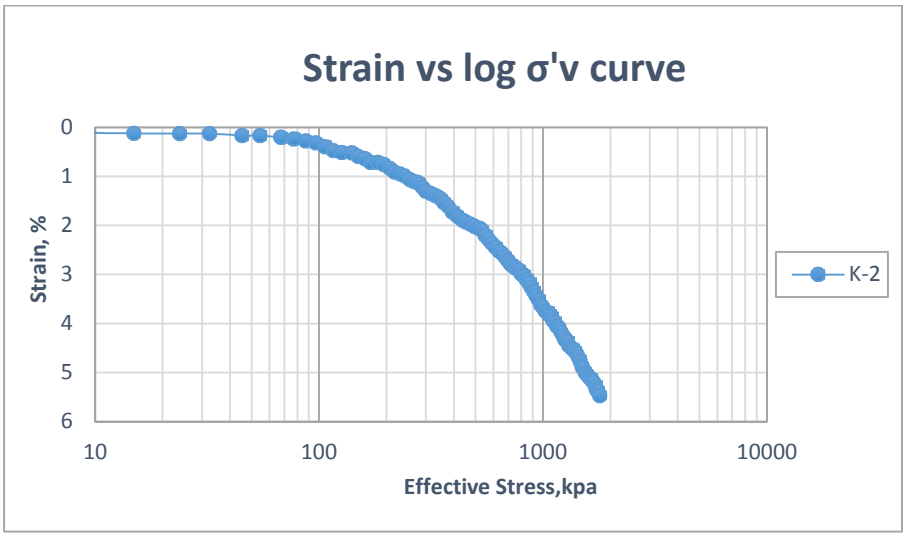

Fig.F-5: Axial strain versus log of average effective vertical stress.

Void Ratio curve

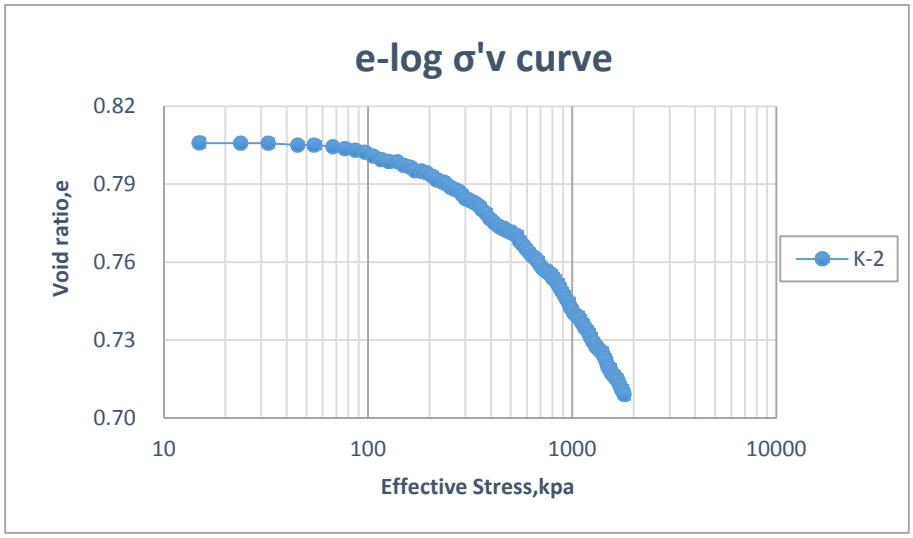

Fig. F-6: Void ratio versus log of average effective vertical stress.

Coefficient of Consolidation Curve

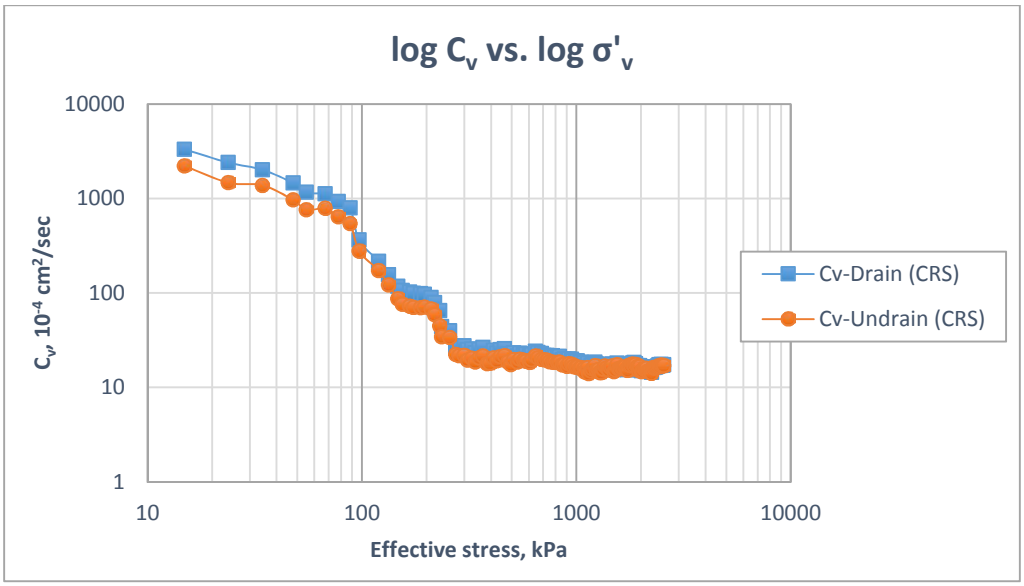

Fig. F-7: Log of coefficient of consolidation versus log of average effective vertical stress for K-2

Excess pore pressure of K-2

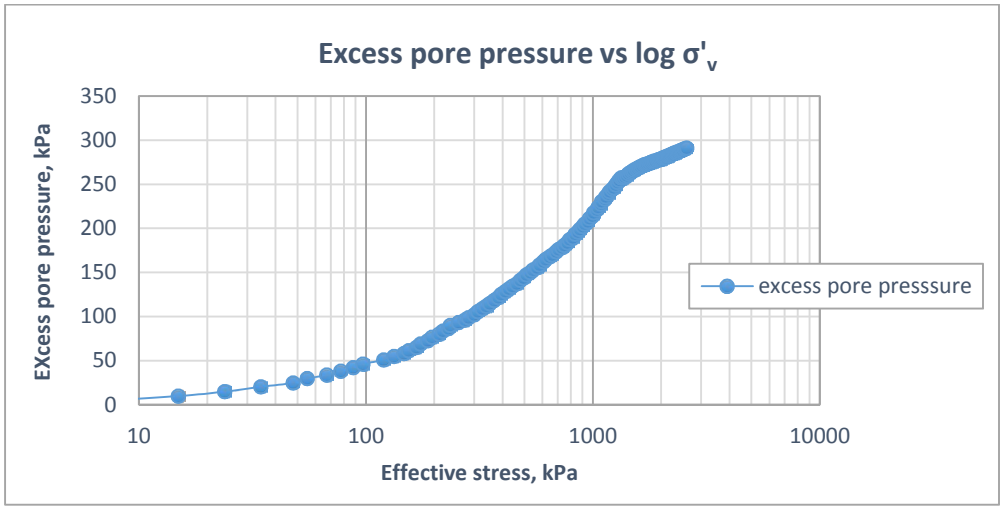

Fig. F-8: Excess pore pressure versus log of average effective vertical stress for K-2

F3. AG-1 CRSC Test Results.

Strain Curve

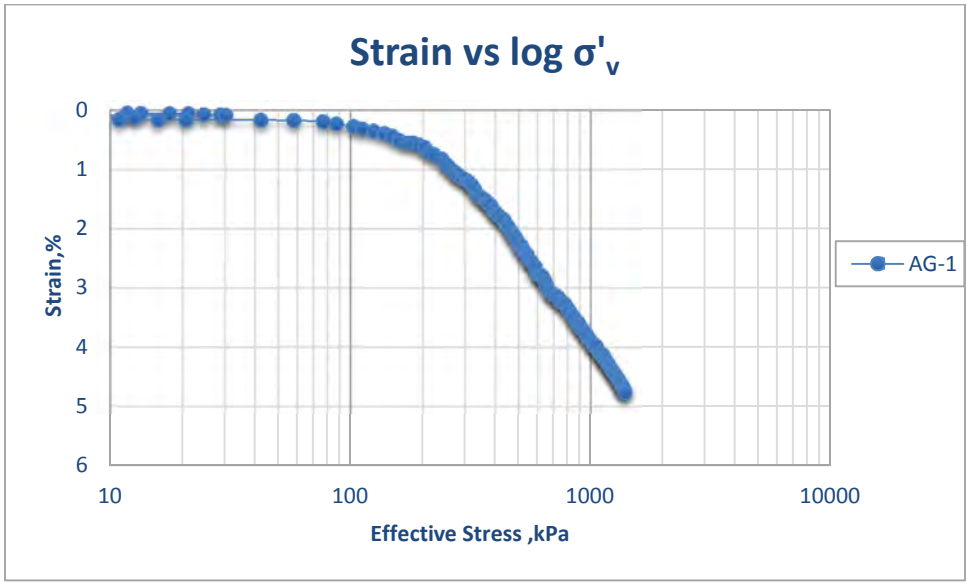

Fig.F-9: Axial strain versus log of average effective vertical stress.

Void Ratio curve

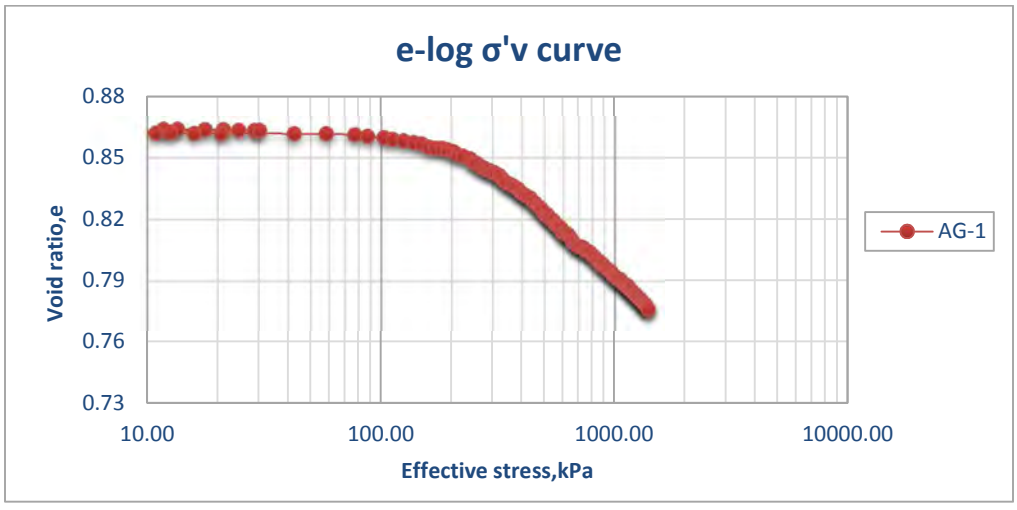

Fig. F-10: Void ratio versus log of average effective vertical stress.

Coefficient of Consolidation Curve

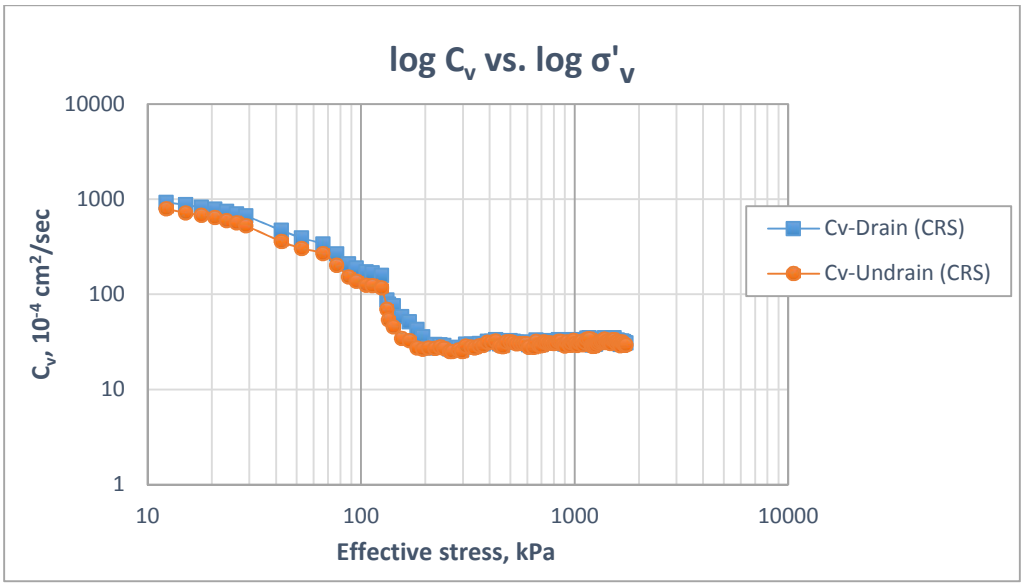

Fig. F-11: Log of coefficient of consolidation versus log of average effective vertical stress for AG-1.

Excess pore pressure of AG-1

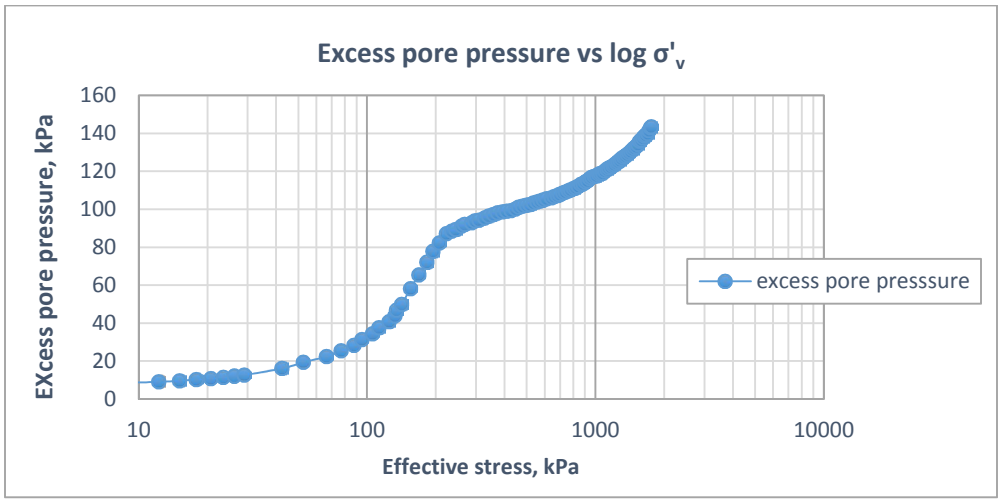

Fig. F-12: Excess pore pressure versus log of average effective vertical stress for AG-1

F4. AG-2 CRSC Test Results.

Strain Curve

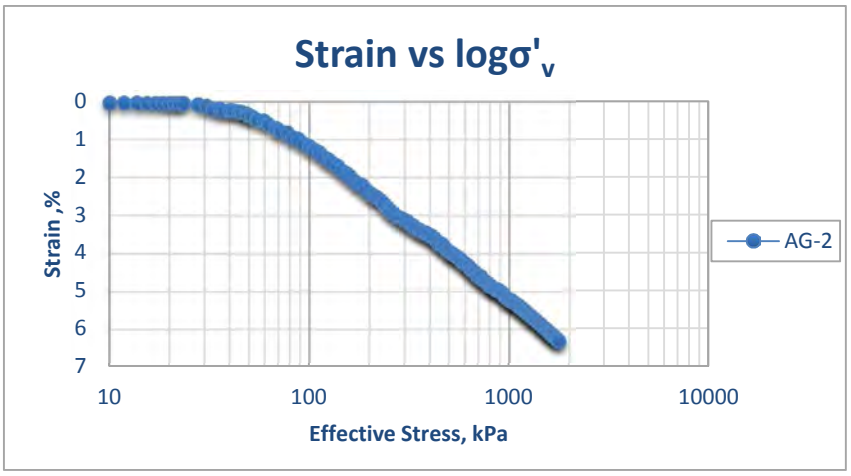

Fig.F-13: Axial strain versus log of average effective vertical stress.

Void Ratio curve

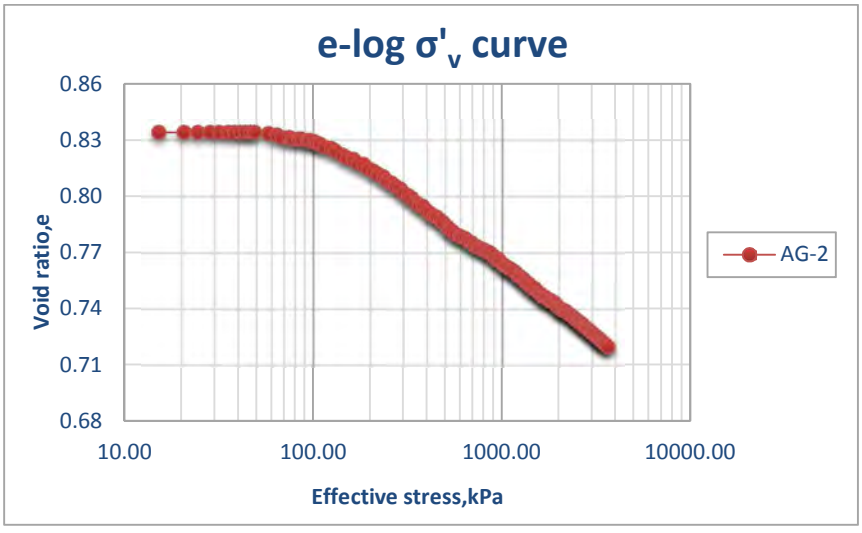

Fig. F-14: Void ratio versus log of average effective vertical stress.

Coefficient of Consolidation Curve

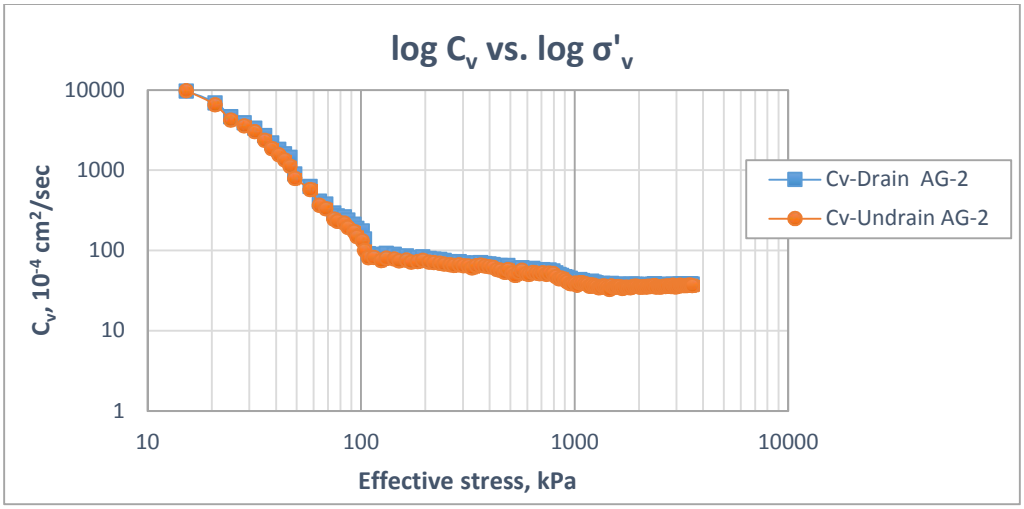

Fig. F-15: Log of coefficient of consolidation versus log of average effective vertical stress for AG-2.

Excess pore pressure of AG-2

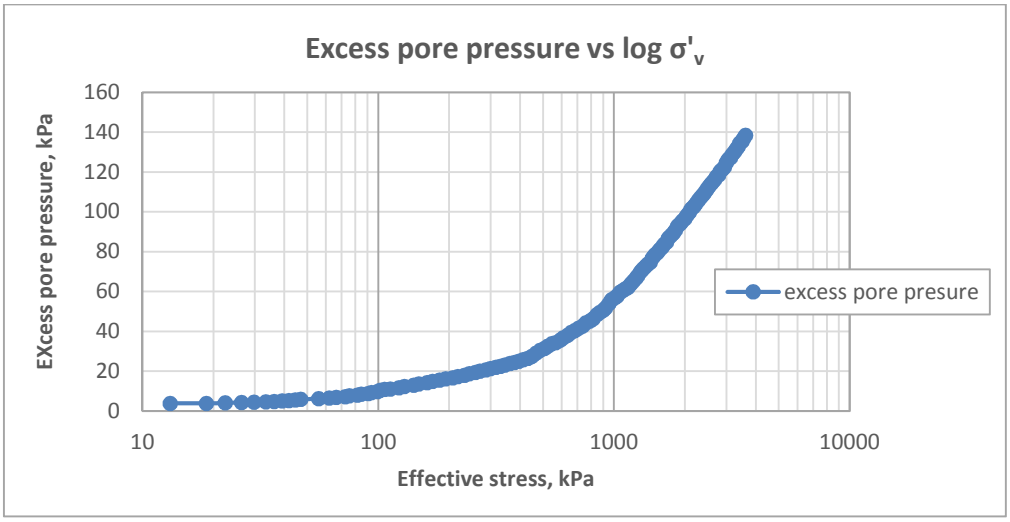

Fig. F-16: Excess pore pressure versus log of average effective vertical stress for AG-2

F5. R-1 CRSC Test Results.

Strain Curve

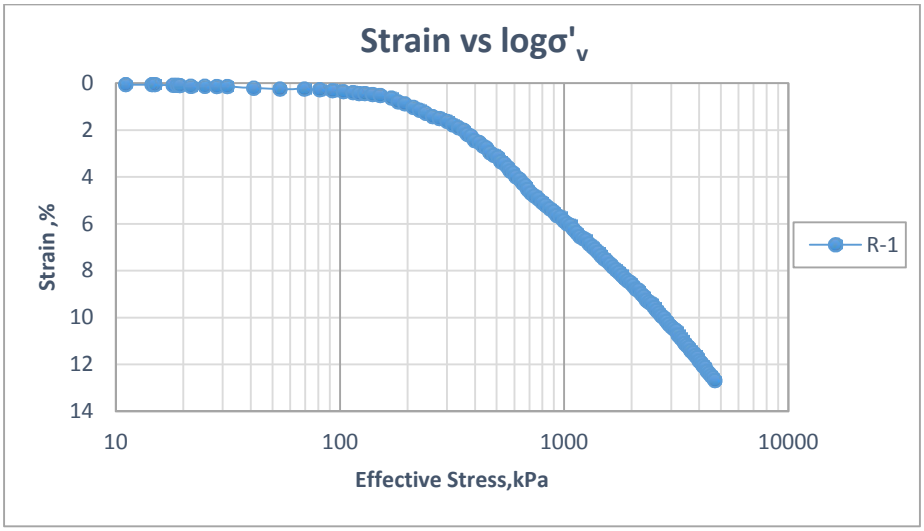

Fig.F-17: Axial strain versus log of average effective vertical stress.

Void Ratio curve

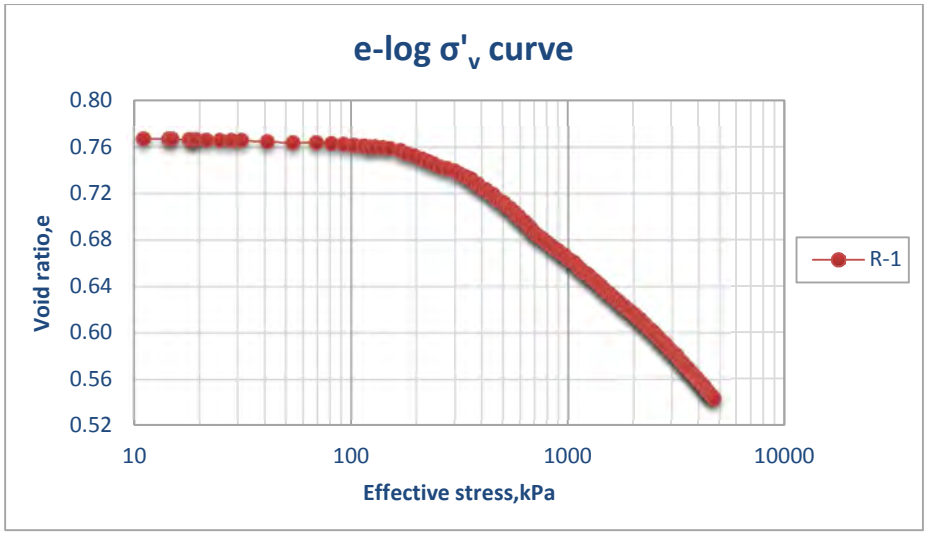

Fig. F-18: Void ratio versus log of average effective vertical stress.

Coefficient of Consolidation Curve

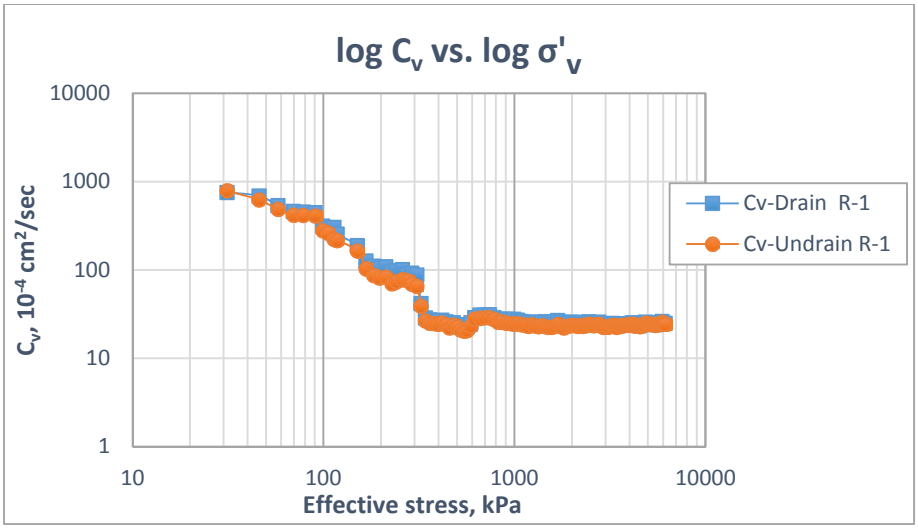

Fig. F-19: Log of coefficient of consolidation versus log of average effective vertical stress for R-1.

Excess pore pressure of R-1

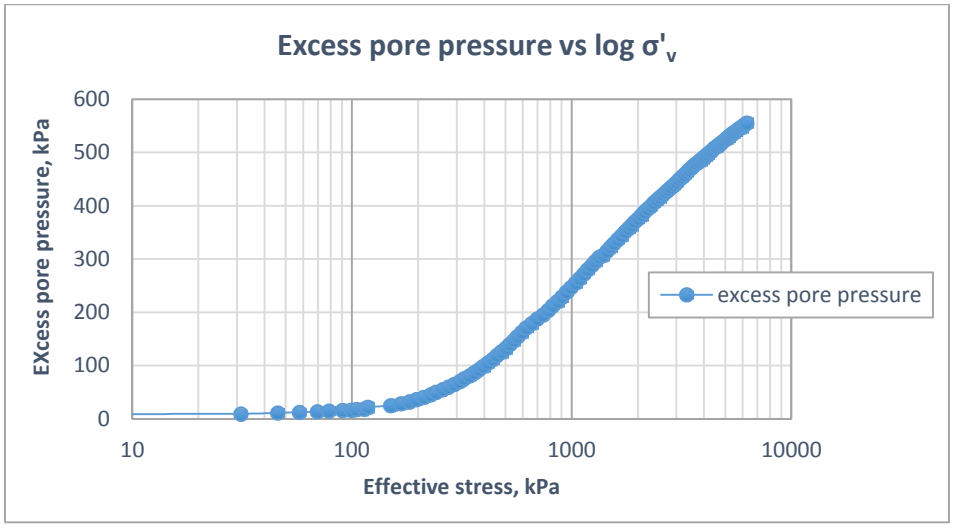

Fig. F-20: Excess pore pressure versus log of average effective vertical stress for R-1

F6. R-2 CRSC Test Results.

Strain Curve

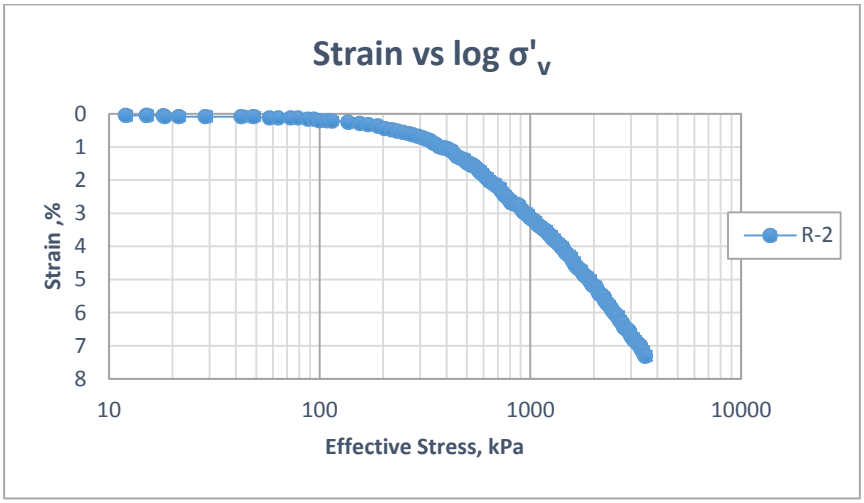

Fig.F-21: Axial strain versus log of average effective vertical stress.

Void Ratio curve

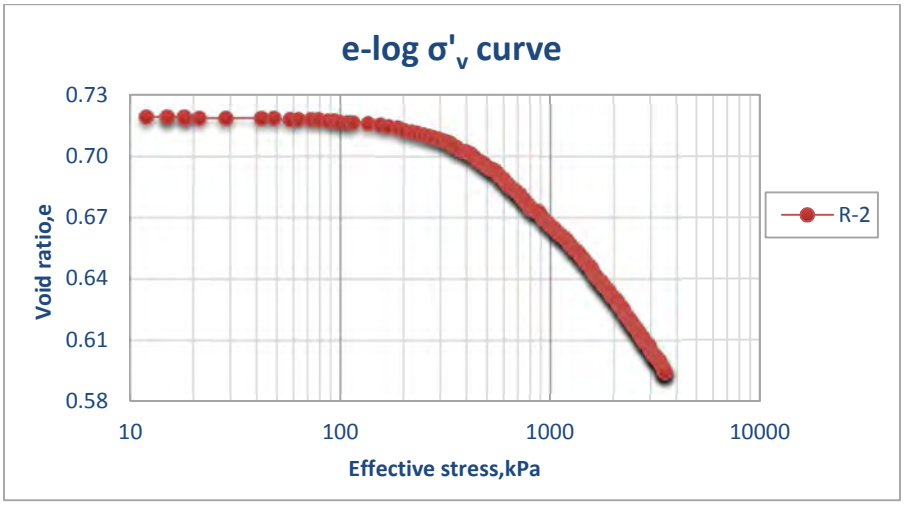

Fig. F-22: Void ratio versus log of average effective vertical stress.

Coefficient of Consolidation Curve

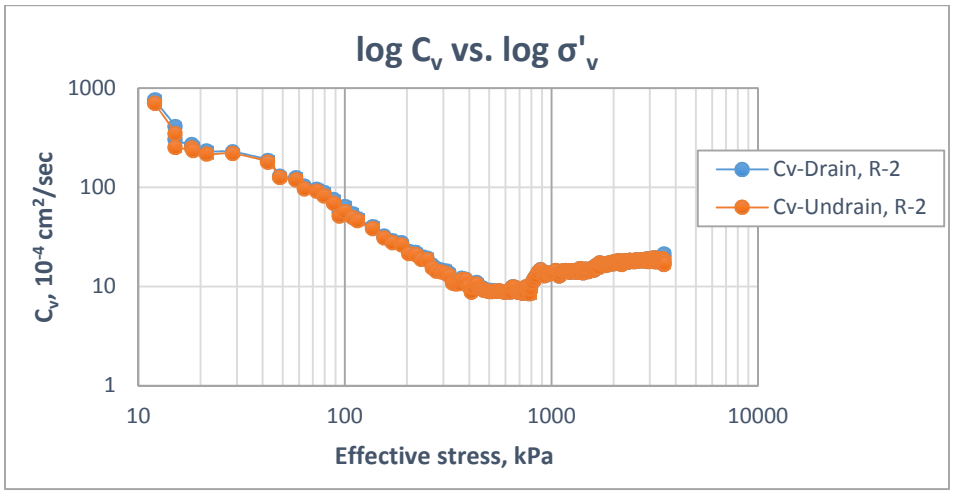

Fig. F-23: Log of coefficient of consolidation versus log of average effective vertical stress for R-2.

Excess pore pressure of R-2

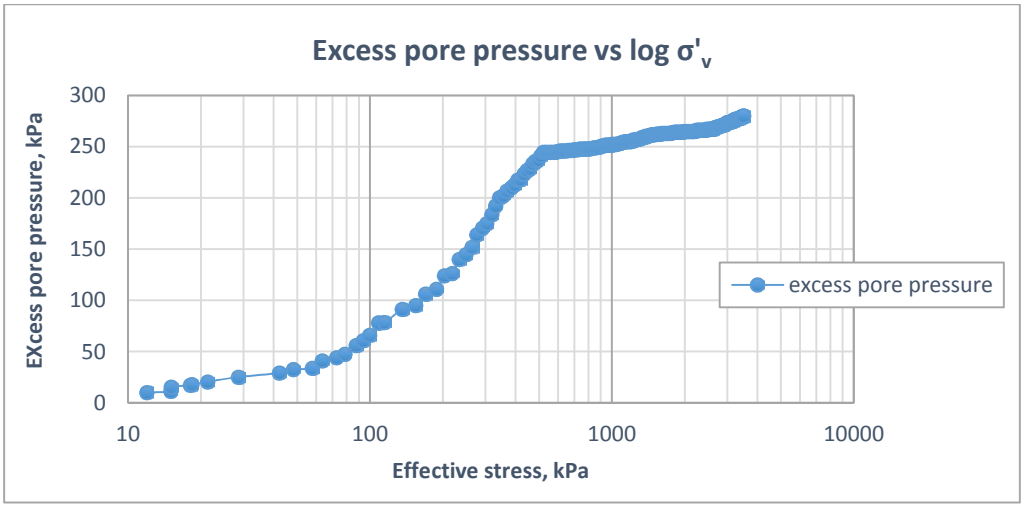

Fig. F-24: Excess pore pressure versus log of average effective vertical stress for R-2.

Appendix G

(Umhera and Zen Charts)

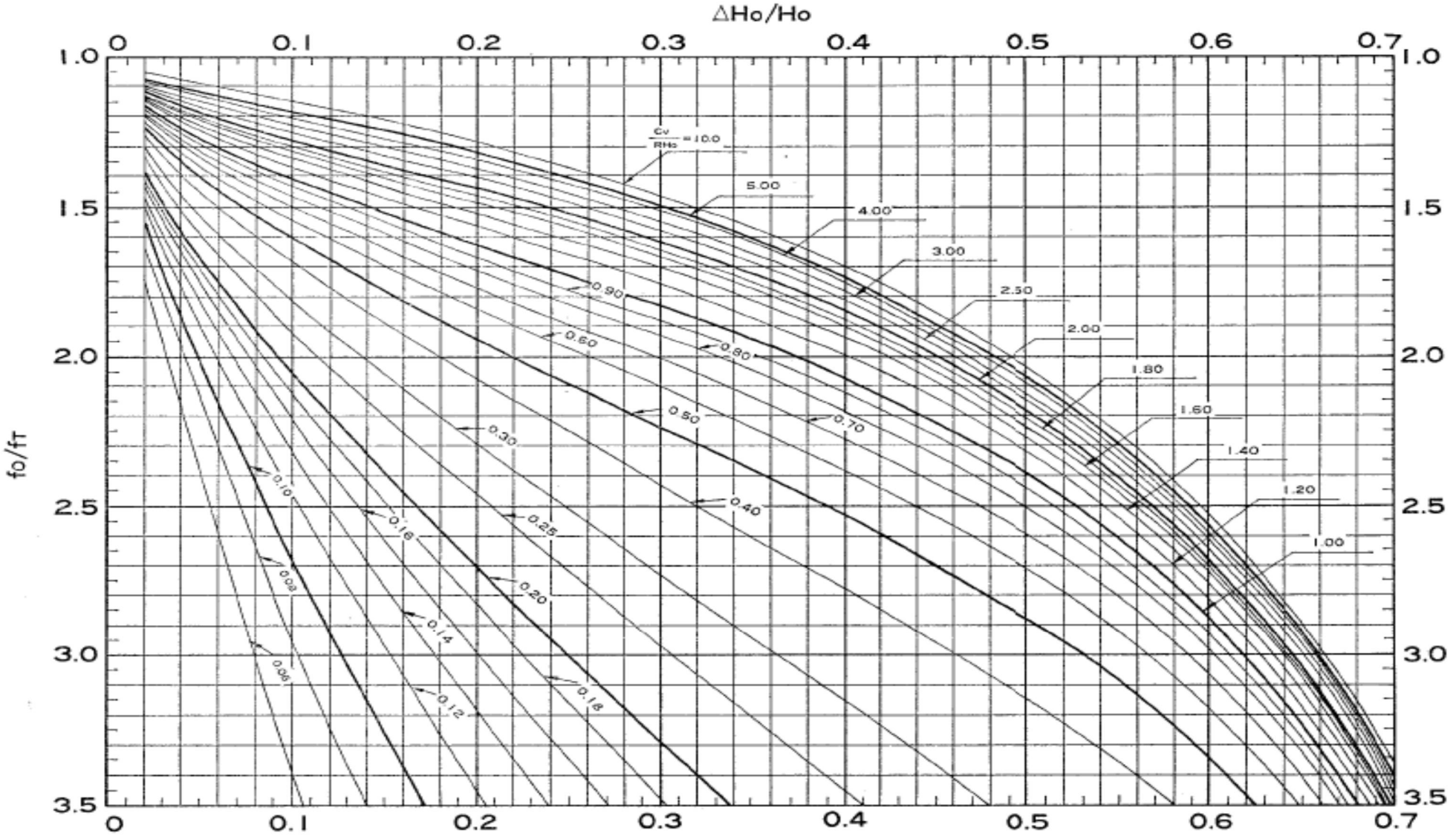

Fig.G-1: Variation of consolidation ratio at the top of the specimen for average strain [35].

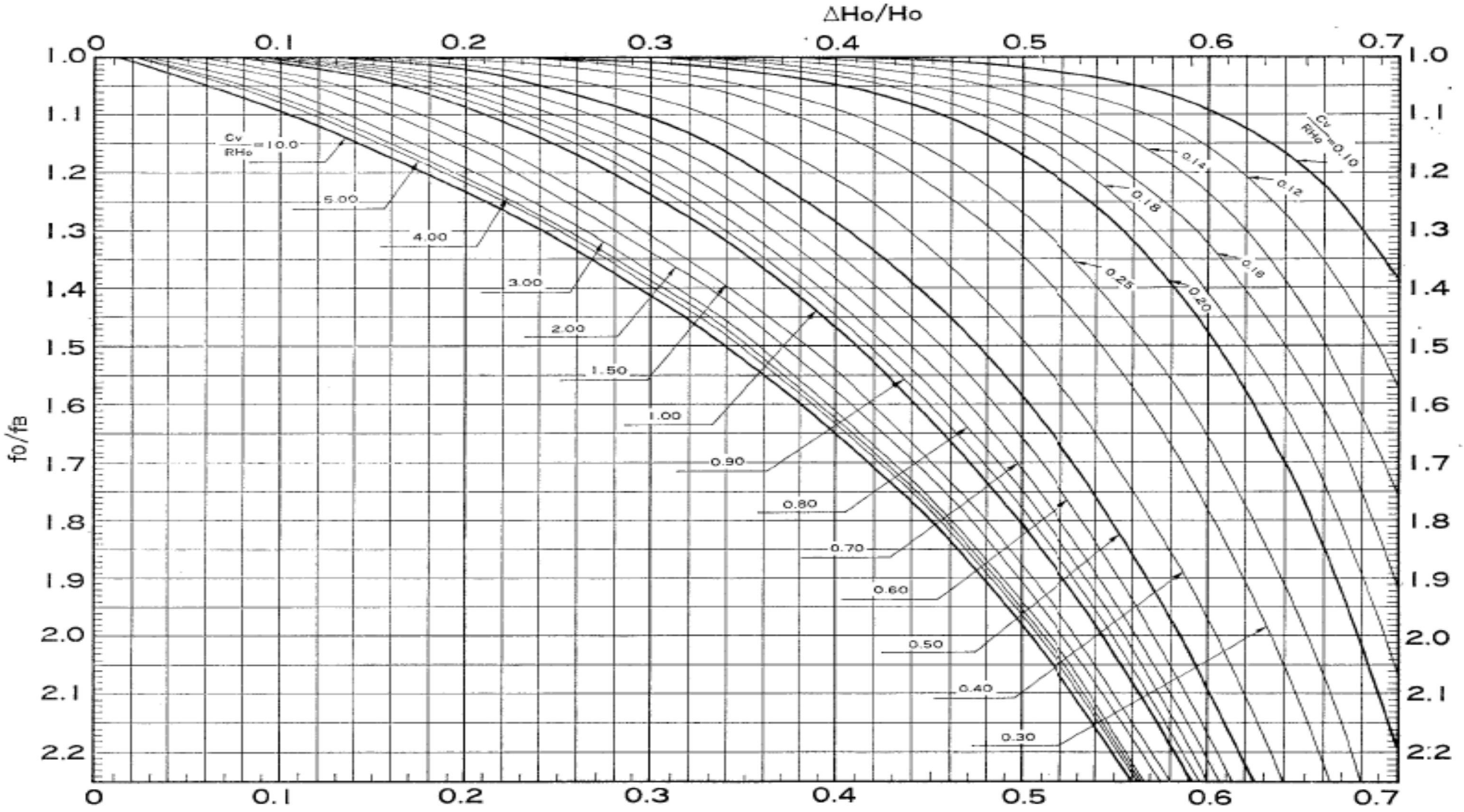

Fig.G-2: Variation of consolidation ratio at the bottom of the Specimen for average strain [35].

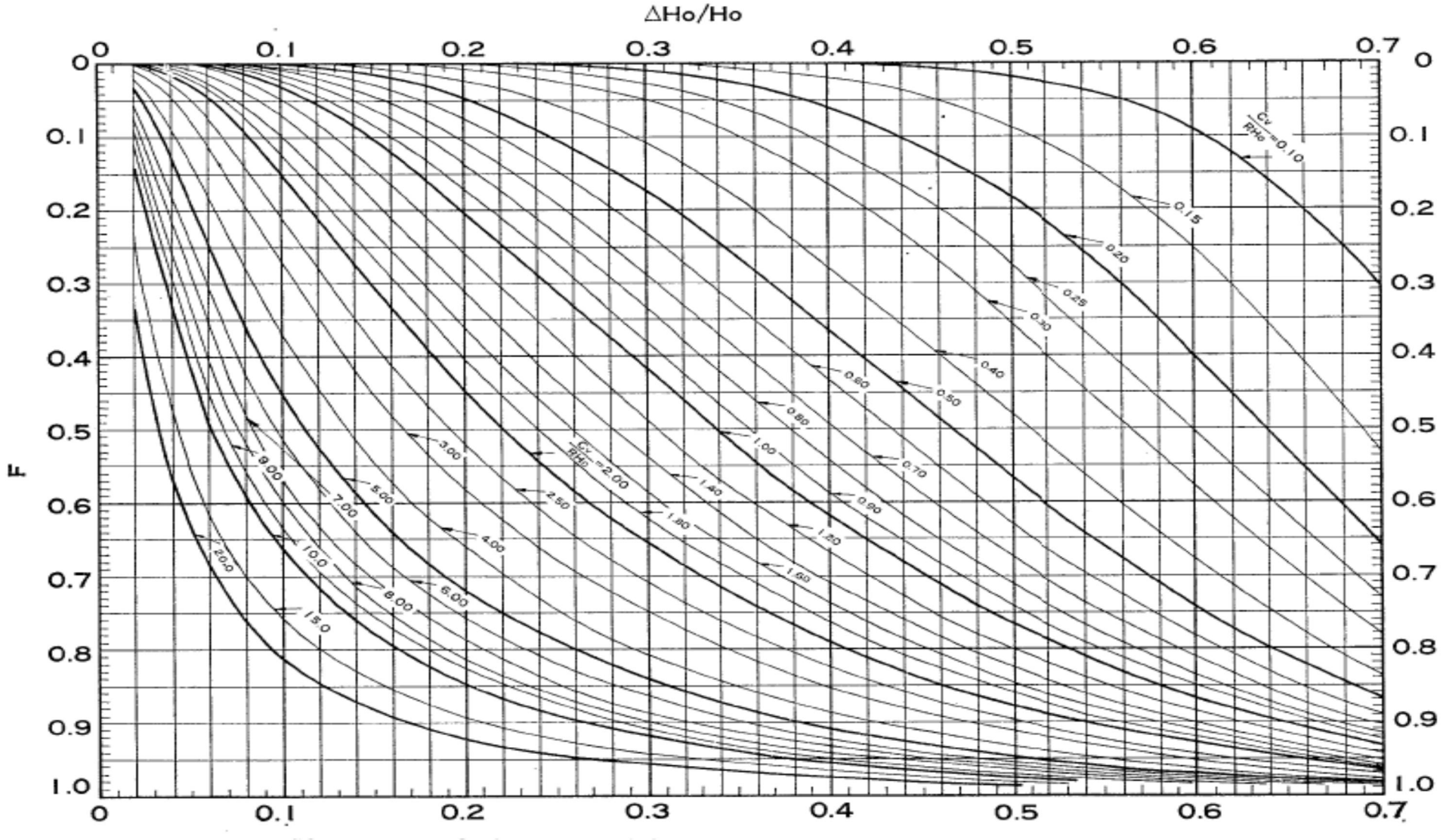

Fig.G-3: Variations of the ratio of bottom strain to top strain for average strain [35]